# Role of the NADPH Oxidase NOX4 in Liver Fibrosis and Hepatocarcinogenesis

Eva Crosas Molist

# ROLE OF THE NADPH OXIDASE NOX4 IN LIVER FIBROSIS AND HEPATOCARCINOGENESIS


Report presented by

**Eva Crosas Molist**


to obtain the title of

Doctor of Philosophy (Ph.D.)

**Supervised by:**


**Isabel Fabregat, PhD.** **Esther Bertran, PhD.**

Biological clues of the invasive and metastasic phenotype group
**Bellvitge Biomedical Research Institute (IDIBELL)**

**PhD program in Biomedicine (Universitat de Barcelona)**

This work has been developed at the Laboratori d'Oncologia Molecular (LOM) at IDIBELL (L'Hospitalet de Llobregat, Barcelona).

The author enjoyed the following financial support:

- "APIF fellowship" from Universitat de Barcelona (October 2009 – September 2010).
- "FPU predoctoral fellowship" from Ministerio de Educación y Ciencia (MEC), Gobierno de España (October 2010 – October 2013).
- "Estancias breves del Programa Nacional de Formación de Profesorado Universitario, Convocatoria 2012" – Allowing the author to complete a three months stage (February – April 2013) in Professor Karl-Heinz Krause's laboratory, at Université de Genève (Geneva, Switzerland).
- "Ajut per fomentar la mobilitat dins els programes de Doctorat en l'àmbit de la Xarxa Eurolife" from Universitat de Barcelona and Campus d'Excel·lència HUBc – Allowing the author to complete a three months stage (April – June 2014) in Dr. Victoria Sanz-Moreno's laboratory, Randall Division, King's College London (London, United Kingdom).

This work has been possible thanks to the finantial support of the following companies and institutions:

- Gobierno de España - Ministerio de Educación y Ciencia (MEC) (2007-2009). BFU2006-01036. Título del proyecto: Señales pro- y anti-apoptóticas inducidas por TGF-beta en hepatocitos. Implicaciones en la Fisiopatología del hígado.
- Gobierno de España - Ministerio de Ciencia e Innovación (MICINN) a través del Instituto de Salud Carlos III - Red Temática de Investigación Cooperativa en Cáncer (RTICC) (2007-2011). RD06/0020.
- Gobierno de España - Ministerio de Ciencia e Innovación (MICINN) (2010-2012). BFU2009-07129. Título del proyecto: Análisis de las vías de transducción de señal inducidas por TGF-beta en células hepáticas humanas como estrategia para el desarrollo de nuevas terapias en patologías del hígado.
- Generalitat de Catalunya - Agència de Gestió d'Ajuts Universitaris i de Recerca (AGAUR) (2009-2013). 2009SGR-312. Título del proyecto: Mecanismos moleculares y celulares asociados al fenotipo tumoral y metastásico.
- Gobierno de España - Ministerio de Economía y Competitividad (MINECO) a través del Instituto de Salud Carlos III -Red Temática de Investigación Cooperativa en Cáncer (RTICC). RD12-0036-0029.
- Gobierno de España - Ministerio de Economía y Competitividad (MINECO) (2013 - 2015). BFU2012-35538. Título del proyecto: Papel del tráfico intracelular, el citoesqueleto y las integrinas en la señalización inducida por TGF-beta en células hepáticas. Relevancia en fibrosis y hepatocarcinogénesis.
- DIGNA BIOTECH (Pamplona, Spain). Project title: Analysis of P144 and P17 peptides (DIGNA BIOTECH) as potential antineoplasic in liver tumor progression.

A vosaltres, perquè tots en formeu part.

# ACKNOWLEDGEMENTS

En el moment que em vaig plantejar començar a escriure la tesi i vaig fer un repàs dels resultats obtinguts al llarg d'aquests anys, em van començar a venir molts records a la memòria, molts moments, moltes persones,… i la veritat, tot i que ja ho sabia, se'm va fer encara més evident que sense tots i cada un de vosaltres arribar fins aquí no hauria sigut possible, MOLTES GRÀCIES A TOTS I TOTES!!!

Amb unes breus línies intentaré fer un repàs de tots els que m'heu ajudat i recolzat al llarg d'aquest recorregut, tot i que ja avanço que n'acabarà sent una mostra perquè m'adono que em serà impossible plasmar amb paraules tot el suport que he rebut i tot l'agraïment que voldria transmetre. Els que em coneixeu bé sabeu que sóc de poques paraules però espero saber-ne suficient per fer-vos arribar el meu missatge.

En primer lloc vull agrair a la meva família tot el suport que he rebut, evidentment no em puc limitar només a aquests últims anys, sinó a tota la vida. Gràcies pels ànims que sempre m'heu donat, per ajudar-me en els moments baixos, per fer-me creure que podia i per fer-me com sóc. Sense vosaltres no seria aquí i sense vosaltres no seria qui sóc. Gràcies!!

Ja centrant-me en els darrers anys, el meu primer agraïment és, com no podria ser d'una altra forma, per la Dra. Fabregat. Gracias Isabel por darme la oportunidad de realizar mi tesis doctoral a tu lado, por guiarme a lo largo de estos años, por enseñarme como funciona el mundo de la ciencia, por transmitirme tu conocimiento, por enseñarme a aprender, por abrirme las puertas del mundo, por ayudarme a conocer gente maravillosa,… podría escribir una larga lista de motivos por los que darte las gracias, así que intentaré resumirlo en pocas palabras: Gracias Isabel por ayudarme en mis primeros pasos en este "mundillo", por todo el soporte que he recibido y por ayudarme a sembrar mi futuro, nunca lo olvidaré.

Sens dubte, el meu següent agraïment és per l'Esther. Buf.. què n'hauria sigut de mi sense tu? Una vegada més, em serà molt complicat resumir en poques paraules tot el que t'hauria d'agrair. Moltes gràcies per ser sempre allà, per ensenyar-me tot el que m'has ensenyat, per guiar-me en tot moment, per tot el teu suport tant a nivell professional com personal, per totes les discussions, per tots els castells de sorra construïts (i desconstruïts...), pels grans moments que hem compartit, i fins i tot per les frases que passen a la història com... (i no m'ho tinguis en compte...) "què és aquesta merda...?". Sense tots aquests records no seria el mateix! Moltes gràcies per tot, Esther!

I continuo amb la resta de membres del laboratori (popularment coneguts com a IFs). Moltes gràcies a tots, als que fa temps que hi sou, als que tots just comenceu i als que no hi sou perquè va arribar l'hora de continuar el vostre camí per una altra banda, sense vosaltres tampoc hauria sigut possible. Que difícil resumir en quatre paraules tot el que m'heu aportat... Patty, mi compañera de NOXs! Que grandes

momentos compartimos y cuanto me enseñaste durante mis primeros años, y todavía estos días, desde la lejanía, transmitiéndome toda esta vitalidad y amor por la ciencia que te caracteriza! Muchas gracias Patricia! Laia, tota tu ets energia, incansable, omnipresent, el meu "Pubmed" preferit! Amb la teva manera de ser i de veure/viure la vida he après un munt, tu sempre tant valenta, optimista, treballadora, intel·ligent,... només espero que amb els anys que hem compartit m'hagis encomanat una miqueta de cada una d'aquestes infinites virtuts que et caracteritzen. Jèssica, la predoc sènior del grup a la meva arribada, gràcies per tota l'ajuda que em vas oferir quan vaig entrar a formar part del lab. Joan, no crec que t'imaginis com d'important ha sigut per mi poder-te tenir de referència, sempre un petit pas per davant! Tu sempre amb aquest tarannà calmat, transmetent tranquil·litat i serenor! Joaquim!!! L'ànima de la festa!! Aquests mesos que no hi has sigut hi havia una calma estranya al lab! Ha sigut senzillament genial compartir tots aquests anys amb tu!! T'asseguro que en la forma en què veig el món hi ha un abans i un després de conèixer-te! I l'Edgar, deu ni do ja els anys que fa que compartim recorregut... Realment un plaer!! Aix Judit... que difícil... quantes coses, dins i fora del lab... tu sempre allà, per escoltar, per donar un cop de mà... Fins i tot per córrer a aquelles hores que els carrers encara no estan posats! Tots hauríem de portar una Judit dins, el món seria un lloc millor! I les últimes incorporacions, Andrea i Dani, que bueno este aire fresco que habéis aportado al grupo! Finalment, ja per acabar amb els IFs, unes últimes línies pel Dr. Estanis Navarro. Sempre amb el teu peculiar punt de vista sobre les coses, gràcies per compartir amb mi la teva experiència i el teu coneixement.

Sortint del grup però encara al COM, un breu pensament per tots aquells que heu format part d'aquesta història, i hi heu aportat el vostre granet de sorra. He tingut la sort d'estar en un departament format per persones amb una increïble qualitat humana. Gràcies a tots!! Amb els IFs al COM 4, Magdiel, un gran placer compartir esas largas charlas contigo! Entrant al COM 5, Miguel y Laura, cuantos buenos momentos hemos compartido! Ja incorporats més recentment, i situats una mica més lluny, al COM 2, però compartint llargues hores de cabina, el Juan, sempre amb el teu humor peculiar, i la Silvia, i darrerament el Santi i el David, els dos super post-doc! Quedant-me una mica més al COM 5, l'Antònia, la veu de l'experiència! i la Dra. Àngels Fabra, moltes gràcies per ser sempre allà, per resoldre els meus dubtes i per donar-me un cop de mà sempre que ha sigut necessari. Acabant de completar el COM 2, un record per tots aquells que ja heu continuat el vostre camí per altres bandes, Anna, Ana, Naiara i Laia, totes sempre amb un somriure i una paraula amable apunt. I finalment cap al COM 3, el guirigall del departament!! Quina vitalitat i quins riures!! Clara, Raffa, Javi, Helena, Adri i Ana gràcies per desprendre aquesta energia, vitalitat i positivitat!!! Sou tots genials!!! I finalment, i com no pot ser d'una altra manera, un agraïment als Drs. Òscar Martinez, Cristina Muñoz, Mariona Graupera, Roser López, Cristina Costa i Àngels Sierra, i tots aquells que m'estic deixant pel camí, amb qui he compartit alguns moments, tots aquells que heu passat pel COM al llarg d'aquests anys, que no sou pocs, i que heu fet que tots aquests anys hagin sigut fantàstics!

Simplement creuant l'autovia, vull agrair al Dr. Joan Gil tot el suport rebut al llarg d'aquests anys, perquè sempre hi has sigut, disposat a ajudar quan ha sigut necessari, i sempre has tingut un somriure i una paraula amable allà on ens haguem trobat.

Encara a Barcelona però sortint de l'IDIBELL, no em puc oblidar del Dr. Gustavo Egea. Moltes gràcies Gustavo per haver-me donat la oportunitat de col·laborar amb tots vosaltres. Crec que ha sigut un plus important en la meva formació al llarg d'aquests anys i una gran experiència.

Ja sortint de Barcelona és el moment de recordar tota aquella gent meravellosa que he tingut la oportunitat de conèixer gràcies a diferents estades i col·laboracions. Per ordre cronològic començo per la Complutense de Madrid. Muchas gracias a todos, con especial mención a Arancha y Marga, por acogerme con los brazos abiertos y ofrecerme toda vuestra ayuda y soporte.

Continuo per Ginebra. I would like to thank Professor Karl-Heinz Krause and Dr. Michelangelo Foti for giving me the opportunity of doing a short stay in their labs, for showing me other ways of thinking and doing science and for allowing me to live a great experience! Of course, I cannot forget marvellous people I met, worked and had great moments there. Thanks a lot Marion, Dorothea, Tamara, Vincent… and a quite long list of people I cannot mention for obvious reasons!

I acabo a Londres. Si hagués de definir aquesta experiència amb una paraula, no hi ha dubte, "velocitat!". Va ser tot tant inesperat i va anar tant de pressa que crec que encara ho estic assimilant. En aquest cas el meu especial agraïment és per la Dra. Vicky Sanz-Moreno. Muchas gracias Vicky por darme la oportunidad, por hacer que todo parezca fácil y por transmitirme tu gran motivación, capacidad de trabajo y máxima auto exigencia, además de permitirme aprender muchísimo al lado de gente maravillosa como Ceci, Jose y Gaia, entre muchos otros. Ceci, hiciste que me sintiera como en casa desde el mismo día que aterricé en Londres, fue simplemente genial compartir esos meses! Y por si fuera poco, gracias a ti conocí una larga lista de personas increibles. Stefano and Luca (and Betta), thanks for being so kind to me, for your help and support, and for the great moments we shared!

I per últim, però no per això menys importants, els meus amics, els de tota la vida, Maria, Ju, Marta, Dolors, Euge… I els que he tingut la sort que han anat apareixent al llarg d'aquesta etapa. Què hauria fet sense vosaltres Alba i Maria, tots els riures que hem fet i totes les neures que m'heu aguantat!!! Moltes gràcies a tots per ser com sou!! Per ser sempre allà!!!

# ABBREVIATIONS

| | |
|---|---|
| **4-HNE** | 4-Hydroxi-2'-Nonena |
| **8-OHdG** | 8-Hydroxydeoxyguanosine |
| **AEBSF** | 4-(2-aminoethyl)-Benzensulfonylfluorid |
| **AFP** | Alfa-Fetoprotein |
| **ALK5** | Activin Receptor-like Kinase 5 |
| **AMH** | Anti-Mullerian Hormone |
| **APC** | Adenomatosis Polyposis Coli |
| **ARE** | Antioxidant Response Elements |
| **$\alpha$-SMA** | Alpha-Smooth Muscle Actin |
| **BCLC** | Barcelona Clinic Liver Cancer |
| **BEC** | Biliary Epithelial cells |
| **BHA** | Butylated Hydroxyanisole |
| **BMP** | Bone Morphogenetic Proteins |
| **BSA** | Bovine Serum Albumin |
| **CAT** | Catalase |
| **CAT** | Collective-to-Amoeboid Transition |
| **$CCl_4$** | Carbon Tetrachloride |
| **CDD** | Choline Deficient Diet |
| **CDK** | Cyclin Dependent Kinase |
| **CGD** | Chronic Granulomatous Disease |
| **CIP** | CDK-Interacting Protein |
| **CKI** | CDK-Inhibitors |
| **CLD** | Chronic Liver Disease |
| **CTGF** | Connective Tissue Growth Factor |
| **DCF** | 2',7'-Diclorofluorescein |
| **$DCFH_2$** | 2',7'-Diclorodihydrofluorescein |
| **DCP** | Descarboxiprothrombin |
| **DEN** | Diethylnitrosamine |
| **DHE** | Dihydroethidine |
| **DLC-1** | Deleted in Liver Cancer 1 |
| **DPI** | Diphenylene Iodonium |
| **DUOX** | Dual oxidase |
| **ECM** | Extracellular Matrix |
| **EGF** | Epidermal Growth Factor |
| **EGFR** | Epidermal Growth Factor Receptor |
| **eIF4E** | Eukaryotic Translation Initiation Factor 4E |
| **ELF** | Embryonic Liver Fodrin |
| **EMT** | Epithelial-to-Mesenchymal Transition |
| **FADH** | Flavin Adenine Dinucleotide plus Hydrogen |
| **FA** | Focal adhesion |

| | |
|---|---|
| **FAK** | Focal Adhesion Kinase |
| **FBS** | Foetal Bovine Serum |
| **FGF** | Fibroblast Growth Factor |
| **GAP** | GTPase Activating Proteins |
| **GDF** | Growth and Differentiation Factor |
| **GDI** | Guanine Nucleotide Dissociation Inhibitors |
| **GDP** | Guanine Diphosphate |
| **GEE** | Gutathione Ethyl Ester |
| **GEF** | Guanine Nucleotide Exchange Factors |
| **GMM** | Genetically Modified Mice |
| **GPx** | Glutathione Peroxidase |
| **GSH** | Reduced Glutathione |
| **GSSG** | Glutathione Disulphide |
| **GST** | Glutathione S-Transferase |
| **HB-EGF** | Heparin Binding EGF-like Growth Factor |
| **HBV** | Hepatitis B Virus |
| **HCC** | Hepatocellular Carcinoma |
| **HCV** | Hepatitis C Virus |
| **$H_2$DCF-DA** | 2′,7′-Dichlorodihydrofluorescein Diacetate |
| **H/E** | Hematoxylin and Eosine |
| **HGF** | Hepatocyte Growth Factor |
| **HIF1$\alpha$** | Hypoxia Inducible Factor 1 alpha |
| **HO-1** | Heme-Oxygenase-1 |
| **HSC** | Hepatic Stellate Cells |
| **IGF** | Insulin-like Growth Factor |
| **IFN** | Interferon |
| **IHC** | Immunohistochemistry |
| **IL-6** | Interleukin-6 |
| **IR** | Ischemia/Reperfusion |
| **LAP** | Latency-Associated Peptide |
| **LMW-PTP** | Low-Molecular-Weight PTP |
| **Mdr2** | Multi drug resistance 2 |
| **MAT** | Mesenchymal-to-Amoeboid Transition |
| **MET** | Mesenchymal-to-Epithelial Transition |
| **MFB** | Myofibroblast |
| **MLC** | Myosin Light Chain |
| **MMP** | Matrix Metalloproteinases |
| **MPO** | Myeloperoxidase |
| **MRTF** | Myocardin-Related Transcription Factor |
| **mTOR** | Mammalian Target of Rapamycin |

| | |
|---|---|
| **MYPT** | Myosin Light Chain Phosphatase |
| **NAC** | N-Acetylcysteine |
| **NADH** | Nicotinamide Adenine Dinucleotide plus Hydrogen |
| **NADPH** | Nicotinamide Adenine Dinucleotide Phosphate |
| **NAFLD** | Non-Alcoholic Fatty Liver Disease |
| **NASH** | Non-Alcoholic Steatohepatitis |
| **NF-κB** | Nuclear Factor–kappa B |
| **NO** | Nitric Oxide |
| **NOS** | Nitric Oxide Synthase |
| **NOX** | NADPH Oxidase |
| **NOXA1** | NOX Activator 1 |
| **NOXO1** | NOX Organizer 1 |
| **Nrf** | Nuclear Factor Erythroid-2-Related Transcription Factor |
| **PBS** | Phosphate-Buffered Saline |
| **PDGF** | Platelet-Derived Growth Factor |
| **PFA** | Paraformaldehyde |
| **PH** | Partial Hepatectomy |
| **PI** | Propidium Iodide |
| **PIVKA-II** | Prothrombin Induced by Vitamin K Absence II |
| **pMLC** | Phospho-Myosin Light Chain |
| **Poldip2** | Polymerase (DNA-directed) Delta-Interacting Protein 2 |
| **PPP** | Pentose Phosphate Pathway |
| **PTP** | Protein Tyrosine Phosphatases |
| **Rb** | Retinoblastoma Protein |
| **RNS** | Reactive Nitrogen Species |
| **ROS** | Reactive Oxygen Species |
| **SEC** | Sinusoidal Endothelial Cells |
| **SMC** | Smooth Muscle Cells |
| **SOD** | Superoxide Dismutase |
| **SRF** | Serum Response Factor |
| **STAT3** | Signal Transducer and Activator of Transcription 3 |
| **TAA** | Thioacetamide |
| **TCA** | Trichloroacetic Acid |
| **TβR** | TGF-β Receptor |
| **TERT** | Telomerase Reverse-Transcriptase |
| **TGF-α** | Transforming Growth Factor alpha |
| **TGF-β** | Transforming Growth Factor beta |
| **TIMP** | Tissue Inhibitors of Metalloproteinases |
| **TLR4** | Toll-Like Receptor 4 |
| **TPA** | 12-*o*-tetradecanoylphorbol 13-acetate |

| | |
|---|---|
| **TNF** | Tumour Necrosis Factor |
| **TXN** | Thioredoxin |
| **VEGF** | Vascular Endothelial Growth Factor |
| **VSMC** | Vascular Smooth Muscle Cells |

# TABLE OF CONTENTS

**I. INTRODUCTION 1**

**1. The liver 3**

1.1. Liver anatomy and physiology 3

1.2. Liver development, regeneration and the proliferative capacity of adult hepatocytes 6

**2. Liver disorders 9**

2.1. Liver fibrosis 10

2.2. Hepatocellular carcinoma 15

**3. Transforming growth factor-beta (TGF-β) 25**

3.1. TGF-β in the progression of liver disease 25

3.2. TGF-β signalling pathway 28

3.3. TGF-β biological roles 30

**4. ROS and NADPH oxidases 35**

4.1. Reactive oxygen species 35

4.2. Oxidative stress and oxidant signalling 36

4.3. Oxidant sources 38

4.4. NADPH oxidase (NOX) family 41

4.5. NADPH oxidase NOX4 48

4.6. Involvement of NOX-derived ROS in liver diseases 54

**5. Cell migration, invasion and metastasis 59**

5.1. Types of cell migration 60

5.2. Role of Rho GTPases 62

**II. HYPOTHESIS 67**

**III. OBJECTIVES 71**

**IV. MATERIAL AND METHODS 75**

**1. Cell culture 77**

1.1. Cell models 77

1.2. Culture conditions 78

1.3. Treatments used 78

**2. Animal experimentation 79**

2.1. Mice models for liver fibrosis studies 79

2.2. Partial hepatectomy in mice 80

2.3. Diethylnitrosamine-induced hepatocarcinogenesis in mice 80

*2.4.* Xenograft model of subcutaneous tumour growth *in vivo* 80

**3. Knock-down assays** **81**
3.1. Transient silencing 81
3.2. Stable silencing 81
**4. Analysis of cell proliferation** **82**
4.1. Crystal violet staining 82
4.2. DNA synthesis assay 83
4.3. Analysis of the percentage of Ki67 positive nuclei 83
4.4. Analysis of DNA content by flow cytometry 83
**5. Analysis of cell death** **84**
5.1. Analysis of Caspase-3 activity 84
**6. Measurement redox state** **85**
6.1. Intracellular ROS 85
6.2. Intracellular superoxide 86
6.3. Mitochondrial superoxide 86
6.4. Extracellular hydrogen peroxide 87
**7. Analysis of gene expression** **87**
7.1. RT-PCR 87
7.2. Semi-quantitative PCR 87
7.3. Quantitative Real Time PCR 88
**8. Protein expression analysis** **90**
8.1. Cell lysis 90
8.2. Protein quantification by Bradford's method 91
8.3. Protein quantification by BCA commercial kit 91
8.4. Protein immunodetection by Western blot 92
**9. Rho GTPase pull-down assays** **94**
**10. Immunocytochemistry** **96**
10.1. Immunofluorescence in 2D cultured cells 96
10.1. Immunofluorescence in cells cultured on thick layers of collagen I 97
**11. Immunohistochemistry** **98**
11.1. Paraffin embedding 98
11.2. IHC on paraffin-embedded tissues 98
**12. Tissue array** **101**
**13. Migration analysis** **102**
13.1. Chemotaxis assay 102
13.2. Wound healing assay 102
13.3. Real time migration assay 102
**14. Invasion analysis** **103**

14.1. Invasive growth assay 103
14.2. 3D invasion assay 103

**15. Adhesion assay 104**

**16. Integrin Array 104**

**17. Statistical analyses 105**

**V. RESULTS 107**

**1. ROLE OF NOX4 IN LIVER FIBROSIS 109**

1.1. Changes in NOX4 expression during liver fibrosis in two different animal models 109

1.2. Effect of silencing NOX4 in the activation of HSC to MFB in response to TGF-β 111

1.3. Effect of silencing NOX4 in the response of hepatocytes to TGF-β in terms of cell death 112

**2. ROLE OF NOX4 IN LIVER CARCINOGENESIS 115**

2.1. Phenotypic characterization of human HCC cell lines: Relevance of TGF-β pathway 115

2.2. Crosstalk between the TGF-β pathway and NOX4 in human HCC cell lines 120

2.3. Role of NOX4 as a negative regulator of proliferation 123

2.4. Role of NOX4 as a negative regulator of invasion 138

**VI. DISCUSSION 161**

**1. NOX4 plays a role downstream of TGF-β during liver fibrosis, participating in the transdifferentiation of HSC to MFB and inducing hepatocyte cell death. 163**

**2. Relevance of the TGF-β pathway in liver cancer. Crosstalk with NOX4. 167**

**3. NOX4 plays a growth inhibitory role in hepatocytes and HCC cells, regulating liver cancer progression. 171**

**4. NOX4 regulates contractility in human HCC cells, influencing its capacity of adhesion and invasion. 175**

**Final discussion 179**

**VII. CONCLUSIONS 181**

**VIII. REFERENCES 185**

**IX. ANNEXES 213**

# I. INTRODUCTION

# 1. The liver

## 1.1. Liver anatomy and physiology

The **liver** is the largest organ, accounting for approximately 2% to 3% of average body weight. It exhibits both endocrine and exocrine properties to carry out numerous functions that are involved in maintaining homeostasis within the organism.

The major exocrine secretion is in form of bile while endocrine functions include the secretion of several hormones (Insuline-like growth factors, Angiotensinogen, Thrombopoietin,…). The liver also holds other essential functions such as glycogen storage; drug detoxification; removal and breakdown of serum proteins, red blood cells and microbes; secretion of an extensive array of plasma proteins including Albumin, Transferrin and Apolipoproteins; control of metabolism: production or removal of glucose during periods of fasting or eating, respectively, processing of fatty acids and triglycerides, regulation of cholesterol synthesis and transport, synthesis and inter-conversion of non-essential amino acids,… (Malarkey et al., 2005; Spear et al., 2006; Si-Tayeb et al., 2010).

**Liver structure** is of important relevance to be able to carry out all these functions. The liver is macro structurally divided in 4 lobes: right, left, quadrate and caudate. Mice and humans have a gall bladder, but not the rat. The liver receives blood from two different sources, the portal vein (supplies about 70% of the blood flow and 40% of the oxygen) and the hepatic artery (supplies 30% of the blood flow and 60% of the oxygen). The hepatic architecture facilitates the exchange of materials between the blood and hepatocytes. In addition, the hepatic biliary system enables the liver to transport bile into intestines (Malarkey et al., 2005; Spear et al., 2006).

The basic architectural unit of the liver is the **liver lobule**. The lobule is a structure that consists of plates of **hepatocytes** lined by sinusoidal capillaries that radiate toward a central efferent vein. Liver lobules are roughly hexagonal with each of six corners demarcated by the presence of a portal triad of vessels, consisting of a portal vein, bile duct, and hepatic artery, in a connective tissue matrix comprised mainly by type 1 collagen. As mentioned before, both the portal vein and the hepatic artery supply blood to the lobule, which flows through a network of sinusoidal capillaries. Sinusoidal blood flow is finally collected by terminal hepatic venules prior to emptying into larger hepatic veins and eventually to the vena cava. Endothelial cells that line the sinusoids form the barrier between the blood and hepatocytes; the narrow region between these two cell types is termed the space of Disse. In the liver, the plates of hepatocytes are one to two cells thick. The sinusoidal side of these hepatocytes interfaces the space of Disse, whereas the opposite (apical) side forms the canalicular membrane. The bile canaliculi, small

channels that are between adjacent hepatocytes, transport bile to the intrahepatic bile duct. The transition region between the canaliculi and intrahepatic bile ducts is called the canal of Hering, narrow channels that are lined by hepatocytes and bile duct epithelial cells (BEC, also called cholangiocytes). These intrahepatic bile ducts converge into larger extrahepatic ducts, which ultimately join the common bile duct that transports bile either to the gall bladder (for storage) or directly to the small intestine. (Fausto and Campbell, 2003; Malarkey et al., 2005; Spear et al., 2006; Si-Tayeb et al., 2010).

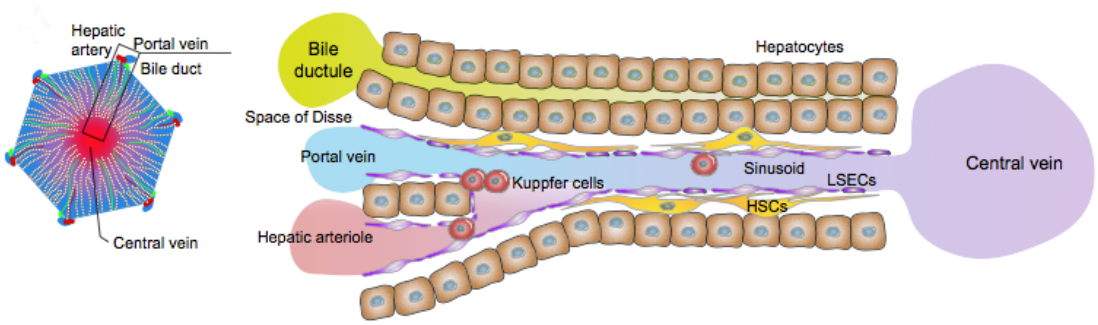


**Figure I.** Schematic hepatic lobule structure (Iwakiri et al., 2014).

Although hepatocytes are the major parenchymal cell type of the liver, other biologically important **cell types** are present: a) biliary epithelial cells (BEC) or cholangiocytes line the bile ducts. b) Sinusoidal endothelial cells (SEC) are the primary barrier between blood and hepatocytes and act as a filter of fluids, solutes and particles between the blood and the space of Disse. They have fenestrae, lack of basal lamina and can transfer molecules and particles by endocytosis. c) Kupffer cells (resident liver macrophages) are phagocytic cells, are the major producers of cytokines as mediators of inflammation and provide crosstalk with other cells. d) Pit cells (natural killer cells) are important in immune function. e) And hepatic stellate cells (HSC) are the major player in regeneration and hepatic fibrogenesis and cirrhosis. HSC are located in the space of Disse and normally produce extracellular matrix (ECM), control microvascular tone, store and metabolize vitamin A and lipids, and when activated transform to myofibroblast (MFB) (Malarkey et al., 2005; Spear et al., 2006; Si-Tayeb et al., 2010).

In addition, it is important to highlight that 5 to 10% of the ECM of the liver is collagen, which is important in the regulation and modulation of hepatic function. The ECM has numerous components including matrix metalloproteinases; glycoproteins like laminin, fibronectin, vitronectin, undulin and nidogen; and proteoglycans such as heparan sulfate (Malarkey et al., 2005).

The lobular organization of the liver has functional significance. While some liver functions can be carried out by all hepatocytes, other functions are limited to a subset of hepatocytes. This compartmentalization of function is determined by the position of hepatocytes within the liver lobule, a phenomenon called **positional (or zonal) heterogeneity** of metabolic zonation. This zonation allows opposing metabolic pathways to be carried out within distinct, non-overlapping regions of the liver. For example, periportal hepatocytes specialize in glycogenolysis and gluconeogenesis, while centrolobular hepatocytes are active in glycolysis and glycogen synthesis. In addition, not only the hepatocytes have gradients of gene and protein activity, but gradients also exist for SEC, Kupffer cells, HSC, and the matrix in the space of Disse (Spear et al., 2006; Fausto and Campbell, 2003; Malarkey et al., 2005).

This zonal heterogeneity is established during the perinatal period, a time when other dramatic changes occur in the liver (Spear et al., 2006).

## 1.2. Liver development, regeneration and the proliferative capacity of adult hepatocytes

Liver development can be separated into several overlapping stages: in the first stage, when specification is established, cells become "**competent**" and are capable of taking a certain fate. Competent cells subsequently become "**committed**" to a particular lineage and exhibit morphological changes and express genes associated with commitment. Cells then "**differentiate**" along that lineage and are ultimately capable of carrying out the functions of a terminally differentiated cell (Spear et al., 2006).

Pluripotent embryonic stem (ES) cells from the blastocyst inner cell mass give rise to three principal germ layers: ectoderm, mesoderm and endoderm. The anterior region of the endoderm will form the foregut. Coordinated signalling of fibroblast growth factors (FGF) from the cardiac mesoderm and bone morphogenetic proteins (BMP) from the septum transversum mesenchyme facilitate the commitment of competent foregut endoderm cells to become hepatoblasts. At the same time, early liver genes such as albumin and alfa-fetoprotein (AFP) are activated and also indicate commitment to the hepatic fate. Following hepatic specification of foregut endoderm, hepatoblasts proliferate and migrate into the septum transversum and continue to proliferate and differentiate (Kung et al., 2010; Spear et al., 2006).

More relevant to this work is the development of new hepatocytes during adulthood where there is **liver regeneration or repair**. Despite the low replicative rate of hepatocytes in the normal adult liver, these highly differentiated cells are not terminally differentiated and replicate in a highly regulated manner after loss of cell or tissue mass (Fausto and Campbell, 2003). Adult hepatocytes maintain the ability to proliferate and regenerate the liver in response to surgical ablation, toxic injury, infections, massive hepatocyte necrosis or apoptosis (Vacca et al., 2013).

A number of models have been proposed for the study of liver regeneration but the most commonly used and best-studied model is that of hepatic growth after **partial hepatectomy (PH)**. Higgins and Anderson first proposed the rodent model of two-thirds hepatectomy, in 1931, which consist on the removal of 70% of the liver mass. Within 5-7 days of surgical removal, the remaining liver has regenerated to a size equivalent to the original. Other models used for the study of liver regeneration include some chemical liver injuries induced by carbon tetrachloride ($CCl_4$) or D-galactosamine treatment, or acetaminophen intoxication (Mao et al., 2014).

Regeneration of the liver is considered a **compensatory hyperplasia** rather than a true restoration of the liver's original gross anatomy and architecture. It is now well accepted that there are two physiological forms of regeneration in the liver in response to different types of

liver injury. In the case of PH and some chemical liver injuries, the liver mass is replaced by replication of existing hepatocytes without activation of progenitor cells. This is considered the quickest and most efficient way to generate hepatocytes for liver regeneration and repair. In other cases of chemical liver injury, when mature hepatocytes are prevented from proliferating, activation and replication of progenitor cells take place (Fausto, 2004; Riehle et al., 2011; Mao et al., 2014).

Mainly three clusters of networks mediate liver regeneration after PH: cytokines, growth factor-mediated pathways and metabolic signals. Given the high redundancy existing among the intracellular components of each network, the loss of an individual gene rarely leads to complete inhibition but only delay of liver regeneration (Riehle et al., 2011; Mao et al., 2014; Vacca et al., 2013). In their quiescent state, hepatocytes do not fully respond to growth factors and need to be "primed" to enter the cell cycle and respond to growth factors. The **cytokine network** acts as the priming phase of liver regeneration. In brief, there is an initial activation of nuclear factor–kappa B (NF-κB) by tumour necrosis factor (TNF) in Kupffer cells with downstream secretion of interleukin-6 (IL-6), which leads to activation of the transcription factor signal transducer and activator of transcription 3 (STAT3) in hepatocytes, among other pathways. After cytokines have triggered the $G_0$ to $G_1$ transition, cell cycle progression is driven by **growth factors**, which override the $G_1$ restriction point, allowing hepatocytes to pass into the S phase. This passage is associated with retinoblastoma (Rb) phosphorylation, and increased expression of the Rb family member p107 and of Cyclins D, E and A. Hepatocyte growth factor (HGF), produced by HSC, and the ligands of the epidermal growth factor receptor (EGFR), produced by hepatocytes, including transforming growth factor alpha (TGF-α), amphiregulin and heparin binding EGF-like growth factor (HB-EGF) drive cell cycle progression during liver regeneration. Ligands of EGFR have different but often overlapping functions. Both c-met (HGF receptor) and EGFR are receptor tyrosine kinases, which recruit enzymes and scaffolding proteins to phosphorylate intracellular domains of each receptor, thus activating multiple intracellular signalling pathways, which in turn regulate a multitude of transcription factors, initiate translation and regulate metabolic pathways. Together with the induction of intermediate and early-delayed genes such as cyclins and cyclin-dependent kinases, it facilitates the transition to DNA synthesis and mitosis (Rozga, 2002; Costa et al., 2003; Fausto et al., 2006; Riehle et al., 2011; Mao et al., 2014). Indeed, the hepatocyte proliferative response during liver regeneration is coincident with a potent activation of immediate early transcription factors including c-Jun, c-Fos, c-Myc, NF-κB, STAT3 and C/EBPβ proteins (Costa et al., 2003).

After PH, the **metabolic demands** of the liver during regeneration are immense. The liver must continue to regulate systemic energy levels while meeting its own demands for significant nucleotide and protein synthesis needed for cell division. Translation is the control point that integrates nutrient levels with mitogenic signals and most proteins involved are downstream of mammalian target of rapamycin (mTOR). Therefore, the mTOR complex may

regulate regeneration by modulating cell size and proliferation based on energy demands (Fausto et al., 2006; Riehle et al., 2011; Mao et al., 2014).

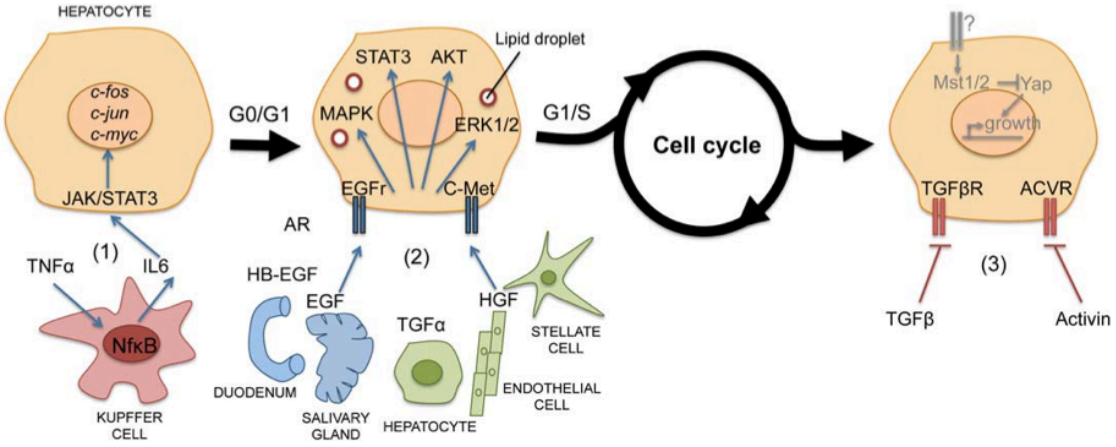


**Figure II.** Main steps of liver regeneration after partial hepatectomy. 1) "Priming" phase. 2) Metabolic and growth factors phase. 3) Termination phase. (Gilgenkrantz and Collin de l'Hortet, 2011).

The initial burst of hepatocyte proliferative activity is followed by secondary waves of mitosis until the original mass of the liver is restored. However, the precise mechanisms leading to the proper termination remain poorly understood. It is known that involves multiple factors, including the transforming growth factor beta (TGF-β) family (Rozga, 2002; Michalopoulos, 2010; Mao et al., 2014).

# 2. Liver disorders

The liver is unique in its response to injury, demonstrating an extraordinary capacity of compensatory growth in response to conditions that induce cell loss by physical, infectious, or toxic injury, simultaneously undergoing regeneration and fibrosis (Rozga, 2002; Zhang and Friedman, 2012).

Liver injuries can be divided into two different groups accordingly to the duration or persistence of liver injury: **acute and chronic liver diseases**. The elimination of the damaging agent can rapidly revert acute liver injuries and usually there is a complete restoration of normal liver architecture and function, without evidence of the preceding insult. However, when the liver injury persists for a long time it drives to a chronic liver disease. Progressive fibrosis is the hallmark of chronic liver injury and it can eventually result in cirrhosis, liver failure or hepatocellular carcinoma (HCC) (Malhi and Gores, 2008).

Briefly, the main liver disorders that affect population these days are acute liver injuries (mainly due to toxic insults), cholestatic liver injuries, chronic viral hepatitis, alcoholic and non-alcoholic steatohepatitis, fibrosis and liver cancer (Malhi and Gores, 2008).

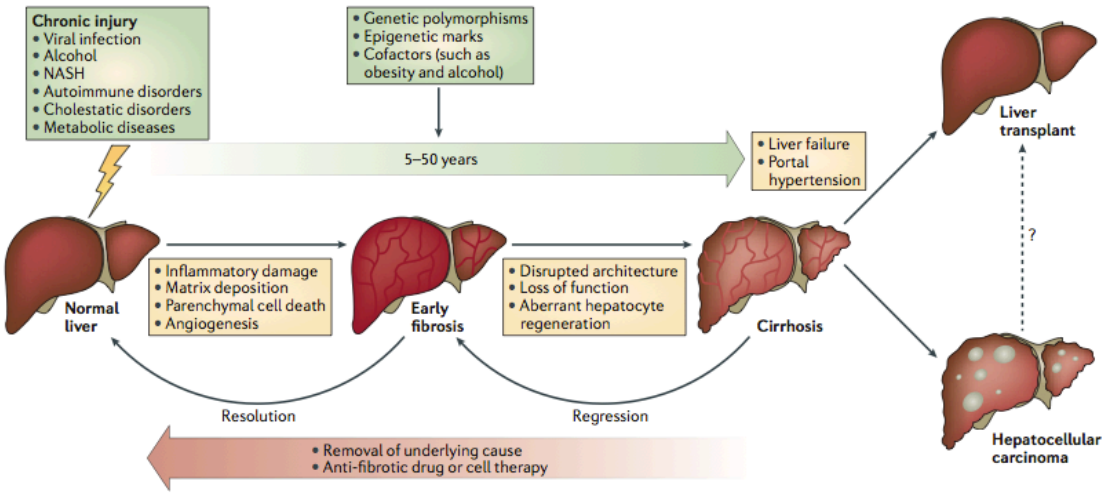


**Figure III.** Natural history of liver disease (Pellicoro et al., 2014).

# 2.1. Liver fibrosis

In all organ systems, the normal mammalian response to injury occurs in three overlapping but distinct stages: inflammation, new tissue formation, and tissue remodelling. A critical step is when repair and regeneration takes place, because excessive deposition of ECM leads to hypertrophic scars, which results in tissue dysfunction (Xue et al., 2013).

## 2.1.1. Epidemiology, aetiology and mechanisms

Liver fibrosis is a common pathological consequence of chronic liver diseases and results from the **progressive accumulation** of a qualitatively altered ECM, that is highly enriched in type I and III fibrillar collagens. Scar deposition results from an altered wound healing response to prolonged parenchymal cell injury and/or inflammation. It is characterized by increased production of matrix proteins and decreased matrix remodelling. In advanced stages, fibrosis leads to cirrhosis, a condition defined by an abnormal liver architecture, with fibrotic septa surrounding regenerating nodules and altered vascularization. Clinical consequences of cirrhosis are liver synthetic failure, portal hypertension, high susceptibility to infection and high risk to develop HCC, thus requiring for a systematic screening for HCC (Mallat and Lotersztajn, 2013; Schuppan and Kim, 2013).

Recent reports from the Global Health Organization indicate that cirrhosis is an increasing cause of morbidity and mortality in more developed countries. It is the 14$^{th}$ most common cause of death in adults worldwide but the 4$^{th}$ in central Europe. It accounts for 170,000 deaths in Europe per year, which is 1.8% of all deaths (Mallat and Lotersztajn, 2013; Tsochatzis et al., 2014). Predominant **causes** of liver fibrosis and cirrhosis in more developed countries are infection with hepatitis C virus (HCV), alcohol misuse, and increasingly, non-alcoholic liver disease. Infection with hepatitis B virus (HBV) is the main cause in sub-Saharan Africa and most parts of Asia (Tsochatzis et al., 2014).

**Mechanisms** that underlie liver fibrogenesis show striking similarities with fibrotic processes that occur with chronic injury in other tissues, including skin, lung, and kidney. However, several clinical reports have documented that regression of liver fibrosis occurs in a substantial proportion of patients, provided that the factor responsible for liver insult is eradicated or controlled (Zeisberg and Kalluri, 2013; Mallat and Lotersztajn, 2013).

The principal source of ECM accumulation and prominent mediators of fibrogenesis are “activated fibroblasts” or MFB. There are different origins of activated fibroblasts: resident fibroblasts, bone marrow-derived fibrocytes, epithelial cells that undergo epithelial-to-mesenchymal transition (EMT), vascular smooth muscle cells and pericytes. Recent knowledge indicates that most fibrogenic MFB are endogenous to the liver, and **activated HSC and fibroblasts** are the major endogenous fibrogenic cells. In liver fibrosis, HSC are considered to

be a major source of fibrogenic cells, while portal fibroblasts play an important role in the fibrogenic process during cholestatic liver diseases (Iwaisako et al., 2014). In the normal liver, HSC are located in the space of Disse and display a quiescent phenotype characterized by the expression of a large number of adipogenic genes and neural markers. Upon acute or chronic liver injury, a complex network of autocrine/paracrine fibrogenic signals promotes the activation, usually called **transdifferentiation**, of quiescent HSC to a myofibroblastic phenotype. This fibrogenic inputs include cytokines, chemokines, growth factors, lipid mediators and reactive oxygen species (ROS) that are produced by epithelial cells (hepatocytes and cholangiocytes), endothelial cells and cells of the immune system (macrophages, dendritic cells, and B and T lymphocytes). Moreover, apoptotic bodies derived from damaged hepatocytes can also transdifferentiate HSC to MFB favouring the fibrogenic process (Mallat and Lotersztajn, 2013; Czaja, 2014). A number of growth factors are associated with MFB differentiation, including Platelet-Derived Growth Factor (PDGF), angiotensin II, Connective Tissue Growth Factor (CTGF), and TGF-β. TGF-β has a pivotal role in fibrogenesis, and some of the other growth factors involved exert their effects by directly stimulating TGF-β production (Barnes and Gorin, 2011).

**MFB** are characterized by the expression of α-smooth muscle actin and a parallel loss of retinoids an lipid droplets, and *de novo* expression of receptors for fibrogenic, chemotactic and mitogenic factors, that leads to increased proliferation and survival, secretion of proinflammatory cytokines and chemokines, enhanced synthesis of matrix proteins, predominantly fibrillar collagens, and inhibitors of matrix degradation, thus provoking the progressive scar formation (Zeisberg and Kalluri, 2013; Mallat and Lotersztajn, 2013).

**Inflammation** plays an essential role in the development of liver fibrosis. When a chronic injury takes place, a large infiltration of mononuclear cells, which include macrophages, lymphocytes, eosinophils, and plasma cells, occur. Mobilization of lymphocytes produces lymphokines that activate macrophages, which, in turn, stimulate lymphocytes, fibroblasts, and other inflammatory cells, thus setting the stage for persistence of an inflammatory response (Wynn and Barron, 2010). Furthermore, macrophages produce pro-fibrotic mediators, including TGF-β and PDGF, and control extracellular matrix turnover by regulating the balance of various matrix metalloproteases and tissue inhibitors of metalloproteases. Examples of knock-out mice that are resistant to fibrosis because they have less inflammation include those with gene deletions of TNF-α or Toll-like receptor 4 (TLR4), among others (Kitamura et al., 2002; Seki et al., 2007). The relevance of TGF-β pathway during liver fibrosis will be further discussed in a following section (**Section 3.1**).

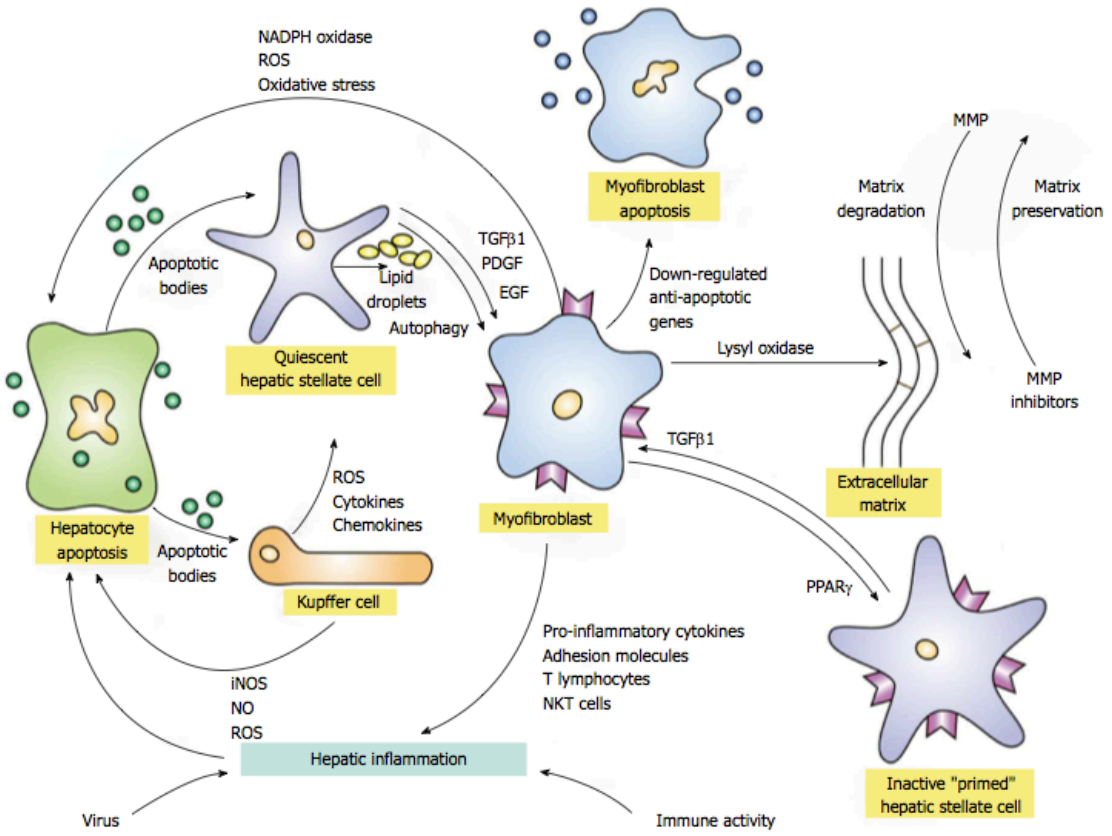


**Figure IV.** Events and signalling pathways involved in liver fibrosis (Czaja, 2014).

Finally, **ROS**, including $H_2O_2$, $OH^{\cdot}$ and $O_2^{-}$, are critical intermediates in both the normal physiology and pathological conditions of liver cells. Indeed, chronic oxidative stress plays a role during both the initial inflammatory phase and its progression to fibrosis. Oxidative stress markers have been detected in the serum and biopsy samples from liver cirrhosis patients and in experimental liver fibrosis/cirrhosis animals (Yadav et al., 2002; Pawlak et al., 2008). Moreover, in liver biopsies, areas of fibrosis were localized to areas with increased 4-hydroxi-2'-nonenal (4-HNE), a marker of lipid peroxidation (MacDonald et al., 2001; Seki et al., 2005). ROS may be generated in the liver by multiple sources, including the mitochondrial respiratory chain, cytochrome p450 family members, peroxisomes, xanthine oxidase, and nicotinamide adenine dinucleotide phosphate (NADPH) oxidases. Accumulating evidence indicates that NADPH oxidases (NOX)-mediated ROS has a critical role in HSC activation and hepatic fibrogenesis (Paik et al., 2013). Sources of ROS and their role during fibrogenesis will be deeply addressed in a future section (**Section 4.6**).

### 2.1.2. Animal models

During the last years, several mouse models have been used for the study of the pathogenesis and molecular mechanisms associated with fibrosis. Among them, chemically induced fibrosis with hepatotoxic agents, being $CCl_4$ the most commonly used, has been extensively studied. These agents cause massive hepatocyte cell death provoking centrilobular parenchymal injury and fibrosis. In addition, Concanavalin A is commonly used to induce immune-mediated liver fibrosis, resembling human chronic hepatitis. Finally, bile duct ligation constitutes a very used model for biliary fibrosis and cirrhosis, since it triggers extrahepatic biliary atresia and primary sclerosing cholangitis. Importantly, during the last decade knock-out mice have become a powerful strategy to study the molecular mechanisms of fibrosis, focusing on the contribution of one or more genes to the pathogenesis of the disease (Hayashi and Sakai, 2011). These knock-out mice, in addition, have helped to establish new genetic models of liver fibrosis such as the Multi drug resistance 2 knock-out ($Mdr2^{-/-}$) mouse, which develops spontaneous sclerosing cholangitis (Fickert et al., 2004).

### 2.1.3. Therapeutic approaches

Regression of fibrosis can be achieved by the successful control of chronic liver injury, owing to termination of the fibrogenic reaction following clearance of hepatic MFB and restoration of fibrolytic pathways. MFB can be eliminated by apoptosis, senescence or reversion to a quiescent (HSC) phenotype. However, inactivated HSC remain primed for re-transdifferentiation, and may be more responsive to recurrent fibrogenic stimuli than its original quiescent state. In advanced stages of fibrosis and cirrhosis the potential for reversibility declines (Mallat and Lotersztajn, 2013; Czaja, 2014).

The first line treatment is, when possible, to counteract the underlying liver disease to stop fibrosis progression. For instance, patients with viral hepatitis should be treated with anti-viral therapies while corticosteroids are useful for autoimmune hepatitis. Recent clinical trials with efficient causal therapy have demonstrated reversibility of advanced liver fibrosis. Treatments focused on the **elimination of the etiological agent** or putative immune-mediated mechanism may be supplemented with antifibrotic agents. Despite experimental characterization of an array of antifibrotic pharmacological targets, there is still no clinical translation. This might be due to multiple causes: liver fibrosis usually progresses slowly in humans, therefore requiring long clinical trials; no non-invasive specific and sensitive markers of fibrosis progression/regression are available; and fibrogenic and fibrolytic pathways are complex, therefore targeting a single pathway may be of limited efficacy. MFB and their products are primary targets for antifibrotic therapies, which in principle would address all types of fibrosis, including advanced fibrosis. Nevertheless, additional cellular elements that are either upstream of MFB or tightly linked to fibrogenic activation may provide a basis for complementary and more disease-specific antifibrotic approaches. A **combined therapy** may

be a more effective approach, given the crosstalk between different cell types that generally underlies the fibrogenic activation (Schuppan and Kim, 2013; Mallat and Lotersztajn, 2013; Czaja, 2014; Tsochatzis et al., 2014).

# 2.2. Hepatocellular carcinoma

## 2.2.1. Epidemiology, risk factors and prevention

**Hepatocellular carcinoma** (HCC) is a major public health problem worldwide with over 700,000 new cases each year and its incidence is increasing in Europe and worldwide. HCC is the sixth most prevalent cancer and the third most frequent cause of cancer-related death, following lung and stomach cancers. HCC represents more than 90% of primary liver cancers. Intriguingly, there are important differences on the incidence when considering the gender, being the male to female ratio estimated to be 2.4. This difference is mainly attributed to the different exposition to risk factors, as well as the influence of androgens and estrogens on HCC progression. Exposition to risk factors also determine the incidence of liver cancer regarding age or ethnicity (European Association For The Study Of The Liver and European Organisation For Research And Treatment Of Cancer, 2012; Bruix et al., 2014; Tabrizian et al., 2014).

In most cases, HCC develops within an **established background** of chronic liver disease, being HBV chronic infection the dominant risk factor in eastern Asia and sub-Saharan Africa, together with exposure to aflatoxin B1. HCV chronic infections together with alcohol are the main risk factors in North America, Europe and Japan. Non-alcoholic fatty liver disease (NAFLD) and non-alcoholic steatohepatitis (NASH) are other clear risk factors for HCC development. Progressive hepatic fibrosis, which is a common pathway for all forms of chronic liver disease, evolves to cirrhosis, which is the largest risk factor for developing liver cancer. Up to 90% of cases of HCC arise in the setting of advanced fibrosis or cirrhosis regardless of aetiology (Wallace and Friedman, 2014; Bruix et al., 2014).

Since HCC develops within an established chronic liver disease, avoiding the exposure to risk factors for these chronic liver diseases is the best option to prevent HCC. HBV infection accounts for more than 50% of all HCC cases. Thus, HCC related to HBV can be prevented by vaccination. When there is already a HBV chronic infection, viral replication can be controlled by means of antiviral drugs, which would prevent progression of liver disease and, perhaps, HCC in the long term. The same strategy can be applied to HCV chronic infection to prevent development of HCC. However, if cirrhosis is already established, risk of HCC is not modified despite antiviral treatment. In the case of HCV, 3-5% of the cases of established cirrhosis evolve to HCC. HCV infection prevention relies on avoidance of viral transmission through contaminated blood. Alcohol consumption constitutes also an important risk factor for HCC and it provokes a synergistic effect when there is an infection with HBV, HCV or both. Individuals co-infected with HIV also have an increased risk of HCC development (Forner et al., 2012).

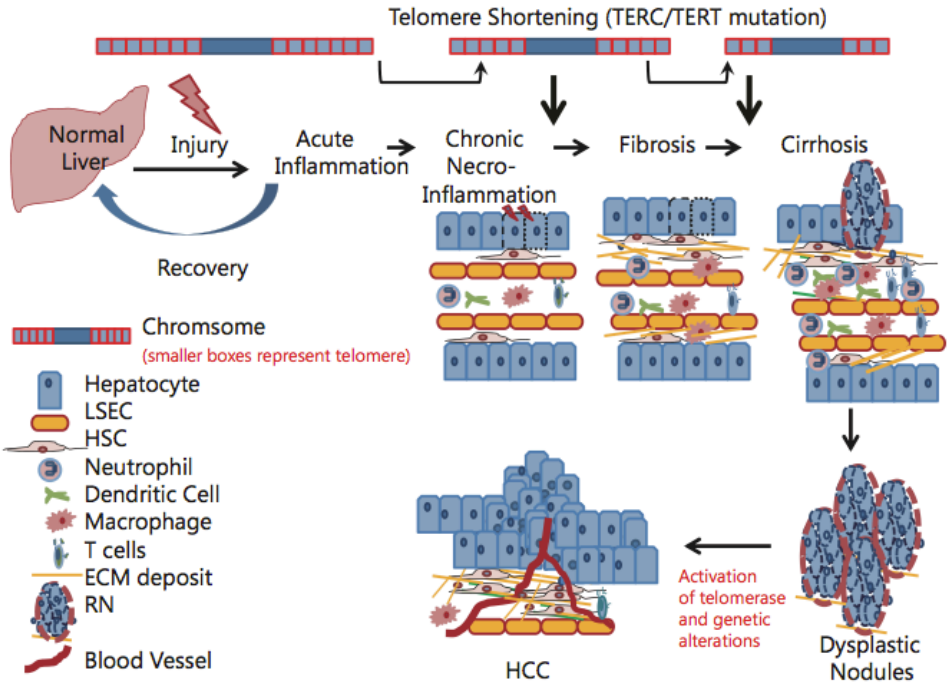


**Figure V.** Diagrammatic representation of various pathological changes that eventually lead to HCC development (Ramakrishna et al., 2013).

## 2.2.2. Animal models

Liver carcinogenesis is a **multi-step process** with several cellular and mechanical dysregulations that eventually lead to malignant transformation of hepatocytes. There are numerous mouse models that successfully produce HCC and are used to try to elucidate mechanisms governing tumour development, at the same time that can be used to test new drugs designed for the treatment of HCC patients. Murine HCC models can be divided into four main categories: chemically induced HCC, oncogene driven HCC, xenograft models and genetically modified mice (GMM) (Hernandez-Gea et al., 2013).

**Chemically induced models**, especially Diethylnitrosamine (DEN) model, are among the most common used in HCC research. DEN belongs to the category of genotoxic chemical carcinogens, as its carcinogenic capacity is due to its capability of alkylating DNA structures. DEN works in a dose dependent manner and the time needed for HCC development also depends on sex, age and strain of mice. The liver lesions appear sequentially, starting with adenomas and the later development of hyperplastic nodules. When associated with $CCl_4$, DEN model mimics the sequence of injury-fibrosis-malignant transformation that usually occurs in humans. Other chemicals used to induce HCC development are Aflatoxin $B_1$, Thioacetamide (TAA) and a choline deficient diet (CDD) (Heindryckx et al., 2009; Fausto and Campbell, 2010; Hernandez-Gea et al., 2013).

Another model of HCC development is by means of conditional **overexpression** of the **oncogenic protein** Myc, in which the expression of human Myc is regulated in murine liver (Hernandez-Gea et al., 2013).

In **xenograft models**, tumours are generated by injecting human cancer cells into immune deficient mice. The tumour xenograft can be established by the implantation of biopsy material or human tumour cell lines either subcutaneous in the flank of the mice (ectopic model) or directly to the liver (orthotopic model). Subcutaneous model enables to follow the appearance and increase of the tumour mass easily while implantation in the liver better replicates the tumour environment.

Finally, **GMM** are engineered to mimic pathophysiological and molecular features of HCC. The most common ones can be divided in two groups, transgenic mice, which carry the overexpression of a specific gene, and knock-out mice, in which a gene was deleted. There are many GMM models, such as overexpressing TGF-$\alpha$, Myc, $\beta$-catenin and HRAS, or PTEN knock-out mice, among others (Sánchez and Fabregat, 2009; Heindryckx et al., 2009; Hernandez-Gea et al., 2013).

### 2.2.3. Molecular mechanisms of HCC: Relevance of proliferation related pathways

Hepatocarcinogenesis is a complex multistep process in which many signalling cascades are altered, leading to a heterogeneous molecular profile. HCC **genetic heterogeneity** is absolutely impressive; there exist differences between patients, between nodules in the same patient and even within a single tumour nodule. However, some molecular pathways are known to be clearly involved in HCC.

There have been described several **mutations** in HCC, the main ones include the tumour suppressor gene *TP53* (in about 25-40% of cancers, depending on tumour stage), and *CTNNB1*, the gene encoding for $\beta$-catenin (in about 25% of HCC, predominantly in HCV-related cases) (Bruix et al., 2014; Llovet, 2014). Recently, mutations in the promoter of the telomerase reverse-transcriptase (TERT) gene have emerged as the most prevalent somatic mutation affecting 60% of HCC cases (Nault et al., 2013). Also chromosomal amplifications, such as 11q13 (Cyclin D1 and FGF19), and deletions are common and affect important oncogenes and tumour suppressors (Sawey et al., 2011). Silencing of tumour suppressors and reactivation of oncogenes by epigenetic alterations have been also described. Finally, transcription of key oncogenes can be also modulated by miRNAs (Toffanin et al., 2011). As a result of all these alterations, several signalling cascades related to cell survival and proliferation, angiogenesis, invasion and metastasis are dysregulated (Wang et al., 2013).

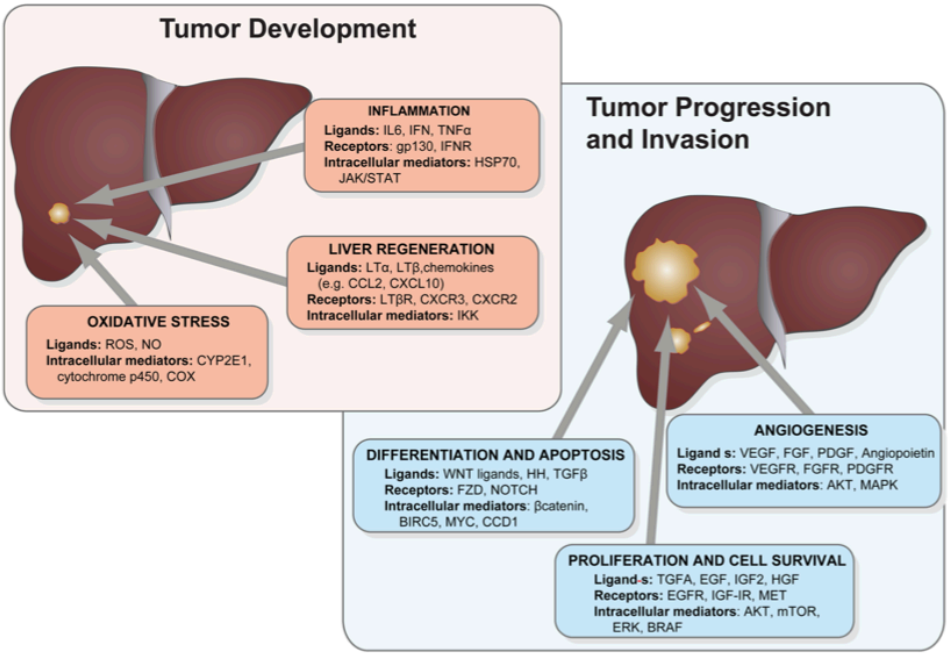


**Figure VI.** Signalling pathways frequently dysregulated in HCC (Zender et al., 2010).

As it happens in most of the cancers, altered **proliferation pathways** have been correlated with liver cancer. Among these alterations, the most frequently reported pathways involve growth factors such as epidermal growth factor (EGF), insulin-like growth factor (IGF) and hepatocyte growth factor (HGF).

EGFR pathway is overactivated in many patients with HCC. It has been reported that this altered signalling can be due to overexpression at mRNA and protein level, reduced turnover of the receptor, DNA copy gain in chromosome 7, where there is the locus of EGFR, and/or modifications in EGFR ligands levels. Our group have demonstrated that increased EGFR signalling not only increases the growth capacity of HCC cells but also confers them resistance to apoptosis (Caja et al., 2011a). Additionally, activation of EGFR stimulates several proteins such as focal adhesion kinase (FAK), caveolin, E-cadherin and β-catenin, which play roles in migration and cytoskeletal reorganization (Nalesnik and Michalopoulos, 2012).

The HGF/Met axis is known to be involved in cell proliferation and metastasis. As mentioned in a previous section (**Section 1.2**), it has a prominent role in liver regeneration. Met activation has been found in 20-40% of HCC, mainly through both the receptor and its ligand (Sia and Villanueva, 2011).

IGF signalling is important for the regulation of growth and development, and it has been shown to be involved in the pathogenesis of several malignancies, including HCC. Allelic lose of the IGFR2 and overexpression of the IGF2 ligand are the most common alterations described in liver cancer (Tovar et al., 2010; Moeini et al., 2012).

Upon EGFR, Met and IGFR activation, extracellular signals can be transduced through different cytoplasmatic intermediates, such as PI3K/AKT/mTOR or RAS/MAPK pathways. The RAS/Raf/MAPK pathway is typically activated in HCC as a result of increased signalling from upstream growth factors, and not due to RAS mutations, as it usually happens in other solid tumours. The PI3K/AKT/mTOR signalling, which controls proliferation, cell cycle and apoptosis, is activated in 30-50% of HCC (Gedaly et al., 2012). AKT can be activated through a tyrosine kinase receptor or through constitutive activation of PI3K or loss of function of the tumour suppressor gene PTEN by epigenetic silencing or somatic mutations (Llovet and Bruix, 2008).

Of special relevance for this work is the control of **cell cycle** by these altered pathways. Cell cycle consists in four phases, the gap 1 ($G_1$) phase, the DNA synthesis (S) phase, the gap 2 ($G_2$) phase and the mitosis (M) phase. The progression of the cell cycle is tightly regulated by cyclins and cyclin dependent kinases (CDKs), whose production and activity is affected by a wide variety of external factors, such as growth factors and hormones that specifically activate or inhibit various signalling pathways that ultimately result in cell cycle progression, cell cycle arrest, differentiation or apoptosis. During each of the phases, a specific cyclin forms a complex with a specific CDK. For instance, Cyclin D forms a complex with CDK4 or CDK6 at the beginning of $G_1$ phase, allowing the activation of CDK4/6. This complex then phosphorylates the retinoblastoma protein (Rb), leading to E2F transcription and subsequent transcription of genes required for cell cycle progression, such as Cyclin E and A. CDKs belong to the family of serine/threonine kinases and its activation consists of several steps of reversible phosphorylation. The cell cycle can be regulated by adjusting the expression of cyclins and CDKs but can also be influenced by modulating CDK activity by kinases and phosphatases such as cdc25. Nevertheless, CDK activity can also be modulated by CDK-inhibitors (CKIs). The CKI family consists of two subfamilies: the inhibitor of CDKs (INK4) family and the CDK-interacting protein (CIP) family. The INK4 family consists of four proteins which inhibit Cyclin D binding to CDK4 and CDK6: $p15^{INK4B}$, $p16^{INK4A}$, $p18^{INK4C}$ and $p19^{INK4D}$. And the CIP family inhibits all cyclin-bound CDKs and consists of three proteins: $p21^{Cip1}$, $p27^{Kip}$ and $p57^{Kip2}$ (Verbon et al., 2012). Cell cycle dysregulation in HCC can be provoked not only as a consequence of the growth factor overactivated signalling pathways but also of direct alteration of cyclins, CDKs and/or their regulators (Che et al., 2012; Ao et al., 2014).

Besides growth factor related pathways, some data indicate aberrant activation of pathways involved in **cell differentiation and development**, such as Wnt signalling. As mentioned before, many studies show mutations in the gene encoding for β-catenin (Villanueva et al., 2007). In addition, Wnt pathway overactivation might be as a consequence of overexpression of Frizzled receptors, or inactivation of E-cadherin or members of the degradation complex (GSK3β, AXIN and adenomatosis polyposis coli (APC)). Other pathways related to cell differentiation such as Hedgehog and Notch are also described to be overactivated in HCC (Sia and Villanueva, 2011).

The **microenvironment**, combined with concurrent tissue responses including angiogenesis, chronic inflammation and oxidative stress, are also critical in the tumour biology. Important proliferative, angiogenic, and regenerative cytokines secreted by HSC contribute to a carcinogenic milieu. These include transforming growth factors (TGF-α and TGF-β), platelet-derived growth factors (PDGF-B and PDGF-C), HGF, vascular endothelial growth factor (VEGF) and IL-6 (Rani et al., 2014).

HCC is a highly vascularised cancer and **neovascularization** is a key event from early stages. Indeed, experimental studies suggest that targeting angiogenesis is of major relevance in HCC. The angiogenic process in HCC is complex and tightly regulated, resulting from the balance between multiple angiogenic and anti-angiogenic factors from the tumour and the host cells. VEGF, angiopoietin-2, PDGF and FGF are considered the key drivers of angiogenesis in HCC. Actually, VEGF and angiopoietin-2 plasma levels have been identified as independent prognostic biomarkers in patients with advanced HCC (Forner et al., 2012; Hernandez-Gea et al., 2013).

Solid evidences support the casual connection between **chronic inflammation** and cancer. Despite the fact that the majority of the cases of HCC occur in a background of chronic inflammation, there still exist big gaps in the understanding of the molecular link between inflammation and HCC. It is suggested that chronic inflammation drives a maladaptive reparative reaction and stimulates liver cell death and regeneration, eventually associated with the development of dysplastic nodules and cancer. Some studies support the role of NF-κB, hypoxia inducible factor 1α (HIF1α) and STAT3 as the major molecular players linking inflammation and cancer. Among all the inflammatory cytokines involved, IL-6, which in turn activates JAK-STAT and MAPK pathways, is thought to be the most abundant. Additionally, several growth factors such as HGF, EGF and TGF-β, are known to regulate the immune and inflammatory response in HCC microenvironment (Capece et al., 2013; Ramakrishna et al., 2013). Considering the relevance of TGF-β pathway in this work, it will be further discussed in a separate section (**Section 3**).

Additionally, several alterations in the **ECM** occurring during progressive fibrosis/cirrhosis predispose to the development of HCC. Accumulation of collagenous and non-collagenous ECM is controlled in part by matrix metalloproteinases (MMP), which degrade substrates, and tissue inhibitors of metalloproteinases (TIMP), which inhibit MMP. Enhanced collagen deposition increases the stiffness of the ECM, which in turn promotes on going HSC activation, and thus, more collagen deposition in a positive feedback loop. HSC are the major source of MMP and TIMP, and their activity is controlled by cytokines. MMP and TIMP are important in progression of hepatocytes from dysplasia to the development of poorly differentiated HCC (Wallace and Friedman, 2014). Moreover, increased matrix stiffness in chronic injured liver favours the growth of HCC cells (Schrader et al., 2011). Many cell-to-matrix interactions are transmitted via transmembrane adhesion molecules, in particular integrins, that bind growth factors and components of the ECM. Integrin expression patterns are altered in

human HCC, potentially mediated by selective pressure from both tumoral and peritumoral stromal cells, and promote established HCC by their actions on cell proliferation, adhesion, invasion, migration and apoptosis, favouring the progression of HCC and metastasis (Wu et al., 2011). Being the metastasis an important process for this work, it will be further analysed in a separate section (**Section 5**).

Finally, during last years it has become evident that **oxidative stress** is playing a relevant role in liver carcinogenesis. For example, overproduction of ROS provokes nitrosative and oxidative stress through interaction with DNA, RNA, lipid and proteins, leading to an increase in mutations, genomic instability, epigenetic changes and protein dysfunction (Hernandez-Gea et al., 2013). However, lower concentrations of ROS can also perturb cell and tissue function by more subtle, often transient and reversible mechanisms, which lead to signal transduction (Choi et al., 2014). Due to the relevance in this work, oxidative stress and ROS will be deeply discussed in a separate section (**Section 4**).

### 2.2.4. HCC and metastasis

HCC is one of the most aggressive human malignancies, with high rate of recurrence that can be divided in intrahepatic and extrahepatic patterns. **Intrahepatic recurrences** can be as a result of multicentric occurrence or intrahepatic metastasis of HCC (Utsunomiya et al., 2010). On the other side, **extrahepatic metastasis** can occur by direct extension, hematogenous spread or lymphatic invasion. Reported HCC metastatic sides include lungs, lymph nodes, bone, peritoneu and/or omentum and brain. Other rare sides of metastasis have also been described (Becker et al., 2014).

### 2.2.5. Diagnosis and management of HCC

HCC is the main cause of death in patients with cirrhosis, and long-term disease-free survival will rely on its early detection and treatment. Patients with high risk of HCC development undergo surveillance through periodic hepatic ultrasonography (US) and AFP blood test. Other serum markers such as descarboxiprothrombin (DCP), also known as Prothrombin Induced by Vitamin K Absence II (PIVKA-II), are currently under study to complement US and AFP (Flores and Marrero, 2014).

**Imaging** has a central role in the diagnosis of HCC, together with a **biopsy** of the lesion. Some biomarkers are currently used for staining of tissue samples when diagnose of HCC is not clear. They include CD34, CK7, glypican 3, HSP-70 and glutamine synthetase. CK19 and EpCAM are recommended stainings for detection of progenitor cell features (Flores and Marrero, 2014).

As in many cancers, assessment of **prognosis** is a crucial step in management of patients with HCC. Prognosis should be assessed accordingly to tumour stage, degree of liver dysfunction and presence of cancer-related symptoms. Among the many HCC staging systems that have been developed around the world, there is a classification widely adopted that stratifies HCC patients according to outcome and simultaneously links it with treatment investigation. This classification is called Barcelona Clinic Liver Cancer (**BCLC**) strategy and it establishes treatment recommendations for all stages of HCC, depending on overall size of the tumour, number and size of the nodules, liver physical and functional status and cancer-related symptoms. BCLC identifies patients with early HCC who are potentially curable, those at intermediate or advanced disease stage for whom non-curative treatment offers the likelihood of extended survival, and those at end stage for whom treatment would provide more harm than benefit (Forner et al., 2012; Bruix et al., 2014). Biomarkers such as AFP, VEGF, angiopoietin-2 or c-kit should enable better stratification. However, they are still not considered for treatment decisions (Bruix et al., 2014).

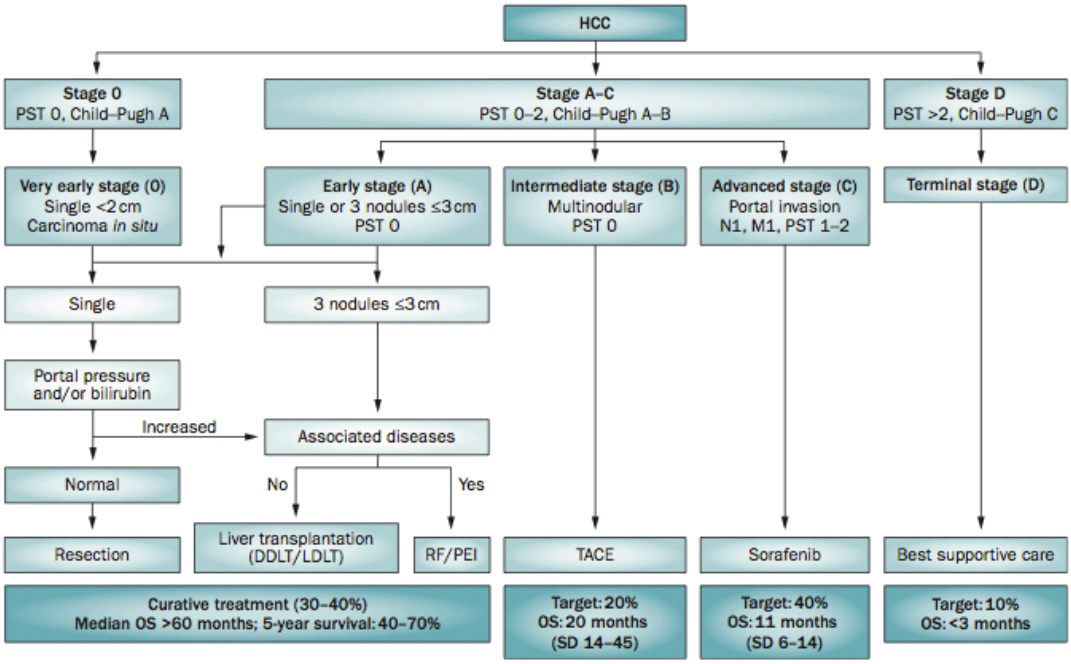


**Figure VII.** BCLC staging system and therapeutic strategy (Villanueva et al., 2013).

Prior to 2007, there was no single systemic therapy with proven efficacy in advanced HCC. This might be due to the high molecular heterogeneity and resistance to conventional chemotherapy. In that year, **sorafenib**, an oral tyrosine kinase inhibitor with a broad inhibitory profile (for example BRAF, PDGFR and VEGFR), showed a substantially increase in survival in patients with advanced HCC (stage C of the BCLC classification). It was demonstrated by the SHARP (Sorafenib Hepatocellular Carcinoma Assessment Randomized Protocol) trial that the

overall survival was 10.7 months in the sorafenib group while it was 7.9 months in the placebo group. The magnitude of the effect of sorafenib was further confirmed in a randomized clinical trial in Asia. Currently, sorafenib is the only treatment approved for patients at advanced stages of HCC, and there is an urgent need to identify biomarkers to accurately predict patient's response to the drug (Forner et al., 2012; Villanueva et al., 2013; Tabrizian et al., 2014). In this sense, a recent work from our group demonstrated that CD44 could play an important role in protecting HCC cells from sorafenib-induced apoptosis in a TGF-β-induced mesenchymal background (Fernando et al., 2014).

Encouraged by the success of sorafenib, a number of other studies are on going using other targeted agents alone or in combination with sorafenib. So far, phase 3 trials testing sunitinib (another oral multikinase inhibitor for receptor tyrosine kinases), everolimus (a mTOR kinase inhibitor), linifanib, brivanib (two anti-angiogenic therapies), or the combination of sorafenib with erlotinib (an EGFR inhibitor) have been negative, as well as all agents tested in second line (Bruix et al., 2014; Flores and Marrero, 2014). The most feasible cause of these failures is the suboptimal understanding of oncogenic drivers and molecular subclasses in HCC, together with the common cirrhotic background of HCC patients, that might facilitate drug liver toxicity, impairing to meet the end points of the clinical trials. To try to improve the results from trials, it appears reasonable that the strategy design should be modified. A possible solution would be to incorporate molecular information of the mechanisms responsible for tumour progression in each patient, to design trials with enriched populations based on pathway activation, instead of including "all comers", in order to maximize the chances of positive clinical outcome benefits. As mentioned before, several critical pathways are known to be activated in subsets of patients with HCC, such as Wnt, JAK-STAT, TGF-β, mTOR, MET, IGF and Notch signalling, among others (Villanueva et al., 2013; Llovet, 2014).

# 3. Transforming growth factor-beta (TGF-β)

Alterations of the transforming growth factor-β (TGF-β) signalling pathway are involved in human diseases including cardiovascular, fibrosis, reproductive, wound healing and immune disorders, and also in cancer. With respect to human malignancies, TGF-β typically exerts tumour-suppressing activities in normal cells, as well as in early-stage carcinomas through its ability to induce cell cycle arrest and apoptotic reactions. However, as carcinomas continue to evolve and ultimately acquire metastatic phenotypes, the tumour suppressing functions of TGF-β are circumvented such that TGF-β is utilized as an oncogenic factor that promotes carcinoma growth, invasion, and metastasis. **Our group** has been focused on the study of the role of TGF-β in the liver. More precisely, we have been studying the relevance of this signalling pathway on cell death, proliferation, differentiation and migration in liver physiology and pathology, analysing its role in liver fibrosis and hepatocarcinogenesis.

## 3.1. TGF-β in the progression of liver disease

Chronic liver diseases (CLD) are leading causes of morbidity and mortality worldwide. In CLD, hepatocyte damage, wound healing and tissue remodelling go awry, resulting in fibrosis and ultimately cirrhosis, the platform on which HCC develops. At the cellular and molecular level, the multistep process of progressive CLD is reflected in the complex modulation of intracellular signal transduction, altered cell-cell communications and, more drastically, an altered differentiation state of most liver resident cell types. It is well-known that TGF-β plays a pivotal role in the sequence of events leading to end-stage CLD (Dooley and ten Dijke, 2012).

### 3.1.1. Role of TGF-β in liver fibrosis

In the normal liver, sinusoidal endothelial cells and Kupffer cells (macrophages) contain relatively high levels of TGF-β mRNA, whereas HSC express little amounts of the cytokine. However, in response to pro-fibrogenic stimuli HSC express the three different isoforms of TGF-β and contribute to the development of fibrosis through both autocrine and paracrine loops of TGF-β-stimulated **collagen production** (Inagaki et al., 2005). As we explained in a previous section (**Section 2.1**), MFB are the main cell responsible for fibrosis and the major source of MFB are activated HSC, being TGF-β a key player in the **transdifferentiation** process of HSC to MFB. In contrast to HSC, where TGF-β plays a growth inhibitory role, MFB demonstrate a growth stimulatory effect in response to the cytokine (Dooley et al., 2000). Several studies have

identified Smad3 as being the main mediator of the fibrogenic response of HSC, especially with respect to the induction of collagen expression (Dooley and ten Dijke, 2012).

In addition to HSC transdifferentiation to MFB, it is now fully accepted that **hepatocyte death** is critical for hepatic fibrosis (Brenner, 2009; Nikolaou et al., 2012). Indeed, it has been proved that apoptosis and phagocytosis of hepatocytes directly induce HSC activation and initiation of fibrosis (Jiang et al., 2010). TGF-β is an important regulatory suppressor factor in hepatocytes, inhibiting proliferation (Carr et al., 1986) and inducing cell death (Oberhammer et al., 1992). However, paradoxically, in addition to its suppressor effects, TGF-β also induces anti-apoptotic signals in proliferating hepatocytes, through the activation of the EGFR pathway (Valdés et al., 2004; Murillo et al., 2005). Cells that survive to TGF-β-induced apoptotic signals undergo EMT (Valdés et al., 2002; Caja et al., 2011b). Although still controversial, it is thought that EMT from hepatocytes could be another source of MFB (Wells, 2010). Additionally, during development of TGF-β-initiated fibroproliferative disorders, NOXs generate ROS, resulting in downstream transcription of a subset genes encoding matrix structural elements and pro-fibrotic factors (Samarakoon et al., 2013a). Apart from being downstream effectors implicated in TGF-β signalling, **ROS** play other roles promoting fibrosis progression, in relation with TGF-β. ROS may promote fibrosis activating latent TGF-β through either latency-associated peptide (LAP) direct activation and subsequent release of the cytokine (Pociask et al., 2004) or via MMP activation (Wang et al., 2005). Indeed, LAP/TGF-β complex has been proposed to function as an oxidative stress sensor (Jobling et al., 2006). Finally, ROS can also stimulate the expression and secretion of TGF-β in a positive feedback loop in many types of cells, including HSC and hepatocytes (Proell et al., 2007; Boudreau et al., 2009). Due to the relevance of ROS and NOX proteins in this work, they will be further addressed in a following section (**Section 4**).

Cirrhosis is not simply extensive fibrosis but is characterised by architectural disruption, aberrant hepatocyte regeneration, nodule formation and vascular changes. These macroregenerative nodules that display foci of hepatocyte dysplasia are considered to be pre-neoplastic lesions of HCC.

### 3.1.2. Role of TGF-β in hepatocarcinogenesis

The key for understanding the complicated role of TGF-β in cancer resides in knowing that it acts as a **tumour suppressor** during the **early stages** of tumorigenesis, but it also **promotes invasiveness and metastasis** in **advanced tumour** cells when cells become resistant to its suppressive effects. Several components of TGF-β suppressor signalling have been found inactivated in pancreatic, colorectal, head-and-neck, ovarian and other tumours. Although mutations and deletions of TGF-β signalling-related genes are found in some cancers, they are rare in HCC (Fabregat et al., 2014).

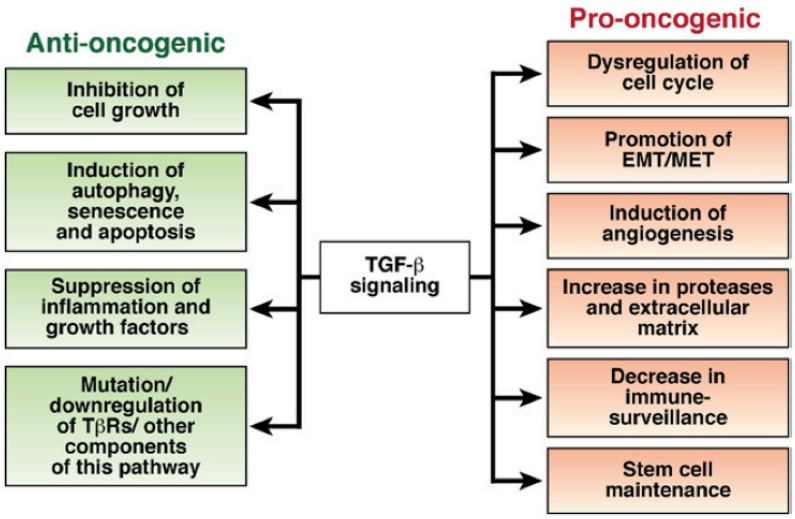


**Figure VIII.** TGF-β signalling exerts both anti-oncogenic and pro-oncogenic activities in carcinogenesis (Achyut and Yang, 2011).

Of remarkable importance to better understand the role of TGF-β in HCC progression, in most of the cases, cancer cells grow embedded in a cirrhotic environment enriched with extracellular matrix that is, in turn, mediated by the cytokine. In these conditions, TGF-β signalling promotes HCC progression by two mechanisms: first, via an intrinsic activity in the tumour as an autocrine or paracrine growth factor and, second, via an extrinsic activity in the stroma. In the **stroma**, TGF-β induces microenvironment changes, including generation of cancer-associated fibroblasts (CAF) which play a relevant role in facilitating the production of growth factors and cytokines that contribute to cell proliferation, invasion and neoangiogenesis. In addition, due to its immunosuppressive actions, TGF-β contributes to tumour cell evasion from immune surveillance. On the other hand, the **intrinsic effects** are mostly observed in highly invasive tumour conditions where TGF-β signalling may stimulate tumour proliferation and survival, and cells that survive to TGF-β suppressor effects undergo EMT favouring tumour metastasis (Fabregat et al., 2014; Giannelli et al., 2014).

All these different effects of TGF-β in liver cells are evidenced in a study by Coulouarn and col., where they define different liver gene signatures in response to TGF-β, based on the response of mice hepatocytes to this cytokine. The **"early" signature** is associated to suppressor genes, whereas the termed **"late" TGF-β signature** is associated to EMT, migration and invasion (Coulouarn et al., 2008). Interestingly, the early response pattern is associated with longer, and the late response pattern with shorter, survival in HCC human patients. In addition, tumours expressing the late TGF-β-responsive genes displayed invasive phenotype, increased tumour recurrence and accurately predicted liver metastasis. Of importance, this study also discriminated HCC cell lines by degree of invasiveness (Coulouarn et al., 2008).

## 3.2. TGF-β signalling pathway

In humans, the **TGF-β superfamily** represents a diverse set of growth factors, including bone morphogenic proteins (BMPs), growth and differentiation factors (GDFs), activins, TGF-β's, nodal and anti-mullerian hormone (AMH), that mediate such diverse processes as cell proliferation, differentiation, motility, adhesion, organization and programmed cell death. Most members of this family exist in variant forms, with the TGF-β cytokine consisting of three isoforms: TGF-$\beta_1$, TGF-$\beta_2$ and TGF-$\beta_3$. The TGF-β ligands are synthesized within the cell as pro-peptide precursors containing a pro-domain, LAP, and the mature domain, and are secreted into the ECM. They need to be cleaved to form active signalling molecules (Heldin et al., 2012).

TGF-β signals via formation of a heterotetrameric complex of type I and type II serine/threonine kinase receptors in which the constitutively active type II receptor phosphorylates and activates the type I receptor. There are several types of both type I and type II receptors but TGF-β preferentially signals through activin receptor-like kinase 5 (ALK5) type I receptor (TβRI) and the TGF-β type II receptor (TβRII). In addition, endoglin and betaglican, also called accessory receptors, bind TGF-β with low affinity and present it to the TβRI and TβRII. Activated receptor complexes propagate **canonical TGF-β signalling** through phosphorylation of the receptor-associated **Smads** (R-Smads). Humans express eight Smad proteins that can be classified into three groups: Receptor-associated Smads (R-Smads), Co-operating Smads (Co-Smads) and Inhibitory Smads (I-Smads). Among the R-Smads, Smad2 and 3 mediate the TGF-β branch of signalling, whereas the BMP branch exclusively utilizes Smad1, 5 and 8. Upon TGF-β stimulation, the R-Smads Smad2 and 3 are phosphorylated and associate with the Co-Smad Smad4, forming a complex that translocates to the nucleus where, in collaboration with other transcription factors, it binds and regulates promoters of different target genes. Two of these genes are the I-Smads Smad6 and Smad7, producing a negative feedback regulation of the TGF-β signalling. The co-activators and repressors recruited by the Smad complex are cell- and context-specific, therefore determining the specific genes induced within particular cells, explaining the diverse set of biological responses exerted by TGF-β signalling (Padua and Massagué, 2009; Drabsch and ten Dijke, 2012; Morrison et al., 2013).

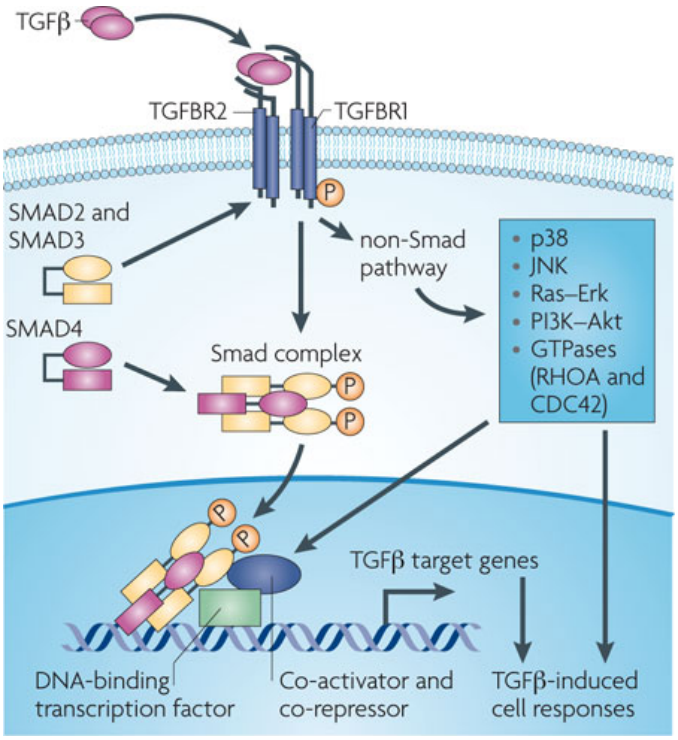


**Figure IX.** TGF-β signalling is transduced through Smad and non-Smad pathways (Ikushima and Miyazono, 2010).

In addition to the canonical Smad pathway, TGF-β is capable of utilising **non-Smad effectors** to mediate some of its biological responses, including non-receptor protein tyrosine kinases such as Src and FAK, mediators of cell survival (e.g., NF-κB, PI3K/AKT pathways), MAPK (ERK1/2, p38 MAPK, and JNK among others), and Rho GTPases like Ras, Rho and Rac1. Interestingly, these pathways can also regulate the canonical Smad pathway (Heldin et al., 2012; Drabsch and ten Dijke, 2012; Morrison et al., 2013).

# 3.3. TGF-β biological roles

As mentioned above, TGF-β is secreted by several cell types and it regulates a diverse array of cellular processes including cell proliferation, morphogenesis, migration, extracellular matrix production, cytokine secretion and apoptosis. To better contextualize the work presented here, this section will summarize the main functions exerted by TGF-β, especially **in liver**, on which our group has focused its effort during the last decades.

## 3.3.1. TGF-β and cell proliferation

In normal epithelial cells, as well as in endothelial, neuronal and hematopoietic cells, TGF-β regulates the expression of several genes promoting **cell cycle arrest** in the $G_1$ phase of the cell cycle, in a Smad dependent manner, through a diverse array of mechanisms, leading to pRb dephosphorylation. In these cells, TGF-β rapidly induces two CDK inhibitors, $p21^{Cip1}$ and $p15^{Ink4b}$, and down-regulates Myc, Id1, Id2 and Id3, all four transcription factors involved in proliferation and inhibition of differentiation. Thus, TGF-β mediates a dual effect on the cell cycle by simultaneously inhibiting the CDK functions and eliminating proliferative drivers (Seoane, 2006; Padua and Massagué, 2009; Drabsch and ten Dijke, 2012). Some of the mechanisms involved in the transcriptional regulation of the TGF-β cytostatic gene responses have been already elucidated. For example, TGF-β induces $p21^{Cip1}$ via a Smad3-FoxO complex that interacts with a specific region of the $p21^{Cip1}$ promoter (Seoane et al., 2004). Besides the canonical Smad-dependent gene responses involved in the cytostatic program, TGF-β can also promote cell cycle arrest through Smad-independent pathways. For instance, the binding of TGF-β receptor complex to the regulatory subunit of PP2A facilitates the dephosphorylation and inhibition of p70 S6 kinase and contributes to the anti-proliferative response (Petritsch et al., 2000). In addition, TGF-β can also induce JNK and p38 to stabilize $p21^{Cip1}$ (Kim et al., 2002).

**In hepatocytes**, TGF-β is known to induce cell cycle arrest at low doses (Sánchez et al., 1996), and to counteract proliferative signals induced by EGF or insulin (Carr et al., 1986; Sánchez et al., 1998). Although hepatocytes from regenerating liver are known to be resistant to the mito-inhibitory effects of TGF-β, maybe due to a decrease in the expression of its receptors, TGF-β has been thought as being a natural stimulus that terminates liver regeneration, preventing uncontrolled hepatocyte proliferation (Michalopoulos, 2007).

In normal cells, the cytostatic effects of TGF-β are often dominant over the opposing mitogenic signals; however, **carcinoma-derived cells** are usually refractory to growth inhibition by the cytokine. In certain cases, this is due to the disruption of TGF-β signalling caused by somatic mutations in components of the TGF-β pathway, such as microsatellite instability leading to mutations in TβRII, inactivating mutations in Smad2 and 4, or with lower incidence,

mutations in the TβRI. Nevertheless, many tumours with an intact, non-mutated TGF-β pathway lack the TGF-β anti-proliferative response, in some cases due to overactivation of non-Smad pathways that can lead to aberrant expression or post-transcriptional modification of the TGF-β pathway components (Seoane, 2006). Indeed, our group has described that TGF-β induces survival signals in both foetal and transformed hepatocytes, but not in adult hepatocytes, through the transactivation of the EGFR pathway. We have demonstrated that this transactivation is through a NOX, NF-κB and Caveolin-1 dependent mechanism (Murillo et al., 2007; Caja et al., 2007; Moreno-Càceres et al., 2014).

### 3.3.2. TGF-β and apoptosis

In addition to its role in regulating the cell cycle, TGF-β also participates in the maintenance of tissue homeostasis through its influence on apoptotic pathways. TGF-β is a well-known **inducer of apoptosis**. However, it is known that the apoptotic signalling induced by TGF-β consists in different mechanisms and a complex network of apoptosis-related events that might occur differently, not only in a cell type-specific manner, but also dependent on the cell context and the extracellular microenvironment. There have been several Smad-dependent and -independent mechanisms described for a variety of cell lines, but in any case, this signal ultimately results in activation of pro-apoptotic caspases as well as changes in the expression, localization and activation of both pro- and anti-apoptotic members of the BCL2 family (Padua and Massagué, 2009).

In epithelial cells, such as foetal hepatocytes, TGF-β-induced apoptosis is coincident with **ROS** production (Sánchez et al., 1996; Sánchez et al., 1997) through either induction of a NOX system, more precisely induction of **NOX4**, to increase extramitochondrial ROS (Herrera et al., 2004; Carmona-Cuenca et al., 2008) or depletion of antioxidant proteins that increase mitochondrial ROS (Franklin et al., 2003; Herrera et al., 2004). TGF-β-induced ROS production is necessary for the apoptotic process in hepatocytes and it is required for an efficient mitochondrial-dependent execution of apoptosis (Herrera et al., 2001a; Herrera et al., 2001b).

Nevertheless, as it happens with the role of TGF-β controlling cell proliferation, when speaking about cell death, TGF-β can also exert both pro- and anti-apoptotic functions. TGF-β is able to activate **survival pathways**, for example activating AKT signalling inducing an increase in anti-apoptotic proteins (Valdés et al., 2004; Wilkes et al., 2005; Song et al., 2006). However, usually, AKT activation is transient and might be related to the capacity of TGF-β to transactivate c-Src and EGFR pathways (Park et al., 2004b; Murillo et al., 2005). Indeed, TGF-β is able to mediate the production of EGFR ligands, which eventually confers resistance to its pro-apoptotic effects in hepatocytes (Del Castillo et al., 2006; Carmona-Cuenca et al., 2006; Murillo et al., 2007) and HCC cells (Caja et al., 2011a), and the inhibition of the EGFR pathway enhances TGF-β induced apoptosis (Sancho et al., 2009). Importantly, the capacity of

hepatocytes to survive to TGF-β is also dependent on their differentiation status (Sánchez et al., 1999). Thus, rat hepatocytes respond to TGF-β inducing survival signals, whereas adult hepatocytes do not (Caja et al., 2007). In the same way, different features of HCC cell lines, like the activation of the EGFR or MEK/ERK pathways, may provoke different outcomes after TGF-β exposure (Caja et al., 2009; Caja et al., 2011a).

### 3.3.3. TGF-β and metastasis

The paradoxical switch in TGF-β function during tumorigenesis has been linked to its ability to **induce EMT** programs, which reflects an evolutionarily conserved cascade in which polarized epithelial cells adopt mesenchymal cell characteristics together with enhanced chemoresistance and evasion from host immunosurveillance, expanded stem-like and tumour-initiating activities, elevated resistance to apoptotic stimuli, and acquired migratory, invasive, and metastatic phenotypes (Morrison et al., 2013). In fact, in contrast to the canonical role in controlling epithelial cell proliferation, TGF-β is considered pro-growth with respect to the mesenchyme. Classically, in response to injury, granulocytes, platelets, leukocytes and additional parenchymal cells increase the presence of TGF-β at the site of the wound. TGF-β, then, induces fibroblast proliferation, MFB differentiation, and remodelling of the ECM, favouring fibrotic processes (Principe et al., 2014).

Epithelial cells show apical-basal polarity, adhere and communicate with each other through specialized intercellular junctions and are positioned on a basement membrane that helps to define their physiology. In this way, epithelia function as permeable barriers that delineate tissues and organs. The transition of epithelial cells into mesenchymal cells, either in development or pathological situations, follows a common and conserved programme. However, it has also inherent flexibility and variability depending on the cell type, tissue context and signals that activate the EMT programme (Lamouille et al., 2014).

EMT starts with dissolution of epithelial cell-to-cell contacts and loss of apical-basal polarity. In addition, the expression of epithelial junction proteins such as E-cadherin, ZO-1 and occludin is down-regulated at the level of gene expression, concomitantly with increases in the expression of mesenchymal adhesion proteins like N-cadherin. Snail/Slug, ZEB1/2 and Twist families of transcription factors potently regulate this epithelial to mesencymal switch in gene expression. Additionally, actin cytoskeleton, as well as microfilaments, microtubules and intermediate filaments (vimentin and α-smooth muscle actin (α-SMA)) are dramatically modified and reorganized promoting phenotypic changes to enable cells to acquire a front-rear polarity and motility. Finally, cells acquire invasive properties through increased expression and secretion of MMPs, and cells that undergo EMT are also efficiently capable of synthesizing components of the ECM to reconstitute their microenvironment following cell invasion. Importantly, EMT can also be reverted through a process called mesenchymal-to-epithelial transition (MET), occurring after migration and homing into new sites within an embryo, during

tumour progression or healing of fibrotic tissue (Heldin et al., 2012; Morrison et al., 2013; Lamouille et al., 2014).

**In cancer**, epithelial cells undergo EMT, which favours intravasation of cells to both lymph and blood vessels and consequent dissemination far from the primary tumour. At secondary loci, cells may undergo a MET process to be able to colonize secondary sites and form metastasis. It is worth to mention that cancer cells may undergo EMT in different extents, it is possible that some cells retain epithelial features at the same time that are acquiring some mesenchymal ones, and other cells become fully mesenchymal (Kalluri and Weinberg, 2009).

It should be noted that both canonical and non-canonical TGF-β pathways participate in driving EMT programs by the cytokine. Indeed, Smad3 and 4 function as positive regulators of EMT programs, while Smad2 functions as a negative regulator of EMT, by regulating different transcription of target genes. Through the activation of PI3K-AKT-mTOR pathway and small GTPases, including RhoA, TGF-β induces increased motility and invasion, and changes in protein synthesis and actin reorganization. MicroRNAs, as well as epigenetic changes and alternative splicing, also regulate the EMT program induced by the cytokine (Heldin et al., 2012; Morrison et al., 2013; Katsuno et al., 2013).

**In the liver**, TGF-β induces an EMT process in foetal hepatocytes that survive to its apoptotic effects (Sánchez et al., 1999). To induce EMT, TGF-β is known to up-regulate the transcription factors Snail and Slug, which in turn repress the expression of epithelial markers, while activating the expression of mesenchymal markers (Katsuno et al., 2013). Interestingly, EMT-inducing factors such as Snail or Twist might help TGF-β to also promote cell dedifferentiation and expression of cell surface presumptive cancer stem cell markers (Mani et al., 2008). In accordance, foetal hepatocytes that undergo EMT become refractory to apoptotic effects of TGF-β, showing characteristics of liver progenitor cells (Valdés et al., 2002). Indeed, TGF-β may contribute to transdifferentiation of foetal hepatocytes into liver progenitors, which later on will be able to differentiate both in mature hepatocytes and cholangiocytes (Del Castillo et al., 2006; Caja et al., 2011b). It is important to note that in absence of the cytokine, cells that underwent a TGF-β-induced EMT revert to an epithelial phenotype (Bertran et al., 2009).

TGF-β is able to induce both pro-apoptotic and survival signals at the same time in hepatocytes, and the balance between them is what decides the **final cell fate**. There is a close link between apoptosis and EMT, not only because initially the EMT process depends on the ability of cells to overcome TGF-β induced apoptosis, but also because EMT induces survival signals that rescue from apoptosis (Valdés et al., 2002; Valdés et al., 2004; Bertran et al., 2009). For instance, Snail overexpression has been shown to confer resistance to TGF-β induced pro-apoptotic effects (Vega et al., 2004; Franco et al., 2010). Furthermore, EMT might confer resistance to TGF-β suppressor effects through the increase in the expression of EGFR ligands and activation of its pathway, which highlights the existence of a cross-talk between TGF-β and EGF signals in hepatocytes (Del Castillo et al., 2006).

Nevertheless, acquiring a mesenchymal phenotype is not the only way through which epithelial cells can invade local and distant sites, since they can move also as a collective group, maintaining epithelial features, as it will be deeply discussed in a following section (**Section 5**). Although it has been less studied by far, it has been described that TGF-β can be implicated in these other kind of movement in different systems, including the liver. For instance, it has been reported that TGF-β has a role in the regulation of collective migration through controling the directional migration of hepatocyte cohorts by modulating their adhesion to fibronectin (Binamé et al., 2008).

# 4. ROS and NADPH oxidases

## 4.1. Reactive oxygen species

**Reactive oxygen species** (ROS) are short-lived, highly electrophilic molecules generated by the partial reduction of oxygen to form superoxide ($O_2^-$), hydrogen peroxide ($H_2O_2$) and hydroxyl radical ($^{\cdot}OH$) as well as secondary metabolites including lipid peroxides, peroxynitrite ($ONO^-$), and hypochlorous acid (HOCl). Reactive nitrogen species (RNS) such as nitric oxide (NO) are sometimes included (Lambeth and Neish, 2014). **Free radicals** are defined by the presence of a single unpaired electron in the outer orbital. This unstable configuration can propagate a chain reaction that includes modification of macromolecules, notably certain proteins, membrane components, and nucleic acids (Lambeth and Neish, 2014). Not all oxygen species are free radicals. For instance, $H_2O_2$ is not a free radical, but it is a precursor of free radicals.

Different types of ROS have different intrinsic chemical properties, which dictate their reactivity, subcellular localization and preferred biological targets:

- **Superoxide** ($O_2^-$) is a free radical whose lifetime in biological systems is few seconds. It is considered a weak oxidant and a weak reductant and rapidly reacts with another molecule of superoxide to form hydrogen peroxide. This is called self-dismutation reaction and it is performed by an enzyme called superoxide dismutase (SOD). Another important reaction in biological systems is the diffusion-controlled reaction between superoxide and nitric oxide (radical-radical reaction) to form a very potent oxidant and reactive nitrogen specie, peroxynitrite. Interestingly, superoxide is membrane impermeant (Kalyanaraman, 2013).
- **Hydrogen peroxide** ($H_2O_2$) is considered a moderate oxidant and its relatively stable (its half-life could be of months if protected against light and trace metal contamination). However, antioxidant enzymes such as catalase and glutathione rapidly destroy it. $H_2O_2$ in the presence of released iron could form hydroxyl radical ($^{\cdot}OH$), a potent oxidant, via the Fenton mechanism ($Fe^{2+} + H_2O_2 \rightarrow Fe^{3+} + {}^{\cdot}OH + OH^-$) or the Haber-Weiss mechanism ($O_2^- + H_2O_2 \rightarrow {}^{\cdot}OH + OH^- + O_2$). Hydroxyl radical is a potent antimicrobial oxidant. Moreover, myeloperoxidase (MPO) is a heme-containing peroxidase that oxidizes halide anion (chloride, bromide and iodide anions) in the presence of $H_2O_2$, forming the corresponding hypohalous acid that is also very reactive. Even more relevant for this work, hydrogen peroxide reacts with cysteine residues from proteins, acting as a signal transducer. It is important to note that hydrogen peroxide is membrane permeable, thus freely diffuses to other compartments in cells. Recent evidences suggest that extracellular hydrogen peroxide preferentially enter the cell through specific plasma membrane aquaporin channels (Finkel, 2011; Kalyanaraman, 2013).

## 4.2. Oxidative stress and oxidant signalling

The term **oxidative stress** refers to the imbalance between the prooxidant and antioxidant levels in favour of prooxidants in cells and tissues, most of the times due to the overproduction of ROS. However, this term is imprecise, because different biological situations create different mixtures of these molecular species, each with its own spectrum of reactivity with different biomolecules (Lambeth and Neish, 2014). For many years, the traditional view of ROS was that their production was unregulated and that their intracellular targets were random. Actually, one of the consequences of oxidative stress is cell injury caused by oxidative damage being the main targets of oxidative damage DNA (mutations caused by AT ↔ GC transition and by GC ↔ TA transversion), lipid (lipid peroxidation) and protein (formation of carbonyls, dityrosine and nitrated and chlorinated tyrosines) (Holmström and Finkel, 2014).

However, there is a growing appreciation that oxidant species such as $O_2^{\cdot-}$ and $H_2O_2$ can also have useful and **beneficial effects** (Holmström and Finkel, 2014). It is true that damaged and oxidized biomolecules are implicated as potential contributors to a range of pathologies, including neurodegenerative diseases, atherosclerosis and the ageing process itself. Nonetheless, when ROS are confined to a phagolysosome, they can mediate microbicidal killing, being beneficial, and additionally, low levels of ROS can function within specific signalling pathways, through **transient and reversible** mechanisms (Lambeth and Neish, 2014).

By oxydizing reactive cysteine residues, which are often located in the enzyme's active site, ROS can activate or inactivate their target proteins. Although the pKa of a thiol group on free cysteine is high (between 8 and 9), in some target molecules due to the surrounding aminoacid microenvironment of the cysteine, its pKa can be substantially modified to result in a pKa as low as 4 to 5, easy to be oxidized. One of the earliest observations in support of a role for ROS in signal transduction was that the increase in tyrosine phosphorylation that occurs after growth factor stimulation is preceded by a burst of ROS generation. Rather than being harmful, this rise in intracellular ROS level was shown to be required for downstream signalling. This tyrosine phosphorylation involved the redox-dependent inactivation of protein tyrosine phosphatases (PTPs). It is now clear that in addition to targeting phosphatases, ROS can also directly affect kinase signalling through the redox-dependent modification of cysteines in certain domains of receptors. Additionally, reversible oxidation and reduction of other aminoacids can occur, and emerging evidences indicate that methionine residues might provide an analogous redox-dependent system (Finkel, 2011; Holmström and Finkel, 2014; Drazic and Winter, 2014).

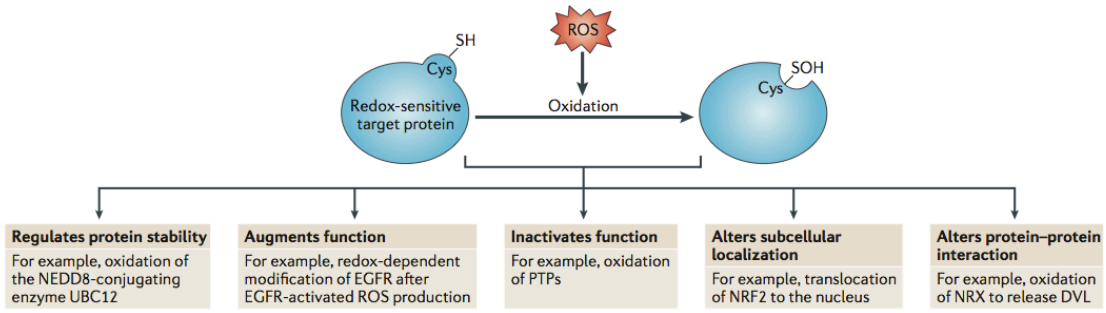


**Figure X.** The multiple ways in which oxidant signalling can affect cellular functions (Holmström and Finkel, 2014).

The number of intracellular targets known for redox-dependent signalling has increased dramatically during the last years. The more recent analyses, based on either computational means or through large-scale proteomic approaches, has suggested that reactive and potentially modulatory cysteine residues might exist in well over 500 individual proteins, thereby extending this form of redox regulation to a wide range of enzymatic activities. Of note, the relevance of redox in signalling relies on its reversibility, oxidized thiols can be reduced by mechanisms involving thioredoxin (TXN) or glutathione, among others, resulting in an off/on regulation analogous to protein phosphorylation/desphosphorylation, allowing the control of critical steps in many signal transduction pathways (Finkel, 2011; Lambeth and Neish, 2014; Holmström and Finkel, 2014).

Some degree of **specificity** is presumably achieved by colocalizing the source of ROS with the intended target, or by confining the spread of ROS to intracellular regions that are enriched in redox targets (Holmström and Finkel, 2014).

## 4.3. Oxidant sources

There are numerous potential sources of ROS within the cell. ROS can be produced as **by-products** of enzymatic processes, which is considered the case of **mitochondrial ROS**. Mitochondria generate ATP in an oxygen-dependent manner during which the flow of electrons down the respiratory chain eventually culminates at complex IV with the reduction of molecular oxygen to water. Throughout this process, superoxide is generated, predominantly at complex I and complex III of the cytochrome chain, when electrons initially derived from NADH or $FADH_2$ react with oxygen. Normal mitochondria provide a low basal level of ROS in most of cells, but this level may increase during aging or mitochondrial damage. Mitochondrial oxidants have been historically viewed as purely toxic, however, recent evidence suggest that they can be also regulators of intracellular signalling pathways. In addition to mitochondria, other redox-active enzymes can generate superoxide and hydrogen peroxide as a by-product. These include xanthine oxidase, cytochrome p450, cyclooxygenase, lipoxygenase, and nitric oxide synthase (NOS) (Finkel, 2011; Lambeth and Neish, 2014).

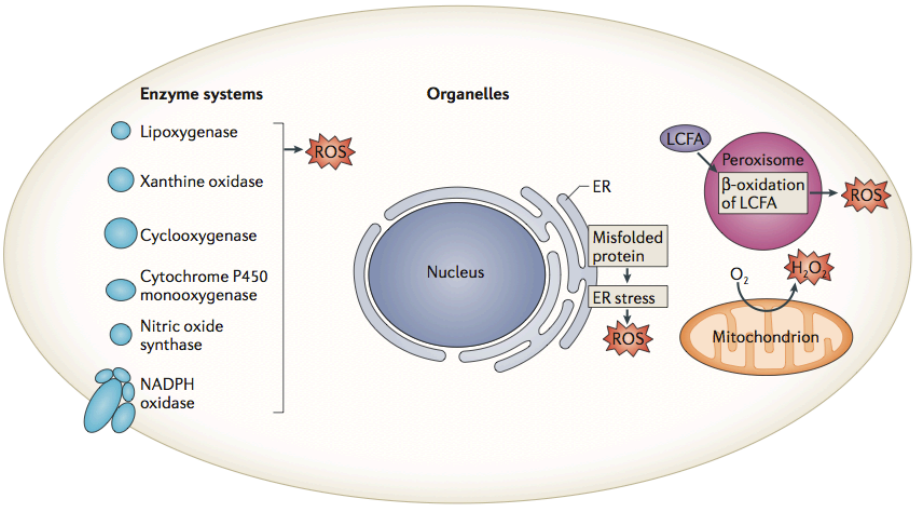


**Figure XI.** Intracellular sources of reactive oxygen species (ROS) (Holmström and Finkel, 2014).

In contrast, **NOXs** are a family of enzymes that generate ROS (either superoxide or hydrogen peroxide) as the **primary species** during the catalytic metabolism of oxygen for a range of host defence and signalling functions. Seven isoforms of NOX are expressed in mammalian cells (NOX1-5, DUOX1 and DUOX2). All NOX isoforms are membrane bound enzymes that rely on NADPH for their activity and the major source of ROS is generated when the flavin- and heme- containing protein complex transfer electrons from cytosolic NADPH to molecular oxygen to produce $O_2^-$ or $H_2O_2$ (Holmström and Finkel, 2014; Lambeth and Neish,

2014). Considering the relevance of NOXs for this work, it will be further reviewed in the next section (**Section 4.4**).

Cells have necessarily developed a variety of mechanisms to keep ROS within acceptable levels. To combat or modulate the production and effect of ROS, the cell is equipped with various potent antioxidant defences. They involve antioxidant enzymes, small molecular-weight antioxidants and adaptive mechanisms leading to antioxidant gene expression.

**Antioxidant enzymes** include superoxide dismutases (SODs), catalases and peroxidases. There are at least three types of SODs: copper-zinc SOD (CuZnSOD), which is cytosolic; manganese SOD (MnSOD), which is mitochondrial; and extracellular SOD (EC-SOD). SOD catalytically enhances the normal dismutation of superoxide forming hydrogen peroxide ($O_2^- + O_2^- + 2H^+ \rightarrow H_2O_2 + O_2$) and it is normally present at low micromolar concentrations in cells. The peroxisomal enzyme catalase (CAT) reduces hydrogen peroxide to molecular oxygen and water. CAT is present in all tissues and it is important when $H_2O_2$ levels are low. At higher concentrations of $H_2O_2$, glutathione peroxidase enzyme (GPx), that is dependent on reduced glutathione, is responsible for detoxifying $H_2O_2$. During this process, reduced glutathione (GSH) is oxidized to glutathione disulphide (GSSG) that is then reduced back to GSH by glutathione reductase using NADPH as a co-factor. In addition, other mechanisms such as peroxiredoxin and thioredoxin, are involved in detoxifying intracellular hydroxiperoxides (Kalyanaraman, 2013; Lambeth and Neish, 2014).

Additionally, cells can modulate the transcription of **cysteine-rich proteins and peptides** such as glutathione, TXNs, and peroxiredoxins that function as redox sinks. These gene products can be transcriptionally up-regulated by the action of redox-sensitive signalling pathways such as the Nuclear Factor Erythroid-2-Related Transcription Factor 2 / antioxidant response elements (Nrf2/ARE) regulatory mechanism. For example, electrophiles formed as by-products of lipid hydroperoxide decomposition, like the aldehydes MDA and 4-HNE, are able to induce antioxidant gene expression through activation of the Keap1-Nrf2 system. Under reducing conditions, Keap1 binds to Nrf2 promoting Nrf2 cytoplasmic degradation through a cullin-dependent E3 ubiquitin ligase. Upon oxidation of redox-sensitive cysteines of Keap1, there is a conformational change that suppresses the proteasomal degradation and provokes the cytosolic accumulation of Nrf2, which translocates to the nucleus and binds to ARE that are contained within the promoters of antioxidant genes, thereby activating its transcription (Kalyanaraman, 2013; Lambeth and Neish, 2014; Holmström and Finkel, 2014).

In addition to enzymatic mechanisms, there exist **non-enzymatic small molecular weight antioxidants** present in certain foods and drinks such as ascorbic acid (vitamin C), alpha-tocopherol (vitamin E), reduced glutathione (present in milimolar levels in cells) and β-carotene, among others. The localization of antioxidants is of relevance for its action. It is important that these antioxidants are not able to deal with hydrogen peroxide as they will only react really slowly with it (Kalyanaraman, 2013). Glucose metabolism through the pentose

phosphate pathway (PPP) is tightly linked to antioxidant defence capacity of cells since it generates the NADPH necessary to maintain glutathione in a reduced form, which is perhaps the most important non-enzymatic ROS scavenger. GSH can get reduced and therefore re-activated by glutathione reductase and NADPH (Holmström and Finkel, 2014; Glasauer and Chandel, 2014).

## 4.4. NADPH oxidase (NOX) family

The **NOX family** has emerged in the last years as important source of ROS in signal transduction (Brown and Griendling, 2009). It consists of seven members, NOX1-5 and two dual oxidases (DUOX1-2), which share analogies in structure and catalytic function, since all of them mediate the reduction of oxygen using NADPH as an electron donor. However, important differences in regulation and cellular functions are observed among them.

The first NOX described was the phagocytic NADPH oxidase or respiratory burst oxidase, whose catalytic subunit is known as NOX2 or gp91phox. Subsequently, p47phox, p67phox and the small GTPase Rac1 and Rac2 were identified as essential regulatory subunits. NOX2 is an enzyme whose main function is to produce large amounts of ROS in a respiratory burst characterized by consumption of $O_2$ and production of superoxide. Mostly during the 90s, investigators in diverse fields had observed that superoxide and hydrogen peroxide were produced in non-phagocytic tissues/cells, often in response to hormones or growth factors. These observations brought to the discovery of the other mammalian NOX homologs. The other members of the NOX family have been cloned and studied in the past fifteen years (Lambeth et al., 2007; Lambeth and Neish, 2014). The first homologue of NOX2 to be cloned was NOX1, originally described in 1999 as MOX1 (Suh et al., 1999), followed by the two dual oxidases (DUOX1 and 2), NOX3, NOX4, and eventually NOX5 in 2001. In addition, new NOX regulatory subunits termed NOXO1 (NOX organizer 1) and NOXA1 (NOX activator 1), homologs of p47phox and p67phox respectively, were identified (Brown and Griendling, 2009; Lambeth and Neish, 2014).

### 4.4.1. NOX structure

All NOXs are **transmembrane flavoproteins** that transport electrons across biological membranes to reduce oxygen to superoxide. In accordance with this preserved function, there are conserved structural properties of NOX enzymes that are common to all family members. Starting from the COOH terminus, these conserved structural features include flavin adenine dinucleotide and nicotinamide adenine dinucleotide plus hydrogen (FADH and NADPH) binding sites at their C-terminus domain and six conserved transmembrane domains. Electrons are transported by two heme groups that are coordinated by four highly conserved histidines within the transmembrane domains. Additionally, NOX5 has an amino-terminal calmodulin-like domain that contains four calcium binding EF-hand structures, and DUOX1 and 2 have an extracellular peroxidase domain in addition to the EF-hand and gp91phox homology domains (Bedard and Krause, 2007; Brown and Griendling, 2009). Thus, the mammalian NOX enzymes can be classified into **two broad groups**, those that require p22phox (NOX1-4) and those that are regulated by calcium through an EF hand-containing calcium-binding domain (NOX5, DUOX1 and DUOX2). Depending on the NOX subunit, p22phox can serve multiple roles, functioning as

a maturation factor required for appropriate glycosylation and localization of the NOX subunit, stabilizing the NOX subunit, and providing a docking site for binding of other regulatory subunits (Lambeth and Neish, 2014).

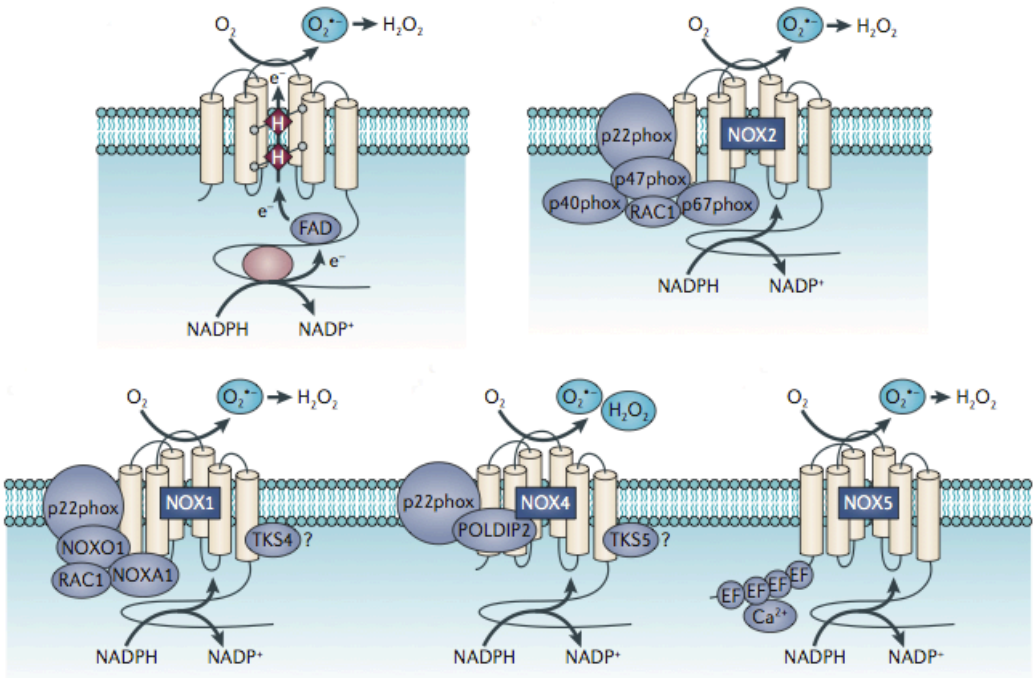


**Figure XII.** Structure and molecular organization of NADPH oxidases (NOX) (Block and Gorin, 2012).

## 4.4.2. NOX activation

The classic activity control of NOX enzymes is exerted by calcium or protein-protein interactions and concerns all NOX enzymes, with the **exception of NOX4**, which is constitutively active. Briefly, the two main elements that contribute to NOX1, NOX2 and NOX3 activation are the interaction with the small GTPase Rac and the interaction with cytosolic activator proteins. NOX activators NOXA1 and p67phox have been identified to require organizing scaffolding proteins to tether them to the large NOX enzyme, which are termed p47phox and NOXO1. As mentioned before, p22phox has a scaffold function for the maturation and the folding of the catalytically active NOX protein through a proline rich region, which also provides a binding platform for the cytosolic activator proteins of NOX1-3. In line with the exclusive dependency of NOX1-3 on cytosolic activators, mutations in the proline rich region of p22phox do not affect NOX4-dependent ROS production. In essence, the activity control of NOX1-3 is therefore primarily achieved through alterations of the cytosolic proteins, which in turn can be modulated by several mechanisms such as phosphorylation, interaction with cytoskeleton, redox status, among others. NOX5 and the DUOX enzymes contain the EF-hands making them directly calcium-dependent, but are independent of Rac. In addition, DUOX1 and 2

require the association of DUOXA1 and 2, respectively, for localization to the plasma membrane. NOX4, in contrast to the other members of the family, is constitutively active and its regulation is believed to be mainly at transcriptional level. It forms stable complexes with p22phox but is Rac-independent and co-expression with p47phox and p67phox or NOXA1/NOXO1 does not increase ROS generation (Lambeth et al., 2007; Serrander et al., 2007; Brandes et al., 2014a). Recently, NOX-interacting partners have been suggested to bind to and enhance NOX4 activity, such as polymerase (DNA-directed) delta-interacting protein 2 (Poldip2) (Lyle et al., 2009) and TLR4 (Park et al., 2004a; Suzuki et al., 2012). Further discussion about NOX4 activity will be done in a separate section (**Section 4.5**).

Although the activity of NOX and DUOX enzymes is acutely regulated by subunits or calcium, the maximum capacity of a cell to generate ROS will be also determined by the **protein expression** of NOX/DUOX (as previously mentioned for NOX4) and their regulatory subunits. Expression of NOXs is ubiquitous in mammals, though the individual NOX isoforms have **different distribution** between tissues and species. It is known that cytokines, growth factors as well as other stimuli such as hypoxia, low pH and bacterial products, can regulate its expression. NOX1 is most highly expressed in colon epithelia, but it is also expressed at lower levels in vascular smooth muscle cells (VSMC), endothelial cells, uterus, placenta, prostate, osteoclasts, hepatocytes, retinal pericytes, neurons, astrocytes and microglia. Though NOX2 is most highly expressed in phagocytes, expression has also been detected in central nervous system, endothelium, VSMC, fibroblasts, cardiomyocytes, skeletal muscle, hepatocytes and hematopoietic stem cells. NOX3 expression is mainly localized in the inner ear. NOX4 was first identified in the kidney, but was subsequently found in many cell types such as VSMC, endothelial cells, fibroblasts, keratinocytes, osteoclasts, neurons, and of special interest for this work, in hepatocytes. NOX5, which is the least well-studied NOX homologue because it is missing in rodents due to gene deletion, has been identified in lymphoid tissues, testes, spleen, smooth muscle cells and endothelial cells. And finally, the dual oxidases DUOX1 and 2 were first described in the thyroid gland but they have been also reported in epithelial cells of the lung (Brown and Griendling, 2009; Paletta-Silva et al., 2013). Furthermore, **subcellular localization** of NOX proteins is considered to be determinant for the specificity of the signalling induced by NOX-derived ROS. Thus, NOX1, NOX2, NOX3 and DUOXes are mainly described to be at the plasma membrane, although other localizations have been reported for NOX1 (for instance, endosomes, nucleus and cytoplasm) and NOX2 (submembranous phagosomes, endosomes and in caveolae on the leading edge of lamellipodia). On the contrary, NOX4 has been identified in focal adhesions, nucleus and endoplasmic reticulum (Brown and Griendling, 2009). Of note, the lack of good specific and reliable antibodies represents one of the biggest obstacles in the field.

Interestingly, NOX enzymes can also be grouped according to the **species of reactive oxygen** that are released. NOX1-3 and NOX5 generate primarily superoxide, whereas the major detected product of NOX4 and DUOX1-2 is hydrogen peroxide (Lambeth and Neish, 2014). Although production of $O_2^-$ is the main biological function of NOX proteins and it is

important in the bactericidal activity of NOX2, its dismutation product $H_2O_2$ directly mediates much of the signalling that occurs. As reported in a previous section, hydrogen peroxide is more stable than superoxide and it is also capable of crossing biological membranes. Because of the presence of SOD in the cell, $H_2O_2$ is formed rapidly from NOX-generated superoxide, or in the case of NOX4, perhaps prior to the release of $O_2^-$ from the enzyme. As mentioned, DUOXes produce $H_2O_2$ directly via a two electron reduction of oxygen, rather than by producing superoxide first as an intermediate (Brown and Griendling, 2009).

### 4.4.3. NOX functions in physiology and pathology

One of the puzzling observations in the NOX field is that cells and tissues often express multiple NOX proteins in the same cell, but that these enzymes regulate different functions in different cell types. All the differences in structure and co-activators, plus the different subcellular localizations of NOX enzymes, the nature, intensity and duration of the activating signal, and the developmental stage of the cell, are a feasible explanation of these different cellular responses to the generated ROS. NOX-derived ROS may mediate fundamental biological processes in cells and tissues, as well as some pathological disorders by participating in gene expression, cytoskeleton remodelling, migration, differentiation, as well as cell proliferation and death. In addition, they have more specialized functions, such as host defence (NOX2), otoconium formation in the inner ear (NOX3), iodination of thyroid hormone (DUOX2), and control of thyroid hormone (NOX2) (Brown and Griendling, 2009; Altenhofer et al., 2012).

There is abundant evidence for the regulation of **gene expression** by ROS. NOX-dependent ROS generation has been shown to induce, for example, the expression of TNF-$\alpha$, TGF-$\beta$, angiotensin II, plasminogen activator inhibitor-1 and HIF1$\alpha$. This regulation can occur through redox-sensitive second messenger systems, like MAPK activation, or through transcription factors including NF-$\kappa$B, AP-1 and p53, which contain redox-sensitive cysteine residues in their DNA binding domain. Alternatively, NOX-derived ROS may also alter gene expression through the regulation of mRNA stability. ROS, through thiol oxidation, also directly activate the transcription factor Nrf2 by oxidizing its inhibitory redox-sensor Keap1, as mentioned before (Bedard and Krause, 2007; Brandes et al., 2014b).

Since studies in the 1990s demonstrated the association between cell division and ROS, many reports have been published attributing NOX-derived ROS to **cell growth**. ROS had been shown to influence proliferation in the form of second messengers in many pathways regulating cell proliferation, such as those involving p21 and MAPK. Furthermore, ROS were shown to be important modulators of ubiquitination and phosphorylation of cell cycle associated enzymes, such as cdc25 and CKIs. Indeed, ubiquitination mediated by ROS is essential for the regulation of the expression of CKIs, such as p21, p27 and p57, and influences proliferation in a context dependent manner, either favouring or impairing cell cycle progression. Additionally, ROS have been recently found to activate growth factor receptors in the absence of the growth

factor receptor ligands, thereby further controlling proliferation (Verbon et al., 2012). One important receptor for cell cycle regulation is the EGFR. Since 1999, ROS are known to affect EGFR signalling by inhibition of EGFR internalization, thus increasing the receptor's signalling potential (de Wit et al., 2000). Interestingly, it has also been described that EGF stimulates the generation of hydrogen peroxide, which is mediated by the activation of NOX1 through a mechanism involving PI3K and Rac1 (Verbon et al., 2012). Hydrogen peroxide markedly stimulates mitotic pathways involving protein tyrosine phosphate as a result of reversible oxidative inactivation of protein tyrosine phosphatase 1B (PTP1B) (Lee et al., 1998). Oxidative inactivation of a variety of PTPs appears to be a widespread phenomenon and it is generally associated with mitotic growth. In addition, our group has described that NOX1 promotes autocrine growth of liver tumour cells through the up-regulation of the EGFR pathway. This proliferation can be impaired by the addition of the NOX inhibitor VAS2870 (Ortiz et al., 2008; Sancho and Fabregat, 2010; Sancho and Fabregat, 2011). In lung epithelia, NOX1 overexpression modifies Cyclin D1 expression leading to the stimulation of mitotic growth (Ranjan et al., 2006). However, growth effects are likely to be cell type/context/isoform specific, as overexpression of NOX enzymes in some cells is associated with **senescence** rather than growth. Indeed, the first description of NOX4 reported a rapid senescence of NOX4-overexpressing fibroblast (Geiszt et al., 2000; Kodama et al., 2013). Furthermore, Senturk et al. demonstrated that TGF-β-induced senescence in well-differentiated HCC cells occurs in a NOX4 and p21 dependent manner (Senturk et al., 2010). Therefore, a role in stimulating growth cannot be generalized.

Furthermore, many studies have described programmed **cell death** in response to ROS and NOX expression/activation. For instance, our group has demonstrated that NOX4 is necessary for the apoptosis induced by TGF-β in HCC cells (Carmona-Cuenca et al., 2008; Caja et al., 2009). Actually, we have described that TGF- β induces the expression of both NOX1 and NOX4 in transformed hepatocytes, and whilst NOX4 induced-ROS are responsible of cell death, NOX1 confers partial resistance to TGF-β-induced apoptosis, through the activation of the EGFR pathway (Sancho et al., 2009). In addition, NOX1-dependent activation of NF-κB pathway mediates the resistance to TGF-β observed in PTP1B knock-out hepatocytes (Ortiz et al., 2012). The same role for NOX4 mediating TGF-β-induced cell death has been recently reported in podocytes (Das et al., 2014). In contrast, other groups demonstrated that ROS from NOX4 in pancreatic cells (Vaquero et al., 2004) and from NOX1 in colon adenoma and carcinoma (Fukuyama et al., 2005), inhibit apoptosis. Therefore, depending on the cell type, genetic background, and probably the NOX isoform, NOX-derived ROS can participate in either pro-apoptotic or anti-apoptotic responses.

NOXs can also regulate **migration and adhesion** in an isoform and cell-specific manner. Cellular movement requires coordinated changes in the structure of the actin cytoskeleton and, as it will be futher described in a following section (**Section 5**), Rho GTPase proteins play a central role. Importantly, both Rho GTPases and actin are sensitive to oxidative

thiol modifications. Among the several potential sites on the actin molecule that are sensitive to redox modifications, $Cys^{374}$ is of particular functional importance since its oxidation and glutathionylation have been associated with decreased actin polymerization. However, it has also been described that ROS production by EGF was correlated with actin deglutathionylation, resulting in increased actin polymerization. Possibly, the role of this actin thiol residue in cell migration is dependent on the cell type (Stanley et al., 2013; Schröder, 2014). Something similar happens when considering the correlation between ROS and Rho GTPases activation, since some studies suggest that increased ROS production is correlated to RhoA activation, whilst others point to an increase in Rac1 activation.

Focal adhesions (FA) can also be modulated by NOX-derived ROS, since it has been described that at least NOX1 and NOX4 can co-localize with focal adhesion complexes (Hilenski et al., 2004). For example, FAK, which, is a master regulator of adhesion turnover, is maintained in an inactive, dephosphorylated form by the constitutive action of the redox-sensitive tyrosine phosphatases (LMW-PTP and SHP-2) (Mitra et al., 2005).

Considering all the processes regulated by NOXs, it is reasonable to associate some **diseases** to the misregulation or absence of certain NOX. The earliest discovery was an immune disorder, chronic granulomatous disease (CGD), caused by the absence of active NOX2 or its subunits. Patients with CGD exhibit chronic infections and impaired wound healing (Segal et al., 2009). NOX-derived ROS have been also implicated in the pathogenesis of a number of neurological disorders, including Parkinson and Alzheimer's diseases (Hernandes and Britto, 2012), cardiovascular disorders such as atherosclerosis and hypertension (Sirker et al., 2011; Montezano and Touyz, 2014), fibrotic processes (Paik and Brenner, 2011; Hecker et al., 2012) and cancer (Bonner and Arbiser, 2012; Weyemi et al., 2013), among others. Implication of NOX proteins in liver disorders will be further discussed in a following section (**Section 4.6**).

### 4.4.4. NOX inhibitors

An important tool for the validation of potential therapeutic targets and proof of principle studies is the pharmacological inhibition of NOX proteins by small chemical compounds. Several compounds have been used for many years, including apocynin, diphenylene iodonium (DPI), and 4-(2-aminoethyl)-benzensulfonylfluorid (AEBSF). However, it has become apparent that these inhibitors are **not specific** for NOX proteins. Apocynin is not a NOX inhibitor but rather a pro-drug with antioxidant actions. It forms adducts with p47phox as well as apocynin multimers which are reported to act as NOX inhibitors through an unknown mode of action. DPI is a general flavoprotein inhibitor, therefore a potent but totally non-specific inhibitor of all NOX enzymes, as well as of other flavoproteins such as cytochrome p450 monooxygenases, xanthine oxidases and NO synthases. It also blocks some proteins of the mitochondrial

respiratory chain. And finally, AEBSF is primarily a serine protease inhibitor (Altenhofer et al., 2012; Brandes et al., 2014a).

Other reported NOX inhibitors are **antioxidants** like ebselen, plumbagagin or fluvene-5, making it difficult to attribute their effects specifically to NOX inhibition (Brandes et al., 2014a).

Recently, several NOX and even **isoform-specific** NOX inhibitors have been published. Vasopharm GmbH developed VAS2870, a triazolo pyrimidine well validated as a NOX inhibitor, as it shows no intrinsic antioxidant activity and does not inhibit other flavoproteins, but it is not NOX isoform-specifc. Apparently, it directly modifies thiols like the ones in p47phox, thus inhibiting NOX1 and NOX2. Some studies also suggest that it can inhibit NOX4 and NOX5 by inhibiting an intra-molecular interaction of different domains of the proteins. Moreover, it has also been described some significant off-target effects (Altenhofer et al., 2012; Brandes et al., 2014a). GenKyoTex developed GKT136901 and GKT137831 in a high-throughput screening for NOX4 inhibitors. GKT compounds potently inhibit NOX1, NOX4 and NOX5, with not known off-target effects, through an unknown mechanism. Importantly, GKT137831 is already in clinical development. In addition, ML171 is another promising hit for NOX1 inhibition, however the pharmacokinetics and safety data available likely enable the use of this compound *in vivo* (Altenhöfer et al., 2014). So far, there are still **no NOX4 specific inhibitors** described.

# 4.5. NADPH oxidase NOX4

## 4.5.1. Structure and activity

The NADPH oxidase homologue NOX4 was originally identified as a NOX homolog highly expressed in the kidney (Geiszt et al., 2000; Shiose et al., 2001) and it is an exception within the family. The enzyme has **constitutive activity**, and so far, no essential cytosolic interacting proteins or other activating mechanisms have been identified. Structurally, NOX4 associates with **p22phox**, but in a different form from NOX1 and NOX2 (von Löhneysen et al., 2010).

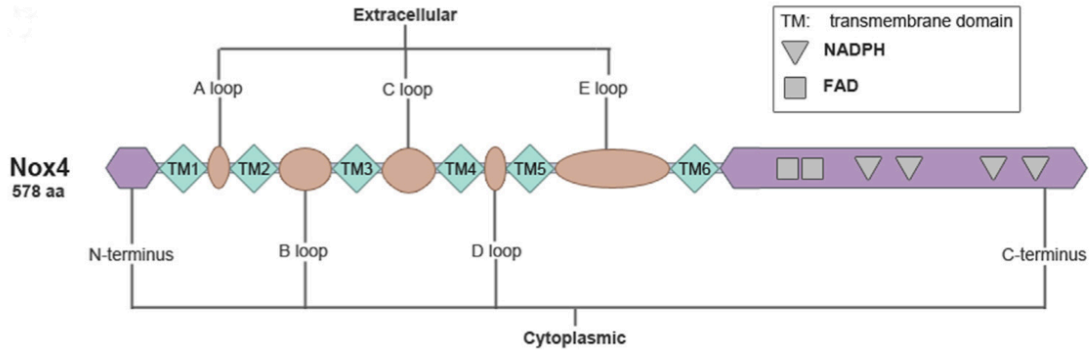


**Figure XIII.** NOX4 protein domain map (Choi et al., 2014).

The activity of NOX4 has generally been thought to be constitutive and thus mRNA formation determines ROS production (Serrander et al., 2007). However, also mRNA stability, translation efficiency and protein stability of NOX4 are controlled (Peshavariya et al., 2009). NOX4-derived ROS production can be enhanced by the binding of Poldip2 to p22phox in the NOX4 complex (Lyle et al., 2009). Another possible interesting interaction facilitates NOX4 degradation. This occurs, at least in some part, through ubiquitination in a process involving the ubiquitin ligase CBl-c, Hic-5 and HSP27 (Desai et al., 2014). Despite this, it is generally believed that the predominant controller of NOX4-dependent ROS formation is the expression level of the enzyme. Indeed, expression control is of particular importance in **TGF-β signalling** since it has been identified as the strongest inducer of NOX4 expression (Sturrock et al., 2007). In addition, several studies focussing on acute agonist-stimulated ROS production, for example responses to angiotensin-II (Dikalov et al., 2008) or bFGF (Schröder et al., 2007), showed that they are mediated by other NOX enzymes, and NOX4 only mediates basal cellular radical formation. Indeed, genetic deletion of NOX4 reduces the constitutive basal ROS formation of murine vessels (Schröder et al., 2012) and kidneys (Babelova et al., 2012). Some reports attribute an acute Rac-dependent ROS production to NOX4, although this is incompatible with

the absence of a Rac-binding site in the protein. A potential explanation for these findings is that Rac does not directly activate NOX4 but alters pathways which control NOX4 degradation or localization through changes in the cytoskeleton (Brandes et al., 2014a).

### 4.5.2. NOX4 localization

The **intracellular localization** of NOX4 is still a matter of discussion. On the one hand, NOX4 localization may vary between cell types and changes with the differentiation state. On the other hand, good enough commercially available antibodies are still missing. Nevertheless, NOX4 expression has been reported for nucleus, perinuclear space, lipid rafts, mitochondria, plasma membrane and endoplasmic reticulum (Helmcke et al., 2009). Moreover, NOX4 has been located in protrusions and focal adhesion of smooth muscle cells in association with vinculin (Hilenski et al., 2004). Importantly, five **splice variants** have been reported for NOX4, NOX4 A-E. NOX4B isoform lacks the first NADPH binding site while NOX4C lacks all FADH and NADPH binding sites. Cells over-expressing both isoforms exhibited a decrease in ROS levels. Finally, NOX4D and NOX4E lack the transmembrane domains, suggesting these as non-membrane associated isoforms. Of special relevance seems to be NOX4D because it contains all FADH and NADPH binding domains, shows the same rate of ROS generation as NOX4 prototype and it is shown to be expressed in the nucleus (Goyal et al., 2005; Anilkumar et al., 2013). Deeper analyses of these splice variants might be the key to understand the different subcellular localizations of the enzyme, as well as a potential explanation of the different functions reported for NOX4. Interestingly, changes in the localization of NOX4 have been associated with activation of the enzyme. For example, insulin stimulates a rapid surface localization of NOX4 in podocytes (Kim et al., 2012).

### 4.5.3. NOX4 expression and functions

An important feature of NOX4 is its **ubiquitous expression**. NOX4, as we said before, is highly expressed in the kidney, but it has also been reported to be expressed in other cell types including mesangial cells, smooth muscle cells, endothelial cells, fibroblasts, keratinocytes, osteoclasts, neurons, and hepatocytes (Brown and Griendling, 2009; Paletta-Silva et al., 2013). Especially in differentiated cells, NOX4 is highly expressed, and potentially NOX4 itself may be necessary for the process of **differentiation**. Indeed, in some mesenchymal cells, in particular MFB and smooth muscle cells (SMC), as well as in cells of the adipocyte linage and chondrocytes, it has been suggested that NOX4 drives the differentiating process itself (Clempus et al., 2007; Schröder et al., 2009; Kim et al., 2010b; Kanda et al., 2011). This idea is supported by the fact that NOX4-dependent ROS production is relatively low and directly correlates with the expression level of NOX4. Differentiation of a cell reduces their mobility, somehow appears to cause quiescence, and opposes activation and proliferation.

NOX4 may contribute to the maintenance of a differentiated state of the cell and thus prevents activation or proliferation (Schröder et al., 2012).

Nevertheless, in addition to cell differentiation, NOX4-derived ROS have been implicated in a variety of physiological processes, including cellular senescence, apoptosis, survival and migration (Brown and Griendling, 2009).

It has been described an important role for NOX4 **mediating TGF-β effects**. In cardiac fibroblasts (Ellmark et al., 2005), lung (Sturrock et al., 2007) and pulmonary artery SMC (Sturrock et al., 2006) and hepatocytes (Carmona-Cuenca et al., 2006), among many other cell types, TGF-β induces NOX4 expression, in a Smad3 dependent manner (Hecker et al., 2009; Bondi et al., 2010; Jiang et al., 2012). NOX4 expression in response to TGF-β plays different roles depending on cell type. Treatment of pulmonary artery SMC with TGF-β promotes proliferation through the expression of NOX4 (Sturrock et al., 2006). NOX4 also mediates TGF-β-induced phosphorylation of Rb and the eukaryotic translation initiation factor 4E (eIF4E) binding protein-1, which regulate cell cycle progression and hypertrophy, respectively, in airway smooth muscle cells (Sturrock et al., 2007). We mentioned before that NOX4 mediates cell senescence. Indeed, it mediates TGF-β-induced senescence both in liver and kidney (Senturk et al., 2010; Hubackova et al., 2012). Importantly for the work presented here, NOX4 plays a key role in TGF-β-induced fibroblast differentiation into MFB (Cucoranu et al., 2005; Amara et al., 2010; Sampson et al., 2011), a process that will be further described later on. Furthermore, TGF-β-induced NOX4 expression is required for TGF-β-induced cell death in hepatocytes, HCC cells and mouse hepatic oval cells (Carmona-Cuenca et al., 2008; Caja et al., 2009; Martínez-Palacián et al., 2013), as well as in podocytes (Das et al., 2014) and endothelial cells (Yan et al., 2014). In the liver, NOX4 mediates TGF-β-induced apoptosis through the liver-specific tumour suppressor STAT5 and the modulation of the expression of key pro-apoptotic genes, such as PUMA, BIM and BMF (Caja et al., 2009; Yu et al., 2012). Moreover, in endothelial cells, NOX4 and ROS have a pivotal role in mediating TGF-β dependent apoptosis and phenotype specification by modulating p38, PTP1B/VEGF/AKT and Notch signalling pathways (Yan et al., 2014). Finally, it has been recently described that ROS and NOX4 may also participate in the TGF-β-induced EMT in several epithelial cell types (Boudreau et al., 2012; Lee et al., 2013b; Hiraga et al., 2013; Prasanphanich et al., 2014). At the same time, NOX4 mediates phenotypic changes induced by TGF-β in vascular smooth muscle cells via activation of p38/serum response factor (SRF)/myocardin-related transcription factor (MRTF) pathway (Martin-Garrido et al., 2011).

Of interest for the work presented here, NOX4 signalling has been linked to the **cytoskeleton**. Most of the work done until now is basically related to vascular smooth muscle cells. It has been suggested that NOX4 could be associated with cytoskeletal structures such as vinculin, in this type of cells (Hilenski et al., 2004). In the same cell type, NOX4-Poldip2 complex may regulate RhoA signalling, thus influencing cell migration (Lyle et al., 2009). Indeed, it has been recently demonstrated that Poldip2 participates in VSMC migration via regulation of focal

adhesion turnover and traction force generation in a NOX4/RhoA/FAK dependent manner (Datla et al., 2014). Also in metabolic-stressed monocytes, NOX4 appears to regulate cell adhesion and migration through its association with FAK, Paxillin and actin (Ullevig et al., 2012; Lee et al., 2013a). Finally, it has also been shown that NOX4 may mediate TGF-β induced cytoskeletal changes in endothelial cells (Hu et al., 2005). Interestingly, both down-regulation and overexpression of NOX4 have been suggested to inhibit migration. In addition, *in vitro* studies point toward an important role of NOX4 *in vivo* in processes that involve cell migration, such as angiogenesis (Schröder, 2014). Indeed, in a NOX4-deficient mouse angiogenesis is reduced. Of note, NOX4 also contributes to the expression of pro-migratory stimuli such as VEGF (Zhang et al., 2010; Schröder et al., 2012).

Many reports suggest a role for NOX4 in **senescence**. In fact, one of the first observation after the discovery of the enzyme was that NIH3T3 fibroblasts overexpressing NOX4 developed signs of cellular senescence (Geiszt et al., 2000). In addition, as we said before, NOX4 is highly expressed in the kidney, where it has also been reported to mediate senescence (Baltanás et al., 2013). Moreover, NOX4 also mediates angiotensin II induced senescence in late endothelial progenitor cells (Li et al., 2011). And, together with NOX1, NOX4-generated ROS mediate senescence in endothelial cells (Schilder et al., 2009), as well as Ras induced senescence, through a mechanism involving DNA damage response and p38 signalling pathway (Weyemi et al., 2012; Kodama et al., 2013).

On the other hand, several reports have shown that NOX4-derived ROS are responsible of mediating **proliferation and survival** in response to different stimuli. Treatment of VSMC with urokinase plasminogen activator results in NOX4-mediated growth and survival (Menshikov et al., 2006). In addition, the vasoactive peptide Urotensin II stimulates proliferation of VSMC through a mechanism involving NOX4/FOXO3a/MMP2, contributing to the progression of vascular diseases associated with vascular remodelling (Diebold et al., 2011). NOX4 is also involved in proliferation in hypoxia-mediated activation of pulmonary adventitial fibroblasts (Li et al., 2008). Growth and survival effects of NOX4 activation have been reported to be mediated by AKT in mesangial cells stimulated with angiotensin II (Gorin et al., 2003), and also through the oxidation-mediated activation of Src (Block et al., 2008). In addition, it has been described a positive feedback loop between NOX4 and PI3K/AKT signalling that contributes to promote proliferation of non-small lung cancer cells (Zhang et al., 2014). Moreover, in pancreatic cancer, NOX4 promotes activation of JAK/STAT pathway in order to enhance the growth response (Lee et al., 2007). NOX4 also plays a role in VEGF-stimulated ERK phosphorylation (Datla et al., 2007), and may also be involved in mediating ERK activation in response to PDGF (Wagner et al., 2007). In endothelial cells, NOX4 is induced upon Prostacyclin stimuli enhancing cell proliferation and angiogenesis (Peshavariya et al., 2014). Moreover, upon TNF-α stimuli NOX4 may mediate both apoptosis and survival in cerebral microvascular endothelial cells, being the survival effects mediated by the endogenous antioxidant carbon monoxide (CO), which is able to inhibit the TNF-α induced ERK and p38 MAPK activities (Basuroy et al., 2011). Finally, autophagy, which is considered an essential survival mechanism during energy stress in the

heart, is promoted by endoplasmic reticulum localized NOX4 in cardiomyocytes (Sciarretta et al., 2013). In addition to the pro-growth effects, in some systems, NOX4 may also mediate anti-apoptotic actions. For example, in pancreatic cells NOX4-derived ROS induced by growth factors have an anti-apoptotic role, since the depletion of NOX4 or ROS promotes apoptosis (Vaquero et al., 2004). Indeed, it has been demonstrated that this NOX4 activation involves transcription up-regulation of p22phox in a NF-κB/AKT dependent manner (Edderkaoui et al., 2011). Moreover, VEGF-induced ROS from NOX proteins (NOX2 and NOX4), increased leukemic cell proliferation and protected cells from apoptosis (Maraldi et al., 2010).

On the contrary, NOX4 has also been associated with **cell death**. NOX4 not only mediates TGF-β induced apoptosis in different models as mentioned before, but also mediates apoptosis induced by other stimuli. It has been described that high insulin level-induced apoptosis involves NOX4-generated oxidative stress and the down-regulation of a complex receptor signalling, involving ERK1, IGF1R and FGFR1 (Scioli et al., 2014). NOX4 also mediates BMP4 induced apoptosis in endothelial cells in a p38MAPK/JNK dependent manner (Tian et al., 2012). A study done in mice deficient in NOX4 ($Nox4^{-/-}$) of either sex demonstrated that those animals are largely protected from oxidative stress, blood-brain-barrier leakage and neuronal apoptosis, after both transient and permanent cerebral ischemia, and that post-stroke inhibition of NOX can be protective (Kleinschnitz et al., 2010). Moreover, using another mice model, in this case cardiac specific Nox4 knock-out mice, it was demonstrated that NOX4 also mediates apoptosis in cardiac myocytes, in addition to hypertrophy and interstitial fibrosis, in response to pressure overload (Kuroda et al., 2010). Finally, Heme-oxygenase-1 (HO-1), the limiting enzyme in the heme catabolism, induced cell death in chondrocytes via NOX4 (Rousset et al., 2013).

### 4.5.4. Role of NOX4 in different disorders

Apart from the different roles stated before, NOXs have also been described to play a role in different **chronic diseases** that are often associated with tissue damage and fibrosis (Lambeth et al., 2007). NOX4 has been proposed to contribute to tissue destruction in asthma (Hoidal et al., 2003). Interestingly, NOX4 induction in response to Urotensin II markedly increases ROS levels contributing to smooth muscle hypertrophy and proliferation associated to pulmonary hypertension (Djordjevic et al., 2005). Later on, it was described that TGF-β-induced expression of NOX4 in pulmonary artery smooth muscle cells, was probably involved in the development of pulmonary hypertension (Sturrock et al., 2006). NOX4-derived ROS have been also associated with pressure overload pulmonary hypertension, contributing to ventricular dysfunction and failure (Frazziano et al., 2014). Both NOX1 and NOX4 have been implicated in mitogenesis and hypertrophy in the cardiovascular system, and therefore might participate in atherosclerosis and hypertension (Brandes, 2003; Brandes and Schröder, 2008; Montezano et al., 2011). Others studies have implicated NOX4 as a major source of ROS in many cell types

and in kidney tissue of diabetic animals (Etoh et al., 2003; Block et al., 2009; Gorin and Block, 2013). Indeed, NOX-derived ROS have been implicated in the development of diabetic nephropathy and a renoprotective effect has been suggested for a NOX1/NOX4 inhibitor in a Type 2 diabetes mouse model (Sedeek et al., 2013; Jha et al., 2014). Moreover, NOX4-derived ROS also contribute to cardiomyopathy at early stages of Type I diabetes (Maalouf et al., 2012). Finally, several lines of evidence suggest that NOX enzymes are involved in promoting fibrotic responses in different organs such as kidney, liver and heart, leading to adverse pathological events (Lambeth et al., 2007). In contrast to previous reports, where NOX4 was mediating TGF-β effects via Smad3, it has been recently reported that TGF-β may mediate kidney myofibroblast activation through RhoA/ROCK pathway activation, which in turn regulates Poldip2/NOX4-derived ROS production (Manickam et al., 2014). Of note, it has been reported that NOX4 inhibition may not only impair the initiation of fibrotic processes but also attenuate established fibrosis (Jarman et al., 2014; Hecker et al., 2014). The implication of oxidative stress and NOX proteins in liver fibrosis will be further discussed in the next section.

Finally, NOX4 has also been implicated in **cancer**. Actually, it has been shown to be expressed in several cancers such as melanoma (Yamaura et al., 2009; Liu-Smith et al., 2014), pancreatic cancer cells (Vaquero et al., 2004; Lee et al., 2007), glioblastoma (Shono et al., 2008; Hsieh et al., 2011; Mondol et al., 2014), prostatic cancer (Lu et al., 2010), non-small cell lung cancer (Zhang et al., 2014), HCC (Choi et al., 2014) and thyroid cancer (Weyemi et al., 2010).

# 4.6. Involvement of NOX-derived ROS in liver diseases

ROS are critical intermediates in both the normal physiology and pathological conditions of liver cells. When the equilibrium between ROS generation and the antioxidant defence of cells is disrupted, it results in oxidative stress.

Both **parenchymal and non-parenchymal** hepatic cells express different members of the NOX family. Thus, hepatocytes and hepatic stellate cells (HSC), either activated or non-activated, express NOX1, NOX2, NOX4, DUOX1 and DUOX2; endothelial cells express mainly NOX1, NOX2 and NOX4; and Kupffer cells, which are hepatic-resident macrophages, express the phagocyte NADPH oxidase NOX2 (Guichard et al., 2008; Paik et al., 2013).

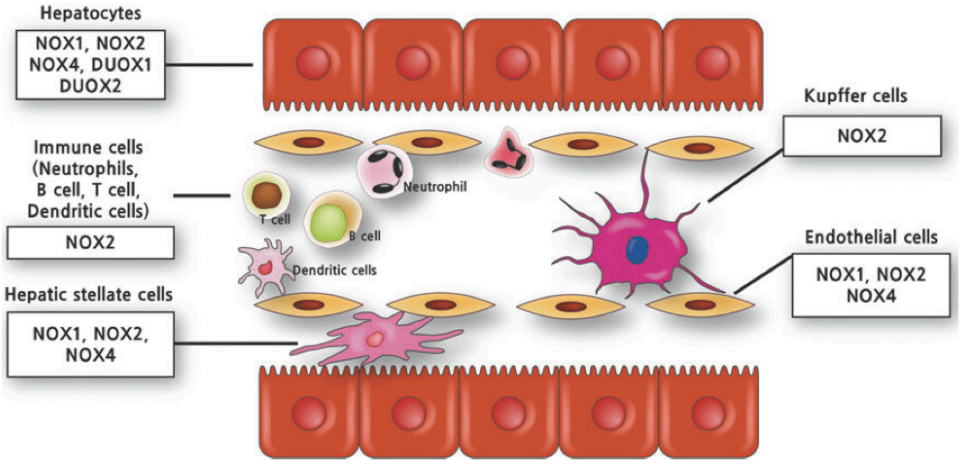


**Figure XIV.** Cellular distribution of NOX isoforms in the liver (Paik et al., 2013).

Until now, little is known about the **physiological roles** of NOX enzymes in liver. However, NOX2 in Kupffer cells should play a similar role to the one played in other macrophages. Thus, a role in killing microorganisms, participation of inflammatory response and possibly also cellular signalling, are the most likely functions of NOX2 in these cells. Indeed, NOX2-derived ROS have been suggested to clear pathogens derived from the gut as well as being essential mediators in antigen presentation by Kupffer cells. In addition, they are also involved in the regulation of gene expression of CD95 (Fas) ligand (CD95L) and NF-κB-dependent production of TNF-α, that can eventually influence on hepatocytes (Bedard and Krause, 2007).

Concerning **HSC**, they generate ROS in response to various stimuli, particularly TGF-β, that play a relevant role during liver fibrosis. However, it is not known whether NOX enzymes develop other roles in these cells.

**Hepatocytes** generate ROS in response to a wide variety of endogenous and exogenous stimuli but not all of them are mediated by NOX enzymes because other systems such as mitochondria, cytochrome p450 enzymes, ER oxidoreductases and cytosolic peroxisomal and xanthine oxidases can also generate ROS in hepatocytes. However, ROS generation in response to at least capsaicin, tamoxifen, CD95L and TGF-β appears to be NOX mediated (Bedard and Krause, 2007). In hepatocytes, ROS, and potentially NOX enzymes, induce a number of functional adaptive changes in the capability of hepatocytes to produce bile and to secrete exogenous and endogenous compounds (Guichard et al., 2008). However, the main function attributed to NOX-derived ROS in hepatocytes is apoptosis. Thus, both CD95L and TGF-β were shown to lead to hepatocyte cell dead through a mechanism involving NOX-derived ROS.

It has been reported that NOX-mediated ROS contributes to various **liver diseases** (Paik et al., 2013). **Hepatic inflammation** accompanies the majority of acute and chronic liver disorders and it is a complex process that originates in response to a variety of stress conditions. Dysregulated inflammatory responses have been associated with most (if not all) hepatotoxic insults, including ischemia/reperfusion (IR) injuries; alcohol overconsumption; intoxications by xenobiotics or heavy metals; bacterial, viral and parasitic infections; as well as systemic metabolic conditions, such as NAFLD, NASH, obesity, diabetes, and the metabolic syndrome (Brenner et al., 2013).

As mentioned above, ROS have been shown to play a central role in mediating effects of **hepatitis virus** core proteins (Perlemuter et al., 2003; Dionisio et al., 2009). Concerning HCV infection, it has been shown to induce oxidative stress through modulation of NOXs in different cell types within the liver. HCV is known to activate the phagocytic NOX2. In addition, it also increases NOX1 and NOX4 mRNA and protein levels in hepatocytes, where HCV has the primary site for replication. Indeed, a dominant negative NOX4 containing a C-terminus deletion, NOX4 or NOX1 knock-down, and DPI, a well-known flavoprotein inhibitor, significantly decreased HCV-induced superoxide and/or hydrogen peroxide production in hepatocytes. Moreover, HCV activated human and murine promoter activity in hepatocytes. Interestingly, HCV increased levels of TGF-β in these cells, which is responsible for inducing NOX4 transcription (Boudreau et al., 2009; de Mochel et al., 2010; Choi et al., 2014). Of note, the nuclear and perinuclear localization of NOX4 was increased with HCV in hepatocytes (de Mochel et al., 2010). Furthermore, not only in hepatocytes but also in HSC, HCV was shown to induce TGF-β transcription through a redox-sensitive mechanism involving NF-κB, AP-1, Sp1, and STAT3 (Presser et al., 2013). HCV induces a marked increase in ROS production in human HSC, an effect that is attenuated by DPI (Bataller et al., 2004). However, the NOX isoforms involved in HCV-induced responses in HSC are not yet identified. In addition, the mechanism by which HCV increases NOX1 is still unknown.

Of note, oxidative stress during chronic liver diseases due to increased ROS production as well as decreased activity of antioxidant systems is not only a consequence of chronic liver injury but also significantly contributes to excessive **tissue remodelling and fibrogenesis** (De Minicis and Brenner, 2007). Mitochondria play a role in ROS production in the liver, since hepatocytes contain hundreds of these organelles and the mitochondrial electron transport is disrupted in a great number of pathophysiological circumstances, resulting in increased electron leak (Murphy, 2009). However, perhaps the main sources of ROS implicated in liver fibrosis are NOXs.

One of the most studied mechanisms of fibrogenesis influenced by ROS is myofibroblast activation, and indeed, it was suggested that NOX proteins would be mediating TGF-β effects on myofibroblasts activation in some systems. NOX-derived ROS have been previously related to fibrosis in several organs such as lung (Hecker et al., 2009), pancreas (Masamune et al., 2008), kidney (Sedeek et al., 2010; Bondi et al., 2010) and heart (Cucoranu et al., 2005). High concentrations of ROS induce HSC dead, however, non-toxic levels of ROS stimulate the activation, proliferation, and collagen production of HSC (Paik et al., 2013). Indeed, in the liver, **HSC transdifferentiation** was shown to be inhibited by antioxidants (Foo et al., 2011; Abhilash et al., 2012). In addition, several reports have demonstrated a key role for NOX proteins in the progression of hepatic fibrosis (De Minicis et al., 2010; Cui et al., 2011; Paik et al., 2011). It has been shown that in HSC, NOX proteins mediate fibrogenic responses induced by various agonists, including angiotensin II, PDGF, leptin, TGF-β and phagocytosis of apoptotic bodies (Paik et al., 2013). As mentioned before, TGF-β is the strongest agonist for HSC activation, and it is released mainly from Kupffer cells. In addition, studies in HSC from p47phox$^{-/-}$ mice demonstrated that angiotensin II stimulates TGF-β production and type I collagen expression in HSC, exerting direct profibrogenic actions on HSC through the activation of the NOX complex and subsequent production of ROS (Paik et al., 2013). Importantly, studies performed in NOX1$^{-/-}$, NOX2$^{-/-}$, or p47phox$^{-/-}$ mice have pointed out the importance of NOX1 and NOX2 in fibrosis development (De Minicis et al., 2010; Jiang et al., 2010; Cui et al., 2011; Paik et al., 2011).

Recent findings also implicate the tumour suppressor p53 as a critical co-factor for several key fibrotic and cell cycle effectors (e.g., TGF-β, CTGF, PAI-1, p21 and angiotensin). Increased oxidative stress associated with the fibrotic process is both a likely initiator and an upstream mediator of p53 signalling in the injured tissue (Samarakoon et al., 2013b). Although appears that p22phox is implicated in the process, it still needs to be proven that a NOX protein is responsible of this ROS production.

Finally, promotion of **hepatocyte apoptosis** is another crucial event during fibrogenesis since it triggers Kupffer cell and HSC activation by secreting cytokines, chemokines and microparticles. Our group described some years ago that TGF-β induces hepatocyte apoptosis through ROS that are derived from both mitochondria and NOX activity (Herrera et al., 2004).

Based on the knowledge of the pathogenic role of ROS and more precisely the role of NOX-derived ROS in hepatic fibrogenesis, the development of novel pharmacological NOX inhibitors is being assessed as potential anti-fibrotic therapeutics. However, the collateral inhibition of some physiological functions of NOX should be considered.

It is worthy to remember that liver fibrosis can lead to cirrhosis, a condition that highly predisposes to develop liver cancer. The hallmarks of cancer were classified by Hanahan and Weinberg some years ago (sustaining proliferative signalling, evading growth suppressors, resisting cell death, enabling replicative immortality, inducing angiogenesis, and activating invasion and metastasis) (Hanahan and Weinberg, 2000; Hanahan and Weinberg, 2011). It has been demonstrated that ROS derived from NOXs can modulate all these hallmarks of cancer (Weinberg and Chandel, 2009; Block and Gorin, 2012). NOX dictate carcinogenesis through the regulation of several cell signalling pathways related to carcinogenesis that respond to stress signals, such as JAK-STAT, protein Kinase C, MAPK and AKT (Paletta-Silva et al., 2013).

When considering the particular case of **liver cancer**, evidence suggests that oxidative stress is a common pathogenic feature in diverse models of HCC. However, what most of the studies showed were altered levels of antioxidants or antioxidant gene expression. For instance, mice deficient in cooper-zinc superoxide dismutase (CuZn SOD, $sod1^{-/-}$) exhibited increased incidence of nodular hyperplasia and HCC (Elchuri et al., 2005). Moreover, liver-specific nuclear factor erythroid-2-related transcription factor-1 (Nrf1) knock-out mice developed liver cancer in 100% of both male and female animals, together with increased lipid peroxidation and oxidative DNA damage (Xu et al., 2005).

In addition, oxidative stress due to increased mitochondrial ROS production has also been reported in animal models of liver cancer, such as DEN- and 12-*o*-tetradecanoylphorbol 13-acetate (TPA)-induced hepatocarcinogenesis. In both cases antioxidants like N-acetylcysteine (NAC) or butylated hydroxyanisole (BHA), or the flavoprotein inhibitor DPI attenuated carcinogenesis and HCC progression (Choi et al., 2014).

Concerning NOX proteins, increased levels of NOX subunits p47phox, p67phox and Rac1 were found increased in pre-neoplastic and neoplastic lesions from c-Myc, TGF-$\alpha$ and c-Myc/TGF-$\alpha$ transgenic mice, where HCC developed with elevated ROS and decreased GSH in hepatocytes (Choi et al., 2014).

Chemical **mutagenesis of DNA**, leading to the mutations of critical cellular genes, it is likely to be a key mechanism whereby oxidative stress contributes to hepatocarcinogenesis. Oxidative stress induces hepatic 8-Hydroxydeoxyguanosine (8-OHdG), which is a product of redox-mediated DNA damage that has been found increased in HCC, and might be responsible to induce G:C to T:A transversions, frequently observed in cancers (Schwarz et al., 2001). The discovery that NOX4 is present in or around the nucleus, especially when there is concomitant

chronic HCV infection, together with increased levels of NOX subunits in HCC models, suggest that NOX activity may increase the probability of DNA damage in the liver.

Another important process occurring during hepatocarcinogenesis, as well as we said it occurs during fibrogenesis, is **inflammation**. Recent studies indicate that TLR4 is a key factor in HCC. It has been shown that TLR4 and intestinal microbiota are not required for HCC initiation but for HCC promotion, mediating increased proliferation and preventing apoptosis (Yu et al., 2010; Dapito et al., 2012). Toll-like receptors are known to participate in the inflammatory response in the liver. Indeed, the extracellular domain recognizes the corresponding ligands having either pathogen-associated molecular pattern or damage-associated molecular pattern, and the cytosolic domain mediates down-stream signal transduction to produce interferon (IFN)-$\alpha$/-$\beta$ or pro-inflammatory cytokines (Paik et al., 2013). In macrophages, ROS play an important role in LPS/TLR4 signalling, that was demonstrated by using NOX inhibitors (DPI and apocynin) or siRNA against p22phox (Martinon et al., 2010). NOX2/p47phox is a key mediator of LPS/TLR4-stimulated ROS generation in polymorphonuclear cells and macrophages (DeLeo et al., 1998; Choi et al., 2014). In addition, LPS induces the expression of NOX1 through TLR4 in the same cells (Kim et al., 2010a). Moreover, a yeast-two hybrid assay and GST-pull-down assay demonstrated that the C-terminal domain of NOX4 interacts with the cytosolic domain of TLR4 (Park et al., 2004a). Furthermore, the 28KDa NOX4 splice variant (NOX4D) was shown to co-immunoprecipitate with TLR4 (Ben Mkaddem et al., 2010). However, whether NOX proteins are involved in TLR4 signalling in hepatocytes is still unknown.

Importantly, inflammation, apoptosis and regenerative DNA synthesis subsequent to DEN-induced liver damage were diminished in p47phox$^{-/-}$ mice. Indeed, it was shown that DEN had a direct stimulatory effect on Kupffer cells to release superoxide and TNF-$\alpha$ during liver damage and inflammation, which aggravated the genotoxic and cytotoxic effects in hepatocytes, contributing to tumour initiation and promotion, effects that were attenuated in mice deficient in p47phox (Teufelhofer et al., 2005). However, a recent study using the same mice model demonstrated that the production of superoxide might be more relevant for the promotion than for the initiation of the hepatocarcinogenesis (Parzefall et al., 2014).

Some work done by **our group and others** demonstrated that NOX-derived ROS have relevant roles in hepatocarcinoma cells, mainly mediating **TGF-β effects**. TGF-$\beta$ induces the expression of both NOX1 and NOX4 in transformed hepatocytes. NOX4 mediates apoptosis induced by TGF-$\beta$ in HCC cells (Carmona-Cuenca et al., 2008; Caja et al., 2009; Yu et al., 2012), and overactivation of the MEK/ERK pathway in liver tumour cells confers resistance to the TGF-$\beta$-induced cell death through impairing NOX4 up-regulation (Caja et al., 2009). Importantly, TGF-$\beta$ also induces senescence in well-differentiated HCC cells through a mechanism involving NOX4 and p21 (Senturk et al., 2010). On the contrary, NOX1 confers partial resistance to TGF-$\beta$-induced apoptosis, through the activation of the EGFR pathway (Sancho et al., 2009).

# 5. Cell migration, invasion and metastasis

**Cancer metastasis** is a highly complex multistep process that involves alterations in growth, angiogenesis, dissemination, invasion and survival, which leads to a subsequent attachment and growth of new cancer cell colonies (Budhu et al., 2005). The initial steps of local invasion include the activation of signalling pathways that control cytoskeletal dynamics in tumour cells and the turnover of cell-to-matrix and cell-to-cell junctions, followed by active tumour cell migration into the adjacent tissue (Friedl and Alexander, 2011).

**Cell migration** is a highly organized process and highly dependent on the actin cytoskeleton dynamics. Actin cytoskeleton is composed of microfilaments scattered throughout the cell from the apical to the basal regions and it is a major component of the whole cytoskeleton. Globular actin (G-actin) is polymerized and compiled in an adenosine triphosphate (ATP)-dependent process to form a helical filamentous structure known as F-actin. F-actin molecules display a distinct polarity in their structure with positive and negative ends, being the positive end (also known as the plus or barbed end) the one that favours the addition of monomers, and the negative end (pointed or minus end) the one that favours the loss of subunits or depolymerisation of F-actin (Stanley et al., 2012).

# 5.1. Types of cell migration

Cells can migrate as collective groups or as individual cells. Two modes of **individual cell migration** have been characterized in a number of systems: an elongated "mesenchymal-like" mode and a rounded "amoeboid" mode of cell migration. **Mesenchymal migration** has been largely studied in two-dimensional systems and is typical of single cells migrating individually while adhering to a surface. It is characterized by cell polarization, requirement for extracellular proteolysis and low actomyosin contractility. Cells largely depend on actin polymerization and depolymerisation that provoke sequential accumulations of actin at the front of the cell, including protrusions such as filopodia, lamelipodia, and membrane ruffles, and retraction at the rear, for achieving a directed cell movement. In addition, actin stress fibers are connected to focal adhesions and with them form a cellular network that is both a generator and a sensor of mechanical force (Stanley et al., 2013). On the contrary, in **amoeboid migration**, which predominantly occurs in cancer cells, cells do not strongly adhere to the extracellular matrix. Instead, they adopt a rounded morphology and rely on actin-myosin contractility for propulsion. This enables them to actively migrate through three-dimensional environments (Stanley et al., 2013). In addition to individual movement, cells can migrate collectively by a coordinated movement of cells as strands, sheets or clusters. Similarly to single-cell migration, **collective cell movement** results from actomyosin polymerization and contractility coupled to cell polarity; however, in the collective movement, cells remain coupled by cell-to-cell junctions at the leading edge as well as in lateral regions inside the moving cell group and the leading cells generate movement through the use of cellular protrusion (similar to mesenchymal migration) (Ilina and Friedl, 2009; Stanley et al., 2013). Importantly, plasticity of inter-convertibility between different forms of migration and cell morphology facilitates tumour cells to metastasize.

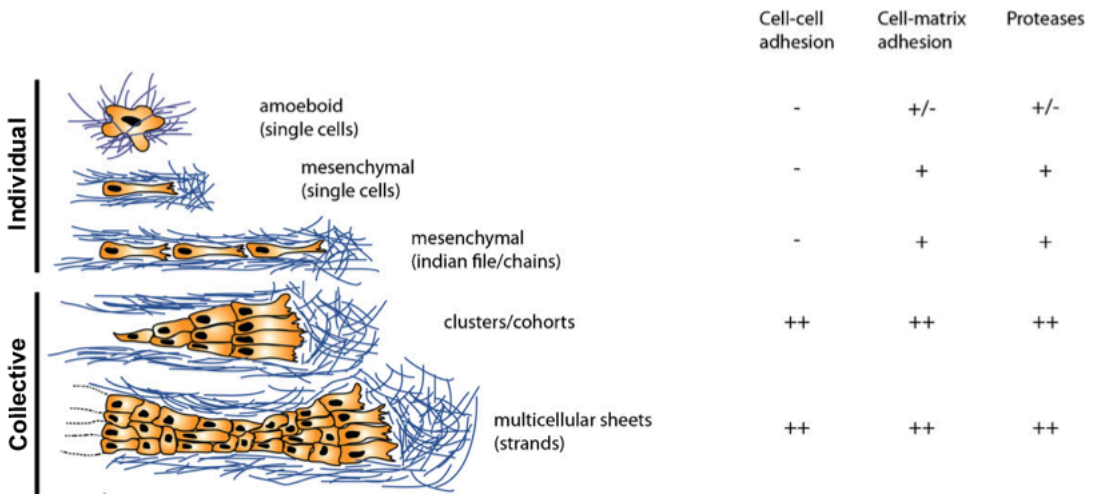


**Figure XV.** Types of cancer cell migration and its characteristics (Spano et al., 2012).

Variations in the physical properties of the environment activate cellular mechano-sensors, which can generate transcriptional responses in the cell, impacting on cell fate, cell shape, and migration. The orchestrated remodelling of the actin cytoskeleton requires spatial and temporal changes in **adhesion to the ECM**. Indeed, integrin receptors and their ligands are important regulators of the actin cytoskeleton since when active, integrins bind ECM and it occurs the recruitment of scaffold proteins, such as paxillin, and signalling proteins, such as the tyrosine kinase FAK which in turn associate with additional molecules, forming the FA complexes that regulate signalling to Rho GTPases (Wiesner et al., 2006; Gardel et al., 2010; Parsons et al., 2010). Interestingly, the adhesion size and distribution reflect the contractile state of the cell. Thus, nascent adhesions initially form in the lamellipodium or filopodium and either disassemble or elongate at the convergence of the lamellipodium and lamellum. Adhesion maturation to focal complexes and focal adhesions is accompanied by the bundling and cross bridging of actin filaments and increase in adhesion size (Wiesner et al., 2006; Parsons et al., 2010).

## 5.2. Role of Rho GTPases

**Rho GTPases family** plays a key role in integrating intracellular signals downstream of mechano-sensors, promoting re-organization of the actin cytoskeleton that is needed for the change in cell shape and, eventually, the mode of migration in a given environment (Sadok and Marshall, 2014). Rho GTPases family is composed of more than 20 small intracellular proteins that are key regulators of cell migration through their actions on **actin assembly and actomyosin contractility**, and they are grouped into eight subfamilies, though the best studied are Rac (composed of 4 members, Rac1, Rac2, Rac3 and RhoG), Rho (composed of 3 members, RhoA, RhoB and RhoC) and Cdc42 (composed of 5 members, Cdc42, TC10, TCL, Chip and Wrch-1) subfamilies.

Upon certain stimuli, Rho GTPase can switch from its inactive guanine diphosphate (GDP)-bound state to its active guanine triphosphate (GTP)-bound state, thus controlling downstream effector proteins. Classically, the control of Rho GTPase activity occurs through the action of three types of cellular proteins: GEFs, which are guanine nucleotide exchange factors that stimulate the exchange of GDP with GTP; GAPs, GTPase activating proteins that stimulate the hydrolysis of intrinsic bound GTP; and GDIs, guanine nucleotide dissociation inhibitors that prevent the dissociation of GDP and are also involved in the membrane localization of the Rho GTPases (Sadok and Marshall, 2014).

The **cellular roles** of Rho GTPases are defined by the nature and the location of their effector proteins, which are activated downstream of the GTPase and can be divided into three groups: protein kinases, phospholipases and scaffold proteins. These wide range of effectors permit that Rho GTPases control many aspects of cell behaviour. Thus, they are involved in progression through the cell cycle, as well as in the formation of cell-to-cell junctions and establishment of cell polarity. However, GTPases are especially well known to regulate actin dynamics. Studies of cell migration in **2D environments** showed that the Rho subfamily is involved in the formation of basolaterally located stress fibers, which are groups of actin filaments banded together to form striking features that are structurally linked to focal adhesion complexes. Cdc42 is primarily involved in the formation of filopodia, which are long and thin cylindrical structures with a diameter of less than 200nm and that can extend many microns away from the main cell body. They are composed of tight bundles of actin filaments whose orientation is in the direction of movement or the forward facing edge. Finally, the Rac subfamily members regulate the formation of lamellipodia, which are thin sheet-like structures, firmly attached to the underlying surface, and dominate the leading edge of motile cells. Membrane ruffles, which are non-adherent parts of the lamellipodia that retract as the cell moves, are also under the control of members of the Rac subfamily (Grise et al., 2009; Stanley et al., 2013; Sadok and Marshall, 2014).

Nevertheless, it is important to note that mechanisms that drive cell movement in 3D can differ from the ones that control cell migration in 2D. Studies in **3D environments**, where

cells have to move through collagen-rich connective tissue with variable physical and chemical properties, have shown that single cancer cells can adopt a round, highly contractile, Rho-driven mode of movement, or an elongated, lower contractility Rac-dependent mode of migration. Importantly, both types of movement rely on actomyosin contractility to generate the force needed for migration but differ in the levels of contractility required. **Actomyosin contractility** is driven by canonical Rho/ROCK signalling, where Rho activates ROCK, which phosphorylates (and thus inactivates) the myosin light chain phosphatase (MYPT), increasing the phosphorylation levels of the Myosin Light Chain (MLC), leading to the activation of the Myosin II. In addition, activation of Cdc42 downstream of DOCK10 can also promote actomyosin contractility through activation of the kinase Pak2, which directly phosphorylates MLC. MLCs, which are structural components of the actin binding motor protein Myosin, are a cross-linker of actin filaments (Stanley et al., 2013; Sadok and Marshall, 2014).

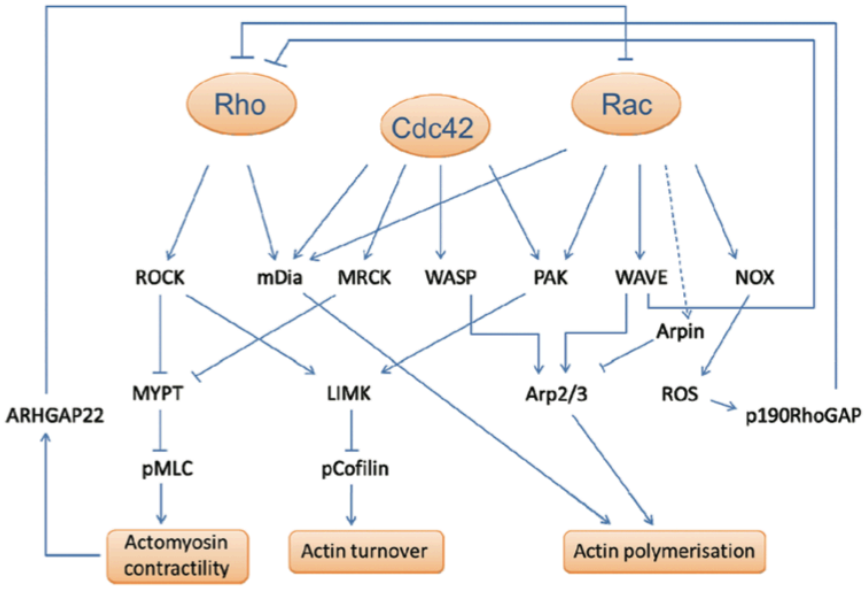


**Figure XVI.** Crosstalk between Rho GTPases and actin remodelling during cell migration (Sadok and Marshall, 2014).

As mentioned before, Rho GTPases have been implicated in all **modes of migration**. Rounded, amoeboid form of movement is driven by high actomyosin contractility through Rho signalling. In this case, cells are less adhesive and have a round shape. On the other hand, Rac signalling is required for actin assembly in elongated-protrusive movement (Sanz-Moreno and Marshall, 2010). Interestingly, Cdc42 is capable of regulating elongated mesenchymal or rounded contractile movement via usage of different GEFs (Sanz-Moreno, 2012).

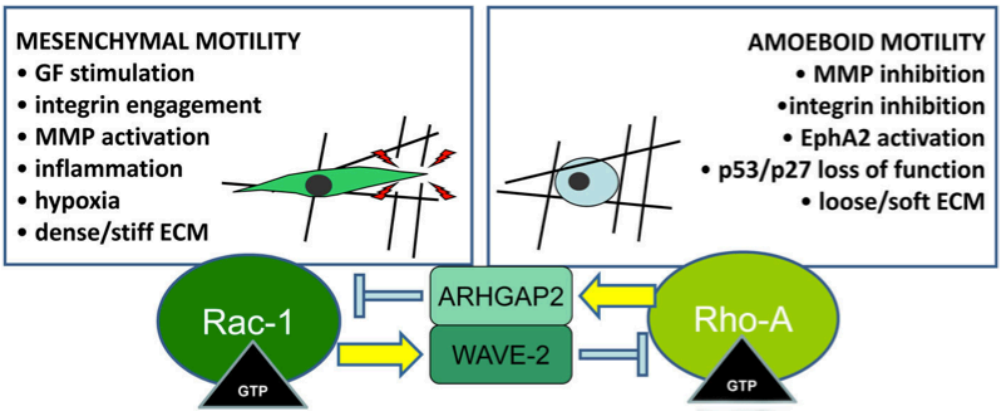


**Figure XVII.** Reciprocal regulation between Rho and Rac during mesenchymal and amoeboid motility (Parri and Chiarugi, 2010).

### 5.2.1. Rho GTPases in HCC

Several studies have highlighted the implication of Rho GTPases in tumour cell invasion and metastasis. Since there have not been found gain- or loss-of-function mutations in Rho GTPases, it is likely that the disturbance of Rho GTPase signalling in cancer may be either caused by alterations of their regulators or by direct regulation of their expression levels, thus resulting in variation of their biological activity (Grise et al., 2009). Thus far, only **few focused studies** have linked human HCC and alteration of Rho GTPase expression. Indeed, reported alterations are limited to the GTPases RhoA, RhoC, Rac1 and Cdc42. For instance, RhoA, which plays a key role in the regulation of cell contractility via the actomyosin system, and RhoC, which is required for cell-to-cell adhesion and invasion, are usually overexpressed in tumours, and both involved in liver tumour progression and metastasis. Also Rac1 is suggested to play a role in HCC progression and development of metastasis. On the other hand, there is controversial literature on the role of Cdc42 during hepatocarcinogenesis. Some studies in mice point that Cdc42 acts as a liver tumour suppressor, suggesting that the absence of Cdc42 can be considered as an initiating agent, whilst the analysis of Cdc42 in human HBV- and HCV-related liver cancers tended to show higher Cdc42 protein expression when compared to normal liver, although it is not known whether this Cdc42 is active or not. In addition, alterations in Rho GAPs, the negative regulators of Rho GTPases, have also been reported in HCC. The best illustration is the Deleted in Liver Cancer 1 (DLC-1) gene. DLC-1 acts as a negative regulator of RhoA and to a lesser extent of Cdc42. Its deletion or loss of function has been related to tumour promotion and tumour metastasis (Grise et al., 2009).

Considering that Rho GTPases seem to play critical roles in the development and progression of HCC, Rho GTPase signalling may constitute an attractive therapeutic target in HCC.

# II. HYPOTHESIS

## II. HYPOTHESIS

Due to the role of NOX4 as a downstream target of TGF-β actions, when we started this work we hypothesised that NOX4 could be mediating TGF-β effects under physiological and pathological situations of the liver where this cytokine plays a relevant role. During liver fibrosis we could expect a pro-fibrotic action, although nothing was known about the type of cell where NOX4 may mediate its effects. Under physiological conditions of liver proliferation, such as liver regeneration, and under pathological conditions, like hepatocarcinogenesis, NOX4 could mediate growth/tumour suppressor actions.

# III. OBJECTIVES

## III. OBJECTIVES

The main aim of this project has been to elucidate the role of the NADPH oxidase NOX4 under physiological and pathological situations of the liver.

**Specific objectives:**

1. **To analyse the involvement of NOX4 in liver fibrosis**
   - 1.1. Changes in NOX4 expression during liver fibrosis in two different animal models.
   - 1.2. Effect of silencing NOX4 in the activation of HSC to myofibroblasts in response to TGF-β.
   - 1.3. Effect of silencing NOX4 in the response of hepatocytes to TGF-β in terms of cell death.
2. **To analyse the crosstalk between the TGF-β pathway and NOX4 expression during liver tumorigenesis**
   - 2.1. Phenotypic characterization of human HCC cell lines: Relevance of TGF-β pathway.
   - 2.2. Crosstalk between the TGF-β pathway and NOX4 in human HCC cell lines.
3. **To analyse the role of NOX4 in liver cell proliferation**
   - 3.1. Effect of silencing NOX4 in human HCC cells on its *in vitro* proliferative capacity. Molecular mechanisms involved.
   - 3.2. Relevance of NOX4 in the regulation of proliferation in non-transformed hepatocytes.
   - 3.3. Regulation of NOX4 expression during liver regeneration after partial hepatectomy in mice.
4. **To analyse the role of NOX4 in liver carcinogenesis**
   - 4.1. Regulation of NOX4 expression during liver carcinogenesis in experimental animal models.
   - 4.2. Effect of silencing NOX4 in HCC cells on their pro-tumorigenic capacity in *in vivo* xenograft experiments in nude mice.
   - 4.3. Analysis of NOX4 expression in human liver tumours.
5. **To analyse the role of NOX4 in the metastatic capacity of HCC cells**
   - 5.1. Characterization of different HCC cell lines in terms of morphology, contractility and invasive capacity.
   - 5.2. Effect of silencing NOX4 on HCC cell morphology and contractility. Relevance in the migratory and invasive capacity of HCC cells.

# IV. MATERIAL AND METHODS

# 1. Cell culture

## 1.1. Cell models

Mice HSC, MBF and hepatocytes were obtained in our or colleagues' laboratories and used in previous published works (Proell et al., 2005; Mair et al., 2010). By employing $p19^{ARF}$ deficiency, we established a non-transformed murine HSC model to investigate their plasticity and the dynamics of HSC activation. The HSC immortal cell line, showed stellate cell characteristics including expression of desmin, glial fibrillary acidic protein, alpha-smooth muscle actin and pro-collagen I (Proell et al., 2005). *In vivo*-activated MFB derived from physiologically inflamed livers of $Mdr2^{-/-}$ / $p19^{ARF-/-}$ double-null mice were obtained as previously described in van Zijl et al., 2009 and used in this study in *in vitro* experiments. Finally, hepatocytes from wild-type mice were isolated and immortalized with a puromycin-resistance retroviral vector pBabe encoding Simian virus 40 large T antigen (LTAg), as described in Gonzalez-Rodriguez et al., 2007 and were generously provided by Dr. AM Valverde (Madrid, Spain).

| Cell line | Tumour type | Morphology / differentiation grade | P53 status | Other characterisics |
|---|---|---|---|---|
| **PLC/PRF/5** | Human liver hepatocarcinoma | Epithelial / Well differentiated | Mutated pR249S | |
| **Huh7** | Human liver hepatocarcinoma | Epithelial / Well differentiated | Mutated pY220S | |
| **Hep3B** | Human negroid hepatocarcinoma | Epithelial / Well differentiated | Deleted | Deficient in functional pRB; mutations within hFas gene |
| **SNU449** | Human asian hepatocarcinoma | Diffusely spreading cells / Poorly differentiated | Mutated pK139R pA161T | Aneuploid; mutations in *CDKN2A* |
| **HLF** | Human hepatoma (non-differentiated) | Diffusely spreading cells / Poorly differentiated | Mutated pG244A | |

**Table I.** Molecular characteristics of human HCC cell lines used

Hep3B and PLC/PRF/5 cell lines were obtained from the European Collection of Cell Cultures (ECACC). Huh7 and HLF cells were from the Japanese Collection of Research Bioresources (JCRB Cell Bank) and were kindly provided by Dr. Perales (University of

Barcelona, Spain) and Dr. Giannelli (University of Bari, Italy), respectively. SNU449 and the human liver cell line CCL-13 (Chang liver, CHL) were from the American Tissue Culture Collection (ATCC). The molecular characteristics of human HCC cell lines are shown in **Table I**.

# 1.2. Culture conditions

## 1.2.1. Cell culture on plastic

For cell culture, HSC, MFB and hepatocytes were grown in DMEM supplemented with 10% foetal bovine serum (FBS) and maintained in a humidified atmosphere of 37ºC, 5% $CO_2$.

Human cell lines were cultured as following for both maintenance of the cell lines and experiments in 2D. Hep3B cells were grown in MEM medium supplemented with non-essential aminoacids, SNU449 and HLF in RPMI medium, and Huh7, PLC/PRF/5, CHL in DMEM medium, supplemented with 10% FBS, in a humidified atmosphere at 37ºC, 5% $CO_2$. Cell lines were never used in the laboratory for longer than 4 months after receipt or resuscitation.

## 1.2.2. Cell culture on thick layers of collagen I

Fibrillar bovine dermal collagen (no. 5005; PureCol, Advanced BioMatrix) was prepared at 1.7mg/mL in DMEM according to the manufacturer's protocol. Volume used differed according to the culture plate: 100μL per well in 96-well plates, 300μL per well in 24-well plates and 700μL per well in 12-well plates. After collagen gel polymerization (4 hours at 37ºC, 10% $CO_2$) cells were seeded on top of the collagen in medium containing 10% FBS and allowed to adhere for 24 hours.

# 1.3. Treatments used

Response to TGF-β on different cells was analysed by adding human recombinant TGF-β (2ng/mL) (Calbiochem, La Jolla, CA, USA) to the culture after 8-12 hours of serum deprivation. For HSC, due to the fact that are very sensitive to serum deprivation, TGF-β was added to complete medium (medium with 10% FBS).

Different pharmacological inhibitors and antioxidant compounds (**Table II**) were added to cell culture 30 minutes before adding TGF-β.

When effects of adding FBS (10%) were analysed, cells were cultured under serum deprivation conditions for 8-12 hours prior treatment.

| Compound / Inhibitor | Dose |
|---|---|
| DPI (Diphenylene iodonium) | 1μM |
| GEE (Glutathione ethyl ester) | 2mM |
| BHA (Butylated hydroxyanisole) | 200μM |

**Table II.** Inhibitors and antioxidants added to cell culture before TGF-β

# 2. Animal experimentation

For the fibrosis study, mice were housed in accordance with European laws and with the general regulations specified by the Good Scientific Practices Guidelines of the Medical University of Vienna (Austria).

For all other studies using mice models, procedures were approved and registered by DARP (Departament d'Agricultura Ramadería i Pesca, Generalitat de Catalunya) and all of them were performed at the Animal Facility Core of the IDIBELL, which is recognized by the Catalunya Government, the Spanish Government and AAALAC (UNIT 1155) (Association for Assessment and Accreditation of Laboratory Animal Care International). All procedures and animal care were carried out in accordance with institutional guidelines.

## 2.1. Mice models for liver fibrosis studies

Two genetically modified mice were used in this study as models of liver fibrosis. $Mdr2^{-/-}$ / $p19^{ARF-/-}$ double null mice displayed a fibrotic phenotype comparable to $Mdr2^{-/-}$ mice, widely used as a model for experimental liver fibrosis (Baghdasaryan et al., 2010; Barikbin et al., 2012), characterized by severe hepatic injury and large periductal accumulation of MFB, showing the additional advantage of allowing the isolation of immortal cells for *in vitro* experiments. $Stat3^{\Delta hc}$ / $Mdr2^{-/-}$ mice show Stat3 conditional inactivation specifically in hepatocytes and cholangiocytes in $Mdr2^{-/-}$ background, which strongly aggravates liver injury and fibrosis.

Animals were sacrificed to evaluate liver histology at 2 and 7 weeks of age. SCID mice have been used as control.

Tissue was collected by Jèssica Máinez, a former PhD student in our group, in Wien, in collaboration and under the supervision of Dr. Mikulits (Medical University of Vienna, Austria).

## 2.2. Partial hepatectomy in mice

Animals used in this study were male C57/BL6 mice, aged 10 to 14 weeks. Partial hepatectomies were performed by removal of two thirds of the adult mouse liver, according to the method described by Higgins and Anderson. Briefly, after cleaning the animal with 70% Ethanol, we made an incision just above the sternum bone and opened a little bit up and down. Next, we made a "V" incision on the muscle layer just delimiting the bone. By pushing with four fingers from down to up surrounding the opened area, the central and left lobe of the liver got out of the body. A ligature surrounding the two lobes was performed and the two lobes were removed simply by cutting them. Finally, the two incision made were closed sewing them. Mice were euthanized at 2, 8, 24, 48 and 72 hours and 7 days after the surgery and tissue samples were frozen immediately in liquid nitrogen for RNA extraction or fixed in 4% paraformaldehyde overnight and paraffin embedded for immunohistochemistry (IHC). Livers from sham-operated animals were used as control.

These experiments were done during a short secondment in Madrid, in collaboration with Aránzazu Sánchez and Margarita Fernández (Universidad Complutense de Madrid, Spain).

## 2.3. Diethylnitrosamine-induced hepatocarcinogenesis in mice

Male mice at day 15 of age received intraperitoneal injections of DEN (5mg/kg) diluted in saline buffer (PBS). Control animals were injected with saline buffer (PBS) intraperitoneally. After 6, 9 or 12 months, mice were sacrificed and their livers removed. For histological studies, liver lobes were fixed in 4% paraformaldehyde overnight and paraffin embedded for IHC staining. Total RNA was isolated from these tissues to analyse gene expression by real time quantitative PCR.

## *2.4.* Xenograft model of subcutaneous tumour growth *in vivo*

Athymic nude mice were purchased from Harlan Laboratories. A total of 16 male mice, 7 weeks of age, were used. Hep3B cells transfected with either a control shRNA or a NOX4 silencing shRNA (shNOX4(#3)) were grown in the presence of 10% FBS. Then, cells were trypsinized and counted, diluting them at a final concentration of $5x10^7$cells/mL in HBSS. The total of 16 nude mice were randomly divided into two groups (shControl and shNOX4(#3), 8 mice per group) and the cell suspension (0.1mL/mouse) was subcutaneously injected into the

left flank of the mouse. Tumour growth was measured every two days. Once tumours reached 1000mm$^3$, animals were euthanized and subcutaneous tumours were removed, fixed overnight in 4% paraformaldehyde and paraffin embedded for IHC analysis.

# 3. Knock-down assays

## 3.1. Transient silencing

For transient siRNA transfection, cells at 70% confluence were transfected using TransIT-siQuest (Mirus, Madison, WI, USA) at 1:300 dilution in complete medium (medium with 10% FBS), with a final siRNA concentration of 50nM. After 8 hours with the transfecting solution, plates were washed and left in fresh medium with 10% FBS overnight before starting experiments.

Oligos were obtained from Sigma-Genosys (Suffolk, UK). Oligo sequences are shown in **Table III**:

| siRNA (gene) | Sequence (5'-3') |
|---|---|
| Human NOX4 | GCCUCUACAUAUGCAAUAA |
| Mouse Nox4 | CAAGAAGAUUGUUGGAUAA |
| Unsilencing | GUAAGACACGACUUAUCGC |

**Table III.** siRNA sequences

## 3.2. Stable silencing

For stable transfection of shRNA, cells at 50–60% confluence were transfected with MAtra-A reagent (IBA GmbH, Goettingen, Germany) at a dilution of 1:600 in complete media, according to the manufacturer's recommendation (15 minutes on the magnet plate), using 2μg/mL of shRNA plasmid. Huh7, Hep3B and PLC/PRF/5 cell lines were stable silenced for NOX4. In addition, Hep3B, PLC/PRF/5, SNU449 and HLF cell lines were stable silenced for TGFBRI. For both NOX4 and TGFBRI four different shRNA plasmids were transfected, separately and combined, as well as a control unspecific shRNA, and the best-silenced clones were selected. After 24 hours, media was changed to complete media, and selection of

transfected cells was done in all cases with puromycin (InvivoGen Therapeutics, France), for at least 50 days prior to experiments. At the beginning, selection was done at a dose of 0.5μg/mL of puromycin and this dose was gradually increased until reaching 2μg/mL, which is the one used for maintaining the silenced clones. shRNA plasmids transfected were selected from Mission SH, Sigma (Madrid, Spain) and sequences are indicated in **Table IV**. The cell line and the clone used for experiments are indicated in each figure.

| shRNA (gene) | Plasmid number | Sequence (5'-3') |
|---|---|---|
| Human NOX4 | #1 | CCGGGAGCCTCAGCATCTGTTCTTACTCGAGTAAGAACAGATGCTGAGGCTCTTTTTG |
| | #2 | CCGGCCCTCAACTTCTCAGTGAATTCTCGAGAATTCACTGAGAAGTTGAGGGTTTTTG |
| | #3 | CCGGCAGAGTTTACCCAGCACAAATCTCGAGATTTGTGCTGGGTAAACTCTGTTTTTG |
| | #4 | CCGGGCTGTATATTGATGGTCCTTTCTCGAGAAAGGACCATCAATATACAGCTTTTTG |
| Human TGFBRI | #1 | CCGGCTCATGTTGATGGTCTATATCCTCGAGGATATAGACCATCAACATGAGTTTTTTG |
| | #2 | CCGGGAAGTTGCTGTTAAGATATTCCTCGAGGAATATCTTAACAGCAACTTCTTTTTTG |
| | #3 | CCGGGATCATGATTACTGTCGATAACTCGAGTTATCGACAGTAATCATGATCTTTTTTG |
| | #4 | CCGGGCTGGTCTTAACTTTAGGTAACTCGAGTTACCTAAAGTTAAGACCAGCTTTTTG |

**Table IV.** shRNA sequences

# 4. Analysis of cell proliferation

## 4.1. Crystal violet staining

Crystal violet staining allows quantifying the amount of cells that survive after a toxic process, being useful when working with adherent cells that detached after undergoing a toxic process. It is useful as well for quantifying the changes in the cell number along time when cells are cultured under certain conditions (Drysdale et al., 1983). The method consists on cell staining with a colorant, crystal violet. Cells were seeded in 24-well plates and cultured under basal conditions (medium supplemented with 10% FBS). After the time of culture required the cell media was removed, cells were washed twice with phosphate-buffered saline (PBS) and the remaining viable adherent cells were stained with crystal violet solution (0.2%(w/v) in 2% ethanol) for 1 hour. Following this, the staining solution was removed, and the wells were

washed several times with PBS or distilled water until the excess staining not incorporated into the cells was eliminated. The plate was air-dried, and the stained cells were lysed in 10% SDS. By spectrophotometric analysis, the absorbance was measured at 595nm. Results were then calculated as the percentage of viable cells at the indicated times relative to time zero.

## 4.2. DNA synthesis assay

To study DNA synthesis, the method of [$^3$H]-Thymidine (GE Healthcare, Barcelona, Spain) incorporation was used. Cells can convert [$^3$H]-Thymidine into [$^3$H]-Thymine, which can then be incorporated into DNA as it is synthesized. This procedure allows the quantification of only newly synthesized DNA. Cells were seeded in 12-well plate and 12 hours after FBS depletion a mix of radioactive and cold Thymidine (0.5μCi/mL, 1μM cold Thymidine) was added. After 40 hours of adding the mix, wells were washed with PBS and cellular products were precipitated by adding to wells cold 10% trichloroacetic acid (TCA), during 20 minutes at 4°C. Next, wells were washed twice with cold 70% ethanol and let dry. Finally, a solution containing 0.1N NaOH, 2% $CO_3Na_2$ and 0.5% SDS was added to wells and was incubated during 20 minutes at 37°C. 100μL from each well was mixed with 5mL of scintillation fluid and radioactivity was counted for [$^3$H] in a liquid scintillation counter using a β-radiation counter 1209 Rackbeta (Wallac). Results were calculated as percentage versus control cells.

## 4.3. Analysis of the percentage of Ki67 positive nuclei

In order to determine the growth fraction of a given cell population Ki67 is considered an excellent marker because it is a protein that can be detected during all active phases of the cell cycle ($G_1$, S, $G_2$ and mitosis) and it is absent in resting cells ($G_0$) (Scholzen and Gerdes, 2000). Cell immunofluorescence using rabbit anti-Ki67 antibody as a primary antibody and DAPI (Molecular Probes, Eugene, OR, USA) staining for nuclei detection was done as explained in Material and Methods 10.1. Cells were visualized in a Nikon eclipse 80i microscope with the appropriate filters and at least ten 40x images were taken with a Nikon DS-Ri1 digital camera. Finally, the percentage of Ki67 positive cells versus the total number of cells was quantified from the images.

## 4.4. Analysis of DNA content by flow cytometry

Twenty-four hours after seeding, cells were trypsinized and collected in a 15mL tube, which was then centrifuged at 1500rpm for 5 minutes. The pellet was resuspended in 200μL of PBS 1X and was added drop by drop into 500μL of cold (stored at -20ºC) 100% ethanol, in

constant motion (gently applied with a vortex), in order to fix cells. At this point, samples can be stored at -20°C. To collect the fixed cells, samples were centrifuged at 2500rpm during 5 minutes at 4°C. The pellet was air-dried and resuspended in 250μL PBS containing 0.1mg/mL of RNAse. After incubation during 30 minutes at 37°C, propidium iodide (PI) was added at a final concentration of 0.05%. Following this process, PI incorporation was directly proportional to the amount of DNA contained by each cell. Finally, this suspension was analysed in a flow cytometer FACScan from Becton-Dickinson at Serveis Cientifico-Tècnics, Universitat de Barcelona. Cell cycle analysis was carried out using the software ModFit LT$^{TM}$ (Verity Software House): DNA content: 2C: $G_0/G_1$ phases; 4C: $G_2$/M phases; >2C and <4C: S phase.

# 5. Analysis of cell death

## 5.1. Analysis of Caspase-3 activity

For the analysis of Caspase-3 activity, after incubation of cells with the desired stimuli, in our case cells were treated with TGF-β for 24 hours, media was preserved and cells were scrapped. Cells and media were collected together in a 15mL tube, which was then centrifuged at 2500rpm for 5 min. Indeed, this pellet contained those cells that were attached to the tissue culture dish and those that were dead and floating in the media. The pellet was resuspended in 30 to 100μL of lysis buffer, **Table V**. The solution was then transferred to an Eppendorf tube, which was incubated for 20 minutes on ice and vortexed every 5 minutes. After this time was elapsed, Eppendorf tubes were centrifuged at 13000rpm during 10 minutes at 4°C. The supernatant was stored at -20 or -80°C until it was used.

When Caspase-3 activity was analysed in tissues, small pieces of frozen tissues were pulverized mechanically in a mortar, previously sterilized at 200ºC for 4 hours to inactivate RNAses. Tissue powder was then transferred to an Eppendorf tube and resuspended in 200μL of lysis buffer, incubated for 20 minutes on ice with a vortex mix every 5 minutes. From this point, the same procedure was used for both, cells and tissue samples.

To determine Caspase-3 activity, first we determined the protein concentration by Bradford's method (Material and Methods 8.2). Then a mix containing 20μg of protein (in a final volume of 25μL), 125μL of Buffer Reaction 2X (**Table VI**) and 2μL of fluorigenic substrate for Caspase-3, Ac-DEVD-AMC (BD Pharmigen) was prepared. This substrate, once it was cleaved by caspase-3, released the AMC fragment that was fluorigenic and could be quantified spectrofluorimetrically. After 2 hours of incubation at 37°C and protected from light, fluorescence was measured in a Microplate Fluorescence Reader Fluostar Optima using an exciting wavelength of 360nm and an emission wavelength of 440nm.

| | |
|---|---|
| Tris-HCl pH 8 | 5mM |
| EDTA | 20mM |
| Triton-X-100 | 0.5% |

**Table V.** Caspase-3 lysis buffer

| | |
|---|---|
| Glycerol | 20% |
| Hepes pH 7.5 | 40mM |
| DTT | 4mM |

**Table VI.** Caspase-3 reaction buffer 2x

A unit of Caspase-3 activity is the amount of active enzyme necessary to produce an increase in 1 fluorescence unit in the spectrofluorimeter. Results were represented as arbitrary units/h/μg protein.

# 6. Measurement redox state

## 6.1. Intracellular ROS

In order to measure the intracellular content of ROS, a fluorimetric method was used. Each condition was analysed in triplicate. Twenty-four hours after seeding the cells in 12-well plates, they were washed with PBS and incubated with 2.5μM 2′,7′-dichlorodihydrofluorescein diacetate ($H_2$DCF-DA, from Invitrogen, UK) in HBSS without red phenol during 30 minutes at 37°C in the dark. This compound is incorporated into the cells, and converted into 2',7'-diclorodihydrofluorescein ($DCFH_2$) by intracellular sterases, that in turn is converted into 2',7'-dicloroflurescein (DCF) when oxidized. Then cells were lysed with 250μl of the lysis buffer described in **Table VII** during 10 minutes at 4°C in motion, and transferred in duplicate into a 96-well plate, each with 100μL. The resting 50μL were used for protein quantification using BCA method (Material and Methods 8.3). Fluorescence was measured in a Microplate Fluorescence Reader Fluostar Optima using an exciting wavelength of 485nm and an emission wavelength of 520nm. Cell auto-fluorescence (produced by cells incubated with HBSS without probe) was

subtracted. Results were calculated as fluorescence units per μg of protein and then expressed as percentage of control.

| | |
|---|---|
| Hepes pH 7.5 | 25mM |
| NaCl | 60mM |
| $MgCl_2$ | 1.5mM |
| EDTA | 0.2mM |
| Triton-X-100 | 1% |

**Table VII.** Lysis buffer

## 6.2. Intracellular superoxide

In order to measure intracellular content of superoxide we incubated the cells with 10μM Dihydroethidine (DHE, from Invitrogen, UK) in HBSS without red phenol during 30 minutes at 37°C in the dark. DHE is a compound able to cross cell membranes. Inside the cells, DHE can be oxidized and converted into 2-hydroxyethidium (2-OH-$E^+$). Then, it intercalates into DNA, resulting in a red fluorescence. The procedure followed was the same as for intracellular content of ROS (Material and Methods 6.1). At the end, fluorescence was measured in a Microplate Fluorescence Reader Fluostar Optima at Ex/Em = 530/620nm. Cell auto-fluorescence (produced by cells incubated with HBSS without probe) was subtracted. Results were calculated as fluorescence units per μg of protein and then expressed as percentage of control.

## 6.3. Mitochondrial superoxide

MitoSOX™ Red reagent (Invitrogen, UK) permeates live cells and specifically targets mitochondria. It was used to determine mitochondrial superoxide production since it is rapidly oxidized by superoxide but not by other ROS and RNS. The oxidized product is highly fluorescent upon binding to nucleic acid. The procedure followed was the same as for intracellular content of ROS (Material and Methods 6.1) incubating cells with 5μM MitoSOX in HBSS during 10 minutes at 37ºC in the dark. Fluorescence was measured in a Microplate Fluorescence Reader Fluostar Optima at Ex/Em = 530/590nm. Cell auto-fluorescence was subtracted. Results were calculated as fluorescence units per μg of protein and then expressed as percentage of control.

## 6.4. Extracellular hydrogen peroxide

Extracellular $H_2O_2$ was measured in intact cells using horseradish peroxidase-linked Amplex Ultra Red (Invitrogen, UK). The non-fluorescent, colourless compound Amplex Red is oxidized by $H_2O_2$ in the presence of HRP to generate resorufin, which is coloured (pink) and highly fluorescent. It is used for the measurement of extracellular $H_2O_2$ since horseradish peroxidase does not penetrate membranes. Twenty-four hours after seeding the cells in 12-well plates, they were washed with PBS and then 250μL of a mix with Amplex Ultra Red (50μM) and horseradish peroxidase (0.1U/mL) were added to the cellular samples and incubated for 2 hours at 37ºC in the dark. Later, fluorescence readings were made in duplicate in a 96-well plate at Ex/Em = 530/590nm using 100μL of media. Fluorescence was measured in a Microplate Fluorescence Reader Fluostar Optima and expressed as percentage of control after correction with cell number (crystal violet assay, Material and Methods 4.1).

# 7. Analysis of gene expression

## 7.1. RT-PCR

RNeasy Mini Kit (Qiagen, Valencia, CA) was used following Manufacturer's protocol for total RNA isolation. When RNA was isolated from cells, culture plates were washed with PBS and cells were scrapped in a solution containing RLT (from the Kit) previously adding 10μl/mL of β-Mercaptoethanol. When RNA was isolated from tissues, small pieces of frozen tissues were pulverized mechanically in a mortar, previously sterilized at 200ºC for 4 hours to inactivate RNAses, then tissue powder was transferred to an Eppendorf tube and resuspended in 600μL of RLT with 10μL/mL of β-Mercaptoethanol. Reverse transcription was carried out with random primers using 1μg of total RNA from each sample for complementary DNA synthesis using High Capacity RNA to cDNA Master Mix Kit (Applied Biosystems, Foster City, CA, USA) following Manufacturer's instructions.

## 7.2. Semi-quantitative PCR

Semi-quantitative Polymerase Chain Reactions (PCR) were performed using 25ng of cDNA, plus a final concentration of 1μM of specific primers (**Table VIII**), dNTPS at 100μM, 1.5mM $MgCl_2$ and 1 unit of Ecotaq (Ecogen, Barcelona, Spain).

| Gene (mouse) | Forward (5'-3') | Reverse (5'-3') |
|---|---|---|
| *Rn18s* | GCGAAAGCATTTGCCAAGAA | CATCACAGACCTGTTATTGC |
| *Acta2* | CCGAGATCTCACCGACTACC | TCCAGAGCGACATAGCACAG |
| *Col1a1* | TCAAGGTCTACTGCAACATGG | TGTAGGTGAAGCGACTGTTG |
| *Fn1* | GGTTTCCCATTACGCCATTG | ATTCTCCCTTTCCATTCCCG |
| *Nox4* | GGAAGCCCATTTGAGGAGTCACTGAAC | TGACTGAGGTACAGCTGGATGTTCAC |
| *Tgfb1* | GTGAAACGGAAGCGCATCGAAG | AGCCGGTTACCAAGGTAACGCC |
| *Vim* | TCCGCCAGCAGTATGAAAG | TGGGTGTCAACCAGAGGAAG |

**Table VIII.** Primers sequences used in semi-quantitative PCR

PCR reactions were carried out following the conditions shown in **Table IX**.

| Phase | Temperature | Time | Nº cycles |
|---|---|---|---|
| Initial denaturalization | 95ºC | 5 minutes | 1 |
| Denaturalization | 94ºC | 30 seconds | 25-40 |
| Hybridization | 55-65ºC | 30 seconds | |
| Elongation | 72ºC | 30-45 seconds | |
| Final elongation | 72ºC | 10 minutes | 1 |

**Table IX.** Semi-quantitative PCR conditions

The obtained PCR products were analysed in 1.5% agarose gels in Ethidium Bromide and imaged using Gel Doc 2000 (BioRad).

## 7.3. Quantitative Real Time PCR

For quantitative Real Time PCR, RNA was obtained as explained in the above section. Expression levels were determined in duplicate in an ABIPrism7700 System, using the SYBR® Green PCR Master Mix (Applied Biosystems, Foster City, CA, USA) in a 96-well plate, for mouse primers. Reaction was prepared using 25μL of SYBR® Green PCR Master Mix, 2.5μL specific primers (10μM) (**Table X**) and 50ng of cDNA plus RNAse free water up to 50μL per

duplicate. For human primers, expression was determined in a LightCycler® 480 Real Time PCR System, using the LightCycler® 480 SYBR Green I Master Mix (Roche Applied Science), in a 384-well plate. In this case, reaction was prepared using 10μL of LightCycler® 480 SYBR Green I Master Mix, 2μL specific primers (5μM) (**Table XI**) and 40ng of cDNA in a final volume of 20μL per duplicate. The levels of mRNA for each gene were determined following Manufacturers' protocols and were normalized with a housekeeping gene.

| Gene (mouse) | Forward (5'-3') | Reverse (5'-3') |
|---|---|---|
| *Rn18s* | CGAGACTCTGGCATGCTAA | CGCCACTTGTCCCTCTAAG |
| *Nox4* | TCCAAGCTCATTTCCCACAG | CGGAGTTCCATTACATCAGAGG |
| *p22phox* | ACACAGTGGTATTTCGGCG | CAGGTACTTCTGTCCACATCG |

**Table X.** Primers sequences used in ABIPrism 7700 SYBR Green System quantitative PCR

| Gene (human) | Forward (5'-3') | Reverse (5'-3') |
|---|---|---|
| *RPL32* | AACGTCAAGGAGCTGGAAG | GGGTTGGTGACTCTGATGG |
| *CDC42* | CAGGGCAAGAGGATTATGACAG | GTTATCTCAGGCACCCACTT |
| *CDH1* | CCCAATACATCTCCCTTCACAG | CCACCTCTAAGGCCATCTTTG |
| *CDH2* | CCCAAGACAAAGAGACCCAG | GCCACTGTGCTTACTGAATTG |
| *CDKN1A* | TGTCACTGTCTTGTACCCTTG | GGCGTTTGGAGTGGTAGAA |
| *NOX4* | GCAGGAGAACCAGGAGATTG | CACTGAGAAGTTGAGGGCATT |
| *RAC1* | GCTTTTCCCTTGTGAGTCCTG | CCTTCAGTTTCTCGATCGTGTC |
| *RHOA* | AGCTGGGCAGGAAGATTATG | CGTTGGGACAGAAATGCTTG |
| *RHOC* | CAAGACGAGCACACCAGG | AGCACTCAAGGTAGCCAAAG |
| *TGFB1* | AAGTGGACATCAACGGGTTC | GTCCTTGCGGAAGTCAATGT |
| *TGFBRI* | ACATGATTCAGCCACAGATACC | GCATAGATGTCAGCACGTTTG |

**Table XI.** Primers sequences used in LightCycler 480 SYBR Green System quantitative PCR

# 8. Protein expression analysis

## 8.1. Cell lysis

After incubation with different factors or after cell culture under basal conditions, the cell culture dishes were placed on ice. The media was collected into tubes, 2mL of cold PBS was added to each dish, and cells were scrapped and collected into the tube. To make sure that most of the cells were collected, other 2mL of cold PBS were added to the dish and collected into the tube. Cells were then pelleted at 2500rpm during 8 minutes at 4°C. The pellet was then washed with 5mL of PBS, and centrifuged at 2500rpm during 5 minutes at 4°C. The pellet was resuspended with RIPA lysis buffer (**Table XII**) and transferred to an Eppendorf tube, being the lysis performed during 1 hour with rotation at 4°C. Then, tubes were centrifuged at 13000rpm during 10 minutes at 4°C, and the supernatants were collected and stored at -20°C or -80°C until they were processed.

| | |
|---|---|
| Sodium Deoxycholate | 5mM |
| TRIS-HCl pH 7.4 | 20mM |
| SDS | 0.1% |
| Triton-X-100 | 0.5% |
| NaCl | 150mM |
| EDTA | 2mM |
| PMSF | 1mM |
| Leupeptin | 5μg/mL |
| $Na_3VO_4$ | 0.1mM |
| DTT | 0.5mM |
| β-Glycerolphosphate | 20mM |

**Table XII.** RIPA lysis buffer

When expression of Myosin Light Chain 2 (MLC2), Rho GTPases and its effectors ROCK I and ROCK II was analysed, the media was removed from culture dishes and 120-150μL of Laemmli lysis buffer (**Table XIII**) were added for a 12-well plate and incubated at room temperature during 5 minutes. Then, cell lysates were collected and transferred into an

Eppendorf tube. Afterwards, samples were denaturalized by heating them at 95 °C for 5 minutes and stored at 4ºC. Next, samples were sonicated for 15 seconds before centrifugation at 13000rpm for 30 minutes at 4ºC, supernatants were then transferred into a new Eppendorf tube and finally stored at -20°C or -80°C until they were processed.

| | |
|---|---|
| TRIS-HCl pH 7.5 | 80mM |
| Glycerol | 10% |
| SDS | 2% |
| DTT | 1mM |
| NaF | 10mM |
| $Na_3VO_4$ | 1mM |
| PMSF | 0.1mM |
| β-Glicerolphosphate | 10mM |
| Protease inhibitor cocktail EDTA-free | |

**Table XIII.** Laemmli lysis buffer

## 8.2. Protein quantification by Bradford's method

Protein quantification was done following the spectrophotometric method described by M. Bradford in 1976. For each measurement a standard curve of protein concentration was prepared with Bovine Serum Albumin (BSA) in a range from 0 to 2μg/mL. The reaction was prepared mixing 200μL of distilled water, 2μL of protein extract and 50μL of Bradford reactive. Absorbance was measured at 595nm.

## 8.3. Protein quantification by BCA commercial kit

If SDS was a component of the lysis buffer, the Bradford method could not be used. Instead, we used the commercial kit BCA. For each measurement a standard curve of protein concentration was prepared with BSA in a range from 0 to 2μg/mL. The reaction was prepared by mixing Solution A and Solution B in a ratio of 50:1. Then, 200μL of this mix were added to 10μL of 1:10 diluted sample, into a 96-well plate. After 30 minutes of incubation at 37°C, absorbance was measured at 595 nm.

## 8.4. Protein immunodetection by Western blot

Protein separation by their molecular weight was done by denaturalizing polyacrylamide gels. The protein samples were prepared by mixing 30 to 100μg of protein with Laemmli loading buffer, and were denaturalized by heating them at 95°C. Once the samples were boiled, they were spun and saved at 4°C. Acrylamide gels consist of two different parts: the stacking and the separating gel, the latter being prepared at different concentrations of acrylamide depending on the size of the proteins to be studied. When Cyclin D1 was analysed, a gel of 15% acrylamide was used. For the other proteins, a gel of 10% or 12% acrylamide was used. Once the gel was ready it was assembled into the gel holder and immersed into the tank, which was filled with an electrophoresis buffer (25mM Tris-HCl; 0.1%SDS; 0.2M glycine; pH 8,3). Then the samples were carefully loaded to the gel together with a molecular weight standard in order to know the molecular weight of the proteins studied. Finally, they were submitted to electrophoresis at a constant voltage.

Once finished the electrophoresis, the proteins were transferred to a PVDF membrane through the passage of electrical current using semi-dry equipment. The PVDF membrane was first immersed into methanol for 1 minute following the manufacturer's instructions. Then the PVDF membrane and the Wattman paper were soaked in transfer buffer (48mM Tris-HCl; Glycine 39mM; SDS 0.4%; Methanol 20%; pH 8.3) for 5 minutes, and the equipment was assembled as follows from bottom to top: 3 Wattman papers - PVDF membrane - Acrylamide gel - 3 Wattman papers. An electrical current of 0.3mA was applied during 0.5-1 hour. After this time, the membrane was stained into a solution of 0.5% red Ponceau in 1% acetic acid to confirm that proteins had uniformly been transferred into the membrane. Then, membrane was washed several times in PBS-Tween 0.05% (PBS-T).

For blotting the desired protein, the membrane was incubated in 5% non-fat dry milk or 5% BSA (depending on the primary antibody to be used) in PBS-T for 1 hour at room temperature (RT). After this time, it was incubated with the primary antibody (see antibodies and conditions in **Table XIV**) in 0.5 % milk/BSA in PBS-T during 16 hours at 4°C in motion. After that, the membrane was washed 3 times during 10 minutes with PBS-T, and subsequently incubated with the secondary antibody (conjugated with peroxidase) at a dilution of 1:5000 in 0.5% milk-PBS-T during 1 hour at RT in motion. Again the membrane was washed 3 times in PBS-T. To visualize the antibody hybridized to the protein of study, the membrane was incubated with a chemiluminescent solution, ECL (Amersham Biosciences) and exposed to an Amersham HyperfilmTM ECL. Secondary antibodies used were obtained from GE-Healthcare: anti-Mouse (NA931V), and anti-Rabbit (NA934V), conjugated with peroxidase.

| Primary antibody | Working conditions | Purchased from | Catalogue nº |
|---|---|---|---|
| Mouse anti-β-actin | 1:5000 (0.5% non-fat milk) | SIGMA | A5441 |
| Rabbit anti-Cdc42 | 1:1000 (4% BSA) | Cell signaling | 2462 |
| Rabbit anti-Cyclin D1 | 1:1000 (0.5% non-fat milk) | Santa Cruz | sc-718 |
| Mouse anti-E-cadherin | 1:1000 (0.5% non-fat milk) | BD Pharmigen | BD-610182 |
| Rabbit anti-MLC2 | 1:500 (4% BSA) | Santa Cruz | sc-15370 |
| Rabbit anti-NOX4 | 1:1000 (0.5% non-fat milk) | SIGMA-Genosys | ---------- |
| Rabbit anti-Nitrotyrosine | 1:1000 (0.5% non-fat milk) | Molecular probes | A21285 |
| Rabbit anti-phospho-MLC2 | 1:500 (4% BSA) | Cell signaling | 3674 |
| Rabbit anti-phospho-Smad2 | 1:1000 (0.5% non-fat milk) | Cell signaling | 3101 |
| Rabbit anti-Rac1 | 1:500 (0.5% non-fat milk) | Millipore | 05-389 |
| Rabbit anti-RhoA | 1:500 (0.5% non-fat milk) | Cell signaling | 21175 |
| Rabbit anti-RhoC | 1:1000 (0.5% non-fat milk) | Cell signaling | 3430 |
| Mouse anti-ROCK I | 1:500 (4% BSA) | BD Pharmigen | 611137 |
| Mouse anti-ROCK II | 1:1000 (4% BSA) | BD Pharmigen | 610624 |
| Rabbit anti-TGF-β RI | 1:1000 (0.5% non-fat milk) | Santa Cruz | sc-399 |
| Mouse anti-Vimentin | 1:1000 (0.5% non-fat milk) | SIGMA | V6630 |

**Table XIV.** Primary antibodies used for Western blot

When expression of MLC2, Rho GTPases and its effectors ROCK I and ROCK II was analysed the protocol used was the following: Cells lysates obtained as explained in Material and Methods 8.1 were fractionated using precast 4–12% gradient SDS–polyacrylamide gel electrophoresis (SDS–PAGE) gels in non-reducing conditions, and transferred subsequently to PVDF membrane. For the blotting of the specific protein, the same procedure explained above was followed.

In both cases, hybridized antibody could be removed with the stripping process consisting in soaking the membrane during 30 minutes at 50°C with stripping solution (62.5nM TRIS-HCl pH 6.8; SDS 0.05%; β-Mercaptoethanol 20%), in motion.

Rabbit anti-NOX4 polyclonal antiserum was created by Sigma-Genosys against a peptide corresponding to the C-terminal loop region (amino acids 499-511), according to our order. Specificity was tested by ELISA assay with the purified peptide. We licensed the antibody to be commercially exploited by Merck Millipore (Billerica, MA) (Catalogue number. ABC459).

Specificity of the antibody was validated in our laboratory (**Figure XVIII**).

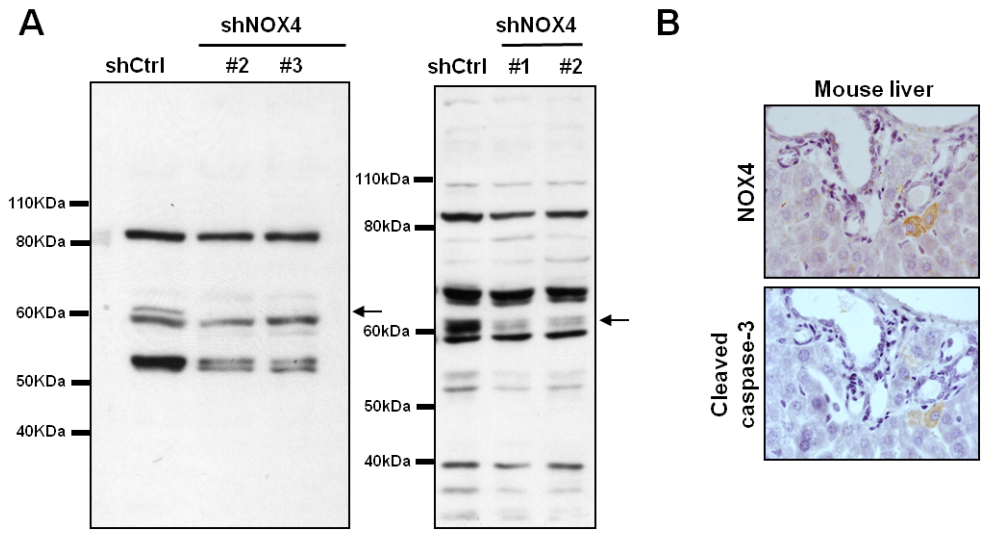


**Figure XVIII. Specificity of NOX4 antibody was tested.** A) Western blot using stable silenced human HCC cells by means of different shRNA plasmids against NOX4, being the silenced band just above 60KDa, as it is expected considering the molecular weight of NOX4. Also a band above 50KDa could be specific considering the pattern observed, representing perhaps a NOX4 splice variant. B) Immunohistochemistry using two serial sections showing coincidence in the expression of NOX4 and the cleaved form of Caspase-3 in the same hepatocytes, since it has been described that NOX4 is required for apoptosis in hepatocytes.

# 9. Rho GTPase pull-down assays

Pull-down assays for determining activated fraction of RhoA and RhoC were performed using Glutathione S-transferase (GST)-Rhotekin and for activated Rac1 and Cdc42 levels using Glutathione S-transferase (GST)-PAK-CRIB expressed from pGEX-Rhotekin and pGEX-PAK-CRIB, respectively.

To prepare GST-Rhotekin, 250mL of bacteria carrying pGEX-Rhotekin were grown to OD600 and then were induced with 0.3mM IPTG for 3 hours. After, bacteria were pelleted by centrifugation at 6000rpm during 15 minutes at 4ºC. Pellets were resuspended with 10mL of cold lysis buffer (**Table XV**) and sonicated for 20 minutes using 10 seconds ON – 10 seconds OFF pulses. Then, 1% Triton-X-100 was added and incubated with rocking during 30 minutes. After a centrifugation at 6000rpm during 30 minutes at 4ºC, supernatant was incubated with glutathione sepharose beads during 2 hours, at 4ºC and rolling. Beads were washed 3 times with TBS washing buffer (**Table XVI**) and kept on ice until needed.

| | |
|---|---|
| TRIS-HCl pH 7.4 | 50mM |
| Glycerol | 10% |
| NP-40 | 1% |
| $MgCl_2$ | 5mM |
| NaCl | 100mM |
| DTT | 1mM |
| Protease inhibitor cocktail EDTA-free | |

**Table XV.** Rho GTPases pull-down lysis buffer

| | |
|---|---|
| $MgCl_2$ | 10mM |
| PMSF | 0.1mM |
| Triton-X-100 | 1% |
| Protease inhibitor cocktail EDTA-free | |

**Table XVI.** GST-Rhotekin washing buffer

To prepare GST-PAK-CRIB, the same procedure was followed using pGEX-PAK-CRIB and the TBS washing buffer from **Table XVII**.

| | |
|---|---|
| $MgCl_2$ | 10mM |
| DTT | 1mM |
| Protease inhibitor cocktail EDTA-free | |

**Table XVII.** GST-PAK-CRIB washing buffer

For the pull-down assays, the same protocol was used for both GST-Rhotekin and GST-PAK-CRIB, with the exception of the washing buffer. Washing buffer from **Table XVI** was used for GST-Rhotekin and from **Table XVII** for GST-PAK-CRIB.

Cells ($2x10^6$) were seeded in 10cm dishes for 48 hours. Then, the medium was removed, cells were washed on ice with cold TBS, and scrapped with 1mL of lysis buffer (**Table XV**). Lysates were transferred to an Eppendorf tube and centrifuged at 13000rpm during 5 minutes at 4ºC. At this point, 100μL of the supernatant were stored in a new Eppendorf tube for the blot of total protein. The remaining supernatant was mixed with 60μL of GST-Rhotekin / -PAK-CRIB bound beads and was incubated at 4ºC with tumbling during 45 minutes. Samples were then briefly spun (1200rpm – 1 minute), the supernatant was removed and beads were washed twice in the corresponding cold washing buffer, before addition of Laemmli buffer and analysis by western blotting with the corresponding primary antibody, as explained in Material and Methods 8.4.

# 10. Immunocytochemistry

## 10.1. Immunofluorescence in 2D cultured cells

Epifluorescence microscopy studies were performed on cells seeded on gelatin-coated glass coverslips. For F-actin staining, after treatment, cells were washed with PBS and fixed with 4% paraformaldehyde (PFA) in PBS for 20 minutes at room temperature, then washed 3 to 5 times with PBS and finally, incubated with rhodamine-conjugated phalloidin (1:500) diluted in 0.1% BSA for 1 hour. To detect E-cadherin and vimentin cells were fixed with cold methanol (stored at -20ºC) during 2 minutes, washed 3 to 5 times with PBS, and then incubated with the primary antibody. For NOX4, phospho-FAK, vinculin, phospho-Paxillin and ZO-1 staining, cells were fixed with 4% PFA in PBS during 20 minutes and washed 3 to 5 times with PBS. For Ki67 and β-catenin staining, after being fixed with 4% PFA in PBS and washed 3 to 5 times with PBS, cells were permeabilized with 0.2% Triton-X-100 during 2 minutes. When cells were permeabilized, prior to the incubation with the primary antibody they were incubated with a blocking solution (BSA 1%; FBS 10%; in PBS) during 1 hour at room temperature.

Primary antibodies, detailed in **Table XVIII**, were diluted in PBS-BSA 1% and incubated during 1 hour at room temperature. Then, after several washes with PBS, samples were incubated with fluorescent-conjugated secondary antibodies (anti-mouse Alexa 488 or anti-rabbit Alexa 488) 1:200 dilution in PBS-BSA 1% during 1 hour at room temperature. Finally, cells were washed 3 to 5 times for 5 minutes each with PBS, adding DAPI in the second last wash for nuclear DNA staining, when necessary. At the end, samples were embedded using Mowiol®. Cells were visualized in a Nikon eclipse 80i microscope with the appropriate filters. Representative images were taken with a Nikon DS-Ri1 digital camera.

| Primary antibody | Dilution | Purchased from | Reference |
|---|---|---|---|
| Mouse anti-β-catenin | 1:50 | BD Pharmigen | 610154 |
| Mouse anti-E-cadherin | 1:50 | BD Pharmigen | BD-610182 |
| Rabbit anti-Ki67 | 1:100 | Abcam | ab16667 |
| Rabbit anti-NOX4 | 1:100 | SIGMA-Genosys | ---------- |
| Rabbit anti-phospho-FAK | 1:50 | Cell signaling | 3283 |
| Rabbit anti-phospho-MLC2 | 1:200 | Cell signaling | 3671 |
| Rabbit anti-phospho-Paxillin | 1:100 | Invitrogen | 44-722G |
| Mouse anti-Vimentin | 1:50 | SIGMA | V6630 |
| Mouse anti-Vinculin | 1:100 | SIGMA | V9131 |
| Mouse anti-ZO1 | 1:50 | SIGMA | V6630 |

**Table XVIII.** Primary antibodies used for immunofluorescence

ImageJ software (NIH) was used to analyse fluorescence from pFAK immunostaining to analyse the number, area and distribution of focal adhesions per cell from TIFF images captured using the same exposure conditions. DAPI staining was used to elucidate the number of cells in each image.

NOX4 staining from cells seeded on gelatin-coated glass coverslips was visualized on a Leica TCS SP5 spectral confocal microscope with a HCX PL APO λ blue 63x 1.4 oil objective lens and excited with the 488nm laser line of an Argon laser. Acquisition software was LEICA application suite advanced fluorescence (LAS AF). The projections of Z-stacks are shown. Fluorescence intensity was quantified using Fiji open source software.

## 10.1. Immunofluorescence in cells cultured on thick layers of collagen I

For the immunostaining of cells seeded on top of a thick collagen I matrix, cells were fixed during 15 minutes at room temperature by adding 50μL of PFA 12% to cells seeded on 100μL of matrix (final concentration of PFA is 4% considering collagen matrix volume) and washed 3 times with PBS during 5 minutes. Afterwards, cells were permeabilized during 10 minutes using a solution containing 0.2% Triton X-100 in PBS-BSA 5% and washed again 3 times with PBS during 5 minutes. Next, samples were blocked in a PBS-BSA 5% solution during 20 minutes, and finally immunostained with specific primary antibodies diluted in blocking

solution. For pMLC2 staining, primary antibody was diluted 1:200 into blocking solution and incubated overnight at 4ºC, in motion. The day after, cells were washed 5 times with PBS for 5 minutes and incubated during 2 hours at room temperature with secondary Alexa Fluor 488 diluted 1:500 in blocking solution. Cells were washed 5 times with PBS during 5 minutes, and finally stained for F-actin during 1 hour at room temperature with Alexa Fluor 546-phalloidin probe diluted 1:500 in blocking solution, and washed again for 5 times with PBS during 5 minutes. During the second last wash nuclei were stained with a DAPI solution 1:200. In all incubations with primary and secondary antibodies, as well as for DAPI staining, dilutions were calculated considering the volume of the collagen matrix.

For the imaging, collagen gels with immunostained cells were transferred to glass-bottomed dishes and visualized on a Zeiss LSM 510 Meta confocal microscope (Carl Zeiss) with C-Apochromat 40x / 1.2 NA (water) and Zen software (Carl Zeiss). Confocal Z-slice images were analysed using ImageJ. pMLC2 fluorescence signal was quantified calculating the pixel intensity in single cells relative to the cell area, determined using F-actin staining, using Fiji open source software.

# 11. Immunohistochemistry (IHC)

## 11.1. Paraffin embedding

After fresh tissue (or tumour) was surgically recovered, it was rinsed with PBS and included into a cassette for paraffin embedding. Then, it was fixed with tamponed formaldehyde (4%) during 12-16 hours. After fixing the samples, they were dehydrated by bathing them in subsequent alcohols as indicated on **Table XIX**. Next, samples were finally embedded in paraffin at 65ºC and taken to 4ºC for solidification.

## 11.2. IHC on paraffin-embedded tissues

Paraffin-embedded samples were cut into 4μm-thick sections. Then, slices were placed in poly-lysined slides. For poly-lysing, slides were incubated for 20 minutes with poly-L-Lysine at 4ºC and let 16 hours of air-drying at 37ºC.

Next, paraffin was removed and samples rehydrated. For this, sample slides were placed at 50ºC during 30 minutes and then soaked in subsequent alcohols as indicated in **Table XX**.

| Step | Time |
|---|---|
| Rinse with tap water | 30 minutes |
| Ethanol 70% | 60 minutes |
| Ethanol 96% | 60 minutes |
| Ethanol 96% (new) | 60 minutes |
| Ethanol 96% (new) | Overnight |
| Ethanol 100% | 60 minutes |
| Ethanol 100% (new) | 90 minutes |
| Ethanol 100% (new) | 90 minutes |
| Xylene | 90 minutes |
| Xylene-Paraffin (50%-65ºC) | 90 minutes |
| Paraffin (65ºC) | Overnight |

**Table XIX.** Samples dehydration for paraffin-embedding

| Step | Time |
|---|---|
| Xylene | 10 minutes |
| Xylene (new) | 10 minutes |
| Xylene (new) | 10 minutes |
| Ethanol 100% | 5 minutes |
| Ethanol 100% (new) | 5 minutes |
| Ethanol 100% (new) | 5 minutes |
| Ethanol 96% | 5 minutes |
| Ethanol 96% (new) | 5 minutes |
| Ethanol 96% (new) | 5 minutes |
| Ethanol 70% | 5 minutes |
| Distilled water | 5 minutes |

**Table XX.** Samples hydration for IHC

Then after, sample slides were stained with Hematoxylin and Eosine (H/E) for tissue structure study or used for immunohistochemical analysis.

For H/E staining, Hematoxylin solution, Harris modified, was used. Samples were stained for 1 minute and washed abundantly with tap water. Next, samples were stained with Eosin solution for 6 minutes and washed again abundantly with tap water. Finally, samples were dehydrated soaking them in subsequent alcohols as indicated in **Table XXI** and slides were mounted in D.P.X. for preservation.

| Step | Time |
|---|---|
| Ethanol 70% | 1 minute |
| Ethanol 96% | 1 minute |
| Ethanol 96% (new) | 1 minute |
| Ethanol 96% (new) | 1 minute |
| Ethanol 100% | 5 minutes |
| Ethanol 100% (new) | 5 minutes |
| Ethanol 100% (new) | 5 minutes |
| Xylene | 10 minutes |
| Xylene (new) | 10 minutes |
| Xylene (new) | 10 minutes |

**Table XXI.** Samples dehydration after IHC

For IHC, after rehydration samples we rinsed during 5 minutes with distilled water and then covered with a mixture of citric acid (0.38mg/mL) and sodium citrate (2.45mg/mL) and boiled during 2 minutes to break the methylene bridges and expose the antigenic sites in order to allow the antibodies to bind. Next, samples were left for 20 minutes at RT, and afterwards rinsed during 5 minutes with distilled water.

At this point, we proceeded to deactivate the endogenous peroxidases of the samples, in order to minimize the background, by incubating the slides in 3% hydrogen peroxide during 10 minutes and then washing them, first during 5 minutes in distilled water, and then in PBS-Tween (0.1%) during 10 minutes.

Afterwards, samples were covered during 2 hours in IHC-blocking solution: 2% BSA and 20% FBS in PBS-Tween (0.1%). Then, slides were incubated overnight with primary antibody diluted in IHC-blocking solution, at 4ºC in a wet chamber. The following primary

antibodies (diluted from 1:50 to 1:100) were used: rabbit anti-Ki67, rabbit anti-cleaved Caspase-3 (Asp-175), rabbit anti-NOX4.

After, slides were washed 3 times with PBS-Tween (0.1%) during 10 minutes and incubated during 1 hour with anti-mouse or anti-rabbit secondary peroxidase-conjugated antibodies (Vectastain ABC KIT, Vector laboratories Inc.), then samples were washed 3 times with PBS-Tween (0.1%) during 10 minutes and incubated in ABC solution for 30 minutes, following the manufacturer's indications, until developing the peroxidase staining with diluted Diaminobenzidine (D.A.B; purchased at DAKO, Inc.) for a maximum of 30 minutes. Once we had acquired an optimum staining the developing reaction was stopped by soaking the samples into tap water during 5 minutes.

The final steps consisted in a Hematoxylin counterstaining as indicated in **Table XXII,** sample dehydration (**Table XXI**) and mounting the slides in D.P.X. for preservation.

Tissues were visualized in a Nikon eclipse 80i microscope with the appropriate filters. Representative images were taken with a Nikon DS-Ri1 digital camera.

| Step | Time |
|---|---|
| Filtered Hematoxylin (Meyer's) | 5 minutes |
| Running tap water | 5 minutes |

**Table XXII.** Hematoxylin counterstaining after IHC

# 12. Tissue array

A human liver tissue array (catalogue number Z7020056, BioChain Institute, San Francisco, USA) containing duplicates of 70 cases covering: 1) HCC and few samples of other types of liver cancer; 2) 3 cases of other non-malignant liver tissues; and 3) 2 normal liver tissues, was incubated with rabbit anti-NOX4 antibody diluted 1:50 into IHC-blocking solution (2% BSA and 20% FBS in PBS-Tween (0.1%)) as a primary antibody. Same procedure as for immunohistochemistry (Material and Methods 11) was used, without counterstaining with Hematoxylin. Staining was densitometered using the software Quantity One (Bio-Rad Laboratories, Hercules, USA) and the ratio between each case and the mean of normal tissues was represented.

# 13. Migration analysis

## 13.1. Chemotaxis assay

Chemotaxis is movement of an organism in response to a chemical stimulus. In order to analyse the chemotactic response of HCC cells to 10% FBS, transwell permeable supports with 8μm pores (Corning) were used. Cells were grown under basal conditions during 24 hours, and then they were trypsinized, washed once with medium without FBS and resuspended in FBS free medium for counting. 200,000 cells suspension was added to the upper chamber, medium 10% FBS was added to the lower chamber of a transwell permeable support, and it was incubated at 37ºC – 5% $CO_2$. After 24 hours, bright field images of the cells that migrated to the lower chamber were taken. Results were expressed as a number of cells per field.

## 13.2. Wound healing assay

Cells were grown under basal conditions up to 95% confluence. Monolayers were scratched with a pipette tip, then culture dishes were washed 2 times with fresh medium and finally, cells were cultured for 48 hours at 37ºC in medium without FBS to avoid proliferation interference. Representative phase contrast pictures were taken just after the scratch as a time zero. Then, cell migration was recorded by phase contrast microscopy (Olympus IX-70) 48 hours after wound scratch.

## 13.3. Real time migration assay

For real time monitoring of cell migration, xCELLigence System was used. For this, we used CIM plates which have an upper chamber sealed at the bottom with a microporous polyethylene terephthalate (PET) membrane with a median pore size of 8μm and a lower chamber that serves as a reservoir for chemo attractant media. xCELLigence System measures electrical impedance across micro-electrodes integrated on the underside of the membrane providing quantitative information about cell migration. CIM plates were placed onto the Real-Time Cell Analyzer (RTCA) station (xCELLigence System, Roche, Mannheim, Germany) for monitoring cell migration.

First, both sides of the membrane were coated during 30 minutes with a collagen IV solution (Sigma) (25.5μg/$cm^2$). Then, cells cultured under basal conditions were trypsinized and counted. Afterwards, 100μL of a suspension containing 4x$10^5$cells/mL were seeded onto the top

chamber of a CIM plate. The lower chamber contained a 48 hours conditioned media from NIH-3T3 cells as a chemo attractant. Cell migration was continuously monitored throughout the experiments by measuring changes in the electrical impedance at the electrode/cell interface, as a population of cells migrated from the top to the bottom chamber. Continuous values were represented as Cell Index (CI), a dimensionless parameter, which reflects a relative change in measured electrical impedance, and quantified as a slope ($hours^{-1}$) of the first five hours.

# 14. Invasion analysis

## 14.1. Invasive growth assay

Spheroid cell culture was performed using the hanging drop method, as described previously by Del Duca et al. (Del Duca et al., 2004). Cells were cultured under basal conditions and then trypsinised and counted. Afterwards, cells were resuspended in 1mL of low viscosity medium (800μL of medium 10% FBS plus 200μL of low viscosity methylcellulose solution) in a concentration of $4x10^5$cells/mL. From this suspension, 25μL droplets were suspended from the lid of tissue culture dishes for 48 hours at 37ºC – 5% $CO_2$, during which time cells clustered into compact sphere-like formation. Then, spheroids were collected into a 15mL tube and centrifuged at 300rpm during 15 seconds, and finally, resuspended in a collagen I solution (1.7mg/mL in DMEM), seeded in 24-well plates and left in the incubator at 37ºC – 10% $CO_2$ for 4 hours until the matrix polymerized. At that point, medium with 10% FBS was added on top and phase contrast pictures were taken every 24 hours, during 4 days. For spheroid invasion quantification, the increase on the area occupied by the spheroids between day 0 (when spheroids were embedded into the collagen I matrix) and day 4 was calculated by using ImageJ software.

## 14.2. 3D invasion assay

For the analysis of the invasive capacity of cells into a matrix, cells were suspended in serum-free bovine collagen I solution at 2.3mg/mL or in a solution of serum-free bovine collagen I / Matrigel (Corning) in a proportion 1:1, to a final concentration of 14,000 cells per 100μL of matrix. Cells were trypsinized, counted and washed twice with cold PBS, finally centrifuged at 1800rpm during 8 minutes at 4ºC and stored on ice. Next, the amount of cells necessary was mixed with the matrix, keeping both the matrix solution and cells always on ice, and 100μL of cell suspension were seeded on 96-well plates, previously coated for at least 30 minutes with a

solution containing BSA 0.2% in DMEM. Cells were then spun down and left in the incubator at 37ºC – 10% $CO_2$ for 4 hours until the matrix was polymerized. At that point, 50μL of 10% FBS-containing media was added on top of the matrix, allowing the cells to invade upwards during 24 hours. Afterwards, cells were fixed for 16 hours by adding 50μL of 20% formaldehyde solution per well (reaching the final concentration of 4% formaldehyde considering the matrix and medium volumes) containing also 5mg/mL Hoechst 33258 for nuclei staining. Plates were then imaged on a Zeiss LSM 510 Meta confocal microscope with a Plan Apochromat 10x / 0.30 objective lenses and Zen software. Confocal Z-slices were collected from each well at the bottom of the well and at 50μm above. Samples were run in quintuplicate and averaged. The 3D migration index was calculated as number of invading cells at 50μm divided by the total number of cells at the bottom.

For 3D imaging of invaded cells, sequential Z sections of embedded cells were obtained using a Zeiss 710 confocal microscope. 3D reconstructions of invaded cells were made using Zen software.

# 15. Adhesion assay

Cell adhesion was examined using a real-time assay through the xCELLigence System. Cells were cultured under basal conditions, trypsinized and counted. Afterwards, $1.25x10^4$cells/well (final volume of 100μL) were seeded onto an E-plate VIEW 16, which features microelectronic sensors integrated on the bottom of the plate. E-plates VIEW 16 were placed onto the Real-Time Cell Analyser (RTCA) station (xCELLigence System, Roche, Mannheim, Germany). Cell adhesion was continuously monitored throughout the experiments by measuring changes in the electrical impedance at the electrode/cell interface every 3 minutes during several hours. To analyse cell adhesion to different extracellular matrix, wells were previously coated during 30 minutes with collagen I (BD Bioscience) (4.5μg/$cm^2$), collagen IV (Sigma) (25.5μg/$cm^2$) or fibronectin (Upstate Biotechnology) (1.5μg/$cm^2$). Continuous values were represented as Cell Index (CI), a dimensionless parameter, which reflects a relative change in measured electrical impedance, and quantified as a slope ($hours^{-1}$) of the first three hours.

# 16. Integrin Array

For the analysis of integrin proteins on the cell surface we used a α/β-Integrin-Mediated Cell Adhesion Array Combo Kit (ECM532, Merck Millipore, Billerica, MA, USA) according to the

manufacturer's instructions. It contained mouse monoclonal antibodies generated against human alpha and beta integrins/subunits, that were immobilized onto a goat anti-mouse antibody coated microtiter plate. Cells were trypsinized and washed twice with PBS/EDTA solution, counted and diluted to a final concentration of $1.5x10^6$cells/mL in assay buffer. From this cell suspension, each well containing mouse anti-$\alpha$- or anti-$\beta$-integrin received 100$\mu$L containing $1.5x10^5$ cells, as did the BSA-coated negative control wells. The plate was then incubated during 2 hours at 37º - 5% $CO_2$ and washed with assay buffer. Cells were then stained with a Cell Stain Solution (provided in the kit), incubated during 5 minutes and washed with distilled water. Extraction buffer (100$\mu$L) was added to each well and left shaking during 5-10 minutes. Fluorescence was measured in Microplate Fluorescence Reader Fluostar optima using an exciting wavelength of 485nm and an emission wavelength of 520nm. Results represent relative cell attachment and were presented as arbitrary fluorescence units and/or as fold change versus control cells.

# 17. Statistical analyses

Statistical analyses were performed as an estimation of the associated probability to a student's t-test (95% confidence interval) or as a one-way ANOVA by Fisher's Least Significant Difference (LSD) method, depending on the involved conditions. In general, experiments were carried out at least 3 independent times with 2-3 technical replicates. Data were represented as mean +/- standard error of the mean (SEM). In all cases statistical calculation was developed using GraphPad Prism software (GraphPad, San Diego).

# V. RESULTS

# 1. ROLE OF NOX4 IN LIVER FIBROSIS

## 1.1. Changes in NOX4 expression during liver fibrosis in two different animal models

$Mdr2^{-/-}$ mice represent a widely used model for experimental liver fibrosis (Baghdasaryan et al., 2010; Barikbin et al., 2012) and are characterized by chronic liver injury and large periductal accumulation of MFB. Similarly, $Mdr2^{-/-}$ / $p19^{ARF-/-}$ double null mice (van Zijl et al., 2009) displayed a fibrotic phenotype comparable to $Mdr2^{-/-}$ mice but importantly, apart from being useful for the investigation of *in vivo* fibrosis development, they permit the isolation of MFB for *in vitro* experiments that become immortalized upon loss of $p19^{ARF-/-}$, a gene involved in the negative control of cell cycle (van Zijl et al., 2009). $Mdr2^{-/-}$ mice and $Mdr2^{-/-}$ / $p19^{ARF-/-}$ mice develop spontaneous fibrosis characterized by periductal accumulation of collagen and MFB, as well as an increased number of Kupffer cells (F4/80 positive). Of note, dying hepatocytes are mostly detected in the surrounding tissue of these fibrotic areas. On the other hand, $Stat3^{-hc}$/$Mdr2^{-/-}$ mice represent a mouse model with conditional inactivation of Stat3 in hepatocytes and cholangiocytes of $Mdr2^{-/-}$ mice (Mair et al., 2010). Loss of the hepatoprotective transcription factor Stat3 strongly aggravated liver injury and fibrosis of the $Mdr2^{-/-}$ fibrotic phenotype to premature lethality. The compensatory hepatocyte proliferation due to parenchymal liver damage is severely reduced in this model.

Previous reports have indicated that several profibrotic genes are up-regulated at early stages of fibrosis development in $Mdr2^{-/-}$ mice, highlighting the major pro-fibrotic cytokine, TGF-β (Fickert et al., 2004). Interestingly, the analysis by immunohistochemistry of the expression levels of the NADPH oxidase NOX4, a well-known target of TGF-β, were found elevated in the two fibrosis models studied ($Mdr2^{-/-}$ / $p19^{ARF-/-}$ and $Stat3^{-hc}$ / $Mdr2^{-/-}$ mice) in both hepatocytes and fibroblastoid cells. In the case of hepatocytes, NOX4 expression was more intense in those cells surrounding the MFB area (**Figure 1**). These data suggested that changes in the expression of NOX4 occur in different experimental animal models of hepatic fibrosis.

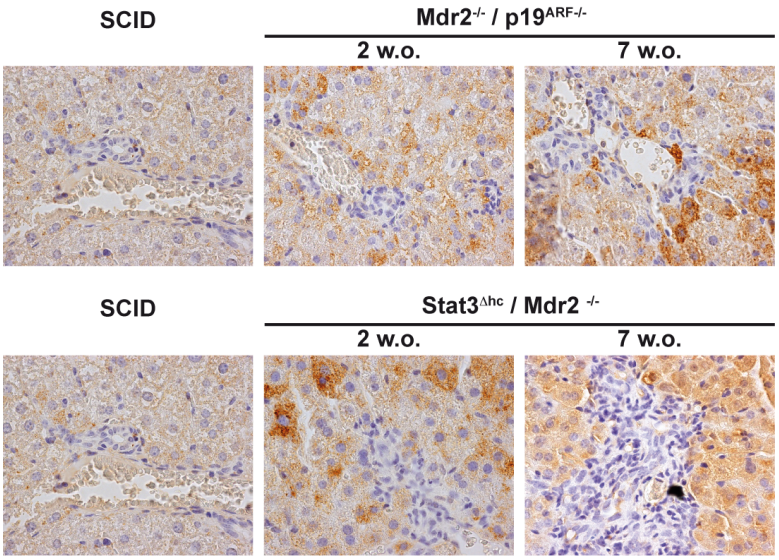


**Figure 1. NOX4 expression is increased concomitant with fibrosis development in Mdr2$^{-/-}$ / p19ARF$^{-/-}$ and Stat3$^{\Delta hc}$ / Mdr2$^{-/-}$ mice.** Representative 60x images of NOX4 immunohistochemistry of livers from control and 2 or 7 weeks old mice models indicated.

p19$^{ARF-/-}$ mice are a tool for the isolation of cells that behave in culture as spontaneously immortalized cells. HSC in an inactive state from p19$^{ARF-/-}$ non-fibrotic livers and activated MFB from Mdr2$^{-/-}$ / p19$^{ARF-/-}$ fibrotic livers were isolated and used to analyse the expression of NOX4 *in vitro*, by quantitative PCR. MFB showed increased expression of NOX4 at the mRNA level when compared to inactive HSC (**Figure 2**), suggesting that NOX4 may be induced during the HSC activation process.

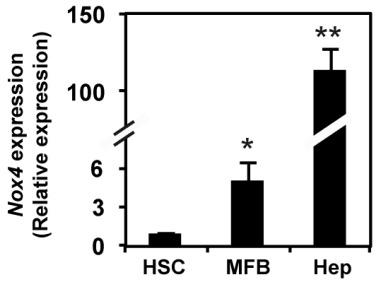


**Figure 2. Comparative analysis of *Nox4* mRNA expression.** Quantitative real time PCR of *Nox4* in HSC isolated from p19$^{ARF-/-}$ mice, *in vivo* activated MFB from Mdr2$^{-/-}$ / p19$^{ARF-/-}$ livers and wild-type immortalized hepatocytes (Hep). Data represent the mean ± SEM of three independent experiments, where relative expression versus HSC was calculated. Student's t-test versus HSC was used: *p<0.05, **p<0.01.

In addition, and corroborating the results at the tissue level where the most positive cells were hepatocytes surrounding fibrotic areas, much more positive than the fibrotic areas *per se*, immortalized hepatocytes showed much higher NOX4 expression when compared to HSC or MFB (**Figure 2**).

## 1.2. Effect of silencing NOX4 in the activation of HSC to MFB in response to TGF-β

Since NOX4 seemed to increase during the transdifferentiation process of HSC to MFB and its role in this process is completely unknown, we decided to focus our study on the potential role of NOX4 in the *in vitro* activation of HSC by TGF-β. For this purpose, HSC isolated from $p19^{ARF-/-}$ mice were used. As expected, TGF-β treatment induced HSC activation, featured by increase in the mRNA levels of α-SMA (*Acta2*) and vimentin, and the extracellular matrix genes collagen I and fibronectin, which was accompanied by NOX4 up-regulation. The same panel shows that all these changes in gene expression induced by TGF-β were inhibited when NOX4 was knocked-down by means of a siRNA, in cultured HSC cells (**Figure 3A**). In order to confirm the role of NOX4 and to determine whether NOX4 ROS production is responsible for mediating the transdifferentiation of HSC to MBF, cells were pre-treated with a permeable form of glutathione (GEE) to counteract ROS effects, and DPI, a well-known inhibitor of NADPH oxidases and other flavoproteins. Results showed attenuation on the changes in gene expression addressed by TGF-β in HSC, highlighting a relevant role played by ROS, and more specifically, NOX-derived ROS, in the activation of HSC (**Figure 3B**).

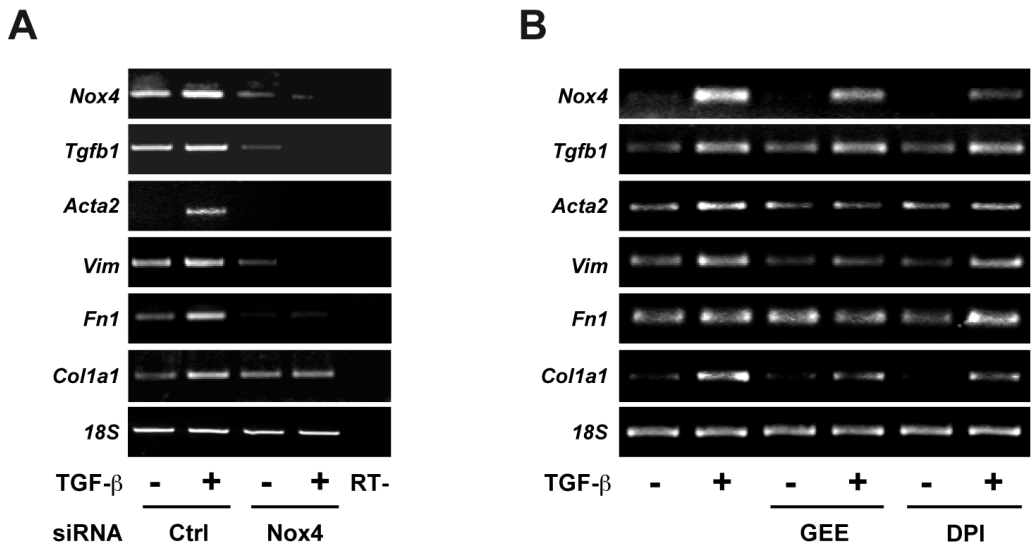


**Figure 3. Attenuation of Nox4 function and antioxidant treatment, inhibit TGF-β dependent activation of HSC.** Semi-quantitative PCR of the genes indicated from $p19ARF^{-/-}$ HSC cells transfected with either an unsilencing siRNA (Ctrl) or a specific siRNA for Nox4 (Nox4 siRNA) and then treated or not with 2ng/mL TGF-β during 48 hours (A) and from $p19ARF^{-/-}$ HSC cells pre-incubated during 30 minutes with 2mM GEE or 1μM DPI, as indicated in the figure, before adding 2ng/mL TGF-β for 48 hours (B). 18S was used as loading control. A representative experiment out of 3 is shown. Since HSC are very sensitive to serum deprivation, all experiments were carried out in the presence of 10% FBS.

## 1.3. Effect of silencing NOX4 in the response of hepatocytes to TGF-β in terms of cell death

Finally, and considering the high expression of NOX4 in hepatocytes, we decided to study the putative role of NOX4 in TGF-β-induced effects in these cells. As shown in **Figure 4A**, NOX4 expression was significantly up-regulated upon TGF-β treatment, reaching the maximum protein level at 24–48 hours after treatment. It has been previously reported in several experimental models that induction of apoptosis by TGF-β is impaired when NOX4 is knocked-down. Thus, we decided to study whether it also occurs in our model. By determining the caspase-3 activity by means of a fluorimetric assay, we confirmed that also in hepatocytes, NOX4 silencing completely blocked the TGF-β-induced apoptosis (**Figure 4B**). Interestingly, supplementation of cell culture medium with either antioxidants (GEE and BHA) or a general inhibitor of NADPH oxidases (DPI) blocked TGF-β-induced ROS production (**Figure 4C**) and caspase-3 activation in hepatocytes (**Figure 4D**), highlighting the relevance of NOX derived ROS in the apoptosis induced by TGF-β in hepatocytes.

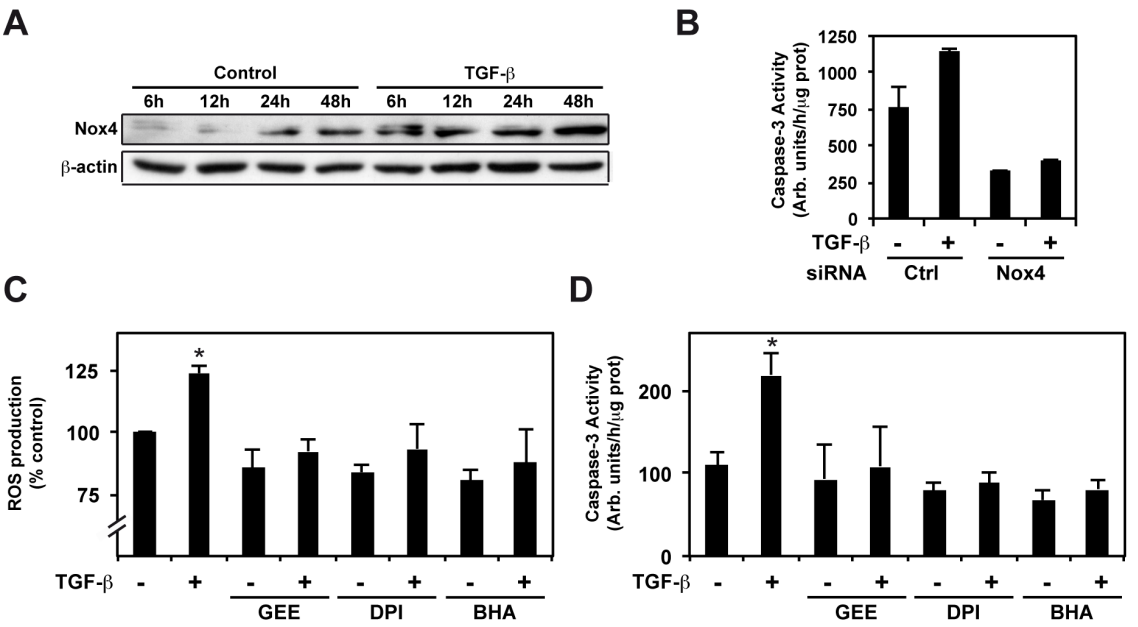


**Figure 4. NOX4-derived ROS mediate TGF-β induced apoptosis in hepatocytes.** A) Nox4 protein levels, analysed by western blot, in hepatocytes after treatment with 2ng/mL TGF-β for the times indicated in the figure. A representative experiment is shown (N=2). B) Analysis of caspase-3 activity in hepatocytes transfected with either an unsilencing siRNA (Ctrl) or a specific siRNA for Nox4 (Nox4 siRNA) and treated or not with 2ng/mL TGF-β for 16 hours. C) Analysis of the intracellular content of ROS through a fluorimetric assay as detailed in material and methods section, after 3 hours treatment with TGF-β. D) Analysis of caspase-3 activity after 16 hours treatment with TGF-β. In (C) and (D), hepatocytes were pre-incubated during 30 minutes with 2mM GEE, 1μM DPI or 200μM BHA, as indicated in the figure, before adding 2ng/mL TGF-β. Data in (B), (C) and (D) represent the mean ± SEM of three independent experiments. Student's t-test comparing TGF-β-treated versus non-treated cells in all pre-treatment conditions was used in (C) and (D): *p<0.05.

# 2. ROLE OF NOX4 IN LIVER CARCINOGENESIS

## 2.1. Phenotypic characterization of human HCC cell lines: Relevance of TGF-β pathway

Considering the relevance of TGF-β pathway in cancer, including liver cancer, and the high heterogeneity both clinical and molecular, described in HCC patients, we wanted to characterize different human HCC cell lines in terms of morphology, actin cytoskeleton and EMT markers, and try to elucidate whether TGF-β would play a role in determining this heterogeneity.

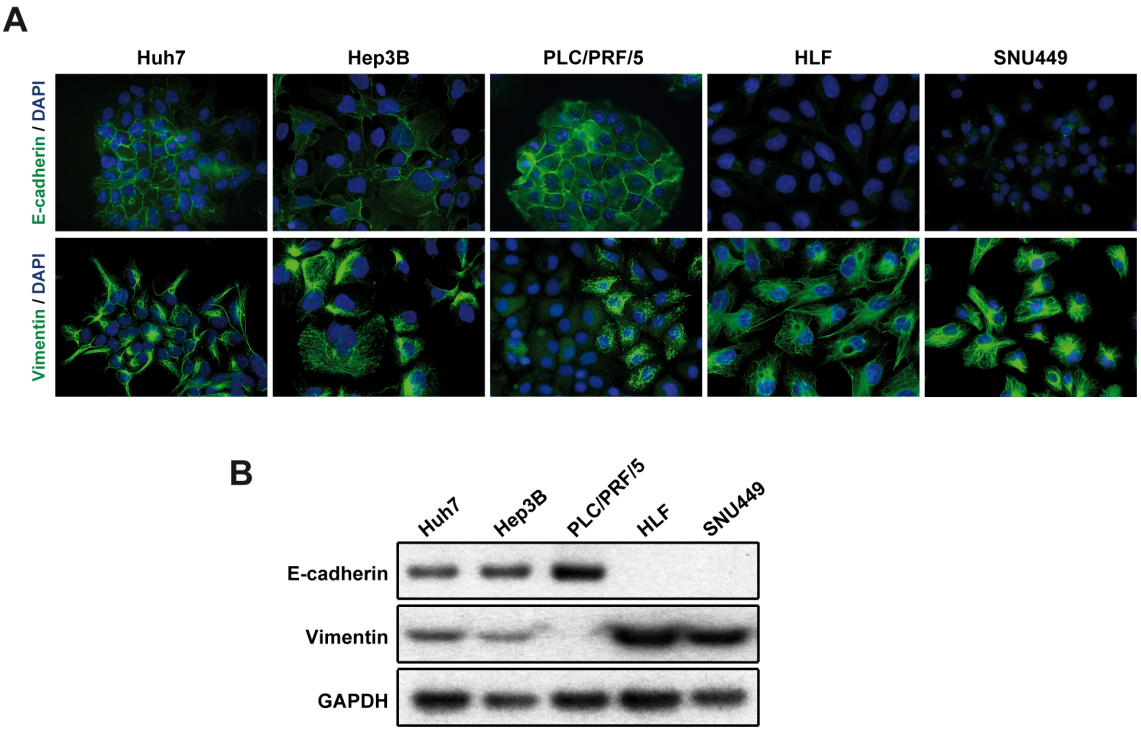


**Figure 5. Expression of epithelial and mesenchymal proteins differs within human HCC cell lines.** A) Immunofluorescence of E-cadherin (green) and vimentin (green). DAPI (blue) was used for nuclei staining. Representative 40x images are shown. B) Analysis of E-cadherin and vimentin protein levels by western blot. GAPDH was used as a loading control. A representative experiment is shown (N=3). HCC cell lines are detailed in each panel.

In order to have a representative sample of the wide range of phenotypes existing in HCC, we selected five different human HCC cell lines whose characteristics are detailed in

material and methods. To begin with, we performed an immunofluorescence of E-cadherin, a well-known protein characteristic of epithelial cells, and of vimentin, a mesenchymal intermediate filament (**Figure 5A**). We observed a correlation between the decrease of epithelial markers and the appearance of cells expressing mesenchymal markers. Furthermore, we can apparently divide the cell lines in two different groups: on the one hand, Huh7, PLC/PRF/5 and Hep3B cells displayed a mixed phenotype, showing both epithelial and mesenchymal characteristics at the same time; while on the other hand, immunofluorescence in SNU449 and HLF cells revealed a full mesenchymal phenotype, since they expressed huge amounts of vimentin without any detection of E-cadherin in cell-to-cell contacts. In addition, western blot analysis of the same EMT markers confirmed the results obtained by immunofluorescence (**Figure 5B**).

To further characterise the HCC cell lines, we did an actin cytoskeleton staining of cells cultured under basal conditions (**Figure 6**). Not surprisingly considering the differences observed in adherent junctions and intermediate filaments, actin structures differ between HCC cell lines. Thus, PLC/PRF/5 cells actin cytoskeleton was structured mainly as cortical F-actin, although some of the cells also showed filopodia. Something similar in terms of filopodia was observed in Huh7 cells. Stress fibres were present in all cell lines. However, its appearance differed between them; on the one hand, both PLC/PRF/5 and Huh7 cells showed few and thin stress fibres, while on the other hand, HLF and SNU449 showed bigger amount of robust, long and thick stress fibres. In contrast, Hep3B cells showed long and thin stress fibres, in addition to membrane ruffles. Moreover, lamellipodia could be observed in some SNU449 cells.

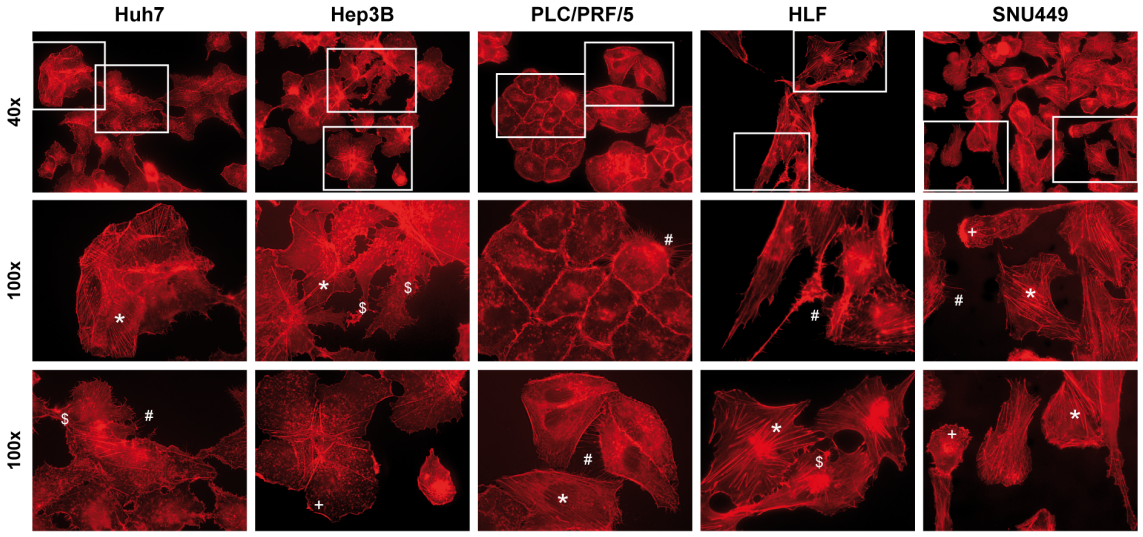


**Figure 6. Analysis of actin cytoskeleton structures in different human HCC cell lines.** Symbols indicate different actin structures: * stress fibres, + lamellipodia, # filopodia and $ membrane ruffles. Representative 40x images are shown (N=3). From 40x images, 100x zoom of specific zones is shown.

HCC cell lines used in this work had already been described to respond with different gene expression profiles to TGF-β treatment (Coulouarn et al., 2008). Interestingly, the three cell lines holding a mixed phenotype belonged to a group called “early”, suppressive responders to TGF-β, while the two other cell lines belonged to a group where the cytokine provoke a “late”, pro-tumorigenic response, inducing a more migratory and invasive phenotype.

Upon TGF-β treatment, cells showing epithelial characteristics responded to the cytokine as a cytostatic factor, whereas cells with a mesenchymal-like phenotype did not arrest proliferation in the presence of TGF-β (**Figure 7A**). This behaviour further confirms the previous classification of these cell lines according to the TGF-β signature (early for Huh7, PLC/PRF/5 and Hep3B and late for SNU449 and HLF). In an attempt to understand what would happen *in vivo*, we wondered whether HCC cells were expressing autocrine TGF-β and whether this production could play a role in determining the cell phenotype. Quantitative analysis of mRNA expression revealed a correlation between TGF-β levels, the acquisition of a mesenchymal phenotype and the lack of response to the cytokine as a tumour suppressor (**Figure 7B**). Of note, cells with higher expression of TGF-β were the same ones showing a robust actin cytoskeleton with many thick and long stress fibres.

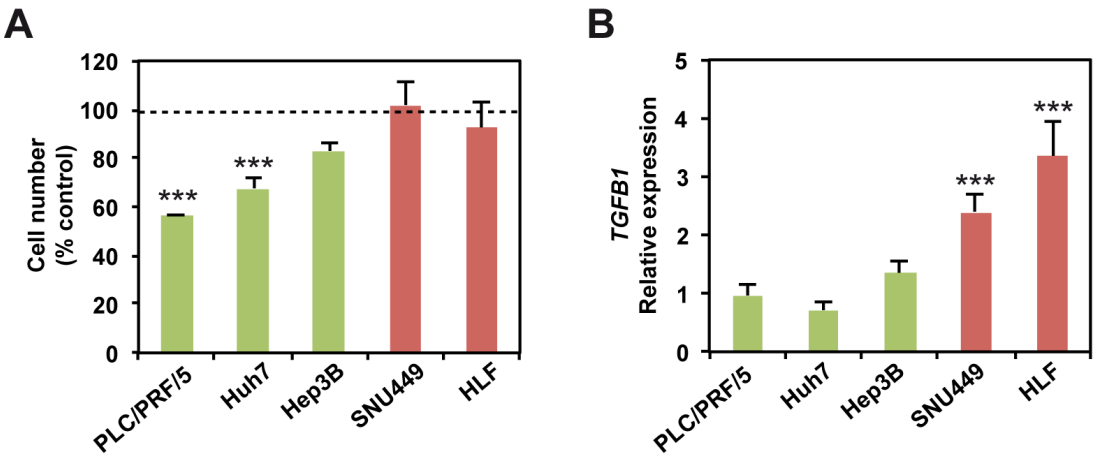


**Figure 7. Mesenchymal-like phenotype in HCC cell lines correlates with resistance to TGF-β-induced suppressor effects and increased expression of TGF-β.** A) Cell viability analysed by crystal violet, after 48 hours treatment with TGF-β 2ng/mL. Data were calculated relative to zero time and represent the mean ± SEM of at least 6 independent experiments. Student’s t-test versus zero time for each cell type was used: ***p<0.001. B) *TGFB1* expression levels analysed by quantitative PCR. Data are mean ± SEM of 5 independent experiments. One way ANOVA versus PLC/PRF/5 cells was used: ***p<0.001.

At this point we analysed whether the autocrine stimulation of the TGF-β pathway is determinant for cell phenotype by stable silencing the expression of TGF-β receptor 1 (TGFBR1), transfecting Hep3B cells with specific shRNA. Briefly, a pool of four different

plasmids containing a shRNA sequence against TGFBR1 were transfected, in addition to an unsilencing shRNA, using MATra-A reagent. After 24 hours the media was changed to complete media and the following day we started the selection of stable transfected cells by adding puromycin into the cell culture, as explained in material and methods. As shown in **Figure 8A and B**, both mRNA and protein TGFBR1 levels were significantly decreased in silenced cells compared to control cells. Furthermore, cells also presented lower levels of phospho-SMAD2, a downstream target of the canonical TGF-β pathway. Interestingly, TGFBR1-silenced Hep3B cells showed increased mRNA and protein levels of E-cadherin, which presented a pericellular distribution, forming cell-to-cell contacts (**Figure 8C-D**).

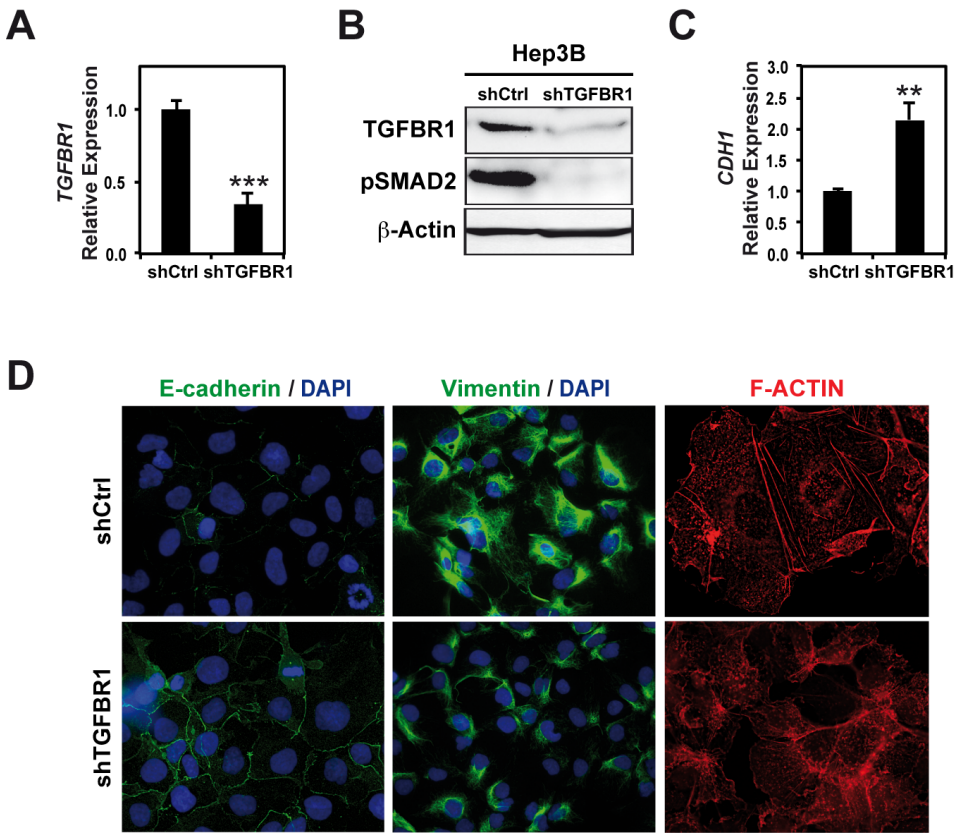


**Figure 8. Stable silencing of TGFBR1 recovers the epithelial phenotype.** Hep3B cells were stable transfected with an unspecific shRNA (shCtrl) or a pool of four different shRNA against TGFBR1 (shTGFBR1). A) Analysis of TGFBR1 expression by quantitative PCR. B) Western blot analysis of TGFBR1 and pSMAD2. β-actin was used as a loading control. A representative experiment is shown (N=3). C) Analysis of E-cadherin (CDH1) expression by quantitative PCR. D) Immunofluorescence of E-cadherin (green), vimentin (green) and F-actin (red). DAPI (blue) staining was used to visualize the nuclei. Representative 40x images are shown (N=3). Data in (A) and (C) represent the mean ± SEM of 3 independent experiments. Student's t-test versus control (unspecific-shRNA-transfected cells) was used: **p<0.01, ***p<0.001.

In addition, we found an apparent decrease in the expression of vimentin and a reorganization of the actin cytoskeleton, showing knock-down cells fewer stress fibers as well

as pericellular redistribution of F-actin, compared to control transfected Hep3B cells (**Figure 8D**).

In order to assess whether these changes on cell morphology had functional relevance, we performed a migration assay through the xCELLigence system. Importantly, silencing of TGFBR1 significantly decreased the migratory capacity of Hep3B cells (**Figure 9**).

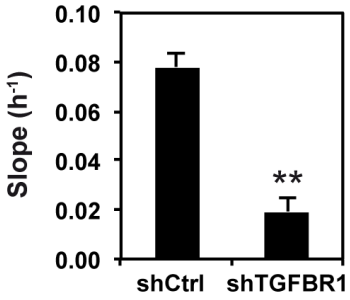


**Figure 9. Stable silencing of TGFBR1 inhibits cell migratory capacity of Hep3B cells.** Analysis of cell migration through a real-time migration assay (xCELLigence System). Data represent the mean ± SEM of 3 independent experiments. Student's t-test versus control (unspecific-shRNA-transfected cells) was used: **p<0.01.

In summary, mesenchymal-like phenotype in HCC cell lines correlates with increased autocrine stimulation of TGF-β pathway and resistance to TGF-β suppressor effects. Furthermore, targeting knock-down TGFBRI recovers epithelial features at the same time that decreases the migratory capacity of the cells.

## 2.2. Crosstalk between the TGF-β pathway and NOX4 in human HCC cell lines

It starts to be well established that in many systems TGF-β induces the expression of the NADPH oxidase NOX4. Indeed, previous works from our group described that TGF-β induces the expression of NOX4 in hepatocytes and HCC cells. Furthermore, we also demonstrated that the induction of NOX4 is necessary for the apoptosis induced by the cytokine (Carmona-Cuenca et al., 2008; Caja et al., 2009). Intriguingly, when we analysed the expression levels of NOX4 in the different human HCC cell lines, and tried to correlate them with the autocrine activation of TGF-β pathway, instead of a direct correlation we found an inverse correlation between NOX4 and TGF-β expression levels. Cells displaying epithelial-like features, that showed lower levels of TGF-β, presented high levels of NOX4 expression, whereas on the contrary, mesenchymal-like cells presenting higher levels of TGF-β showed lower mRNA levels of NOX4 (**Figure 10**).

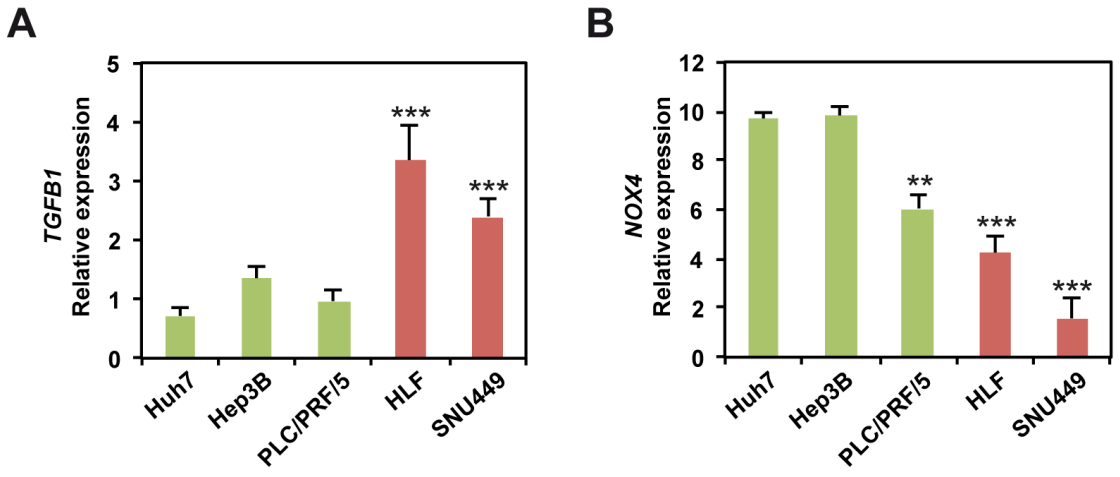


**Figure 10. Inverse correlation between TGF-β and NOX4 expression in human HCC cell lines.** Analysis of TGF-β (A) and NOX4 (B) expression levels by quantitative PCR. Data represent the mean ± SEM of at least 3 independent experiments. One way ANOVA versus Huh7 cells was used: **p<0.01, ***p<0.001.

Importantly, immunofluorescence analysis in normal hepatocytes (CHL) and different HCC cell lines (PLC/PRF/5, Hep3B and HLF) revealed that NOX4 is down-regulated in transformed cell lines when compared to normal cells (**Figure 11**).

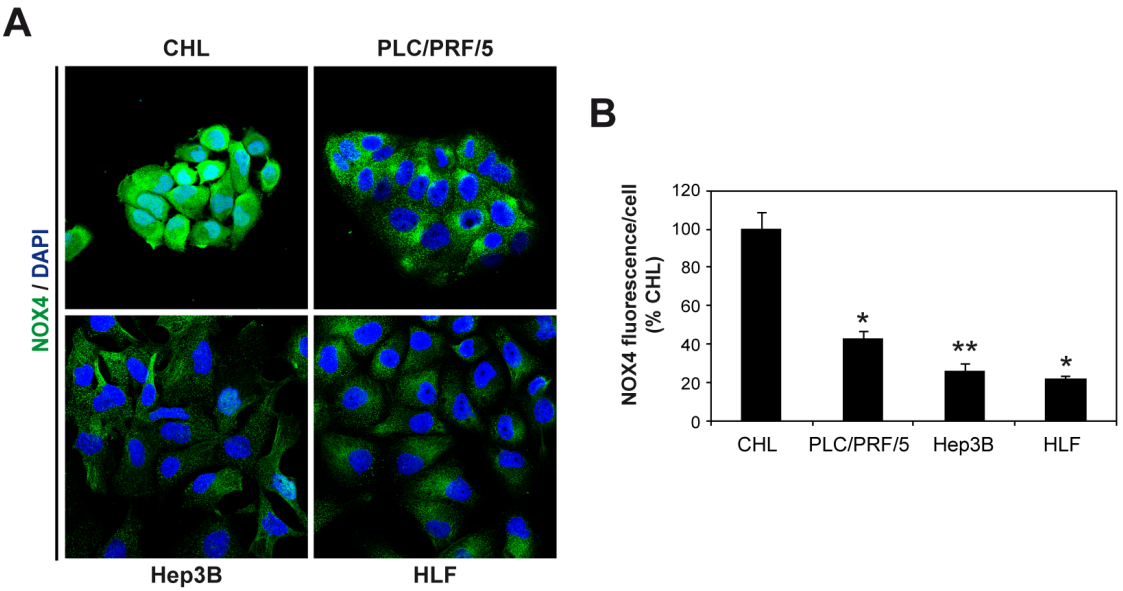


**Figure 11. NOX4 is down-regulated in HCC cell lines.** A) NOX4 (green) and DAPI (blue) staining in human hepatocytes (CHL) and human HCC cell lines (PLC/PRF/5, Hep3B and HLF). B) Quantification of NOX4 fluorescence per cell represented as percentage versus CHL. Data are mean ± SEM (N=3, 3 images/experiment) and Student's t-test versus normal hepatocytes (CHL) was used: *p<0.05, **p<0.01.

In an attempt to find an explanation for this unexpected result we wondered whether NOX4 expression levels on basal culture conditions were dependent on the autocrine TGF-β levels. If so, blocking the TGF-β pathway would have an impact on NOX4 expression. Thus, we decided to examine NOX4 protein levels in cells silenced for TGFBR1. Interestingly, in PLC/PRF/5 and Hep3B cells, which increased NOX4 expression upon TGF-β treatment (Carmona-Cuenca et al., 2008), knocking-down of the TGF-β receptor 1 provoked a decrease in NOX4 levels when compared to control cells (**Figure 12**).

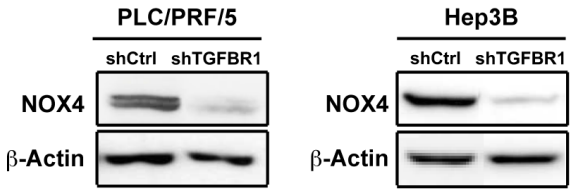


**Figure 12. Stable silencing of TGFBR1 decreases NOX4 levels in early TGF-β signature HCC cells.** Western blot analysis of NOX4 in PLC/PRF/5 and Hep3B cells silenced for TGFBR1. β-actin was used as a loading control. A representative experiment is shown (N=4).

However, when the effect of cancelling TGFBR1 on NOX4 levels was analysed in SNU449 and HLF, results revealed the opposite outcome, NOX4 expression was increased after blocking TGF-β pathway (**Figure 13A**). These data brought us to think that in these cell lines, the response to TGF-β treatment might be different. Indeed, when we treated these cells with TGF-β, surprisingly again, but in accordance to the results obtained upon blockage of the pathway, TGF-β decreased the expression levels of NOX4 in SNU449 and HLF cells (**Figure 13B**).

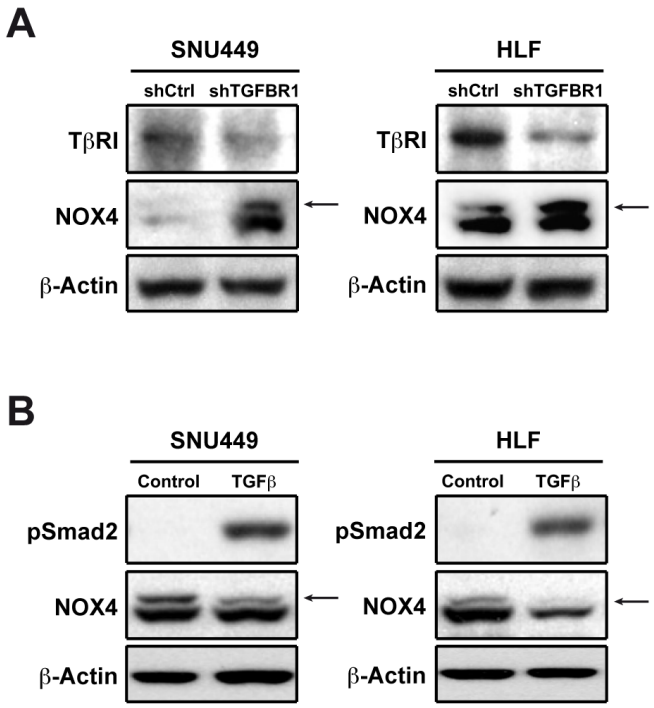


**Figure 13. Effect of TGF-β on NOX4 levels in late TGF-β signature HCC cells.** A) Western blot analysis of NOX4 in SNU449 and HLF cells silenced for TGFBR1. B) Western blot analysis of NOX4 in SNU449 and HLF cells after TGF-β treatment (2ng/mL). β-actin was used as a loading control. A representative experiment is shown (N=3).

At this point it is important to remember that TGF-β plays a dual role in some cancers, including HCC. It is shown in here (**Figure 7A**), and it was previously suggested by Coulouarn et al., that PLC/PRF/5 and Hep3B cells respond to TGF-β as a suppressor factor, while SNU449 and HLF display a late TGF-β signature, where TGF-β behaves as a pro-tumorigenic cytokine. Therefore, we can speculate that NOX4-TGF-β correlation might be cell context dependent, being a direct correlation during early stages of hepatocarcinogenesis, when TGF-β still acts as a tumour suppressor, but an inverse correlation in advanced stages when TGF-β already behaves as a tumour promoter. However, further experiments are needed to confirm this hypothesis.

# 2.3. Role of NOX4 as a negative regulator of proliferation

## 2.3.1. *In vitro* analysis of the effect of silencing NOX4 on the proliferation of liver tumour and untransformed cells

Considering the relevance of NOX4 in liver fibrosis presented in previous sections, one might think of the convenience of NOX4 targeting drugs to be used as therapeutic tools in this disease. However, we wondered which would be the consequences of sustained treatment with NOX4 inhibitors in liver carcinogenesis. We cannot forget that HCC usually develops in a background of a chronic liver disease such as fibrosis and cirrhosis.

In order to address this question, NOX4 was targeted knock down with specific shRNA in different HCC cell lines. We used the human HCC cell lines PLC/PRF/5 and Hep3B, not only because they express high levels of NOX4 but also because they respond to TGF-β with an early tumour suppressor signature, thus we could consider them as representative of the first steps of tumour development. Cells were transfected with four different plasmids of NOX4 shRNA, as well as with a plasmid control, following the procedure explained in material and methods section. Stable silenced clones were selected for the future experiments. In **Figure 14** are shown the best silenced clones for each cell line: clone #1 for PLC/PRF/5 and clones #2 and #3 for Hep3B cells. NOX4 levels were evaluated by western blot (**A**) and immunofluorescence (**B**), using a NOX4 antibody generated by our laboratory. Both assays showed a high reduction of NOX4 protein levels in the selected clones, when compared to cells transfected with the control shRNA.

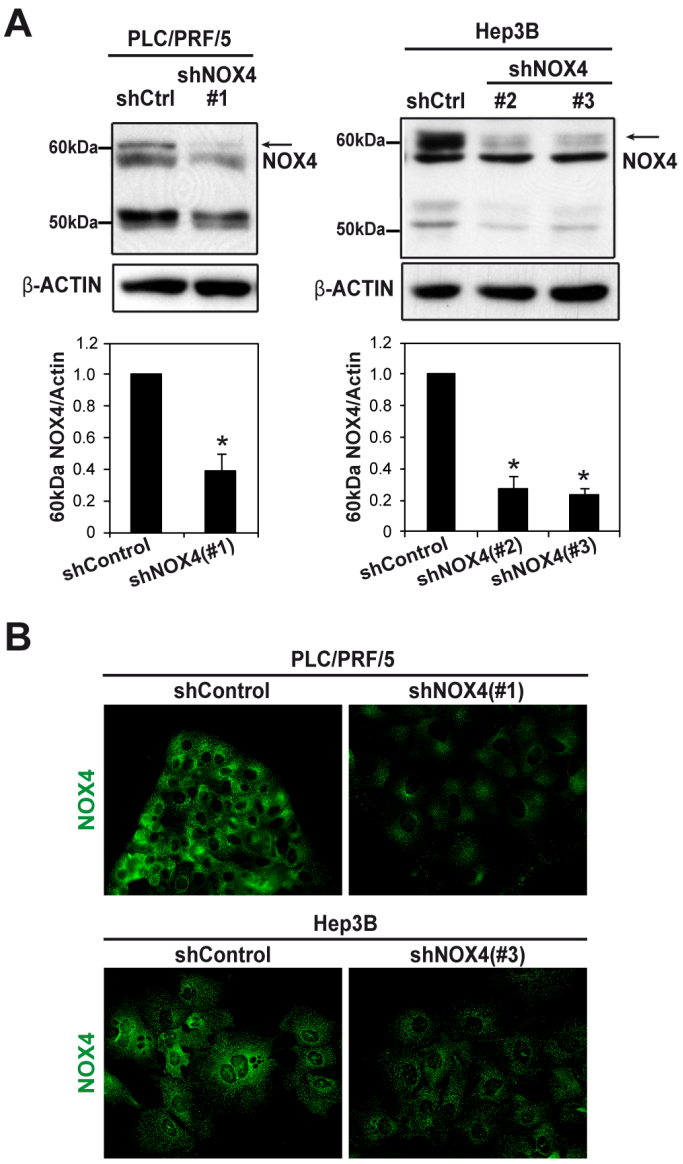


**Figure 14. Molecular analyses of the stable silencing of NOX4 in two human HCC cell lines.** Human HCC cells PLC/PRF/5 and Hep3B were stably transfected either with an unsilencing shRNA (shControl) or with four different plasmids against NOX4, separately. Best-silenced clones were selected: in PLC/PRF/5, clone#1: shNOX4(#1); in Hep3B, clones #2 and #3: shNOX4(#2) and shNOX4(#3), respectively. A) Up: Analysis of NOX4 protein levels by Western blot. β-actin was used as loading control. Down: Densitometric analysis of at least 3 independent experiments. Data are mean ± SEM and Student's t-test versus control (unspecific-shRNA-transfected cells) was used: *p<0.05. B) Immunofluorescence analysis of NOX4 (green) in control and NOX4 silenced cells. A representative experiment of 3 is shown.

Considering the NOX4 silencing achieved by the targeting knock-down, it was not surprising to find a decrease in intracellular ROS levels, when they were determined through $H_2$DCFDA fluorescence analysis, as well as in extracellular hydrogen peroxide levels, through Amplex Red assay (**Figure 15A**). Neither the analysis of mitochondrial superoxide using the MitoSOX Red reagent nor the analysis of intracellular superoxide through DHE fluorescence indicator showed differences between NOX4 targeted knock-down cells and control cells,

meaning that hydrogen peroxide was the main ROS source modified by silencing NOX4 in HCC cells (**Figure 15B**).

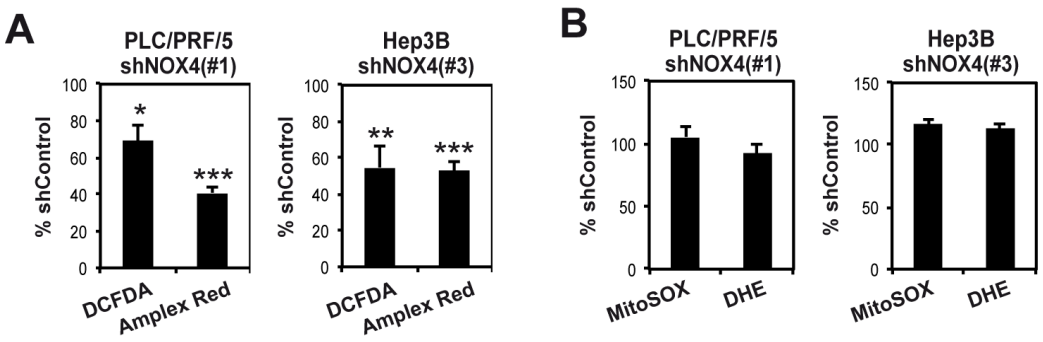


**Figure 15. Analysis of ROS production in NOX4 silenced cells.** A) Intracellular ROS levels ($H_2$DCFDA) and extracellular hydrogen peroxide levels (Amplex Red) analyzed fluorimetrically. B) Mitochondrial (MitoSOX) and intracellular superoxide (DHE) levels analyzed fuorimetrically. Left panels correspond to PLC/PRF/5 cells, right panels to Hep3B cells. Data are represented as percentage versus shControl and they are mean ± SEM of at least 3 independent experiments. Student's t-test versus control (unspecific-shRNA-transfected cells) was used: *p<0.05, **p<0.01, ***p<0.001.

Interestingly, it appears that NOX4 silencing does not provoke a massive change in protein oxidation but on the contrary, only specific changes were detected by using an antibody against nitrotyrosilated proteins (**Figure 16**). The nitration of tyrosyl groups in proteins, which is usually due to its reaction with peroxynitrite ($ONOO^-$) species that are produced as a consequence of the reaction of nitric oxide ($NO\cdot$) with ROS, modifies protein activity either in a loss or gain of function. Thus, nitration can contribute to signal transduction mechanisms (Kalyanaraman, 2013).

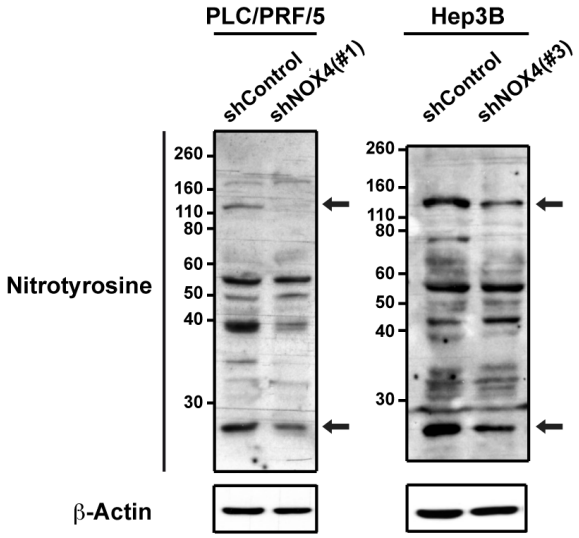


**Figure 16. NOX4 knock-down induces specific changes in protein nitration.** Western blot analysis of protein nitration in tyrosyl groups by using an anti-nitrotyrosine antibody. A representative experiment out of 3 is shown.

To further confirm the NOX4 silencing, we decided to analyse the loss of NOX4 function in Hep3B cells. We evaluated the cell response to TGF-β in terms of apoptosis, a process that requires NOX4 (Carmona-Cuenca et al., 2008). As expected, TGF-β-induced activation of caspase-3 was significantly diminished in both clones where NOX4 was knocked-down (**Figure 17**).

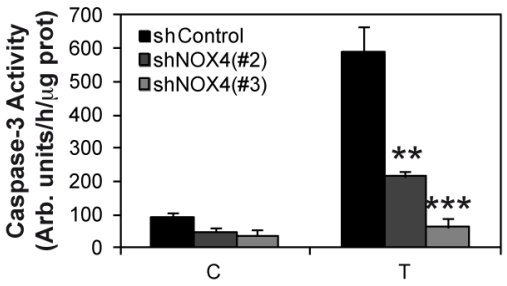


**Figure 17. Functional analysis of the stable silencing of NOX4 in HCC cells.** Caspase-3 activity analysis after 24 hours of TGF-β treatment (2ng/mL) in Hep3B shControl versus shNOX4(#2) and shNOX4(#3) cells. Data are mean ± SEM of 3 independent experiments. Student's t-test versus TGF-β treated shControl cells was used: **p<0.01, ***p<0.001.

Once the working model was verified, we first decided to analyse the effect of cancelling NOX4 on *in vitro* growth of HCC cells. For this, we performed experiments to compare the proliferative capacity of NOX4 silenced cells versus their respective control. Growth capacity was determined by performing several assays. To start with, increase in cell number upon time was assessed by crystal violet staining. Both cell lines (PLC/PRF/5 and Hep3B) showed a higher increase in the number of cells after NOX4 knock-down. Afterwards, DNA synthesis was analysed as [$^3$H]-Thymidine incorporation into TCA-precipitable material and, again, NOX4 silenced cells displayed a significant increase in proliferation compared to control cells. Finally, proliferating cells were determined by immunofluorescence of Ki67. Ki67 is an excellent marker for determining the growth fraction of a given cell population since it is a protein that can be detected during all active phases of the cell cycle ($G_1$, S, $G_2$ and mitosis) and is absent in resting cells ($G_0$) (Scholzen and Gerdes, 2000). Once more, reduction in NOX4 levels was coincident with increased number of Ki67 positive proliferating cells. Thus, all assays performed pointed to a significantly increased growth capacity in NOX4 knocked-down cells (**Figure 18**).

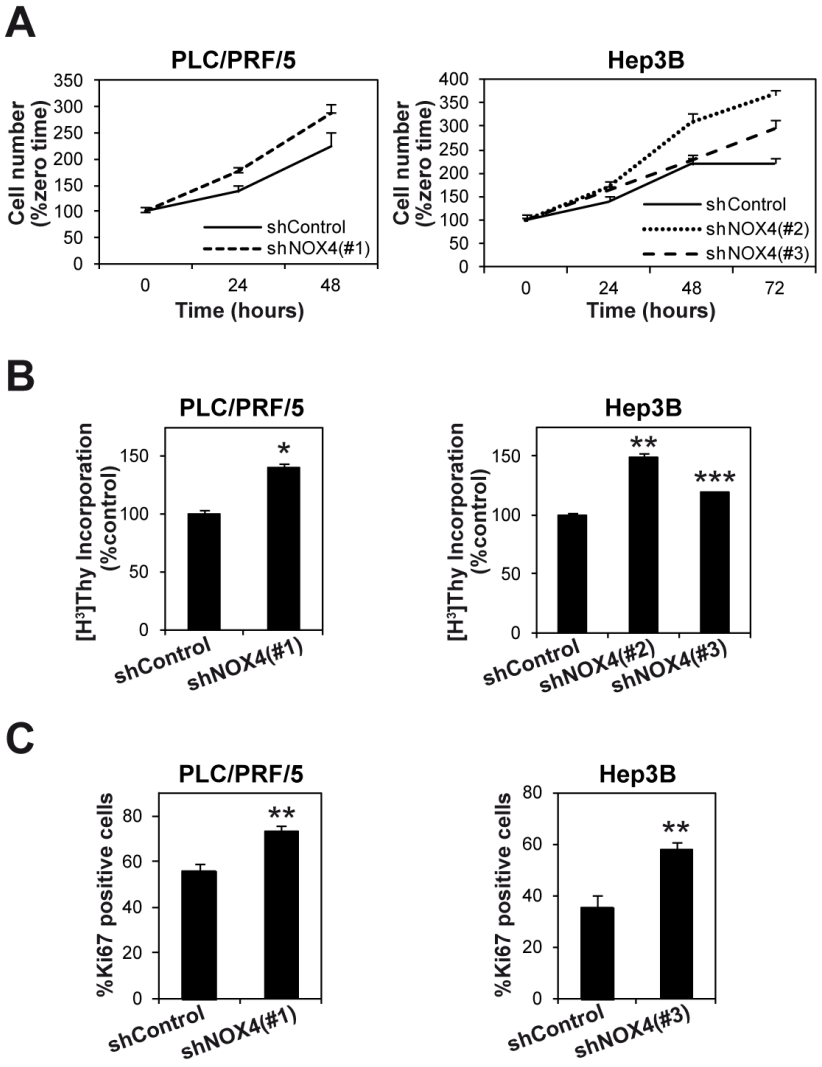


**Figure 18. Stable silencing of NOX4 confers a proliferative advantage to human HCC cells.** Comparison of the proliferative capacity of NOX4 silenced cells (shNOX4) versus cells transfected with an unspecific shRNA (shControl). The cell line and the shNOX4 used are detailed in each panel. A) Number of viable cells analyzed by crystal violet at the times indicated in the figure. Results are expressed as percentage of increase relative to zero time. B) DNA synthesis analyzed as [$^3$H]-Thymidine incorporation (48h) and expressed as percentage of the control (unspecific-shRNA-transfected) cells. C) Ki67 immunofluorescence; quantification of the positive nuclei expressed as percentage of total nuclei number. Data are mean ± SEM of 3 independent experiments. Student's t-test versus control (unspecific-shRNA-transfected) cells was used in (B) and (C): *p<0.05, **p<0.01, ***p<0.001.

Enhancement in cell proliferation correlated with significant lower percentage of cells in $G_1$-phase of the cell cycle and significant increase in the percentage of cells in S-phase (**Figure 19A**). Previous reports had proposed a role for NOX4 in TGF-β-induced senescence through up-regulation of $p21^{Cip1}$ and $p15^{INK4b}$ (Senturk et al., 2010). For this, we decided to analyse the expression of these cyclin-dependent kinase inhibitors. We found that attenuation of NOX4

expression provoked a decrease in the transcript levels of *CDKN1A* ($p21^{Cip1}$) (**Figure 19B**). Correlating with this, analysis of Cyclin D1 protein by Western blot revealed higher levels in NOX4 silenced versus control cells (**Figure 19C**).

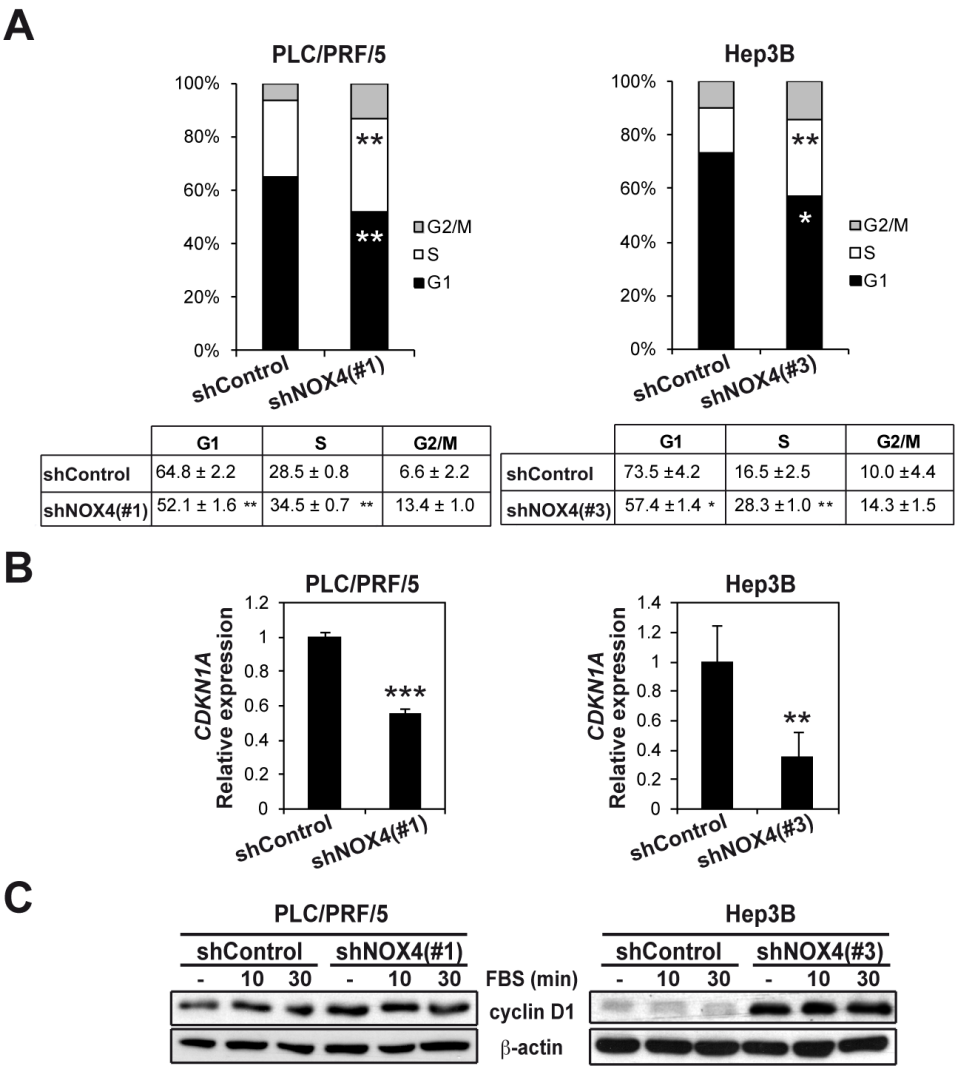


| | G1 | S | G2/M |
|---|---|---|---|
| shControl | 64.8 ± 2.2 | 28.5 ± 0.8 | 6.6 ± 2.2 |
| shNOX4(#1) | 52.1 ± 1.6 ** | 34.5 ± 0.7 ** | 13.4 ± 1.0 |

| | G1 | S | G2/M |
|---|---|---|---|
| shControl | 73.5 ±4.2 | 16.5 ±2.5 | 10.0 ±4.4 |
| shNOX4(#3) | 57.4 ±1.4 * | 28.3 ±1.0 ** | 14.3 ±1.5 |

**Figure 19. Stable silencing of NOX4 increases the proportion of HCC cells in proliferating phases of the cell cycle.** The cell line and the shNOX4 used are detailed in each panel. A) Analysis of the percentage of cells in the different phases of the cell cycle in control and NOX4 silenced (shNOX4) cells. B) Analysis of *CDKN1A* expression by quantitative PCR. C) Analysis of Cyclin D1 by Western blot at 10 and 30 minutes after 10% FBS stimulation. (C) shows a representative experiment (N=3). Data in (A) and (B) are mean ± SEM of at least 3 independent experiments. Student's t-test versus control (unspecific-shRNA-transfected) cells was used: *p<0.05, **p<0.01, ***p<0.001.

Interestingly, by immunofluorescence analyses, HCC cells where NOX4 expression was knocked-down showed higher nuclear localization of β-catenin, which was coincident with a decrease in the expression levels and/or membrane localization of E-cadherin (**Figure 20**). It is well characterized that under conditions of strong adhesion, cadherins and β-catenin interact in cell-to-cell adhesion complexes, forming a cluster together with actin filaments. However, when adhesion is lost, cadherins are de-clustered, connections with the cytoskeleton are dissolved and β-catenin is translocated to the nucleus where modifies gene expression, being Cyclin D1, a key inducer of transition from $G_1$ to S phase of the cell cycle, one of its target genes (Fagotto, 2013; Monga, 2014).

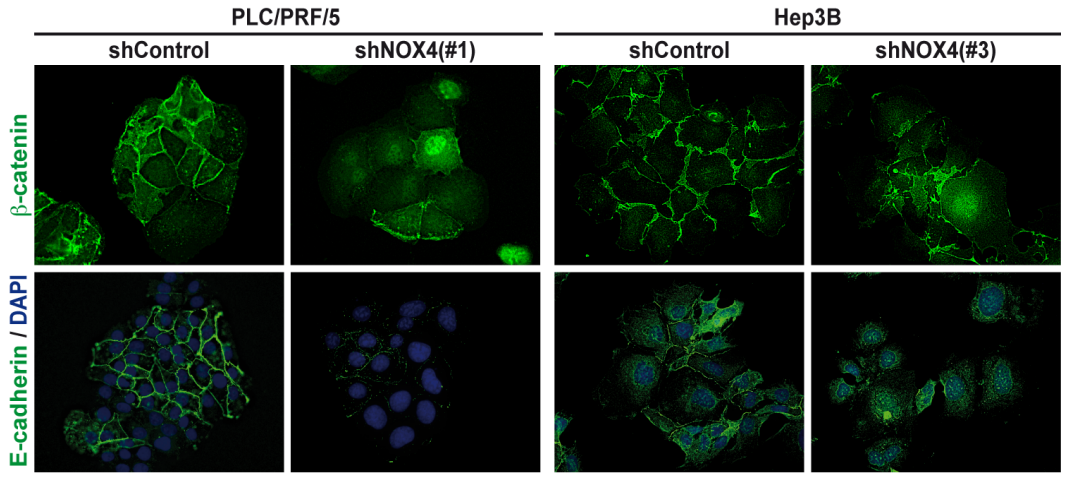


**Figure 20. NOX4 knock-down promotes β-catenin translocation to the nucleus.** Immunofluorescence analysis of β-catenin (green), E-cadherin (green). DAPI (blue) was used to detect the nuclei. Representative 40x pictures are shown (N=3).

In order to know whether the role of NOX4 in controlling proliferation was a specific characteristic of tumour cells or it also occurs in untransformed cells, experiments of transient targeting knock-down of NOX4 were performed in the untransformed human hepatocyte cell line Chang Liver (CHL) and in an immortalized mouse hepatocyte cell line. As shown in **Figure 21**, silencing of NOX4 (**A**), which correlated with a significant decrease in the intracellular ROS levels (**B**), significantly increased the growth of both cell lines (**C**).

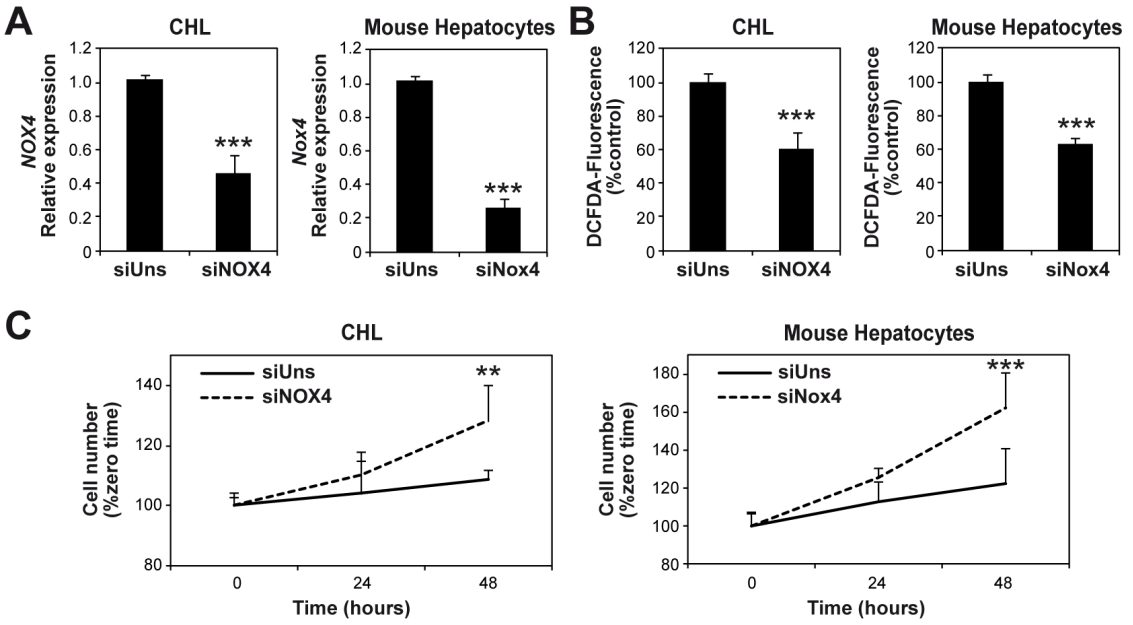


**Figure 21. NOX4-targeted knock-down increases proliferation in both human and mice hepatocytes.** CHL cells and mice hepatocytes were transfected with an unsilencing siRNA (siUns) or a specific NOX4 siRNA (siNOX4). A) Analysis of *NOX4* mRNA expression by quantitative PCR. B) Analysis of intracellular ROS levels (DCFDA). C) Number of viable cells analyzed by crystal violet at the indicated times. Results are expressed as percentage of increase relative to zero time. Data are mean ± SEM of 3 independent experiments. Student's t-test versus control (unspecific-siRNA-transfected) cells was used: **p<0.01, ***p<0.001.

All these results indicated that NOX4 negatively controls the proliferation of liver tumour and untransformed cells.

### 2.3.2. Nox4 expression is down-regulated during liver regeneration after partial hepatectomy in mice

Since results described above indicated an inverse correlation between NOX4 expression and liver cell growth in *in vitro* experiments, we hypothesized that NOX4 expression may inversely correlate with hepatocyte proliferation under physiological and/or pathological situations where proliferation of liver cells takes place. To confirm this hypothesis, changes in the expression of NOX4 were studied after 2/3 partial hepatectomy in mice, situation that pushes hepatocytes to leave $G_0$ phase of the cell cycle to proliferate and regenerate the liver. As shown in **Figure 22A**, partial hepatectomy provoked a down-regulation of *Nox4* expression between 2 and 72 hours, completely recovered after 7 days, without changes in *p22phox* expression, correlating with lower NOX4 protein levels in hepatocytes, analysed by immunohistochemistry (**Figure 22B**).

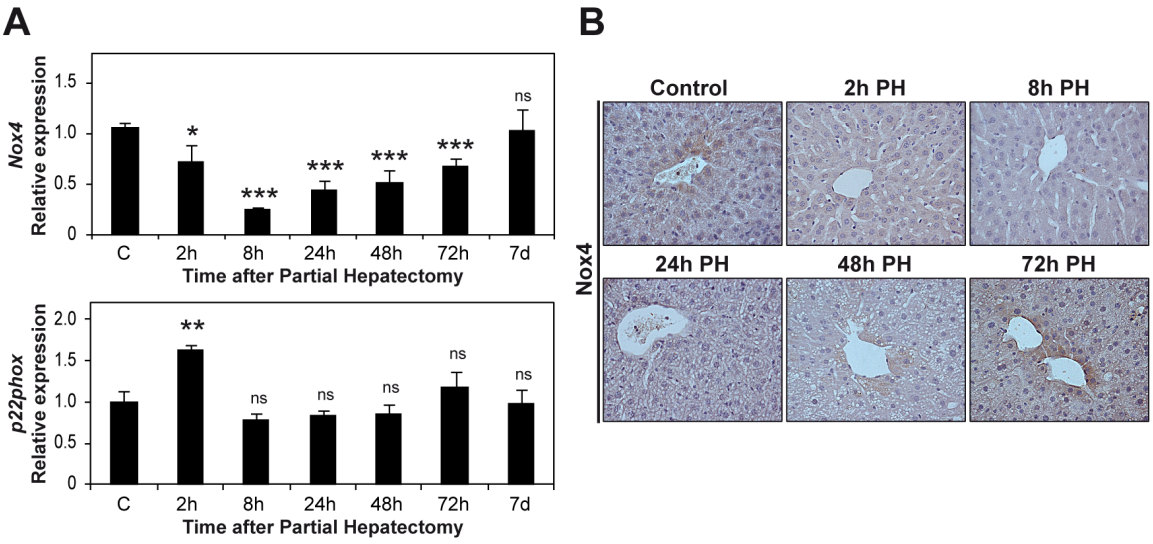


**Figure 22. Down-regulation of NOX4 during liver regeneration after partial-hepatectomy in mice.** A) Analysis of *Nox4* and *p22phox* mRNA expression by quantitative PCR at the indicated times after partial-hepatectomy. B) Immunohistochemistry of Nox4 at the indicated times after partial-hepatectomy. Data in (A) are mean ± SEM of at least 3 mice per group. Student's t-test versus control was used: *p<0.05, **p<0.01, ***p<0.001.

This effect on NOX4 expression preceded the peak of maximal DNA synthesis in hepatocytes (**Figure 23**). Thus, *in vivo* liver cell proliferation correlates with a decrease in *Nox4* expression.

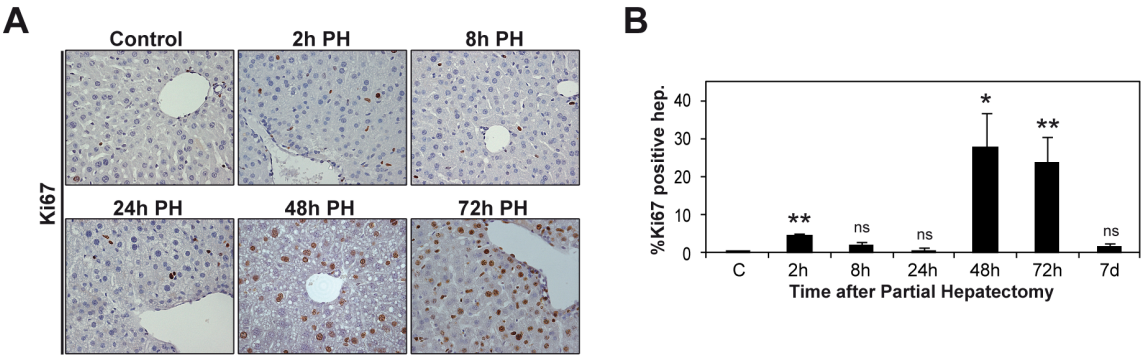


**Figure 23. NOX4 down-regulation during liver regeneration after partial-hepatectomy precedes the peak of maximal DNA synthesis in hepatocytes.** A) Immunohistochemistry of Ki67 at the indicated times after partial-hepatectomy. B) Quantification of the percentage of Ki67 labeled nuclei. Data in (B) are mean ± SEM of at least 3 mice per group. Student's t-test versus control was used: *p<0.05, **p<0.01.

### 2.3.3. Inverse correlation between Nox4 expression and liver tumour progression in experimental animal models

The treatment of mice with a single dose of DEN at day 15 of age provokes a situation of liver injury that develops in the appearance of liver tumours between 9 and 12 months of age in mice. As a control, mice of the same age were treated with PBS. The appearance of tumours was microscopically observed in all mice at 9 months of age, but macroscopic masses were observed at 12 months. At 6 months of age, already half of the animals treated with DEN showed microscopic tumours. Importantly, no tumours were found in any of the control animals (**Figure 24**).

A

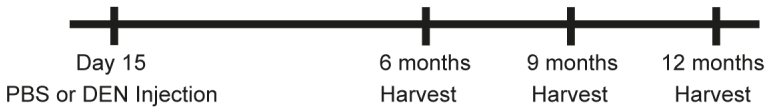


B

| Tumour Incidence | | | |
|---|---|---|---|
| Treatment | 6 months | 9 months | 12 months |
| PBS | 0% | 0% | 0% |
| DEN | 50% | 100% | 100% |

C

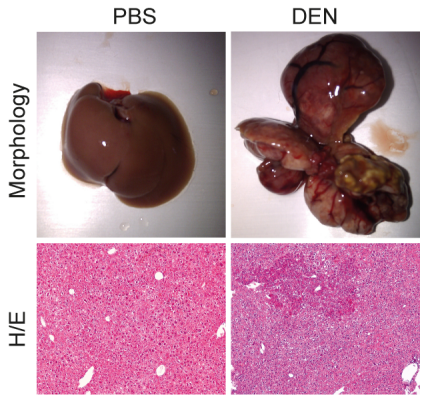


**Figure 24. Diethylnitrosamine (DEN) was used to induce HCC in mice.** A) Scheme of the timing followed to induce hepatocarcinogenesis in mice. B) Summary of tumour incidence in control (PBS) and DEN-injected mice at 6, 9 and 12 months. C) Up: Representative images of livers 12 months after injection. Down: Hematoxylin and Eosin (H/E) staining of 12 months old liver paraffin sections from both control (PBS) and DEN injected mice.

Neoplastic areas with high proliferative cells were localized both by Hematoxylin and Eosin and Ki67 staining (**Figure 25A**). Quantification of the Ki67 positive hepatocytes per field is shown in **Figure 25B**, and it clearly confirmed the presence of high proliferative areas in DEN-treated mice, which were not present in PBS-treated mice, where only few hepatocytes were positive, as expected considering the low replicative rate of hepatocytes in adult liver.

Interestingly, when *Nox4* mRNA levels were analysed in the livers of DEN-treated mice, a significant decrease of *Nox4* expression was observed in 12 month-old animals, coincident with the appearance of macroscopic liver tumours (**Figure 25C**). No significant differences between control and DEN-treated mice were observed in earlier samples. These results indicated that *in vivo* liver tumour cell proliferation also correlates with a decrease in *Nox4* expression in an experimental model of hepatocarcinogenesis in mice.

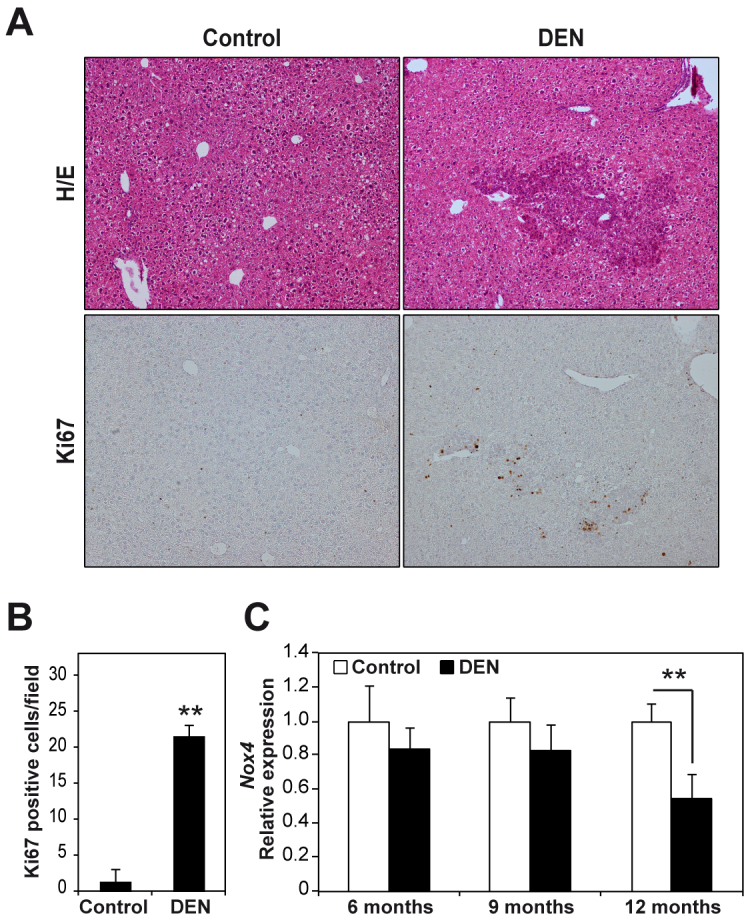


**Figure 25. Tumorigenesis in mice following DEN treatment is associated with decreased *Nox4* expression.** A) Serial sections immunohistochemistry of 12 months old mice livers. Up: Hematoxylin and Eosin (H/E) staining section. Down: Immunohistochemistry of Ki67. B) Quantification of the number of Ki67 labeled nuclei per field. C) *Nox4* transcript levels analysed by quantitative PCR in control liver (PBS treatment) versus tumoral tissues in animals at 6, 9 and 12 months of age. Data represent mean ± SEM (number of animals: 4 in control animals; 3 in DEN-treated animals; analysis in two different pieces of tissue/animal). Student's t-test was used: **p<0.01.

Considering all the results described above, we wondered whether the effect of silencing NOX4 in terms of proliferation observed *in vitro*, would have relevance in *in vivo* studies. We hypothesized that NOX4 silencing might increase the tumorigenic capacity of HCC cells. To confirm so, the tumour formation and progression capabilities of control and NOX4

knocked-down Hep3B cells were studied in xenograft experiments into athymic nude mice. Briefly, as explained in material and methods, cells were subcutaneously injected in left flank of the mice and tumour appearance and its progression were followed every two days until they reached a size of 1000mm$^3$. It is noteworthy that all the animals, both the ones injected with control Hep3B cells and the ones injected with NOX4 silenced Hep3B cells, developed tumours within the 20 days following injection. However, animals injected with cells NOX4 knocked-down developed those tumours significantly earlier than mice injected with shControl transfected cells (**Figure 26A**). Moreover, the measurement of tumour size revealed that tumour growth was much quicker in those from Hep3B shNOX4 cells (**Figure 26B**). Maintenance of the NOX4 silencing in tumours from NOX4 knock-down HCC cells was corroborated by immunohistochemical analysis of the paraffin embedded tumour tissues (**Figure 27**). Additionally, a study of tumour morphology by Hematoxylin and Eosin staining revealed no significant changes between tumours from NOX4 silenced cells and control cells, neither at tissue structure nor at vasculature organization (**Figure 27**).

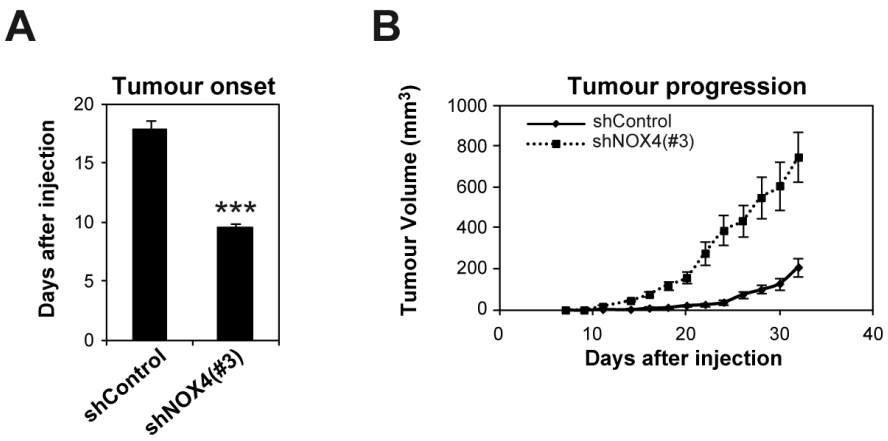


**Figure 26. Stable silencing of NOX4 in human HCC cells increases their tumorigenic capacity when injected subcutaneously into athymic nude mice.** A) Number of days after injection when tumours appeared. B) Tumour volumes over time. Data are mean ± SEM of at least 6 mice per group. Student's t-test versus control (unspecific-shRNA-transfected cells) was used: ***p<0.001.

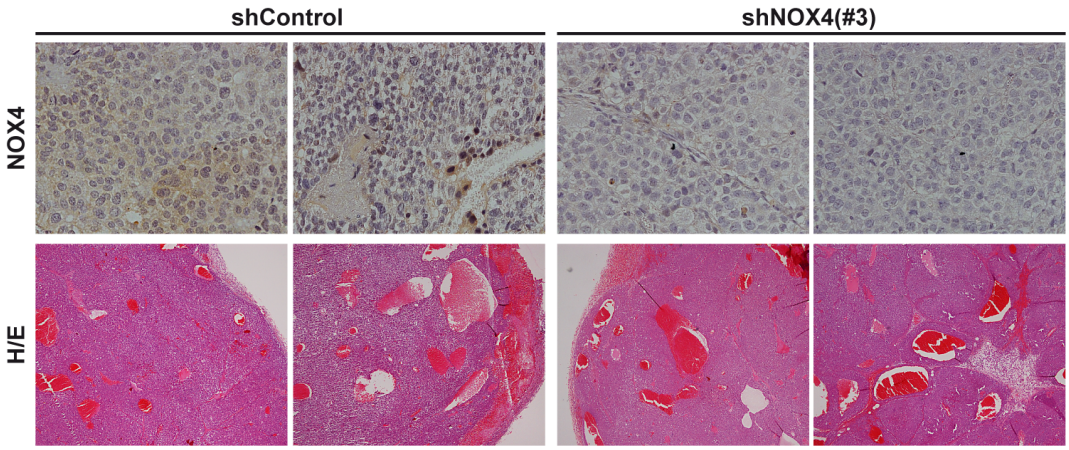


**Figure 27. Analysis of NOX4 levels in subcutaneous tumours formed after injection of NOX4 silenced Hep3B cells in athymic nude mice.** Hep3B cells stably transfected with a plasmid containing either a shRNA against NOX4 (shNOX4(#3)) or an unsilencing sequence (shControl) were injected subcutaneously into athymic nude mice. Representative images of subcutaneous tumours from shControl and shNOX4 Hep3B cells. Up: Representative 40x images of NOX4 immunohistochemistry. Down: Representative 10x images from Hematoxylin and Eosin (H/E) staining.

To sum up, results indicated that attenuation of NOX4 significantly increased cell tumorigenic capacity, as tumours appeared earlier and reached a higher volume than those induced by shControl Hep3B cells.

At this point, taking into account data from *in vitro* studies we considered likely that increased proliferation would be responsible of the increased tumorigenic capacity, however, we couldn't discard that apoptosis could be playing a role as well. Thus, we performed immunostainings of both Ki67, to analyse cell growth, and cleaved caspase-3 to address apoptosis, in paraffin embedded tumours. Additionally, also caspase-3 activity was analysed by a fluorimetric assay from tumour lysates. Results confirmed that increased rate in tumour progression was in correlation with significant enhancement in tumour cell proliferation (**Figure 28A**). Number of apoptotic cells was low in both cohorts of tumours (**Figure 28B**) and when caspase-3 activity was analysed in tissues, although a tendency to a decrease was observed in the tumours originated from NOX4 knock-down cells, the effect was not statistically significant (**Figure 28C**). Therefore, increase in proliferation was the main responsible of the increase in tumorigenesis after NOX4 silencing, further confirming *in vitro* data.

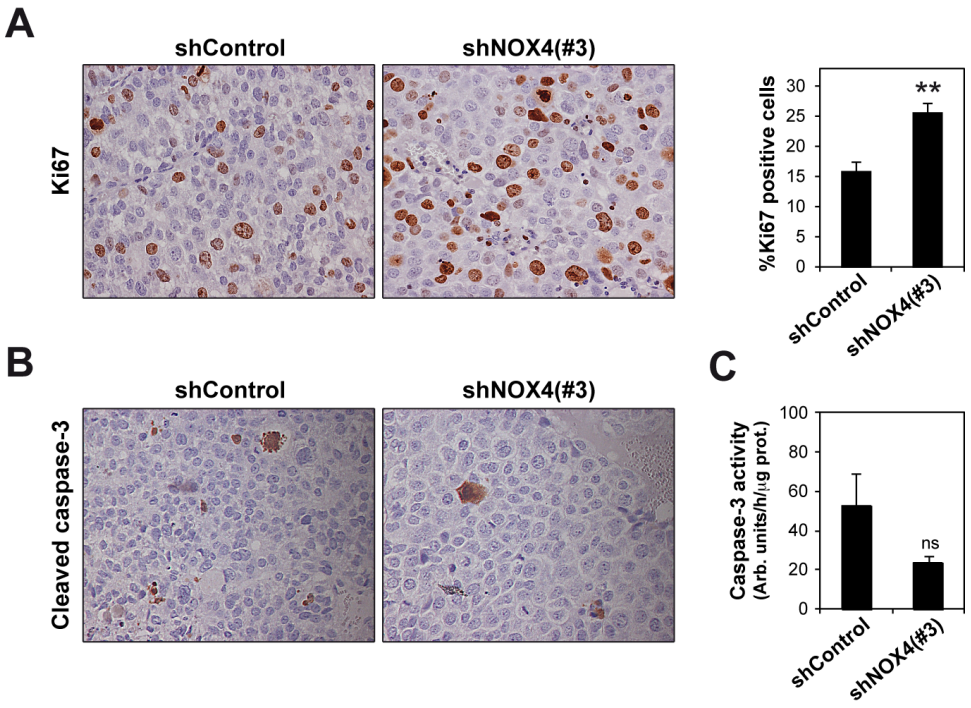


**Figure 28. Increased tumorigenic capacity of NOX4 knock-down cells is due to increased proliferation.** A) Left: Immunohistochemistry of Ki67. Right: Quantification of the percentage of labeled nuclei. B) Immunohistochemistry of cleaved caspase-3. C) Analysis of caspase-3 activity. In (A) and (B) representative 40x images are shown. Data are mean ± SEM of at least 6 mice per group. Student's t-test versus control (unspecific-shRNA-transfected cells) was used: **p<0.01.

### 2.3.4. Human liver tumours show decreased levels of NOX4 protein

Due to the observed effect of targeting knock-down NOX4 on liver tumour progression in animal models, we next decided to evaluate NOX4 protein levels in tissues from human liver tumours. A human tissue array that contained 65 samples (in duplicate) of liver tumours, from which 62 were HCC, as well as 2 samples (in duplicate) of healthy tissue (as control) and 3 samples (in duplicate) of non malignant lesions, was used for immunohistochemical analysis of NOX4 levels. It was evidenced that most of the HCC tissues showed lower NOX4 expression when compared to the control samples or even when compared to the non-malignant lesions (**Figure 29A**). Quantitative analysis corroborated decreased levels of NOX4 in most of the tumour samples (**Figure 29B**). In 47% of the cases the ratio of NOX4 expression in tumour versus healthy tissues was lower than 0.8 and in 13% of the cases lower than 0.5.

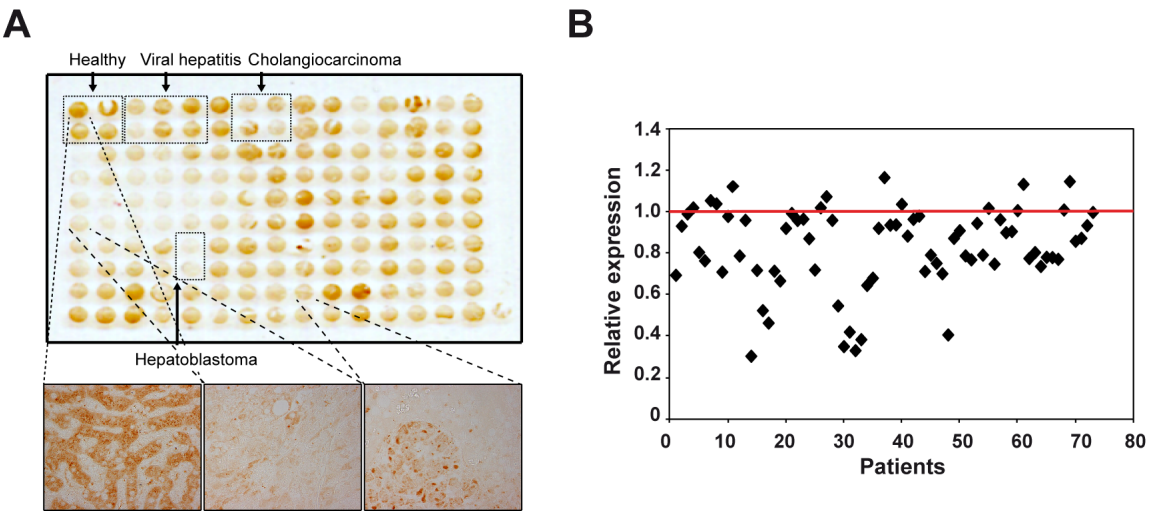


**Figure 29. NOX4 is down-regulated in human HCC tissues.** A) Up: Macro overview of the NOX4 immunohistochemistry staining of the human liver tumour tissue array. Spots corresponding to healthy donors, viral hepatitis patients, cholangiocarcinoma or hepatoblastoma are indicated. All the other spots correspond to hepatocellular carcinoma. Down: Representative 40x images of one healthy liver spot and two of HCC patients spots. B) Densitometric quantification of each HCC tissue spot versus healthy tissue. Red line represents healthy tissue values.

Altogether, these results suggest that NOX4 might be a potential biomarker in HCC patients, since most of the HCC tumours analysed showed decreased levels of the protein. In addition, both *in vitro* and *in vivo* studies revealed that low NOX4 levels correlate with increased cell proliferation.

# 2.4. Role of NOX4 as a negative regulator of invasion

## 2.4.1. NOX4 is important for maintaining epithelial parenchymal structures both in 2D and 3D cell culture systems

In addition to changes in the cell growth capacity, NOX4 stable silencing provoked a change in the morphology of human HCC cells, as it is shown in **Figure 30**. Phase contrast analysis of morphology in PLC/PRF/5 cells, which show an epithelial phenotype forming parenchymal areas, suggested that NOX4 might have an effect on cell-to-cell adhesion, since in those cells where NOX4 was silenced a more spindle appearance and disruption of parenchymal structures were observed. In Hep3B cells, which show a mixed epithelial-mesenchymal phenotype, the effect observed was milder compared to PLC/PRF/5 cells.

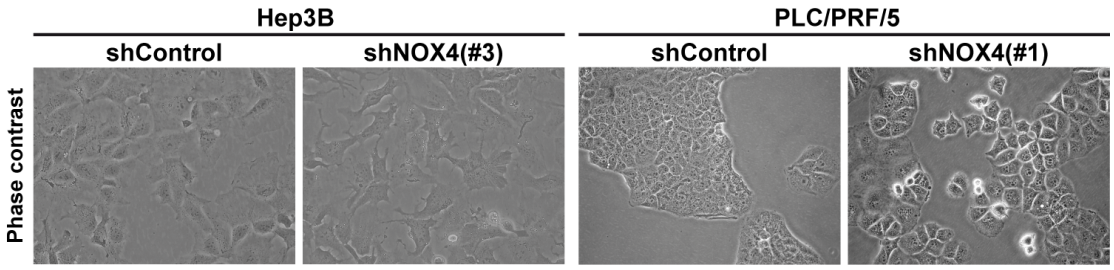


**Figure 30. NOX4 silencing provokes changes in cell morphology.** 20x representative bright-field images of cells cultured at basal conditions on top of plastic.

Disruption of parenchymal structures was corroborated at the molecular level through analysis of the expression and intracellular localization of proteins regulating cell-to-cell adhesion. Results indicated that NOX4 targeted knock-down cells expressed lower mRNA levels of E-cadherin, a component of adherent junctions, both in Hep3B and PLC/PRF/5 cells, while N-cadherin expression was only decreased in PLC/PRF/5 (**Figure 31A**). In addition, immunofluorescence staining of E-cadherin, as well as ZO-1 staining, which are components of adherent junctions and tight junctions respectively, evidenced their lower presence in the cell membrane of NOX4 silenced cells, indicating lower cell-to-cell contact areas in both cell lines analysed (**Figure 31B**).

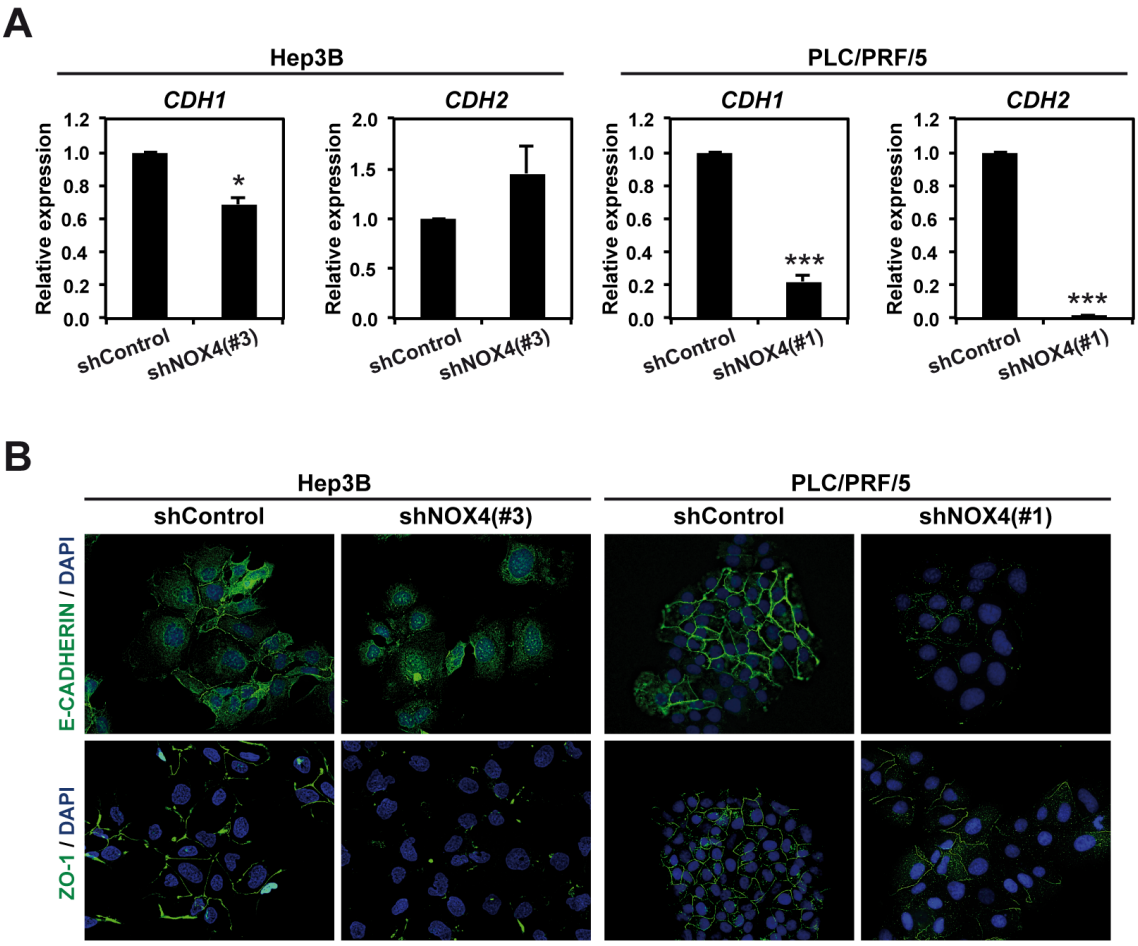


**Figure 31. NOX4 is important for maintaining cell-to-cell contacts.** A) Analysis of *CDH1* (E-cadherin) and *CDH2* (N-cadherin) expression by quantitative PCR. Data are mean ± SEM of 4 independent experiments. Student's t-test versus control (unspecific-shRNA-transfected) cells was used: *p<0.05, ***p<0.001. B) Cell-to-cell contact imaging, by immunofluorescence of E-cadherin (green) and ZO-1 (green); DAPI (blue) used to detect nuclei. Representative 40x images are shown (N=3). The cell line and the shNOX4 used are detailed in each panel.

In parallel to the study of cell-to-cell adhesion, we analysed the migratory capacity of cells when NOX4 expression was attenuated, by using two different approximations. On the one hand, a wound-healing assay pointed out that in both cell lines analysed (Hep3B and PLC/PRF/5), NOX4 silencing provoked an increase in cell migration (**Figure 32A**). On the other hand, real time monitoring of cell migration (xCELLigence System) also demonstrated that cancelling NOX4 increased migration in both Hep3B and PLC/PRF/5 cell lines, being stronger the effect on PLC/PRF/5 (**Figure 32B**), result not fully unexpected considering that the major morphological differences were observed in this cell line (**Figure 30 and 31**).

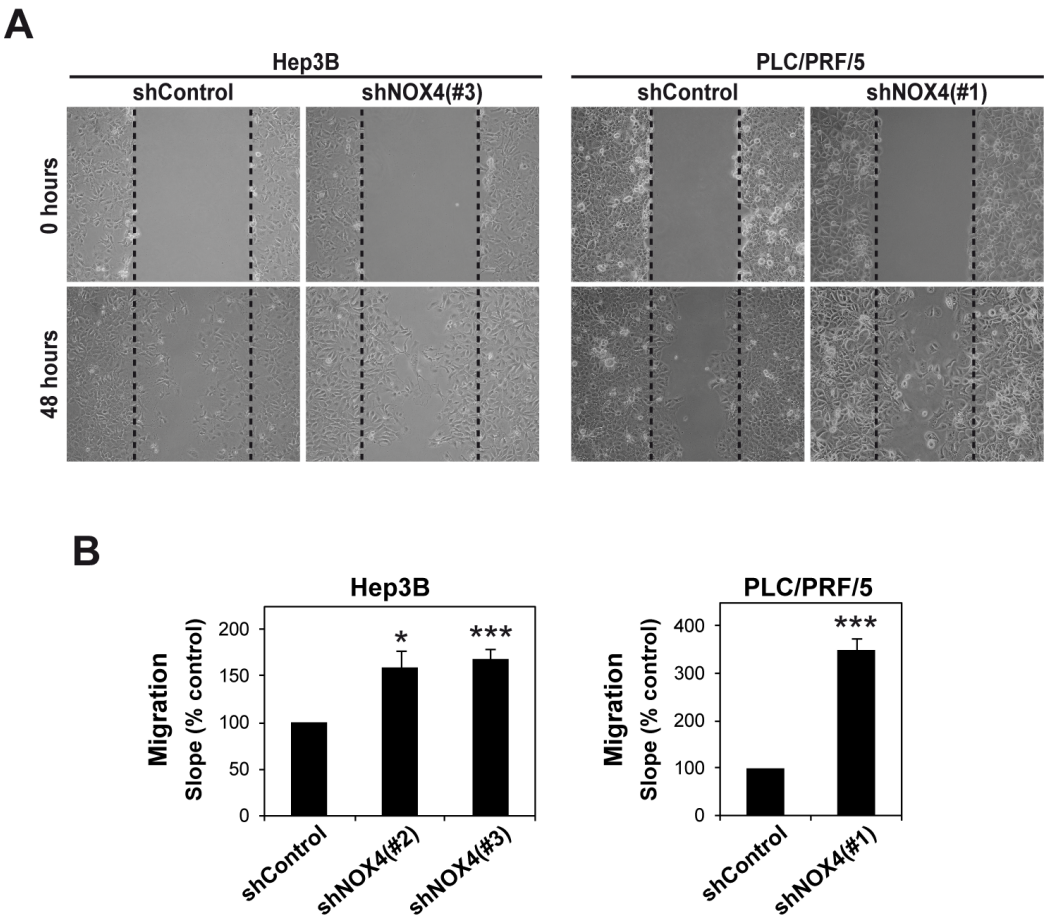


**Figure 32. NOX4 depletion increases the migratory capacity of human HCC cells.** A) Wound healing assay (N=3). B) Real-time migration assay (xCELLigence system). Data are expressed as percentage versus control (unspecific-shRNA-transfected) cells and they are mean ± SEM of 3 independent experiments. Student's t-test versus control (unspecific-shRNA-transfected) cells was used: *p<0.05, ***p<0.001.

Cell movement is tightly related to cell shape and morphology since it determines the mode of migration that cells adopt to invade surrounding tissues. Cancer cells disseminate from the primary tumour to form metastasis, either as individual cells, using amoeboid or mesenchymal type movement, or as cell sheets, strands and clusters using collective migration (Friedl and Wolf, 2003). Among other characteristics, these types of movement differ on cell adhesion requirements. Considering the morphological differences, as well as the changes in cell-to-cell contacts observed by silencing NOX4, we hypothesized that NOX4 would be regulating the kind of movement that HCC cells adopt to invade. Taking into account that mechanisms driving cell movement might differ between 2D and 3D environments, we decided to do a phenotypic characterisation of five different HCC cell lines (Huh7, Hep3B, PLC/PRF/5, HLF and SNU449), when were seeded on a matrix of bovine collagen I, one of the main components of the extracellular matrix that HCC cells have to invade to metastasize. These five cell lines were the same ones previously characterized in a 2D system (**Figure 5, 6 and 10**). As

a reminder, the three former cell lines showed a mixed phenotype, holding both epithelial and mesenchymal characteristics, and high NOX4 expression, while the two latter showed a mesenchymal-like phenotype and low NOX4 levels. Surprisingly, we found a wide range of phenotypes among the human HCC cell lines studied when seeded on top of a thick layer of collagen I, and the classification in two groups was not as evident as when we studied EMT markers. Thus, Huh7 cells showed an elongated morphology, with a big number of long protrusions, likely filopodia, while Hep3B and PLC/PRF/5 cells were mainly rounded. Cell lines with low levels of NOX4 showed a mixed population; HLF tend to adopt a spindle-like morphology although around 40% of the cells were rounded, while most of SNU449 cells were rounded, only 20% of the cells were elongated (**Figure 33**).

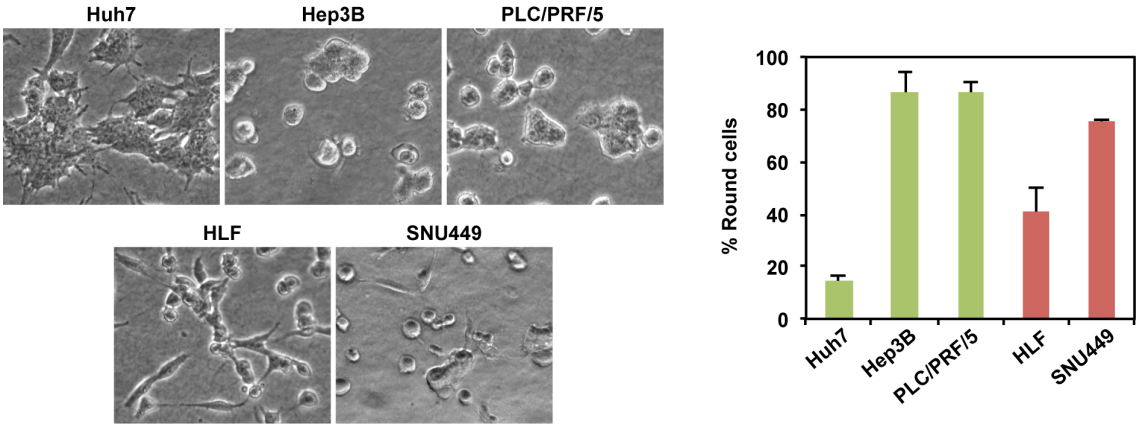


**Figure 33. High heterogeneity of phenotypes when HCC cell lines are cultured on collagen I.** A) 20x representative bright-field images of cells cultured on top of a bovine collagen I matrix. B) Quantification of the percentage of round cells. Data are mean ± SEM of at least 3 images from 3 independent experiments.

In addition, while HLF and SNU449 cells were individual, Huh7 and PLC/PRF/5 cells (and in a less extend, Hep3B cells) tended to form groups of cells, correlating with higher NOX4 expression levels (**Figure 34A**). When the effect of cancelling NOX4 was analysed, results revealed that there was a disruption of parenchymal structures formed by the parental cell lines and most of the cells became individual when NOX4 was silenced (**Figure 34B-C**). Noteworthy is that the remaining groups formed by NOX4 silenced cells were smaller (formed by fewer cells) compared to the ones formed by control cells (**Figure 34D**).

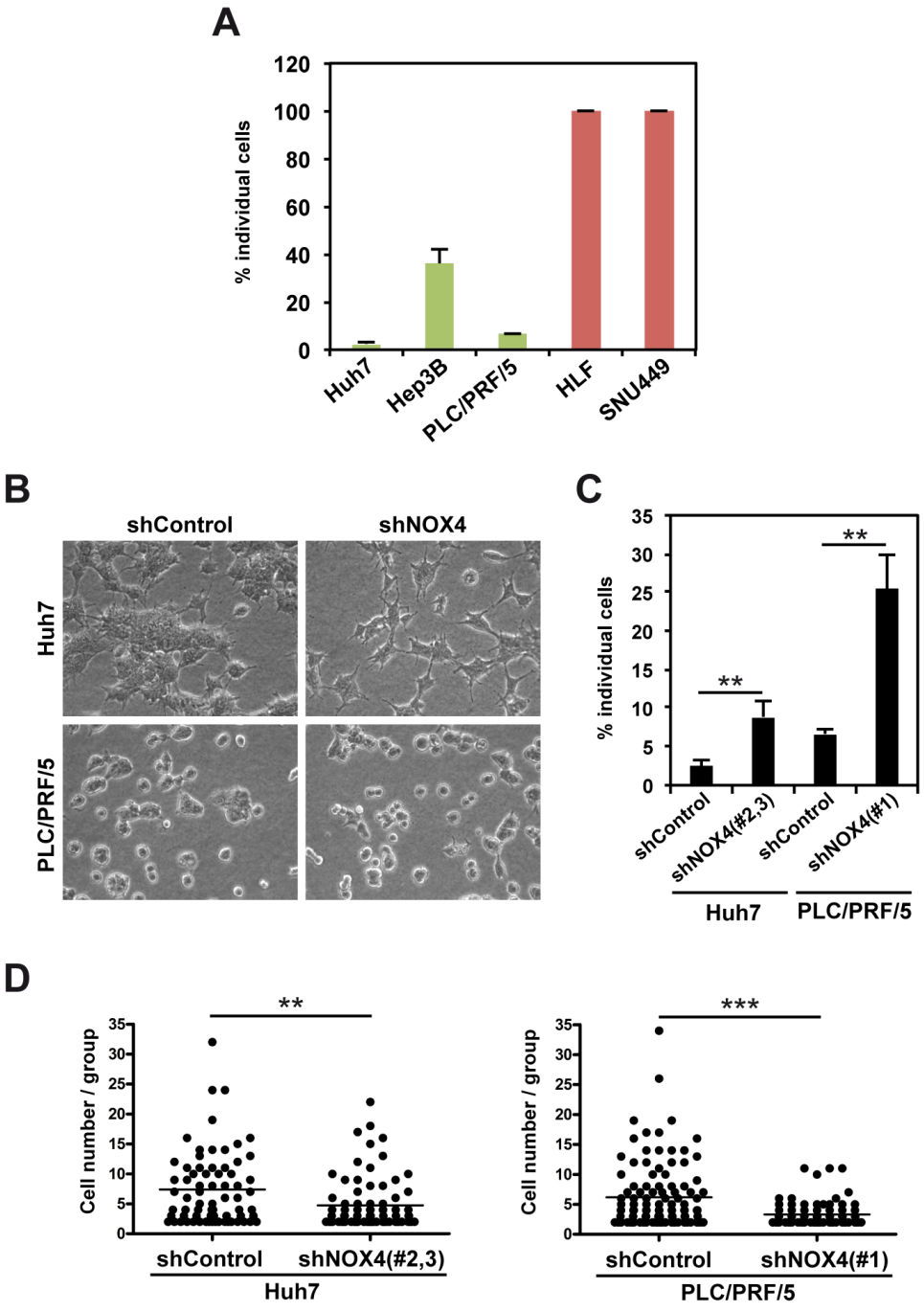


**Figure 34. NOX4 is important for maintaining parenchymal structures.** Cells were cultured on top of a bovine collagen I matrix. The cell line and the shNOX4 used are detailed in each panel. A) Quantification of the percentage of individual cells. B) 20x representative bright-field images of cells on top of a bovine collagen I matrix. C) Quantification of the percentage of individual cells cultured when NOX4 is knocked-down. D) Quantification of the number of cells per group. Data in (A), (C) and (D) are mean ± SEM of 3 independent experiments (5 pictures/experiment). Student's t-test versus control (unspecific-shRNA-transfected) cells was used: **p<0.01, ***p<0.001.

### 2.4.2. NOX4 expression inversely correlates with the invasive growth capacity of HCC cells

In order to analyse the relevance of the phenotypes observed among the different HCC cell lines on their invasive behaviour in a 3D system, we started by determining the invasive growth capacity of the cells when cultured as spheroids embedded in a collagen I matrix, one of the main components of the extracellular matrix in the liver. Results revealed a huge difference between epithelial-like and mesenchymal-like HCC cell lines. Cells with high levels of NOX4 showed much lower invasive growth capacity when compared to cells with low NOX4 expression. Thus, when considering Huh7, Hep3B and PLC/PRF/5 cells we could mainly see an increase in the size of the spheroids when day zero and day four were compared. In the case of HLF and SNU449 cells, we could observe that the rate of increase in the area occupied by the spheroids was much faster, easily seen already at day two, in comparison to the other cell lines. In addition, the spheroid structure of HLF and SNU449 cells was partially disrupted along time, being possible to observe a great number of individual cells invading the collagen matrix, phenomena difficult to observe in the other cases (**Figure 35A**). Importantly, NOX4 silencing in Huh7, Hep3B and PLC/PRF/5 cells increased the invasive growth capacity of all of them (**Figure 35B**), suggesting an inverse correlation between the invasive growth capacity and NOX4 expression levels.

Proliferation, invasion, or both at the same time, can determine invasive growth capacity of cells, making difficult to speculate which of those phenomena are involved in each of the situations analysed. However, considering all the results previously exposed in this work, it was reasonable to think that cell growth was involved in the effects observed, especially when considering results from NOX4 silencing. Nevertheless, nothing was known about the possible contribution of invasion to this process in our model.

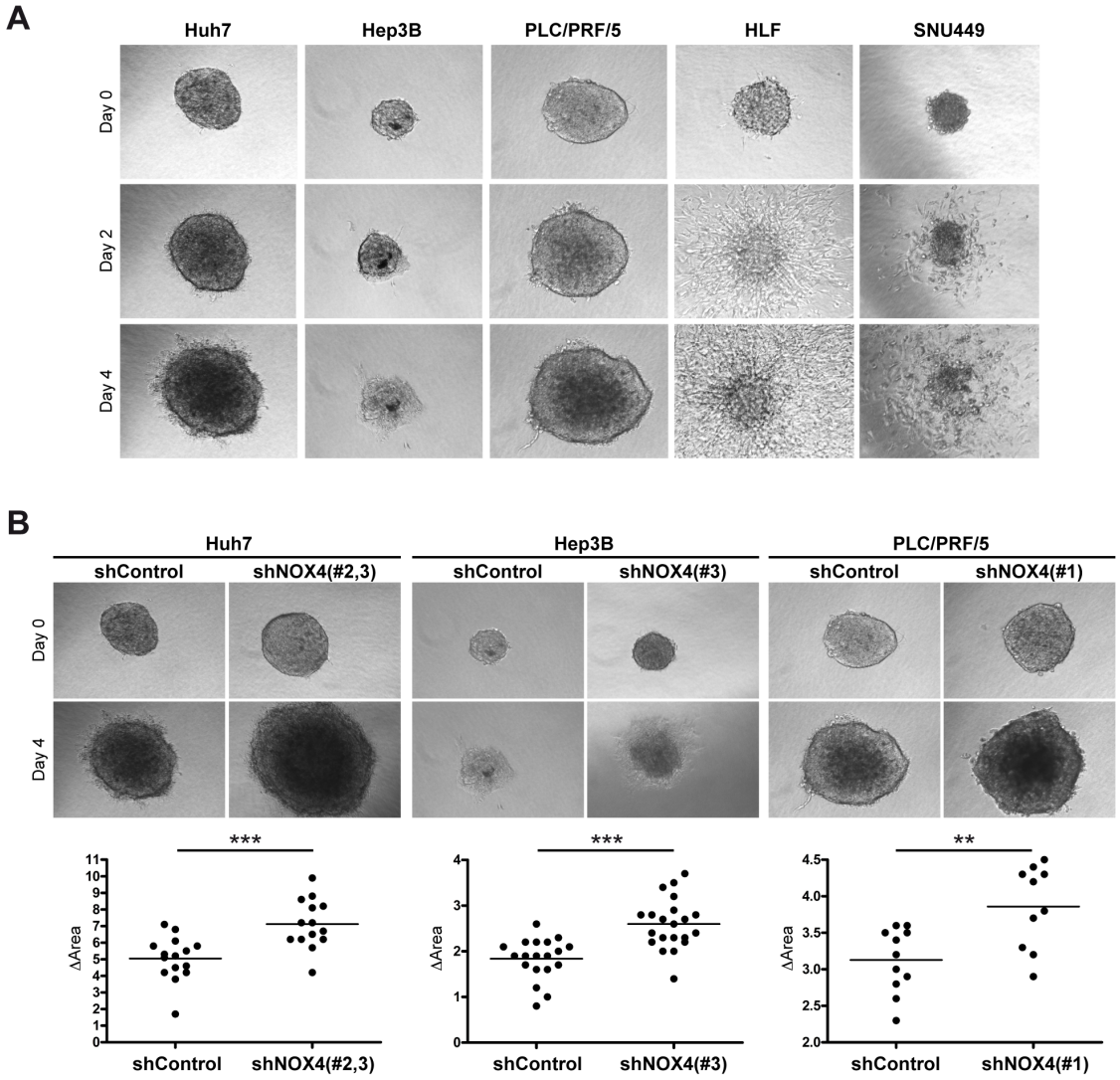


**Figure 35. NOX4 expression inversely correlates with the invasive growth capacity of human HCC cells.** A) Representative images of the spheroids from Huh7, Hep3B, PLC/PRF/5, HLF and SNU449 cell lines embedded in a bovine collagen I matrix. B) Up: Representative images of the spheroids from control (shControl) and NOX4 silenced (shNOX4) cells. The cell line and the shNOX4 used are detailed in each panel. Down: Quantification of the increase in area between day 0 and day 4. Student's t-test versus control (unspecific-shRNA-transfected) cells was used: **p<0.01, ***p<0.001 (N=2).

### 2.4.3. NOX4 knock-down induces high actomyosin contractility and increases the migratory and invasive capacity of human HCC cells

Cell movement is not only determined by cell shape but also by actomyosin contractility. Thus, an elongated “mesenchymal-like” mode of movement is characterized by cell polarization and low actomyosin contractility, while rounded “amoeboid” mode of cell migration is driven by high levels of actomyosin contractility. Collective migration requires high contractility but differing from individual migration, it is necessary to maintain cell-to-cell contacts (Sanz-Moreno, 2012). Considering this, NOX4 would be a regulator of the mode of movement of cells because of the differences observed in cell shape and cell-to-cell adhesion, and taking into account the different behaviour of cells during the invasive growth assay, we decided to study the contractility status of different HCC cell lines, as well as whether NOX4 silencing could modify it. Actomyosin contractility was determined by analysing the percentage of blebbing cells, as well as the protein levels of pMLC2 (phospho-MLC 2), a down-stream effector of the canonical Rho/ROCK signalling, that represents a readout of high actomyosin contractility, in cells seeded on top of a thick collagen I matrix. Results revealed an inverse correlation between actomyosin contractility and NOX4 expression levels, being HLF and SNU449 the most contractile cell lines, since they showed a high percentage of round cells with blebs (**Figure 36A**) and high levels of pMLC2, when analysed both by western blot and immunofluorescence (**Figure 36B-D**). Considering epithelial-like cells, PLC/PRF/5 were the most contractile ones (**Figure 36**). Of note, protein levels of MLC2 were much higher in mesenchymal-like cells when compared to epithelial-like cells (**Figure 36B**).

Interestingly, NOX4 stable silenced PLC/PRF/5 cells showed higher actomyosin contractility, presenting increased percentage of blebbing cells, in addition to increased phosphorylation of MLC2 (**Figure 37**). This effect on cell contractility was mild or not observed in Huh7 and Hep3B cells (**Figure 37**).

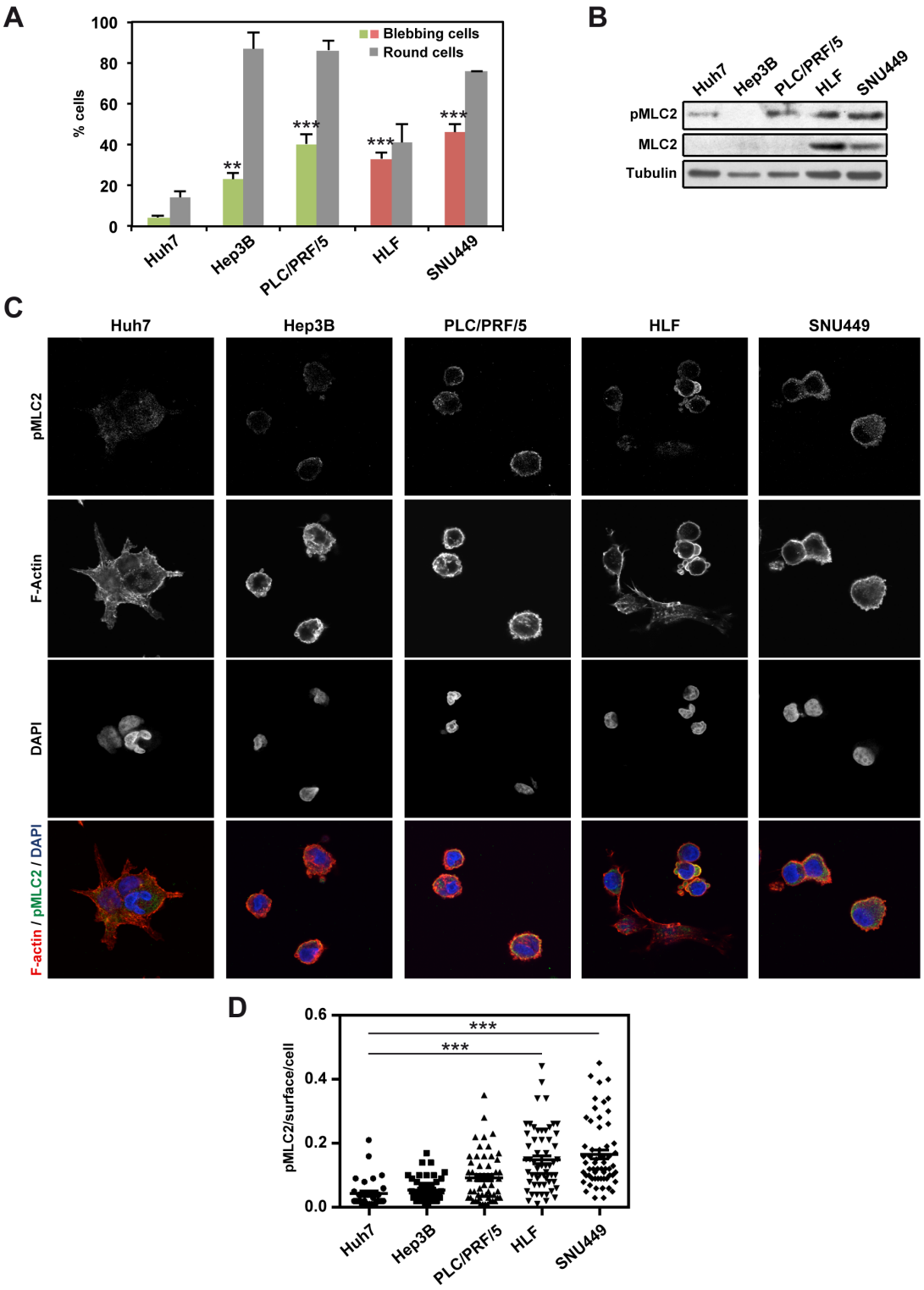


**Figure 36. NOX4 levels inversely correlate with actomyosin contractility in human HCC cells.** Cell lines are detailed in each panel. A) Quantification of both the percentage of round cells and cells with blebs. B) Analysis of the protein levels of pMLC2 and MLC2. Tubulin was used as a loading control. A representative experiment is shown (N=4). C) Representative 40x confocal images of immunostaining of pMLC2 (green), F-actin (red), and DAPI (blue) of HCC cells (N=3). D) Quantification of pMLC2 immunostaining intensity per cell surface. In all experiments cells were cultured on top of a bovine collagen I matrix. Data in (A) and (D) are mean ± SEM of 3 independent experiments (at least 5 pictures/experiment). One way ANOVA versus Huh7 cells was used in (A) and (D): **p<0.01, ***p<0.001.

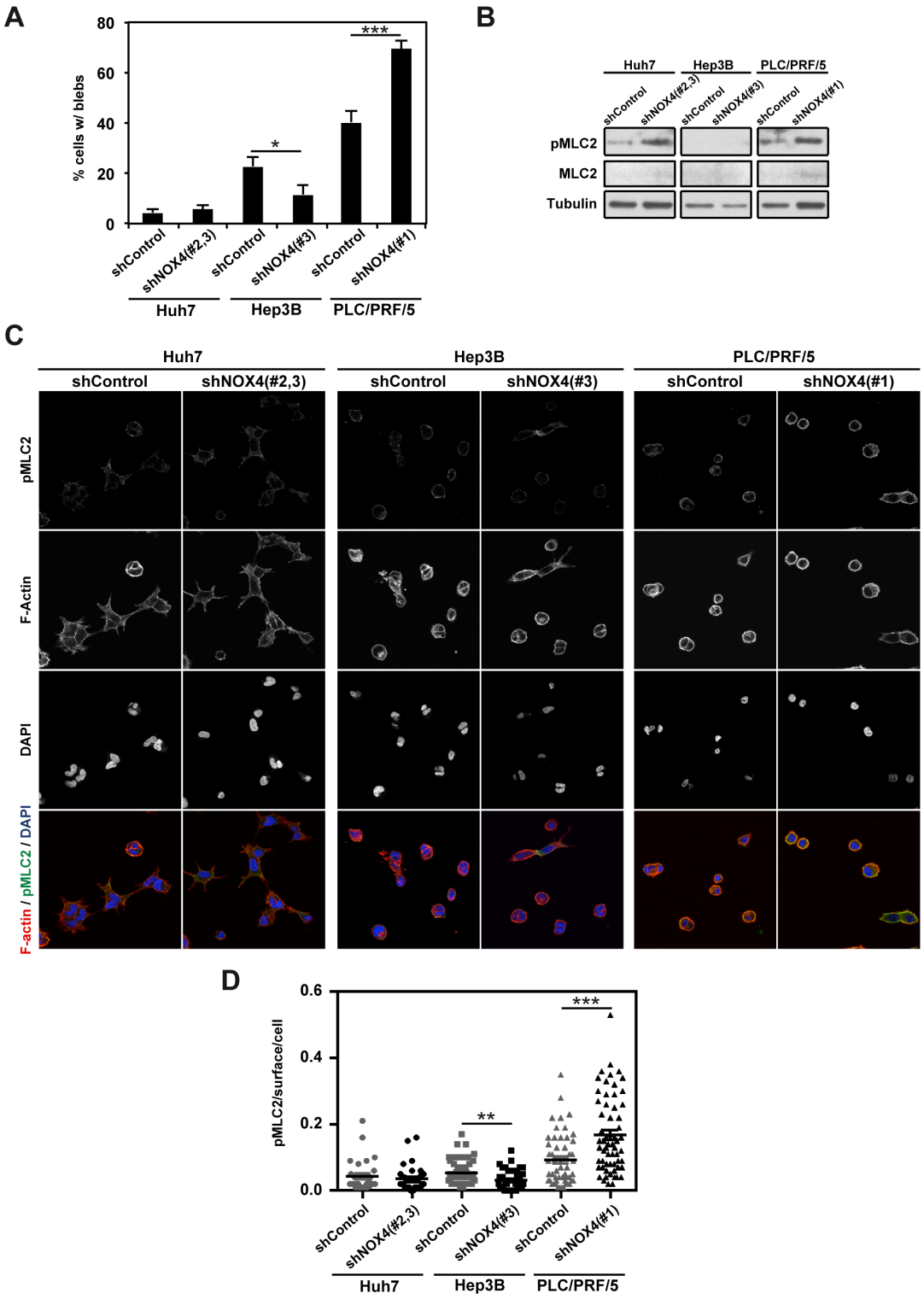


**Figure 37. NOX4 silencing increases actomyosin contractility of PLC/PRF/5 cells.** The cell line and the shNOX4 used are detailed in each panel. A) Quantification of the percentage of cells with blebs. B) Analysis of the protein levels of pMLC2 and MLC2. Tubulin was used as a loading control. A representative experiment is shown (N=4). C) Representative 40x confocal images of immunostaining of pMLC2 (green), F-actin (red), and DAPI (blue) of HCC (N=3). D) Quantification of pMLC2 immunostaining intensity per cell surface. In all experiments cells were cultured on top of a bovine collagen I matrix. Data in (A) and (D) are mean ± SEM of 3 independent experiments (at least 5 pictures/experiment). Student's t-test versus control (unspecific-shRNA-transfected) cells was used: *p<0.05, **p<0.01, ***p<0.001.

Once determined that low expression of NOX4 in HCC cells correlates with increased contractility and that the fact of cancelling NOX4 expression could also increase actomyosin contractility, we analysed its relevance in the migratory and invasive capacity of HCC cells. To start with, we compared the migratory capacity of HCC cell lines by means of a chemotaxis assay using 10% FBS as a chemoattractant. Eight hours after seeding the cells, only very few HLF and SNU449 cells migrated to the lower chamber. Cells were let to migrate longer to assess whether it was a matter of time, but after 24 hours, even though more HLF and SNU449 cells were counted in the lower chamber, no Huh7, Hep3B and PLC/PRF/5 cells were visualized (**Figure 38**). In addition, we showed before that cancelling NOX4 expression increased migration (**Figure 32**). At the same time, the wound-healing assay corroborated results from the chemotaxis assay, since neither Hep3B nor PLC/PRF/5 showed high migratory capacity and the scratch could still be visualized after 48 hours. Therefore, the most contractile cell lines were also the most migratory ones.

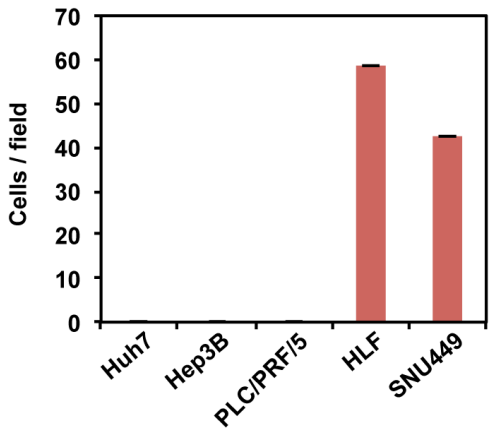


**Figure 38. Low levels of NOX4 are coincident with high migratory capacity of human HCC cells.** 24 hours chemotaxis assay using 10% FBS as a chemoattractant (N=1, in duplicates).

To asses the invasive capacity of cells, we used two different matrixes, collagen I and collagen I / Matrigel mix (1:1). The protocol used is extensively explained in material and methods but briefly, cells were seeded on the bottom of the corresponding matrix, and once the matrix was polymerized, the chemoattractant was added on top and cells were let invade for 24 hours, a time short enough to avoid cell proliferation interference. Invading cells were considered those found 50μm above the bottom layer of cells. In accordance to migration, results from the invasion assay revealed that invasive capacity was higher in those cells with low NOX4 levels (HLF and SNU449), in both matrixes studied (**Figure 39**), correlating with higher actomyosin contractility. These data suggested that NOX4 might be important for HCC

cells invasion. Intriguingly, HLF were more prompted to invade collagen I matrix whilst SNU449 invaded preferentially the collagen I / Matrigel mixed matrix. By using 3D imaging we could determine that SNU449 invading cells were rounded while spindle-like HLF cells were the ones invading (**Figure 40**). Regarding epithelial-like cells, PLC/PRF/5 was the cell line with higher invasive capacity, mainly in the collagen I / Matrigel matrix, accordingly to lower NOX4 levels and higher contractility in comparison to the others (Huh7 and Hep3B) (**Figure 39**).

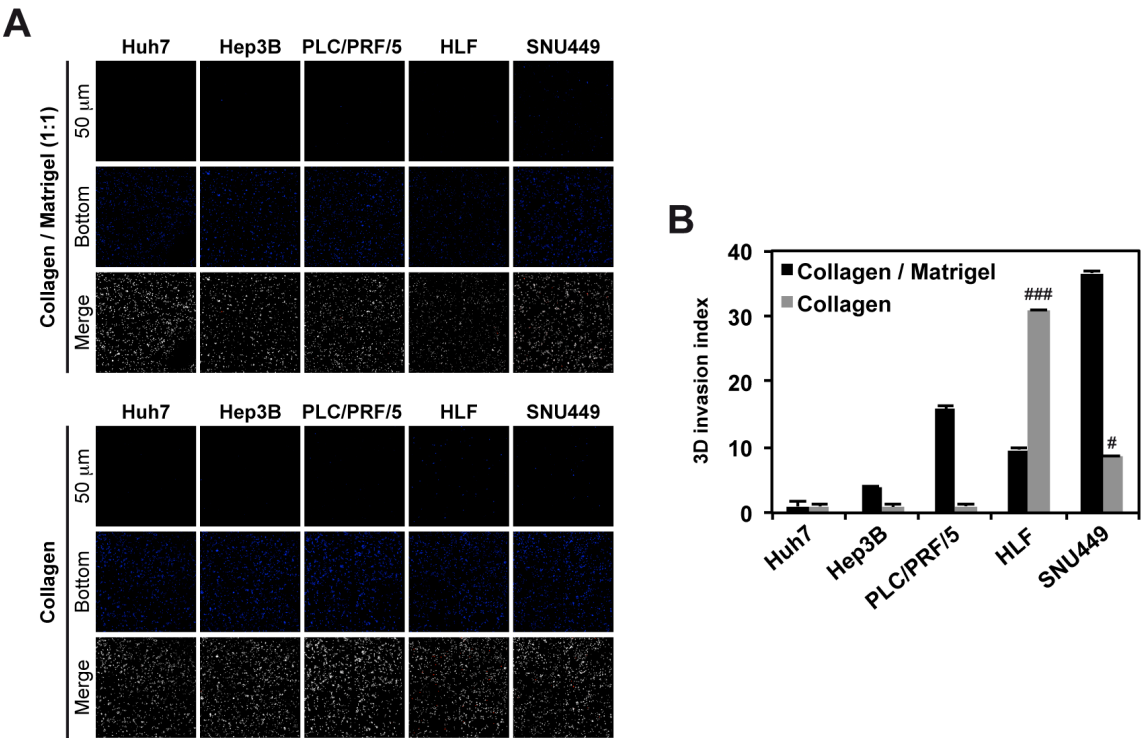


**Figure 39. Low NOX4 levels correlate with high invasive capacity in human HCC cells.** Cell lines are detailed in each panel. A) 3D invasion into a matrix of bovine collagen I / Matrigel mix (1:1) (Up) and collagen I (Down). B) Quantification of the invasion into both matrixes. Data are expressed as fold increase versus Huh7 cells and are mean ± SEM (N=2 for collagen / Matrigel, N=4 for collagen). One way ANOVA versus Huh7 cells was used: $^{\#}p<0.05$, $^{\#\#\#}p<0.001$.

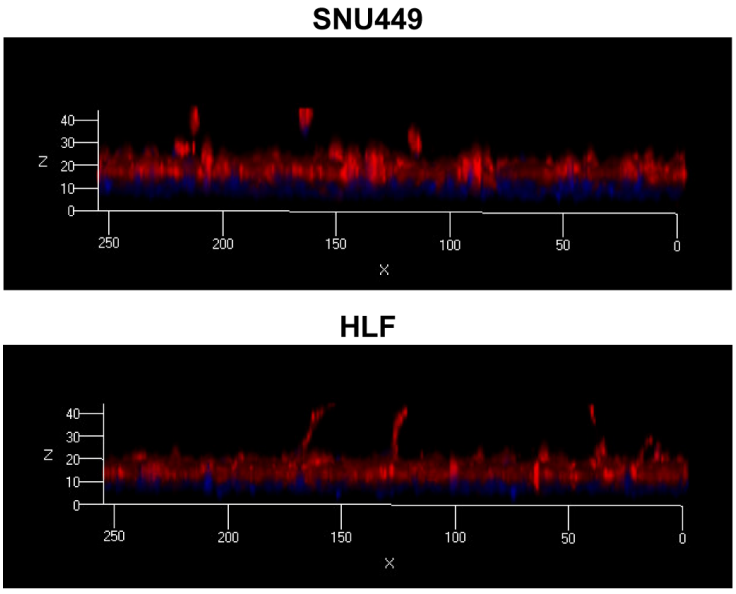


**Figure 40. HCC cells adopt different morphologies when invading collagen I / Matrigel matrix.** 3D imaging of invading cells. Representative 10x images are shown (N=1, in quintuplicates).

NOX4 silencing did not increase Hep3B cell invasion but provoked a slight increase in Huh7 and a huge increase in PLC/PRF/5 cell invasion capacity in both collagen I / Matrigel mix and collagen I matrixes (**Figure 41**). Interestingly, 3D imaging determined that NOX4 silenced cells invaded as rounded cells (**Figure 42**).

At this point, going back to the results obtained from the invasive growth assay (**Figure 35**), we would propose that increased invasion may contribute to the higher invasive growth capacity of those cells with low NOX4 levels (HLF and SNU449), as well as in the increase in invasive growth capacity of Huh7 and PLC/PRF/5 cells after NOX4 silencing.

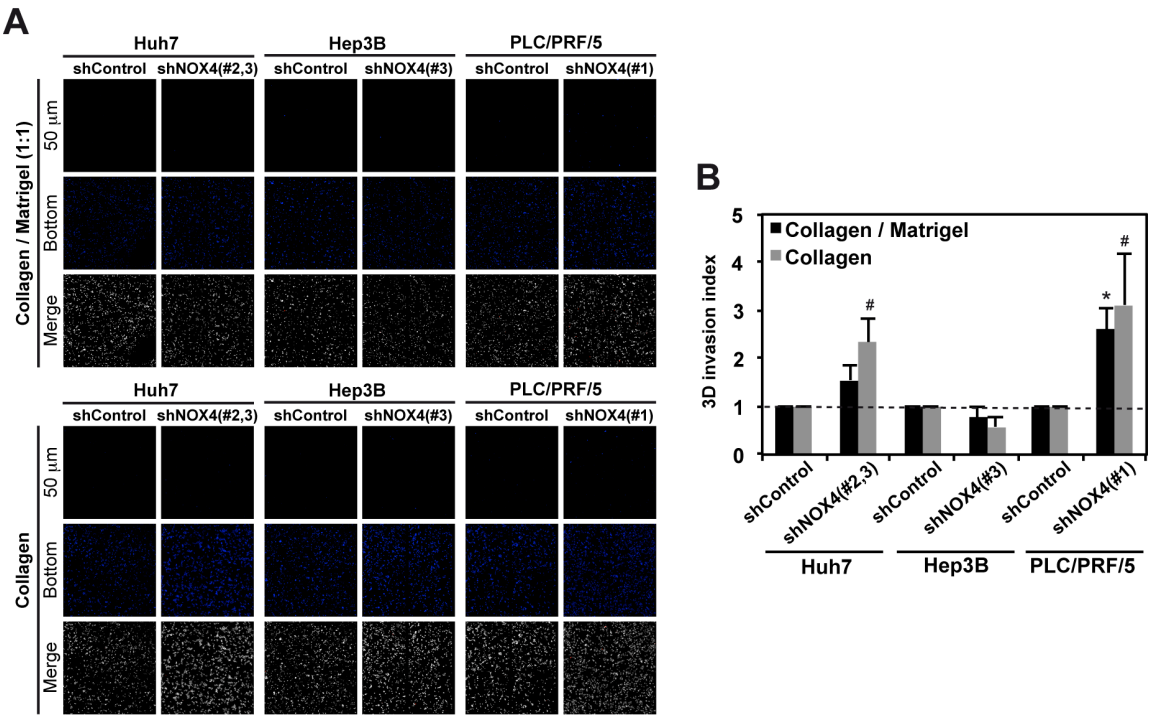


**Figure 41. Cancelling NOX4 in human HCC cells increases their invasive capacity.** The cell line and the shNOX4 used are detailed in each panel. A) 3D invasion into a matrix of bovine collagen I / Matrigel mix (1:1) (Up) and collagen I (Down). B) Quantification of the invasion into both matrixes. Data expressed as fold increase versus their control (unspecific-shRNA-transfected) cells are mean ± SEM (N=2 for collagen / Matrigel, N=4 for collagen). Student's t-test versus control (unspecific-shRNA-transfected) cells was used: * (for collagen / Matrigel matrix) and # (for collagen matrix) $p<0.05$.

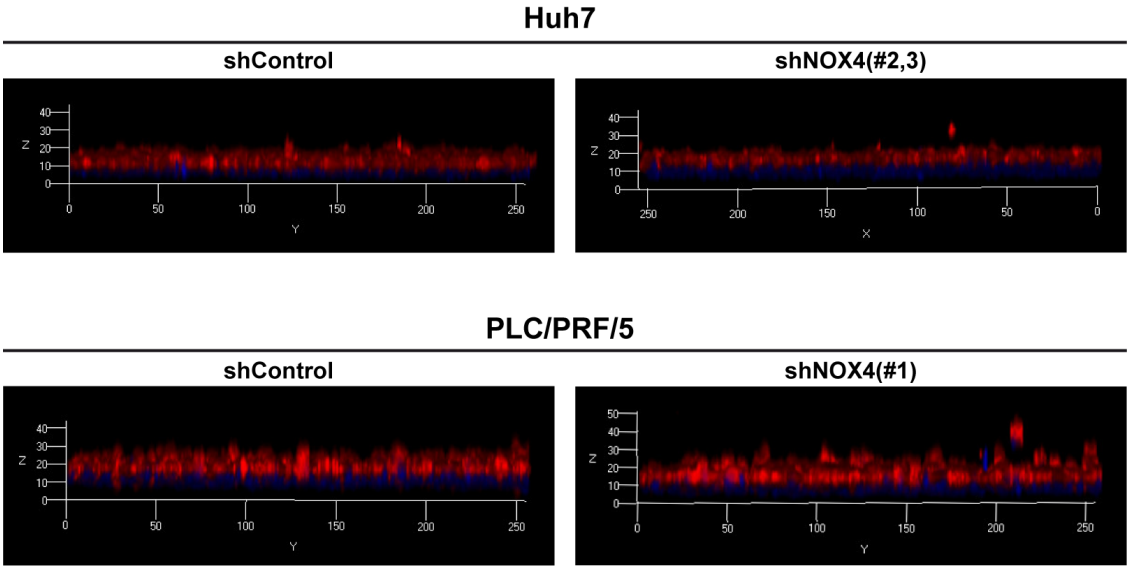


**Figure 42. NOX4 silenced Huh7 and PLC/PRF/5 cells invade the extracellular matrix as rounded cells.** 3D imaging of Huh7 and PLC/PRF/5 control (unspecific-shRNA-transfected) and NOX4 knock-down cells invading a collagen I / Matrigel mix matrix. Representative 10x images are shown (N=1, in quintuplicates).

Rho GTPases family are key regulators of cell migration through their actions on actin assembly and actomyosin contractility. Thus, rounded, amoeboid form of movement is driven by high actomyosin contractility through Rho signalling, while Rac signalling is required for actin assembly in elongated-protrusive movement (Sanz-Moreno and Marshall, 2010). Interestingly, Cdc42 through different GEFs is capable of regulating both kinds of movement (Sanz-Moreno, 2012). Trying to elucidate the mechanism by which NOX4 is modifying the invasive capacity of HCC cells, we analysed protein levels of different Rho GTPases and their effectors. Cells with low NOX4 expression presented high expression of RhoA, RhoC and Cdc42 (**Figure 43A**), all of them related to high cell contractility. By contrast, Hep3B cells, as well as HLF, showed high levels of Rac1. No conclusive pattern was observed when ROCK I and ROCK II were analysed, though it appears clear that their expression is lower in Hep3B cells in comparison to all other HCC cell lines studied. Interestingly, an increase in the expression of all Rho GTPases and their effectors analysed was observed when NOX4 expression was cancelled in PLC/PRF/5 cells. This effect was not observed as a consequence of NOX4 silencing neither in Huh7 nor in Hep3B cells (**Figure 43B**). These data is in accordance with the differences observed in both contractility and the invasive assay, where the major effects of silencing NOX4 were observed in PLC/PRF/5 cells (**Figure 37 and 41**).

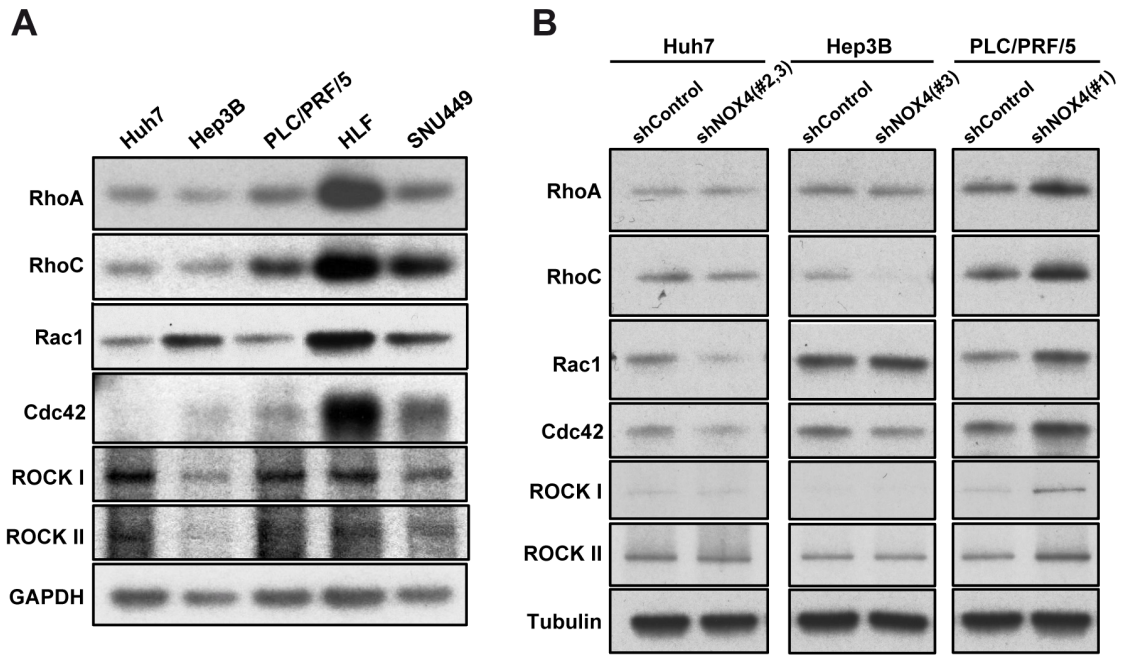


**Figure 43. NOX4 depletion increases the migratory and invasive capacity of human HCC cells by modifying Rho GTPases expression levels.** Representative western blot, out of 5 experiments, of Rho GTPases, ROCK I and ROCK II of Huh7, Hep3B, PLC/PRF/5, HLF and SNU449 cells (A) and NOX4 silenced Huh7, Hep3B and PLC/PRF/5 cells (B). GAPDH and tubulin were used as loading control.

Changes at protein level may be due to either modifications in transcription or alterations in protein translation or degradation. We analysed Rho GTPases expression at mRNA level by quantitative PCR. Preliminary data suggested that there is already a transcriptional regulation since similar patterns were observed at protein and mRNA level. However, these results are not sufficient to discard also a possible post-transcriptional regulation and further analysis would be needed (**Figure 44**).

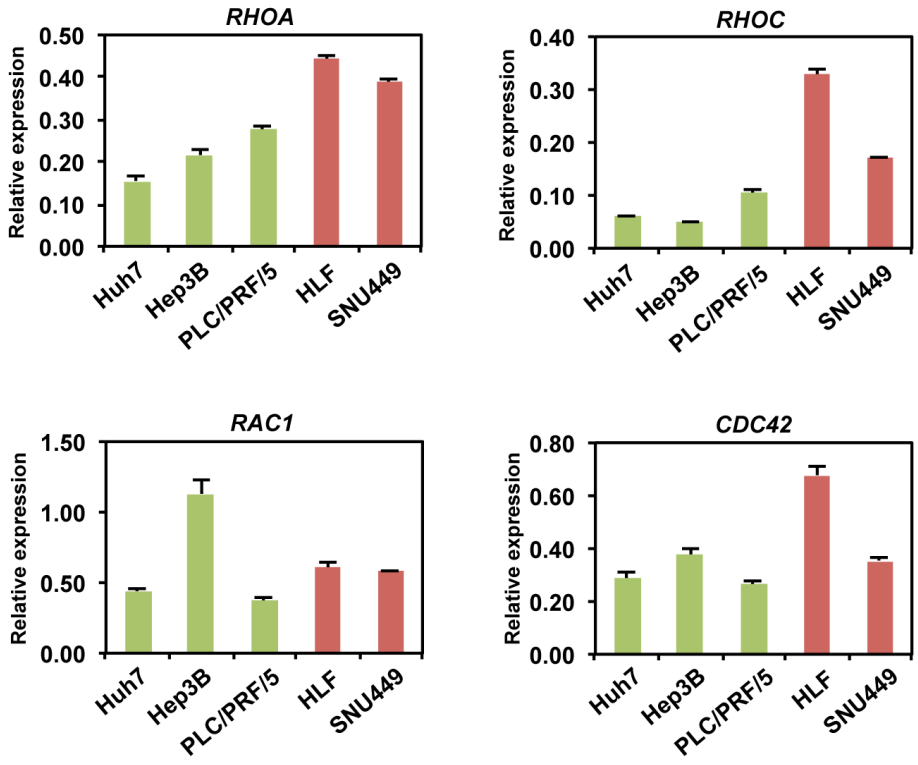


**Figure 44. Rho GTPases levels are regulated at transcriptional level.** Analysis of RhoA, RhoC, Rac1 and Cdc42 expression levels by quantitative PCR. Data represent the mean ± SEM of 2 independent experiments.

In view of these results, we wondered whether the differences in expression were translated into differences in Rho GTPases activation. Thus, Rho GTPases activity was analysed by pull-down with Rhotekin beads for RhoA and RhoC, and PAK-CRIB beads for Rac1 and Cdc42. Preliminary results have revealed that in most of the cases, activity is proportional to the protein level of each Rho GTPase, only Cdc42 showed discrepancies (in Hep3B and PLC/PRF/5 cells when NOX4 was silenced), since we could observe little differences in expression levels while clear differences were observed in the activation status. But, in general, these results would suggest that regulation of Rho GTPases is rather at expression level than at activation, in our system (**Figure 45**).

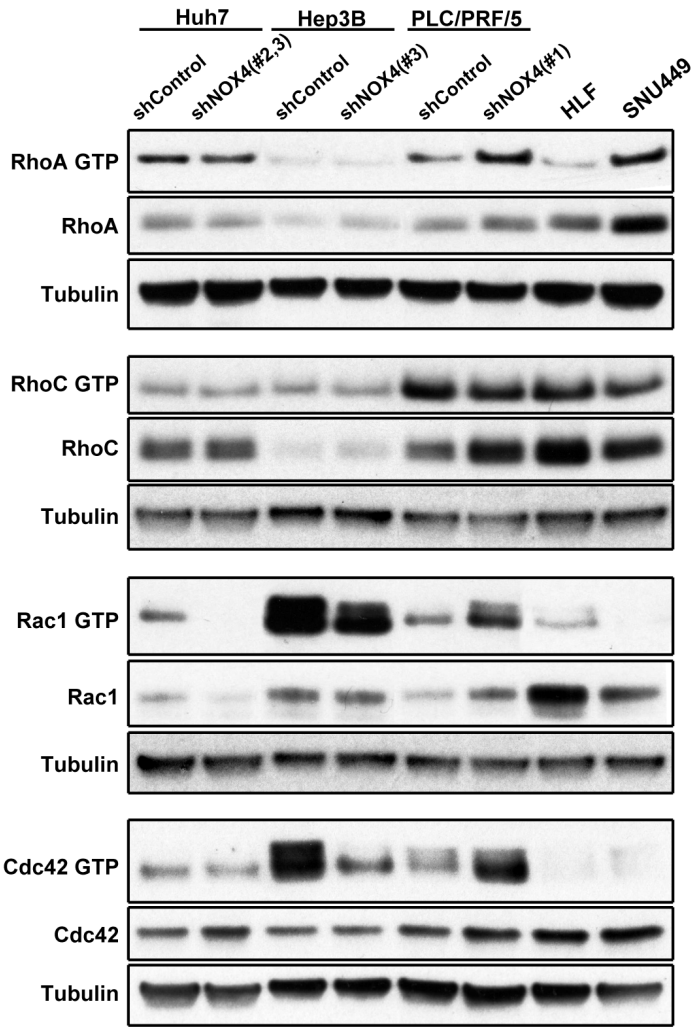


**Figure 45. Direct correlation between Rho GTPases expression and their activation in human HCC cells, both at basal conditions and after NOX4 silencing.** Rho GTPases activation levels analysed by pull-down assays with Rhotekin beads for RhoA and RhoC and with PAK-CRIB beads for Rac1 and Cdc42. A representative experiment is shown (N=2).

### 2.4.4. NOX4 down-regulation drives to a decrease in cell-to-matrix adhesion

Finally, considering that high actomyosin contractility is related to low adhesion to extracellular matrix, and that NOX4 expression could modify contractility, we also explored whether NOX4 silencing may have altered cell-to-matrix adhesion. Analysis of cell adhesion through the xCELLigence system, after seeding cells on regular cell culture plates, revealed lower cell-to-plastic adhesion in NOX4 silenced cells (**Figure 46A**). In addition, using different extracellular matrix proteins for coating the culture plates, such as collagen I, collagen IV or

fibronectin, we could observe lower adhesive capacity of NOX4 silenced cells on any of the extracellular matrixes used (**Figure 46B**).

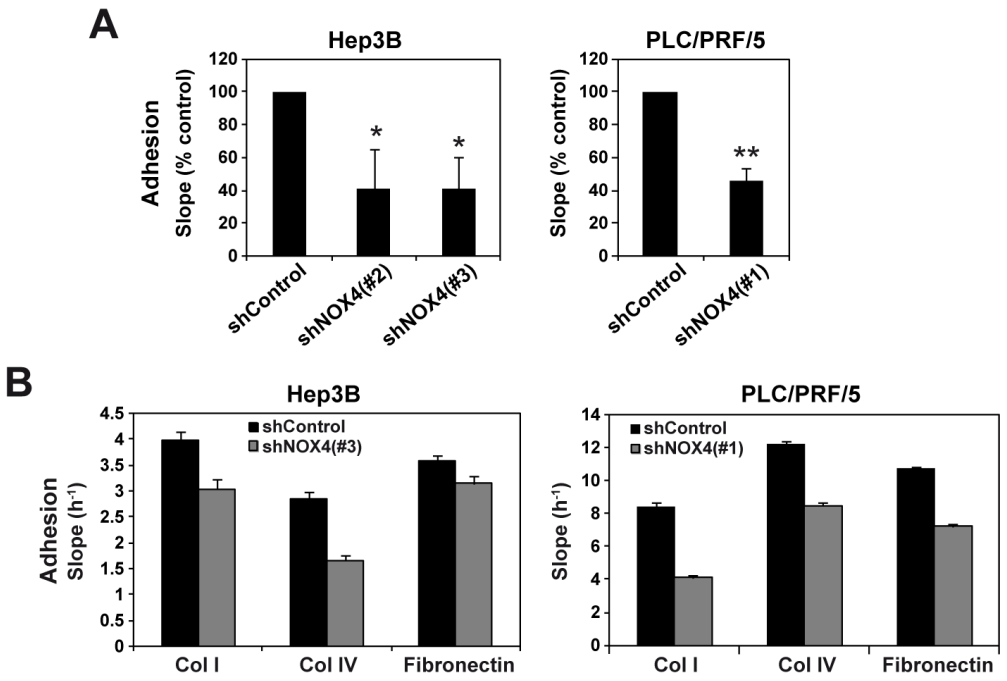


**Figure 46. NOX4 down-regulation drives to a decrease in cell-to-matrix adhesion.** Cell line and shNOX4 used are detailed in each panel. A) Real-time adhesion assay (xCELLigence system), data are expressed as percentage versus control (unspecific-shRNA-transfected) cells and are mean ± SEM of at least 3 independent experiments. Student's t-test versus control (unspecific-shRNA-transfected) cells was used: *p<0.05, **p<0.01. B) Real-time adhesion assay (xCELLigence system) after pre-coating the culture plates with either collagen I (4.5 μg/cm$^2$), collagen IV (25.5 μg/cm$^2$) or fibronectin (1.5 μg/cm$^2$). Mean ± SEM of a representative experiment performed in triplicate is shown (N=1).

These results suggested that NOX4 might be regulating focal adhesions, which are large protein complexes through which the cytoskeleton of the cell connects to the extracellular matrix. In support of this hypothesis, immunoluorescence analysis of pFAK (phospho-FAK, an important regulatory protein of focal adhesion formation), vinculin (involved in the anchoring of actin to the plasma membrane, participating in cell-to-cell and cell-to-matrix adhesion) and pPaxillin (phospho-Paxillin, an adaptor protein of focal adhesions and actin cytoskeleton), showed important differences in NOX4 silenced cells when compared to control cells (**Figure 47A**). These changes were confirmed and quantified by the analysis of pFAK images using Image J software. Image analysis revealed a decrease in the number of focal adhesion complexes as well as changes in their distribution within the cell surface after NOX4 silencing. Indeed, the remaining focal adhesions were the ones on the edge of the cells, while the focal adhesion complexes distributed within the cell body in control cells were missing when NOX4 was cancelled (**Figure 47B**). In addition, the quantification of both the area occupied by focal adhesions and the focal adhesion number per cell showed a significantly decrease in NOX4

silenced cells (**Figure 47C-D**). These results suggested a disruption/decrease in focal adhesions when expression of NOX4 was attenuated.

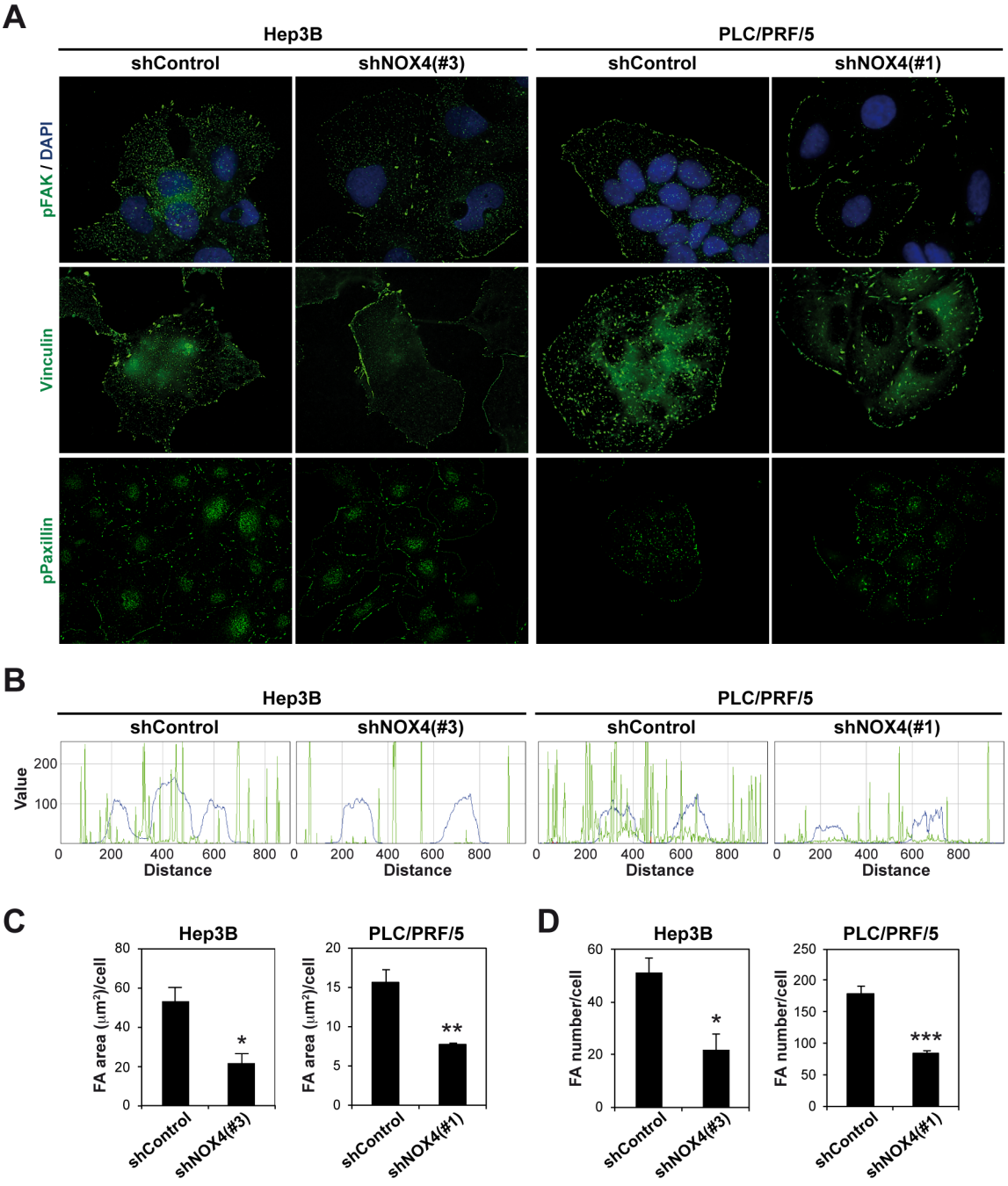


**Figure 47. Stable silencing of NOX4 disrupts focal adhesions in human HCC cells.** The cell line and the shNOX4 used are detailed in each panel. A) Immunofluorescence analysis of pFAK (green); vinculin (green) and pPaxillin (green). DAPI (blue) used to detect nuclei. Representative 40x images are shown. pFAK image processing using ImageJ software: analysis of focal adhesions (green) and nuclei (blue) distribution (B), analysis of the area occupied by focal adhesions per cell (C), and quantification of the number of focal adhesions per cell (D). Data in (C) and (D) are mean ± SEM of at least 3 independent experiments (5 pictures/experiment). Student's t-test versus control (unspecific-shRNA-transfected) cells was used: *p<0.05, **p<0.01, ***p<0.001.

It is well known that integrins play an essential role mediating cell-to-matrix interactions thereby linking cues from the extracellular environment to actin cytoskeleton through focal adhesion complexes. Integrins transmit signals from the outside to the inside of the cell through the phosphorylation and activation of adhesion-linked protein tyrosine kinases that facilitate the linkage of the actin cytoskeleton and integrin receptors. This provokes activation of numerous downstream effectors, including Rho GTPases, together with other signalling pathways, that have a pivotal function in cellular processes such as cell proliferation, survival, motility and cytoskeletal remodelling (Ushio-Fukai, 2009).

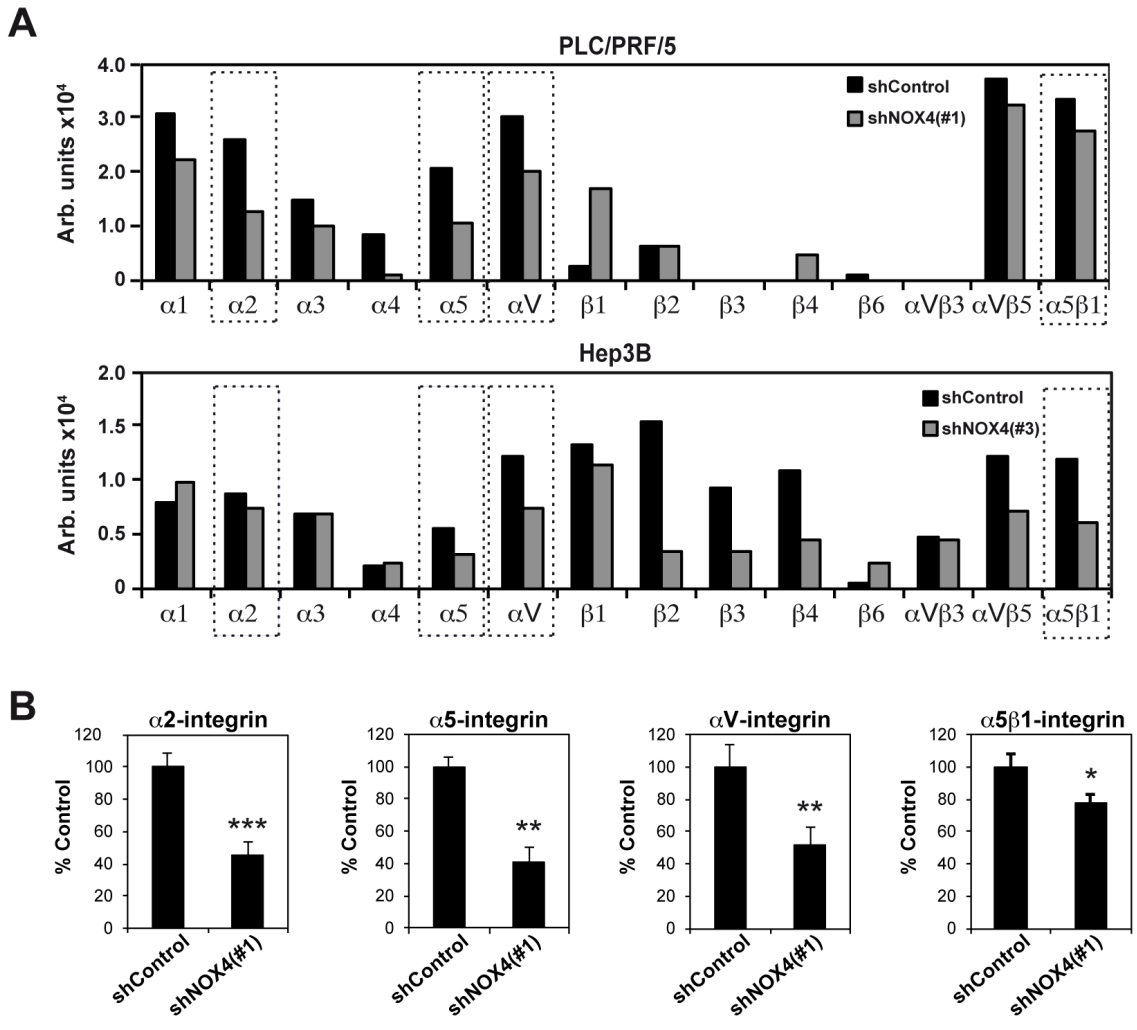


**Figure 48. NOX4 down-regulation drives to a change in the integrin pattern on the surface of HCC cells.** A) Analysis of cell surface integrins using a α/β Integrin-mediated cell adhesion array (Millipore) in PLC/PRF/5 and Hep3B NOX4 silenced cells. A representative experiment is shown (N=3 for PLC/PRF/5, N=1 for Hep3B). B) Selection of those integrins that presented significant changes in PLC/PRF/5 shControl versus shNOX4(#1) cells. Data in (B) are mean ± SEM of 3 independent experiments. Student's t-test versus control (unspecific-shRNA-transfected) cells was used: *p<0.05, **p<0.01, ***p<0.001.

Due to the differences observed in cell-to-matrix adhesion and focal adhesion complexes, we wondered whether NOX4 silencing was affecting integrin signalling. By using a $\alpha/\beta$-integrin-mediated cell adhesion array we observed changes in levels of different integrin proteins on the cell surface. Consistently in the two cell lines analysed, Hep3B and PLC/PRF/5, significant lower levels of $\alpha$2-, $\alpha$5- and $\alpha$V-integrins, as well as the complex $\alpha5\beta1$-integrin, were observed (**Figure 48**).

In summary, results presented here suggest that NOX4 may participate in the control of cell-to-cell contacts (modifying both adherent- and tight-junctions), cell-to-extracellular matrix adhesion (modifying the integrin pattern on the cell surface of HCC cells and focal adhesion complexes), small GTPases expression and activation, and the actomyosin contractility status of cells. Altogether leads to a role for NOX4 in the regulation of the mode of movement of human HCC cells.

# VI. DISCUSSION

# 1. NOX4 plays a role downstream of TGF-β during liver fibrosis, participating in the transdifferentiation of HSC to MFB and inducing hepatocyte cell death.

The discovery of new members of the NADPH oxidase family opened perspectives about the role of these ROS-producing enzymes in human physiology and pathology. Indeed, it has been reported that ROS from NOX proteins participate in the development of various liver diseases such as hepatitis (both alcoholic and viral hepatitis), cholestatic liver injury and hepatic fibrosis.

Liver fibrosis is the final consequence of many chronic liver injuries that later develop in cirrhosis and HCC (Brenner, 2009). Different models of hepatic fibrosis have been used to study the molecular pathogenesis of this disease. From these studies, several key generalizations have been done (Brenner, 2009): 1) TGF-β is the most potent liver pro-fibrogenic cytokine; 2) oxidative stress induces liver fibrosis; 3) blocking normal liver regeneration by massive hepatocyte apoptosis turns out to be pro-fibrogenic. Indeed, although the pathogenesis of liver fibrosis varies according to the aetiology of the injury, oxidative stress seems to play a crucial role in most types of hepatic fibrogenesis (Bataller and Brenner, 2005). One of the most studied mechanisms of fibrogenesis actually influenced by ROS is MFB activation. ROS can stimulate the production of the type I collagen, and may act as intracellular signalling mediators of the fibrogenic actions of TGF-β (Paik et al., 2013). Of relevance, NOX4 downstream TGF-β has been described as the main mediator for MFB activation in different organs such as heart (Cucoranu et al., 2005; Chan et al., 2013), lung (Hecker et al., 2009), kidney (Bondi et al., 2010) and diseased prostatic stroma (Sampson et al., 2011). However, at the beginning of this work, very few were known about the role of NOX4 in liver fibrosis but it had been demonstrated in cultured HSC that TGF-β-induced transdifferentiation is accompanied by ROS (Proell et al., 2007).

Results presented here show that there is an increased expression of NOX4 concomitant with the fibrotic process in two different animal models. In addition, they also indicate that NOX4 plays a key role in liver fibrosis development, downstream TGF-β, at least at two different levels. Thus, NOX4 appears to be required not only for the transdifferentiation of HSC into MFB but also for the TGF-β-induced apoptosis in hepatocytes. Regarding HSC, results revealed that NOX4-derived ROS are essential for MFB activation since both NOX4 silencing/inhibition and antioxidant treatments impaired TGF-β-induced transdifferentiation of

HSC into MFB. Corroborating our data, there is a study showing that TGF-β-mediated HSC activation is dependent on NOX4-generated ROS by using NOX4-deficient HSC. Moreover, they show that NOX4 is acting downstream of both TGF-β and the Smad complex (Jiang et al., 2012).

However, the role of NOX proteins in liver fibrogenesis is not only circumscribed to NOX4. HSC express both phagocytic NOX2 and non-phagocytic NOX, including NOX1 and NOX4, in addition to other NOX regulatory components (p22phox, p40phox, p67phox, NOXO1, NOXA1 and Rac1). It has been shown that both NOX proteins and NOX components are increased when quiescent HSC activate to MFB. Moreover, studies performed in $Nox1^{-/-}$, $Nox2^{-/-}$ or $p47phox^{-/-}$ mice have demonstrated the importance of other NOX proteins, concretely NOX1 and NOX2 in fibrogenesis. NOX1 promotes MFB proliferation by PTEN inactivation to positively regulate an AKT/FOXO4/p27 signalling pathway (Cui et al., 2011). Indeed, NOX1 seems to mediate the pro-fibrogenic effects exclusively in endogenous liver cells, while NOX2 could be implicated in both endogenous liver cells and bone marrow-derived cells (Paik et al., 2011), possibly acting in the process of phagocytosis of dead hepatocytes (Jiang et al., 2010). Furthermore, NOX1 activity might further contribute to the inflammatory process that concomitantly occurs during liver fibrosis, promoting COX-2 expression and prostaglandin synthesis in hepatocytes (Sancho et al., 2011). In addition to TGF-β, angiotensin II also activates HSC, actually in a TGF-β dependent manner. Fibrogenic responses to angiotensin II in HSC are blunted by antioxidant (NAC) and NOX inhibitor (DPI) treatments (Bataller et al., 2003). Interestingly, NOX4 up-regulation after angiotensin II stimuli requires NOX1, since it was shown to be impaired in NOX1 knock-out HSC, while TGF-β by itself induces NOX4 in a NOX1 independent manner (Aoyama et al., 2012). Importantly, it has been recently reported that activated HSC have increased ROS-detoxifying capacity compared to quiescent HSC that protects them from ROS-induced apoptosis and necrosis (Dunning et al., 2013).

Furthermore, results presented here also demonstrate that the highest expression of NOX4 occurs in hepatocytes when compared to HSC or MFB, and that TGF-β induces NOX4 expression in hepatocytes, which mediates TGF-β-induced cell death. Moreover, hepatocyte caspase-3 activation is prevented when cells are treated either with a NOX inhibitor (DPI) or antioxidant compounds (GEE and BHA). These results are in accordance to previous results from our group where we demonstrated that NOX4 mediates TGF-β-induced apoptosis in rat and human hepatocytes (Carmona-Cuenca et al., 2008). In addition, NOX4 also mediates apoptosis induced by other stimuli since $NOX4^{-/-}$ hepatocytes are resistant to apoptosis induction by CD95L and TNF-α/actinomycin D (Jiang et al., 2012). Hepatocyte apoptosis during fibrosis might be relevant to blunt regeneration and create a pro-fibrogenic microenvironment. In agreement with these results, it has been proposed a role for NOX4 in epithelial cell death during development of bleomycin-induced lung fibrosis. Using a model of NOX4 deficient mice, authors demonstrated that these animals were resistant to fibrosis due to the abrogation of TGF-β-induced apoptosis in epithelial cells (Carnesecchi et al., 2011). Of note, hepatocytes

express not only NOX4 but also other NOX proteins, and they play opposite roles in the control of hepatocyte survival and death. Indeed, as we just said, NOX4 is necessary to mediate apoptosis induced by TGF-β (Carmona-Cuenca et al., 2008; Caja et al., 2009), however, this pro-apoptotic effect of the cytokine can be attenuated when NOX1 is active (Sancho et al., 2009; Sancho and Fabregat, 2011).

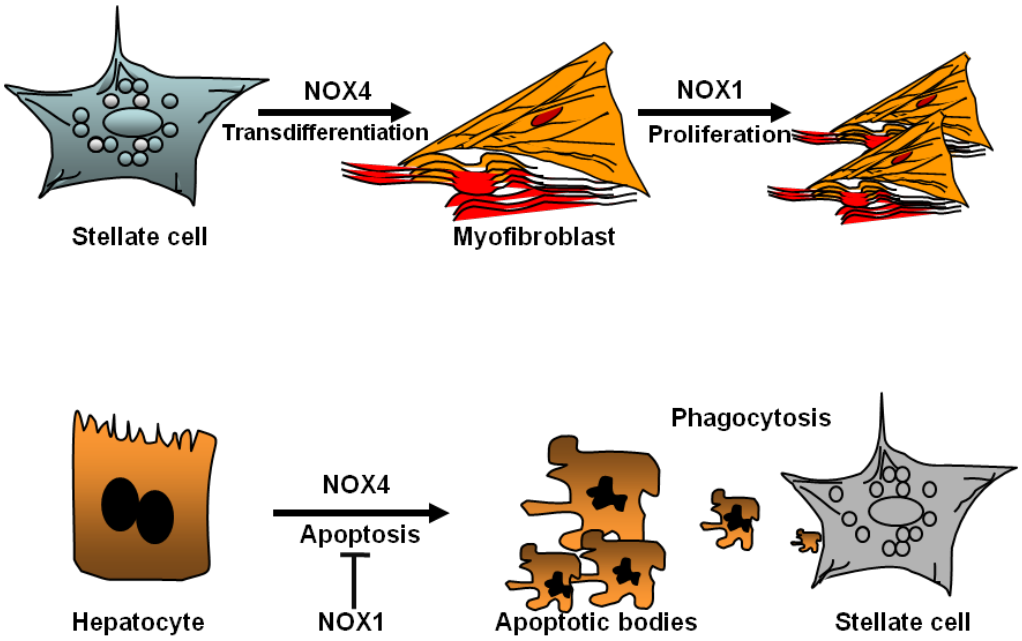


**Figure XIX.** NOX proteins play different roles during liver fibrosis development.

The development of novel pharmacological NOX inhibitors is being assessed as potential anti-fibrotic therapeutics for hepatic fibrosis. Interestingly, evidences for the role of dual NOX4/NOX1 pharmacological inhibitor GKT137831 in decreasing both the apparition of fibrogenic markers and hepatocyte apoptosis *in vivo*, upon bile duct ligation and $CCl_4$ treatment, are reported (Aoyama et al., 2012; Jiang et al., 2012). However, further experimental work is required for a better knowledge of the physiological functions of NOX proteins in the liver to predict the consequences of using NOX inhibitors.

# 2. Relevance of the TGF-β pathway in liver cancer. Crosstalk with NOX4.

TGF-β is a central regulator in chronic liver disease contributing to all stages of disease progression from initial liver injury through inflammation and fibrosis to cirrhosis and HCC. Nevertheless, it has been described a double-edged role of TGF-β in various liver disease stages. The ability of TGF-β to contribute to tumour progression depends on the capacity of the cells to overcome its growth inhibitory and pro-apoptotic effects. Different mechanisms could account for this resistance, among others, alteration of oncogenic pathways, such as Ras/ERKs or p53 (Caja et al., 2009; Morris et al., 2012); alterations in the TGF-β suppressor arm, such as dysregulation of embryonic liver fodrin (ELF), a crucial Smad3/4 adaptor (Baek et al., 2008) or up-regulation of Smad7 (Matsuzaki et al., 2000; Dooley et al., 2009); or interaction with hepatitis B virus X (HBx) protein (Murata et al., 2009). Tumour cells that overcome TGF-β suppressor effects become susceptible to respond to this cytokine inducing other effects, such as EMT processes that contribute to either fibrosis and/or tumour dissemination (Moustakas and Heldin, 2012).

In the liver, TGF-β signalling has been shown to play a tumour suppressor role, however, different studies have identified overexpression of TGF-β in HCC, which correlates with tumour progression and bad prognosis (Coulouarn et al., 2008; Fransvea et al., 2008). TGF-β may stimulate tumour proliferation and survival through the production of mitogenic growth factors, and cells that survive to TGF-β later induce EMT that favours cell migration and invasion, which clearly contributes to tumour metastasis (Fabregat et al., 2014).

Results presented here show that the mesenchymal-like phenotype observed in some human HCC cell lines are coincident with autocrine overactivation of the TGF-β pathway in these cells. In addition, a correlation between the expression of mesenchymal features and the lack of response to TGF-β as a tumour suppressor is observed. Interestingly, the human HCC cell lines that responded to TGF-β as a suppressor cytokine (Huh7, PLC/PRF/5 and Hep3B) are included within the group of early TGF-β signature, while the non-responder cell lines (SNU449 and HLF) belong to the late TGF-β signature, in the classification designed by Coulouarn and colleagues (Coulouarn et al., 2008). Moreover, late TGF-β signature is associated with increased invasiveness, and in accordance, our cells displayed a higher migratory capacity in a TGF-β/CXCR4 dependent manner, being CXCR4 a chemokine receptor previously associated with higher invasive potential of HCC (Schimanski et al., 2006; Liu et al., 2008; Bertran et al., 2013). Furthermore, it has been described in liver cancer cells that EMT process through Snail1 up-regulation overcome TGF-β-induced tumour-suppressor effects, switching its response to

tumour progression, making cells resistant to cell death and prone to acquire invasive properties (Franco et al., 2010).

Interestingly, mesenchymal-like characteristics are attenuated in cells where TGFBR1 expression is silenced with a specific shRNA. Furthermore, decreased expression of mesenchymal markers correlates with the impairment of migratory capacity of the cells. Importantly, it was demonstrated that inhibition of migration in TGFBR1 silenced cells concurs with decreased CXCR4 expression and impaired asymmetric distribution of the protein in cells (Bertran et al., 2013). Inhibition of the TGF-β pathway is emerging as a new therapeutic tool in cancer (Giannelli et al., 2011). Since it regulates several steps in tumour progression, blocking this mediator should have multiple beneficial effects. So far, blocking antibodies and ligand traps, antisense oligos, TβRII and/or TβRI (ALK5) inhibitors and immune response-based strategies are being developed to block TGF-β pathway in cancer (Fabregat et al., 2014). Interference of TGF-β signalling in various short-term animal models has provided promising results. However, liver disease progression in humans is a process of decades with different phases where targeting of TGF-β might have both beneficial and adverse effects (Dooley and ten Dijke, 2012). Nevertheless, preliminary results from a phase II clinical trial with the TβRI inhibitor LY2157299 have shown improved clinical outcome and changes consistent with a reduction of EMT in HCC patients (Giannelli et al., 2014). Importantly, the results presented here, where overactivation of the TGF-β pathway differs among the different cell lines tested and the heterogeneity of the tumours, suggest that these might condition the response to the inhibitors. For this reason, dissecting the downstream signals that govern the suppressor and the pro-tumorigenic effects of TGF-β pathway in liver tumour cells may help in the design of more specific targeted therapies for downstream TGF-β receptors and/or to select patients in whom a potential positive response to TGF-β inhibitors is predicted.

Due to the observed relevant role played by NOX4 in mediating some of TGF-β effects in both normal and transformed hepatocytes (Carmona-Cuenca et al., 2008; Caja et al., 2009), we wondered whether autocrine expression of TGF-β would be regulating NOX4 levels in HCC cells. Surprisingly, results show that there is not a direct correlation between NOX4 expression and autocrine levels of TGF-β but on the contrary, cells with higher levels of NOX4 are those with lower levels of TGF-β, and on the other way round. Importantly, high NOX4 expression occurs in early TGF-β signature cell lines, whereas late TGF-β signature is coincident with low NOX4 levels. Furthermore, TGF-β treatment and/or disruption of TGF-β signalling by means of silencing TβRI resulted in different outcomes depending on the TGF-β signature. Thus, cancelling TβRI in early TGF-β signature cell lines decreases NOX4 levels while TGF-β treatment induces NOX4 expression (Carmona-Cuenca et al., 2008), and the opposite result is shown when the late TGF-β signature cell lines are treated with TGF-β or knocked-down for the TβRI. These results showing that TGF-β only induces NOX4 in those cells that are able to respond to TGF-β as a tumour suppressor but not in those that are refractory to these effects

are in accordance to previously reported roles for NOX4 mediating TGF-β suppressor effects in different models, including in the liver, such as induction of apoptosis (Carmona-Cuenca et al., 2008; Caja et al., 2009; Das et al., 2014; Yan et al., 2014) and senescence (Senturk et al., 2010; Hubackova et al., 2012). Furthermore, previous results from our group demonstrated that NOX4 is dispensable for TGF-β-induced EMT in hepatocytes, being EMT a pro-tumorigenic effect of the cytokine (Sancho et al., 2012), suggesting that at least in the liver, NOX4 may be only mediating TGF-β suppressor effects. We show here that mesenchymal characteristics of HCC cells are dependent on TGF-β. Considering that cells displaying a mesenchymal-like phenotype are the ones with lower NOX4 levels, and that accordingly to the fact that TGF-β induced EMT might be NOX4 independent, we can speculate that the capacity of TGF-β for inducing NOX4 expression is circumvented to its suppressor activity, and it might be lost when the switch to pro-tumorigenic actions occurs. Nevertheless, in other models such as breast epithelial cells, it has been reported that NOX4 is mediating TGF-β pro-tumorigenic actions, including EMT and invasion (Boudreau et al., 2012). A possible explanation for these contradictory results is that NOX4 role might be dependent on the cell system and the intracellular compartment where it acts. For example, as we said before, NOX4 has a pro-apoptotic effect in liver cells, but on the contrary, in pancreatic cells it has been shown that NOX4 induces anti-apoptotic actions (Vaquero et al., 2004). Nevertheless, further studies will be necessary to confirm the differential role of NOX4 mediating TGF-β effects, depending on the TGF-β signature in HCC cells and whether genetic or epigenetic alterations in the NOX4 promoter may be responsible for these differences.

# 3. NOX4 plays a growth inhibitory role in hepatocytes and HCC cells, regulating liver cancer progression.

So far, results presented here show that NOX4 mediates TGF-β effects both as a fibrogenic cytokine and a tumour suppressor in the liver. Therefore, we can already speculate that it is necessary to be cautious on the usage of NOX4 inhibitors as a treatment for liver fibrosis because the consequences on transformed hepatocytes may be deleterious due to the inhibition of at least some of the TGF-β suppressor actions. Nevertheless, results presented in this work also indicate that NOX4 may also play a tumour suppressor function in the liver by itself by controlling hepatocyte proliferation. Different evidences support this hypothesis: 1) Targeting NOX4 confers selective advantage to liver cells to proliferate *in vitro*; 2) during liver regeneration after 2/3 partial hepatectomy in mice, a process that requires hepatocytes to leave quiescence and enter in cell cycle, *Nox4* expression is transiently down-regulated; 3) liver tumorigenesis in an experimental model in mice correlates with down-regulation of *Nox4*; 4) targeting NOX4 in HCC cells confers advantage for tumour progression in a xenograft model of *in vivo* tumorigenesis; and 5) lower levels of NOX4 are found in human HCC cell lines and in a great percentage of human liver tumour tissues.

Stable NOX4 silencing in human HCC cell lines decreased intracellular ROS production, modifying mainly hydrogen peroxide levels, since no changes were detected when intracellular superoxide levels were measured while a significant reduction was observed through both DCFDA and Amplex Red assays, which detect intracellular unspecific ROS and $H_2O_2$, respectively. These results are consistent with data from other groups suggesting that $H_2O_2$ is the only reactive oxygen specie that can be detected from NOX4 activity. The explanation might lay on the protein structure since it is reported that the third extracytosolic loop (E-loop) of NOX4 differs from NOX1 and NOX2, being longer and containing a highly conserved histidine that could serve as a source for protons to accelerate spontaneous dismutation of superoxide to form $H_2O_2$ (Serrander et al., 2007; Takac et al., 2011).

Correct progression through the cell cycle and its precise regulation is essential to an organism for proliferation and survival. Here we show that when cancelling NOX4 expression in human HCC cells there is a substantial increase in the growth capacity of cells, concurring with higher percentage of cells actively proliferating together with down-regulation of the cell cycle inhibitor *CDKN1A* ($p21^{Cip1}$) and up-regulation of Cyclin D1, a central mediator in the transition from $G_1$ to S phase of the cell cycle. Cyclin D1 is considered to play a relevant role in the increased progression of HCC cells and it has been found to be overexpressed in HCC tissues (Che et al., 2012; Ao et al., 2014).

ROS have been proposed to play a role on cell proliferation. Indeed, low concentrations of $H_2O_2$ are generally growth stimulatory, but higher concentrations of $H_2O_2$ and superoxide can have deleterious effects leading to mammalian cell death. Already in 1999 an effect of ROS on cell growth was shown on PDGF stimulation where down-regulation of NOX1 before PDGF stimulation resulted in decreased levels of ROS and decreased serum dependent growth after PDGF stimulation (Suh et al., 1999). Moreover, our group has described that NOX1 promotes autocrine growth through the up-regulation of the EGFR pathway in liver cells (Sancho and Fabregat, 2010). The production of ROS in early growth factor-induced signalling pathways has led to the proposal that ROS regulate cell cycle progression through the regulation of Cyclin D1 expression (Burch and Heintz, 2005). Furthermore, recent results indicate that NOX4 in normal human fibroblasts is required to suppress p53-dependent check-point of proliferation (Salmeen et al., 2010). However, different pieces of evidence locate ROS in a completely opposite role. For example, $H_2O_2$ mediates oxidation and inactivation of the cell cycle phosphatase cdc25, which is required for cell cycle progression from $G_2$ to M phase (Glasauer and Chandel, 2014). In addition, oxidative stress induced by NOX4 has been also associated to decreased cell growth by inducing cell cycle arrest and cell death through either senescence or apoptosis. A possible explanation for these pleiotropic and sometimes contradictory actions of ROS may be related to the duration and intensity of the activating signal, the developmental stage of the cell, and also to the intracellular compartment where ROS are produced, because different redox targets might be affected (Lambeth and Neish, 2014). In this sense, NOX4 is associated with intracellular compartments, including ER, mitochondria and nucleus. In addition, cells harbouring mutations in tumour suppressor genes such as p53 or in oncogenes such as Ras, may be able to bypass senescence-mediated ROS-dependent growth arrest (Holmström and Finkel, 2014). Nuclear NOX4 has been proposed to mediate ROS-induced DNA damage that leads to a loss of replicative potential and subsequent senescence (Weyemi and Dupuy, 2012; Weyemi et al., 2012). In this same line of evidence, NOX4 mediates TGF-β-induced senescence in HCC cells through up-regulation of $p21^{CIP1}$ and $p15^{INK4B}$ (Senturk et al., 2010). Moreover, NOX4 has been implicated in cell differentiation, and in maintenance of the differentiated state, which usually is associated with a quiescent state of the cells (Schröder et al., 2009; Schröder et al., 2012). Intracellular NOX4-derived ROS may mediate signal transduction in normal cells by regulating redox-sensitive cysteine residues in specific effector proteins including tyrosine phosphatases (Finkel, 2011). Several works have reported that ROS-induced p38 MAPK may trigger blockage of proliferation in different cell lines including hepatocytes. However, in some cell lines and under specific circumstances, p38 MAPK activation induced by ROS can also promote cell proliferation, rarely occurring in hepatocytes. It has been described that in liver injury and hepatocarcinogenesis, activated p38 MAPK induces growth arrest and senescence through a mechanism involving cell cycle regulators such as $p21^{Cip1}$ (Tormos et al., 2013). NOX4 has been reported to mediate TGF-β-stimulated p38 MAPK phosphorylation (Martin-Garrido et al., 2011). Moreover, low concentrations of $H_2O_2$ induce cell proliferation by ERK and PI3K/AKT pathways through stimulation of growth-factor receptors,

mimicking the action of natural ligands and determining survival (Yoon et al., 2002; Tormos et al., 2013).

Liver is a quiescent tissue that rarely divides under normal conditions. However, under certain conditions such as toxic injury, viral infection and partial hepatectomy, hepatocytes divide in order to compensate the loss of liver mass. It has been reported that NOX2-derived ROS are not essential for liver regeneration after partial hepatectomy (Ueno et al., 2006). Here we show that both physiological proliferative situations in the liver, such as liver regeneration after partial hepatectomy in mice, and neoplastic liver pathologies, such as that found in the mouse model of DEN-induced hepatocarcinogenesis, concur with significant decrease in NOX4 expression. These results, together with the higher tumorigenic capacity of NOX4-silenced HCC cells in xenograft experiments in mice, where it is demonstrated that the higher tumorigenic capacity is due to increased proliferation rather than altered apoptosis, point to the *in vivo* relevance of the *in vitro* results, where the attenuation in NOX4 expression is coincident with cell growth capacity. Interestingly, NOX4 knock-down cells show nuclear translocation of β-catenin and it has been reported that HCC with β-catenin activation display significantly higher proliferation rate and larger tumour size when compared with β-catenin negative tumours (Calvisi et al., 2005). Indeed, one of the main target genes of activated β-catenin is Cyclin D1, thus promoting cell proliferation. It has been shown that activation of β-catenin after partial hepatectomy always precedes Cyclin D1 expression and appearance of cells in the S phase of cell cycle (Monga, 2014). All these results together indicate that NOX4 in liver tumour cells acts as a growth inhibitor, compatible with its potential role counteracting growth factor signals and/or inducing senescence. In support of this, it is worthy to note that NOX4 levels appear to be decreased in a cohort of tissues from human liver tumours, most of them HCC.

To sum up, our results suggest a role for NOX4 as a redox enzyme involved in controlling proliferation of liver cells. Considering that fibrotic processes frequently develop in cirrhosis, it is necessary to be cautious when using NOX4 inhibitors.

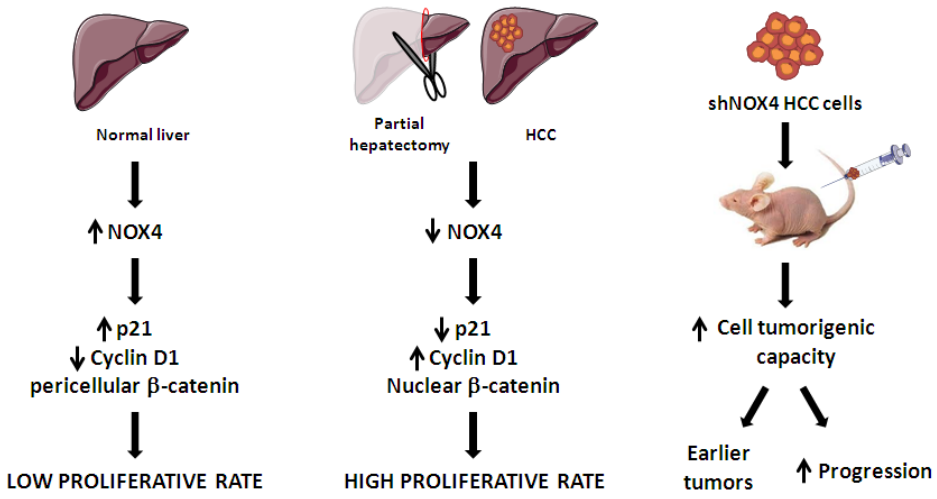


**Figure XX.** NOX4 inhibits proliferation and favours tumorigenesis in liver.

# 4. NOX4 regulates contractility in human HCC cells, influencing its capacity of adhesion and invasion.

HCC is characterized for being a highly heterogenic cancer and for harbouring a high rate of tumour recurrences, in addition to be usually presented as a multifocal cancer, being difficult to elucidate whether these multiple focus are different primary tumours or intrahepatic metastasis from a single primary tumour. In advanced stages, it is possible to find extrahepatic dissemination, being lungs, lymph nodes and bones the most frequent metastatic sides. More than 90% of HCC-related deaths are the result of secondary local or distant disease. Therefore, it is important to investigate the molecular mechanisms involved in the recurrence and metastasis of HCC. Accordingly, they will provide potential therapeutic targets for HCC.

Metastasis involves a complex cascade of signal events between tumour cells and stromal microenvironment, and accumulating evidences support the idea that alterations in cell-to-cell or cell-to-matrix interactions contribute to the occurrence of cancer metastasis, since cancer cells need to remodel their adhesion to gain migratory capabilities and thus, to invade adjacent tissues (Spano et al., 2012). It is shown in this work that liver tumour cells are able to migrate and invade the surrounding ECM. Results demonstrate that some human HCC cells display a mesenchymal-like phenotype and migratory capacity under basal conditions. When we analysed whether NOX4 was playing a role in the migratory and invasive capacity of HCC cells, results revealed that NOX4 down-regulation in some human HCC cells increases actomyosin contractility with an altered pattern of expression and activation of Rho GTPases, which concurs together with diminished cell-to-cell and cell-to-matrix adhesion, leading to increased migration and invasion capabilities, mainly as rounded cells.

Advanced cancers can display plasticity with respect to morphological characteristics and the modes of migration and invasion they use (mesenchymal, amoeboid, collective migration). These can be altered and adapted according to interactions with and signals they receive from the local tumour environment (Canel et al., 2013). Rho GTPases family are key regulators of cell migration through their actions on actin assembly and actomyosin contractility. Until now, only few focused studies have linked human liver cancer and alteration in Rho GTPase expression. Nevertheless, it has been described overexpression of RhoA (Li et al., 2006) and RhoC (Wang et al., 2004) in HCC, as well as of Rac1, participating in tumour progression and metastasis (Grise et al., 2009). Cdc42 has been associated to both suppression and promotion of liver cancer (Grise et al., 2009). Recently, it has been described that ROCK II, a Rho effector, promotes invasion and metastasis of HCC by preventing ubiquitination and degradation of MMP2 (Huang et al., 2014).

Of relevance for the results presented here, previous works support functional and physical links among the actin cytoskeleton and Rho GTPases, and the NADPH oxidase systems, although many points are still unknown. NOX-derived ROS can target proteins that in turn will interact with actin, thus providing an indirect ROS-mediated (and Rho GTPase) control of actin function, and eventually, of cell migration (Stanley et al., 2013).

Most of the studies relating NOX-derived ROS with cell migration and adhesion do not characterize the type of movement analysed. However, considering the assumptions done in most of the reports, where increased migration and invasion is associated to increased adhesion and usually to increased protease activity, we can speculate that what is basically described in the literature is the association between ROS and single cell mesenchymal mode of migration, most of them reporting a link between NOX-derived ROS, Rac signalling and increased migration. For example, it has been described that upon several endogenous physiological stimuli, such as growth factors and integrin engagement with the epithelial basement membrane, local ROS production is induced via activation of NOX1, which results in a rapid oxidative inactivation of PTPases, consequent FAK phosphorylation and initiation of cellular motility (Chiarugi et al., 2003). ROS production and inactivation of PTPases facilitate cell spreading through the down-regulation of RhoA activity activating p190RhoGAP (Hurd et al., 2012). Intriguingly, almost nothing is known about the role of NOX-derived ROS regarding single cell amoeboid migration or collective migration.

Results presented here show that low expression of NOX4 is related to increased expression of RhoA, RhoC and Cdc42, both at RNA and protein level. Moreover, NOX4 silencing in PLC/PRF/5 cells, which present intermediate levels of NOX4 expression when compared to the other cell lines, provokes an increase in the expression of the same Rho GTPases, further confirming the link between NOX4 and these proteins, suggesting a transcriptional regulation. Furthermore, RhoA activation is also increased after NOX4 silencing in PLC/PRF/5 cells. Regarding Hep3B, these cells present high expression and activation of Rac1 compared to the other cell lines. Rac and RhoA signalling have opposing effects and reciprocally dampen each other activity. Indeed, regulatory proteins that favour the amoeboid mode of movement either activate RhoA/ROCK signalling or inhibit Rac activation, and on the other way round for mesenchymal migration (Lämmermann and Sixt, 2009), suggesting tight mechanistic links between alternative modes of movement. Of note, a redox regulation between Rho GTPases has been reported. Thus, Rac-derived ROS inhibit the low-molecular-weight PTP (LMW-PTP), which provokes activation of p190RhoGAP that in turn down-regulates Rho signalling (Nimnual et al., 2003; Parri et al., 2007). Indeed, NOX1-dependent ROS production is necessary for the down-regulation of RhoA during directed cell migration in colon epithelial cells (Sadok et al., 2009). Moreover, Rac1 and RhoA/ROCK signalling pathways are inversely regulated in hypoxia/reoxygenation-induced actin cytoskeleton remodelling. During hypoxia, reduced production of ROS results in a reduction in the activity of Rac1, with subsequent activation of RhoA, while during reoxygenation occurs the other way round, there is an increase

in NOX-dependent ROS production, resulting in an increase in Rac1 activity with subsequent decrease in RhoA activity (Wojciak-Stothard et al., 2005).

Thus, considering that Rho and Rac play opposite roles, that they regulate each other, and that Rac activity appears to be a key determinant of the inter-conversion or plasticity between modes of movement, it is feasible that RhoA expression and activity are barely detectable in Hep3B as a consequence of the overexpression of Rac1. Interestingly, NOX4 silencing in Hep3B reduces Rac1 activation, although the effect is not sufficient to increase neither RhoA expression nor activity.

Some reports suggest that RhoA and RhoC have different roles during cell migration by acting through different downstream targets. However, other studies suggest that RhoA, B and C act redundantly to generate actomyosin contractility (Sadok and Marshall, 2014). Results presented here show that increases in expression and/or activity of both RhoA and C are coincident with low levels of NOX4 and correlate with increased actomyosin contractility. Indeed, we show that highest levels of pMLC2, a readout of high actomyosin contractility, are found in HLF and SNU449 cells, and importantly, NOX4 silencing in PLC/PRF/5 cells also increases pMLC2 levels, confirming the relevance of NOX4 expression in the process. Of note, high levels of pMLC2 correlate with membrane blebbing, which requires high contractility.

High actomyosin contractility is related to a decrease in cell-to-matrix adhesion. Indeed, results presented here show that adhesion to different matrixes is partially impaired when NOX4 silencing increases cell contractility, showing a decrease in the number and the area occupied by focal adhesion complexes, as well as a decrease in the functional integrins on the plasma membrane. In accordance, Ribeiro-Pereira et al. described that NOX4 silencing in melanoma cells resulted in a decrease in FAK phosphorylation and cytoskeleton rearrangement (Ribeiro-Pereira et al., 2014). Importantly, it has been described that FAK-mediated phosphorylation and activation of p190RhoGAP may decrease Rho and ROCK-mediated Myosin II activity (Gardel et al., 2010).

Furthermore, results in this work also show an individualization of HCC cells, together with a disruption of cell-to-cell adhesion in highly contractile cells, when NOX4 expression is low or silenced. These effects are likely to be due to the increased actomyosin contractility. It has been shown that ROCK-mediated actomyosin contractility downstream of Rho disrupts adherent junctions (Sahai and Marshall, 2002). Also Cdc42 has been reported to be crucial for the disassembly of E-cadherin junctions (Shen et al., 2008). In fact, a key factor that determines the net outcome in terms of invasive migration and its underlying mechanism is the balance between E-cadherin-mediated adherent junctions and integrin-mediated cell-to-matrix contacts (Canel et al., 2013).

Altogether our results suggest that NOX4 controls actomyosin contractility of human HCC cells through the regulation of expression and activation of Rho GTPases, which in turn modifies cell-to-cell and cell-to-matrix adhesion capabilities. All these phenomena may determine the mode of cell migration and invasion of HCC cells. Indeed, it has recently been

described that targeting of RhoA signalling by the microRNA-122 enhances cell adhesion and suppresses HCC cell motility and invasion (Wang et al., 2014). Cancer cells can follow two distinct strategies to migrate as single cells. On the one hand, there is the elongated "mesenchymal-like" mode that is a directed migration driven by Rac-induced cell protrusions requiring high adhesion and low actomyosin contractility. On the other hand, there is the rounded "amoeboid" mode of cell migration, which does not involve significant cell-to-matrix adhesion and proteolytic activity, and do not require cell-to-cell adhesion at all. This movement is mainly driven by Rho/ROCK mediated bleb-like protrusions with active myosin-actin contractions (Sanz-Moreno and Marshall, 2010; Sanz-Moreno, 2012). Importantly, mesenchymal migration is relatively low (0.1-1μm/min) while intravital imaging showed that cells move at very high speed with an amoeboid morphology (up to 4μm/min) (Parri and Chiarugi, 2010). In addition, cell can migrate collectively maintaining cell-to-cell adhesion and forming a cortical actin filament assembly along cell junctions. This allows the formation of a larger-sized, multicellular contractile body. Collective movements are sensitive to integrin antagonists and protease inhibitors (Friedl and Wolf, 2003). Importantly, cancer cell migration mechanisms can be reprogrammed, including the epithelial-to-mesenchymal transition (EMT), the mesenchymal-to-amoeboid transition (MAT) and the collective-to-amoeboid transition (CAT) (Friedl and Wolf, 2003).

Considering the different types of migration described, it appears that amoeboid movement is favoured when NOX4 is down-regulated in HCC cells since they show higher Rho signalling and contractility, leading to higher migratory and invasive capabilities. Accordingly, both PLC/PRF/5 silenced for NOX4 and SNU449 invading cells displayed round morphology. Considering that cells expressing high levels of NOX4 form parenchymal structures that are disrupted by NOX4 silencing or not observed in cell lines expressing low levels of NOX4, it is likely that by decreasing NOX4 levels a CAT is induced.

In conclusion, NOX4 is controlling actomyosin contractility of liver tumour cells that in turn regulates cell-to-cell and cell-to-matrix adhesion. Therefore, NOX4 might be a key regulator of the mode of movement that liver cancer cells adopt to metastasize, favouring amoeboid migration when it is down-regulated.

# Final discussion

Due to the causal role of ROS in promoting cancer, and that various antioxidant promoters, such as Nrf2, are considered tumour suppressors, research has been focused on antioxidant treatments to dampen ROS levels as therapeutic strategies against tumorigenesis. However, most of clinical trials have failed to show beneficial effects of antioxidants on a variety of pathologies, including cancer (Glasauer and Chandel, 2014). Cancer therapeutics designed to target adhesion receptors or proteases have not yet been shown to be effective in clinical trials and this might be due to the fact that cancer cell migration mechanisms are inter-convertible (Friedl and Wolf, 2003). Results presented here suggest that neither antioxidants nor drugs targeting adhesion related molecules might be effective strategies for cancer treatment. In here it is shown that NOX4, a ROS producing enzyme, may be a key player during the inter-conversion of different modes of migration. Indeed, NOX4 may play an essential tumour suppressor role in the liver through the control of both cell proliferation and cell contractility, therefore modifying at the same time the tumorigenic capacity and metastatic potential of HCC cells. Finally, as mentioned before, new pharmacological inhibitors of NOX proteins are being assessed for fibrotic processes. Considering that fibrosis frequently develops in cirrhosis, which is a pre-neoplastic situation, it will be necessary to be cautious in the use of NOX4 inhibitors in this pathology.

# VII. CONCLUSIONS

1. *Nox4* expression is up-regulated during liver fibrosis in mice and it is required for TGF-β-induced transdifferentiation of HSC to MFB and hepatocyte apoptosis.

2. High levels of autocrine TGF-β provoke loss of epithelial characteristics, gain of mesenchymal features and resistance to TGF-β suppressor effects in HCC cells. There is an inverse correlation between autocrine TGF-β and NOX4 expression in HCC cell lines.

3. NOX4 is a negative regulator of hepatocyte proliferation in both untransformed and liver tumour cells. Its expression is down-regulated during liver regeneration after partial hepatectomy in mice.

4. *Nox4* expression is down-regulated during DEN-induced liver tumorigenesis in mice and targeting knock-down of NOX4 in HCC cells confers them advantage for tumour progression in xenograft models in mice. Low levels of NOX4 are found in human HCC cell lines and in a relevant percentage of human liver tumour tissues.

5. Down-regulation of NOX4 increases the invasive growth capacity of HCC cells when embedded in a pliable matrix, increasing both proliferation and invasion. Low levels of NOX4 correlate with high actomyosin contractility, which provokes loss of epithelial parenchymal characteristics, decreasing both cell-to-cell contacts and cell-to-matrix adhesion, and increasing invasive capacity.

# Final conclusion:

In the liver, NOX4 plays pro-fibrotic roles, mediating TGF-β-induced HSC activation and hepatocyte death, but plays a tumour suppressor role during carcinogenesis, being a negative regulator of liver tumour growth and invasion.

# VIII. REFERENCES

## VIII. REFERENCES


Abhilash, P.A., Harikrishnan, R., and Indira, M. (2012). Ascorbic acid supplementation down-regulates the alcohol induced oxidative stress, hepatic stellate cell activation, cytotoxicity and mRNA levels of selected fibrotic genes in guinea pigs. Free Radic. Res. *46*, 204–213.

Achyut, B.R., and Yang, L. (2011). Transforming growth factor-β in the gastrointestinal and hepatic tumor microenvironment. Gastroenterology *141*, 1167–1178.

Altenhofer, S., Kleikers, P.W.M., Radermacher, K.A., Scheurer, P., Rob Hermans, J.J., Schiffers, P., Ho, H., Wingler, K., and Schmidt, H.H.H.W. (2012). The NOX toolbox: validating the role of NADPH oxidases in physiology and disease. Cell. Mol. Life Sci. *69*, 2327–2343.

Altenhöfer, S., Radermacher, K.A., Kleikers, P.W.M., Wingler, K., and Schmidt, H.H.H.W. (2014). Evolution of NADPH Oxidase Inhibitors: Selectivity and Mechanisms for Target Engagement. Antioxid. Redox Signal.

Amara, N., Goven, D., Prost, F., Muloway, R., Crestani, B., and Boczkowski, J. (2010). NOX4/NADPH oxidase expression is increased in pulmonary fibroblasts from patients with idiopathic pulmonary fibrosis and mediates TGFbeta1-induced fibroblast differentiation into myofibroblasts. Thorax *65*, 733–738.

Anilkumar, N., San Jose, G., Sawyer, I., Santos, C.X.C., Sand, C., Brewer, A.C., Warren, D., and Shah, A.M. (2013). A 28-kDa splice variant of NADPH oxidase-4 is nuclear-localized and involved in redox signaling in vascular cells. Arterioscler. Thromb. Vasc. Biol. *33*, e104–e112.

Ao, R., Zhang, D.-R., Du, Y.-Q., and Wang, Y. (2014). Expression and significance of Pin1, β-catenin and cyclin D1 in hepatocellular carcinoma. Mol. Med. Rep. *10*, 1893–1898.

Aoyama, T., Paik, Y.-H., Watanabe, S., Laleu, B., Gaggini, F., Fioraso-Cartier, L., Molango, S., Heitz, F., Merlot, C., Szyndralewiez, C., et al. (2012). Nicotinamide Adenine Dinucleotide Phosphate Oxidase (NOX) in Experimental Liver Fibrosis: GKT137831 as a Novel Potential Therapeutic Agent. Hepatol. Baltim. Md *56*, 2316–2327.

Babelova, A., Avaniadi, D., Jung, O., Fork, C., Beckmann, J., Kosowski, J., Weissmann, N., Anilkumar, N., Shah, A.M., Schaefer, L., et al. (2012). Role of Nox4 in murine models of kidney disease. Free Radic. Biol. Med. *53*, 842–853.

Baek, H.J., Lim, S.C., Kitisin, K., Jogunoori, W., Tang, Y., Marshall, M.B., Mishra, B., Kim, T.H., Cho, K.H., Kim, S.S., et al. (2008). Hepatocellular cancer arises from loss of transforming growth factor beta signaling adaptor protein embryonic liver fodrin through abnormal angiogenesis. Hepatol. Baltim. Md *48*, 1128–1137.

Baghdasaryan, A., Claudel, T., Kosters, A., Gumhold, J., Silbert, D., Thuringer, A., Leski, K., Fickert, P., Karpen, S.J., and Trauner, M. (2010). Curcumin improves sclerosing cholangitis in Mdr2−/− mice by inhibition of cholangiocyte inflammatory response and portal myofibroblast proliferation. Gut *59*, 521–530.

Baltanás, A., Solesio, M.E., Zalba, G., Galindo, M.F., Fortuño, A., and Jordán, J. (2013). The senescence-accelerated mouse prone-8 (SAM-P8) oxidative stress is associated with upregulation of renal NADPH oxidase system. J. Physiol. Biochem. *69*, 927–935.

Barikbin, R., Neureiter, D., Wirth, J., Erhardt, A., Schwinge, D., Kluwe, J., Schramm, C., Tiegs, G., and Sass, G. (2012). Induction of heme oxygenase 1 prevents progression of liver fibrosis in Mdr2 knockout mice. Hepatol. Baltim. Md *55*, 553–562.

Barnes, J.L., and Gorin, Y. (2011). Myofibroblast differentiation during fibrosis: role of

NAD(P)H oxidases. Kidney Int. *79*, 944–956.

Basuroy, S., Tcheranova, D., Bhattacharya, S., Leffler, C.W., and Parfenova, H. (2011). Nox4 NADPH oxidase-derived reactive oxygen species, via endogenous carbon monoxide, promote survival of brain endothelial cells during TNF-α-induced apoptosis. Am. J. Physiol. Cell Physiol. *300*, C256–C265.

Bataller, R., and Brenner, D.A. (2005). Liver fibrosis. J. Clin. Invest. *115*, 209–218.

Bataller, R., Schwabe, R.F., Choi, Y.H., Yang, L., Paik, Y.H., Lindquist, J., Qian, T., Schoonhoven, R., Hagedorn, C.H., Lemasters, J.J., et al. (2003). NADPH oxidase signal transduces angiotensin II in hepatic stellate cells and is critical in hepatic fibrosis. J. Clin. Invest. *112*, 1383–1394.

Bataller, R., Paik, Y.-H., Lindquist, J.N., Lemasters, J.J., and Brenner, D.A. (2004). Hepatitis C virus core and nonstructural proteins induce fibrogenic effects in hepatic stellate cells. Gastroenterology *126*, 529–540.

Becker, A.K., Tso, D.K., Harris, A.C., Malfair, D., and Chang, S.D. (2014). Extrahepatic metastases of hepatocellular carcinoma: A spectrum of imaging findings. Can. Assoc. Radiol. J. J. Assoc. Can. Radiol. *65*, 60–66.

Bedard, K., and Krause, K.-H. (2007). The NOX family of ROS-generating NADPH oxidases: physiology and pathophysiology. Physiol. Rev. *87*, 245–313.

Bertran, E., Caja, L., Navarro, E., Sancho, P., Mainez, J., Murillo, M.M., Vinyals, A., Fabra, A., and Fabregat, I. (2009). Role of CXCR4/SDF-1 alpha in the migratory phenotype of hepatoma cells that have undergone epithelial-mesenchymal transition in response to the transforming growth factor-beta. Cell. Signal. *21*, 1595–1606.

Bertran, E., Crosas-Molist, E., Sancho, P., Caja, L., Lopez-Luque, J., Navarro, E., Egea, G., Lastra, R., Serrano, T., Ramos, E., et al. (2013). Overactivation of the TGF-β pathway confers a mesenchymal-like phenotype and CXCR4-dependent migratory properties to liver tumor cells. Hepatology *58*, 2032–2044.

Binamé, F., Lassus, P., and Hibner, U. (2008). Transforming Growth Factor β Controls the Directional Migration of Hepatocyte Cohorts by Modulating Their Adhesion to Fibronectin. Mol. Biol. Cell *19*, 945–956.

Block, K., and Gorin, Y. (2012). Aiding and abetting roles of NOX oxidases in cellular transformation. Nat. Rev. Cancer *12*, 627–637.

Block, K., Eid, A., Griendling, K.K., Lee, D.-Y., Wittrant, Y., and Gorin, Y. (2008). Nox4 NAD(P)H oxidase mediates Src-dependent tyrosine phosphorylation of PDK-1 in response to angiotensin II: role in mesangial cell hypertrophy and fibronectin expression. J. Biol. Chem. *283*, 24061–24076.

Block, K., Gorin, Y., and Abboud, H.E. (2009). Subcellular localization of Nox4 and regulation in diabetes. Proc. Natl. Acad. Sci. U. S. A. *106*, 14385–14390.

Bondi, C.D., Manickam, N., Lee, D.Y., Block, K., Gorin, Y., Abboud, H.E., and Barnes, J.L. (2010). NAD(P)H Oxidase Mediates TGF-β1–Induced Activation of Kidney Myofibroblasts. J. Am. Soc. Nephrol. *21*, 93–102.

Bonner, M.Y., and Arbiser, J.L. (2012). Targeting NADPH oxidases for the treatment of cancer and inflammation. Cell. Mol. Life Sci. CMLS *69*, 2435–2442.

## VIII. REFERENCES


Boudreau, H.E., Emerson, S.U., Korzeniowska, A., Jendrysik, M.A., and Leto, T.L. (2009). Hepatitis C virus (HCV) proteins induce NADPH oxidase 4 expression in a transforming growth factor beta-dependent manner: a new contributor to HCV-induced oxidative stress. J. Virol. *83*, 12934–12946.

Boudreau, H.E., Casterline, B.W., Rada, B., Korzeniowska, A., and Leto, T.L. (2012). Nox4 involvement in TGF-beta and SMAD3-driven induction of the epithelial-to-mesenchymal transition and migration of breast epithelial cells. Free Radic. Biol. Med. *53*, 1489–1499.

Brandes, R.P. (2003). Role of NADPH oxidases in the control of vascular gene expression. Antioxid. Redox Signal. *5*, 803–811.

Brandes, R.P., and Schröder, K. (2008). Composition and functions of vascular nicotinamide adenine dinucleotide phosphate oxidases. Trends Cardiovasc. Med. *18*, 15–19.

Brandes, R.P., Weissmann, N., and Schröder, K. (2014a). Nox family NADPH oxidases: Molecular mechanisms of activation. Free Radic. Biol. Med.

Brandes, R.P., Weissmann, N., and Schroder, K. (2014b). Redox-mediated signal transduction by cardiovascular Nox NADPH oxidases. J. Mol. Cell. Cardiol. *73*, 70–79.

Brenner, D.A. (2009). Molecular pathogenesis of liver fibrosis. Trans. Am. Clin. Climatol. Assoc. *120*, 361–368.

Brenner, C., Galluzzi, L., Kepp, O., and Kroemer, G. (2013). Decoding cell death signals in liver inflammation. J. Hepatol. *59*, 583–594.

Brown, D.I., and Griendling, K.K. (2009). Nox proteins in signal transduction. Free Radic. Biol. Med. *47*, 1239–1253.

Bruix, J., Gores, G.J., and Mazzaferro, V. (2014). Hepatocellular carcinoma: clinical frontiers and perspectives. Gut *63*, 844–855.

Budhu, A.S., Zipser, B., Forgues, M., Ye, Q.-H., Sun, Z., and Wang, X.W. (2005). The molecular signature of metastases of human hepatocellular carcinoma. Oncology *69 Suppl 1*, 23–27.

Burch, P.M., and Heintz, N.H. (2005). Redox Regulation of Cell-Cycle Re-entry: Cyclin D1 as a Primary Target for the Mitogenic Effects of Reactive Oxygen and Nitrogen Species. Antioxid. Redox Signal. *7*, 741–751.

Caja, L., Ortiz, C., Bertran, E., Murillo, M.M., Miró-Obradors, M.J., Palacios, E., and Fabregat, I. (2007). Differential intracellular signalling induced by TGF-beta in rat adult hepatocytes and hepatoma cells: implications in liver carcinogenesis. Cell. Signal. *19*, 683–694.

Caja, L., Sancho, P., Bertran, E., Iglesias-Serret, D., Gil, J., and Fabregat, I. (2009). Overactivation of the MEK/ERK Pathway in Liver Tumor Cells Confers Resistance to TGF-β–Induced Cell Death through Impairing Up-regulation of the NADPH Oxidase NOX4. Cancer Res. *69*, 7595–7602.

Caja, L., Sancho, P., Bertran, E., and Fabregat, I. (2011a). Dissecting the effect of targeting the epidermal growth factor receptor on TGF-β-induced-apoptosis in human hepatocellular carcinoma cells. J. Hepatol. *55*, 351–358.

Caja, L., Bertran, E., Campbell, J., Fausto, N., and Fabregat, I. (2011b). The transforming growth factor-beta (TGF-β) mediates acquisition of a mesenchymal stem cell-like phenotype in human liver cells. J. Cell. Physiol. *226*, 1214–1223.

## VIII. REFERENCES


Calvisi, D.F., Conner, E.A., Ladu, S., Lemmer, E.R., Factor, V.M., and Thorgeirsson, S.S. (2005). Activation of the canonical Wnt/beta-catenin pathway confers growth advantages in c-Myc/E2F1 transgenic mouse model of liver cancer. J. Hepatol. *42*, 842–849.

Canel, M., Serrels, A., Frame, M.C., and Brunton, V.G. (2013). E-cadherin–integrin crosstalk in cancer invasion and metastasis. J. Cell Sci. *126*, 393–401.

Capece, D., Fischietti, M., Verzella, D., Gaggiano, A., Cicciarelli, G., Tessitore, A., Zazzeroni, F., and Alesse, E. (2013). The Inflammatory Microenvironment in Hepatocellular Carcinoma: A Pivotal Role for Tumor-Associated Macrophages. BioMed Res. Int. *2013*.

Carmona-Cuenca, I., Herrera, B., Ventura, J.-J., Roncero, C., Fernández, M., and Fabregat, I. (2006). EGF blocks NADPH oxidase activation by TGF-beta in fetal rat hepatocytes, impairing oxidative stress, and cell death. J. Cell. Physiol. *207*, 322–330.

Carmona-Cuenca, I., Roncero, C., Sancho, P., Caja, L., Fausto, N., Fernández, M., and Fabregat, I. (2008). Upregulation of the NADPH oxidase NOX4 by TGF-beta in hepatocytes is required for its pro-apoptotic activity. J. Hepatol. *49*, 965–976.

Carnesecchi, S., Deffert, C., Donati, Y., Basset, O., Hinz, B., Preynat-Seauve, O., Guichard, C., Arbiser, J.L., Banfi, B., Pache, J.-C., et al. (2011). A Key Role for NOX4 in Epithelial Cell Death During Development of Lung Fibrosis. Antioxid. Redox Signal. *15*, 607–619.

Carr, B.I., Hayashi, I., Branum, E.L., and Moses, H.L. (1986). Inhibition of DNA synthesis in rat hepatocytes by platelet-derived type beta transforming growth factor. Cancer Res. *46*, 2330–2334.

Del Castillo, G., Murillo, M.M., Alvarez-Barrientos, A., Bertran, E., Fernández, M., Sánchez, A., and Fabregat, I. (2006). Autocrine production of TGF-beta confers resistance to apoptosis after an epithelial-mesenchymal transition process in hepatocytes: Role of EGF receptor ligands. Exp. Cell Res. *312*, 2860–2871.

Chan, E.C., Peshavariya, H.M., Liu, G.-S., Jiang, F., Lim, S.-Y., and Dusting, G.J. (2013). Nox4 modulates collagen production stimulated by transforming growth factor β1 in vivo and in vitro. Biochem. Biophys. Res. Commun. *430*, 918–925.

Che, Y., Ye, F., Xu, R., Qing, H., Wang, X., Yin, F., Cui, M., Burstein, D., Jiang, B., and Zhang, D.Y. (2012). Co-expression of XIAP and cyclin D1 complex correlates with a poor prognosis in patients with hepatocellular carcinoma. Am. J. Pathol. *180*, 1798–1807.

Chiarugi, P., Pani, G., Giannoni, E., Taddei, L., Colavitti, R., Raugei, G., Symons, M., Borrello, S., Galeotti, T., and Ramponi, G. (2003). Reactive oxygen species as essential mediators of cell adhesion: the oxidative inhibition of a FAK tyrosine phosphatase is required for cell adhesion. J. Cell Biol. *161*, 933–944.

Choi, J., Corder, N.L.B., Koduru, B., and Wang, Y. (2014). Oxidative stress and hepatic Nox proteins in chronic hepatitis C and hepatocellular carcinoma. Free Radic. Biol. Med. *72*, 267–284.

Clempus, R.E., Sorescu, D., Dikalova, A.E., Pounkova, L., Jo, P., Sorescu, G.P., Schmidt, H.H.H., Lassègue, B., and Griendling, K.K. (2007). Nox4 is required for maintenance of the differentiated vascular smooth muscle cell phenotype. Arterioscler. Thromb. Vasc. Biol. *27*, 42–48.

Costa, R.H., Kalinichenko, V.V., Holterman, A.-X.L., and Wang, X. (2003). Transcription

factors in liver development, differentiation, and regeneration. Hepatol. Baltim. Md *38*, 1331–1347.

Coulouarn, C., Factor, V.M., and Thorgeirsson, S.S. (2008). Transforming Growth Factor-beta Gene Expression Signature in Mouse Hepatocytes Predicts Clinical Outcome in Human Cancer. Hepatol. Baltim. Md *47*, 2059–2067.

Cucoranu, I., Clempus, R., Dikalova, A., Phelan, P.J., Ariyan, S., Dikalov, S., and Sorescu, D. (2005). NAD(P)H Oxidase 4 Mediates Transforming Growth Factor-β1–Induced Differentiation of Cardiac Fibroblasts Into Myofibroblasts. Circ. Res. *97*, 900–907.

Cui, W., Matsuno, K., Iwata, K., Ibi, M., Matsumoto, M., Zhang, J., Zhu, K., Katsuyama, M., Torok, N.J., and Yabe-Nishimura, C. (2011). NOX1/nicotinamide adenine dinucleotide phosphate, reduced form (NADPH) oxidase promotes proliferation of stellate cells and aggravates liver fibrosis induced by bile duct ligation. Hepatology *54*, 949–958.

Czaja, A.J. (2014). Hepatic inflammation and progressive liver fibrosis in chronic liver disease. World J. Gastroenterol. WJG *20*, 2515–2532.

Dapito, D.H., Mencin, A., Gwak, G.-Y., Pradere, J.-P., Jang, M.-K., Mederacke, I., Caviglia, J.M., Khiabanian, H., Adeyemi, A., Bataller, R., et al. (2012). Promotion of hepatocellular carcinoma by the intestinal microbiota and TLR4. Cancer Cell *21*, 504–516.

Das, R., Xu, S., Quan, X., Nguyen, T.T., Kong, I.D., Chung, C.H., Lee, E.Y., Cha, S.-K., and Park, K.-S. (2014). Upregulation of mitochondrial Nox4 mediates TGF-β-induced apoptosis in cultured mouse podocytes. Am. J. Physiol. Renal Physiol. *306*, F155–F167.

Datla, S.R., Peshavariya, H., Dusting, G.J., Mahadev, K., Goldstein, B.J., and Jiang, F. (2007). Important role of Nox4 type NADPH oxidase in angiogenic responses in human microvascular endothelial cells in vitro. Arterioscler. Thromb. Vasc. Biol. *27*, 2319–2324.

Datla, S.R., McGrail, D.J., Vukelic, S., Huff, L.P., Lyle, A.N., Pounkova, L., Lee, M., Seidel-Rogol, B., Khalil, M.K., Hilenski, L.L., et al. (2014). Poldip2 controls vascular smooth muscle cell migration by regulating focal adhesion turnover and force polarization. Am. J. Physiol. Heart Circ. Physiol. *307*, H945–H957.

DeLeo, F.R., Renee, J., McCormick, S., Nakamura, M., Apicella, M., Weiss, J.P., and Nauseef, W.M. (1998). Neutrophils exposed to bacterial lipopolysaccharide upregulate NADPH oxidase assembly. J. Clin. Invest. *101*, 455–463.

Desai, L.P., Zhou, Y., Estrada, A.V., Ding, Q., Cheng, G., Collawn, J.F., and Thannickal, V.J. (2014). Negative regulation of NADPH oxidase 4 by hydrogen peroxide-inducible clone 5 (Hic-5) protein. J. Biol. Chem. *289*, 18270–18278.

Diebold, I., Petry, A., Burger, M., Hess, J., and Görlach, A. (2011). NOX4 mediates activation of FoxO3a and matrix metalloproteinase-2 expression by urotensin-II. Mol. Biol. Cell *22*, 4424–4434.

Dikalov, S.I., Dikalova, A.E., Bikineyeva, A.T., Schmidt, H.H.H.W., Harrison, D.G., and Griendling, K.K. (2008). Distinct roles of Nox1 and Nox4 in basal and angiotensin II-stimulated superoxide and hydrogen peroxide production. Free Radic. Biol. Med. *45*, 1340–1351.

Dionisio, N., Garcia-Mediavilla, M.V., Sanchez-Campos, S., Majano, P.L., Benedicto, I., Rosado, J.A., Salido, G.M., and Gonzalez-Gallego, J. (2009). Hepatitis C virus NS5A and core proteins induce oxidative stress-mediated calcium signalling alterations in hepatocytes. J. Hepatol. *50*, 872–882.

## VIII. REFERENCES


Djordjevic, T., BelAiba, R.S., Bonello, S., Pfeilschifter, J., Hess, J., and Görlach, A. (2005). Human urotensin II is a novel activator of NADPH oxidase in human pulmonary artery smooth muscle cells. Arterioscler. Thromb. Vasc. Biol. *25*, 519–525.

Dooley, S., and ten Dijke, P. (2012). TGF-β in progression of liver disease. Cell Tissue Res. *347*, 245–256.

Dooley, S., Delvoux, B., Lahme, B., Mangasser-Stephan, K., and Gressner, A.M. (2000). Modulation of transforming growth factor beta response and signaling during transdifferentiation of rat hepatic stellate cells to myofibroblasts. Hepatol. Baltim. Md *31*, 1094–1106.

Dooley, S., Weng, H., and Mertens, P.R. (2009). Hypotheses on the role of transforming growth factor-beta in the onset and progression of hepatocellular carcinoma. Dig. Dis. Basel Switz. *27*, 93–101.

Drabsch, Y., and ten Dijke, P. (2012). TGF-β signalling and its role in cancer progression and metastasis. Cancer Metastasis Rev. *31*, 553–568.

Drazic, A., and Winter, J. (2014). The physiological role of reversible methionine oxidation. Biochim. Biophys. Acta *1844*, 1367–1382.

Drysdale, B.E., Zacharchuk, C.M., and Shin, H.S. (1983). Mechanism of macrophage-mediated cytotoxicity: production of a soluble cytotoxic factor. J. Immunol. Baltim. Md 1950 *131*, 2362–2367.

Del Duca, D., Werbowetski, T., and Del Maestro, R.F. (2004). Spheroid preparation from hanging drops: characterization of a model of brain tumor invasion. J. Neurooncol. *67*, 295–303.

Dunning, S., Ur Rehman, A., Tiebosch, M.H., Hannivoort, R.A., Haijer, F.W., Woudenberg, J., van den Heuvel, F.A.J., Buist-Homan, M., Faber, K.N., and Moshage, H. (2013). Glutathione and antioxidant enzymes serve complementary roles in protecting activated hepatic stellate cells against hydrogen peroxide-induced cell death. Biochim. Biophys. Acta *1832*, 2027–2034.

Edderkaoui, M., Nitsche, C., Zheng, L., Pandol, S.J., Gukovsky, I., and Gukovskaya, A.S. (2011). NADPH oxidase activation in pancreatic cancer cells is mediated through Akt-dependent up-regulation of p22phox. J. Biol. Chem. *286*, 7779–7787.

Elchuri, S., Oberley, T.D., Qi, W., Eisenstein, R.S., Jackson Roberts, L., Van Remmen, H., Epstein, C.J., and Huang, T.-T. (2005). CuZnSOD deficiency leads to persistent and widespread oxidative damage and hepatocarcinogenesis later in life. Oncogene *24*, 367–380.

Ellmark, S.H.M., Dusting, G.J., Fui, M.N.T., Guzzo-Pernell, N., and Drummond, G.R. (2005). The contribution of Nox4 to NADPH oxidase activity in mouse vascular smooth muscle. Cardiovasc. Res. *65*, 495–504.

Etoh, T., Inoguchi, T., Kakimoto, M., Sonoda, N., Kobayashi, K., Kuroda, J., Sumimoto, H., and Nawata, H. (2003). Increased expression of NAD(P)H oxidase subunits, NOX4 and p22phox, in the kidney of streptozotocin-induced diabetic rats and its reversibity by interventive insulin treatment. Diabetologia *46*, 1428–1437.

European Association For The Study Of The Liver, and European Organisation For Research And Treatment Of Cancer (2012). EASL-EORTC clinical practice guidelines: management of hepatocellular carcinoma. J. Hepatol. *56*, 908–943.

Fabregat, I., Fernando, J., Mainez, J., and Sancho, P. (2014). TGF-beta signaling in cancer treatment. Curr. Pharm. Des. *20*, 2934–2947.

## VIII. REFERENCES


Fagotto, F. (2013). Looking beyond the Wnt pathway for the deep nature of β-catenin. EMBO Rep. *14*, 422–433.

Fausto, N. (2004). Liver regeneration and repair: Hepatocytes, progenitor cells, and stem cells. Hepatology *39*, 1477–1487.

Fausto, N., and Campbell, J.S. (2003). The role of hepatocytes and oval cells in liver regeneration and repopulation. Mech. Dev. *120*, 117–130.

Fausto, N., and Campbell, J.S. (2010). Mouse models of hepatocellular carcinoma. Semin. Liver Dis. *30*, 87–98.

Fausto, N., Campbell, J.S., and Riehle, K.J. (2006). Liver regeneration. Hepatol. Baltim. Md *43*, S45–S53.

Fernando, J., Malfettone, A., Cepeda, E.B., Vilarrasa-Blasi, R., Bertran, E., Raimondi, G., Fabra, A., Alvarez-Barrientos, A., Fernández-Salguero, P., Fernández-Rodríguez, C.M., et al. (2014). A mesenchymal-like phenotype and expression of CD44 predict lack of apoptotic response to sorafenib in liver tumor cells. Int. J. Cancer J. Int. Cancer.

Fickert, P., Fuchsbichler, A., Wagner, M., Zollner, G., Kaser, A., Tilg, H., Krause, R., Lammert, F., Langner, C., Zatloukal, K., et al. (2004). Regurgitation of bile acids from leaky bile ducts causes sclerosing cholangitis in Mdr2 (Abcb4) knockout mice. Gastroenterology *127*, 261–274.

Finkel, T. (2011). Signal transduction by reactive oxygen species. J. Cell Biol. *194*, 7–15.

Flores, A., and Marrero, J.A. (2014). Emerging trends in hepatocellular carcinoma: focus on diagnosis and therapeutics. Clin. Med. Insights Oncol. *8*, 71–76.

Foo, N.-P., Lin, S.-H., Lee, Y.-H., Wu, M.-J., and Wang, Y.-J. (2011). α-Lipoic acid inhibits liver fibrosis through the attenuation of ROS-triggered signaling in hepatic stellate cells activated by PDGF and TGF-β. Toxicology *282*, 39–46.

Forner, A., Llovet, J.M., and Bruix, J. (2012). Hepatocellular carcinoma. The Lancet *379*, 1245–1255.

Franco, D.L., Mainez, J., Vega, S., Sancho, P., Murillo, M.M., de Frutos, C.A., Del Castillo, G., López-Blau, C., Fabregat, I., and Nieto, M.A. (2010). Snail1 suppresses TGF-beta-induced apoptosis and is sufficient to trigger EMT in hepatocytes. J. Cell Sci. *123*, 3467–3477.

Franklin, C.C., Rosenfeld-Franklin, M.E., White, C., Kavanagh, T.J., and Fausto, N. (2003). TGFbeta1-induced suppression of glutathione antioxidant defenses in hepatocytes: caspase-dependent post-translational and caspase-independent transcriptional regulatory mechanisms. FASEB J. Off. Publ. Fed. Am. Soc. Exp. Biol. *17*, 1535–1537.

Fransvea, E., Angelotti, U., Antonaci, S., and Giannelli, G. (2008). Blocking transforming growth factor-beta up-regulates E-cadherin and reduces migration and invasion of hepatocellular carcinoma cells. Hepatol. Baltim. Md *47*, 1557–1566.

Frazziano, G., Al Ghouleh, I., Baust, J., Shiva, S., Champion, H.C., and Pagano, P.J. (2014). Nox-derived ROS are acutely activated in pressure overload pulmonary hypertension: indications for a seminal role for mitochondrial Nox4. Am. J. Physiol. Heart Circ. Physiol. *306*, H197–H205.

Friedl, P., and Alexander, S. (2011). Cancer invasion and the microenvironment: plasticity and reciprocity. Cell *147*, 992–1009.

## VIII. REFERENCES


Friedl, P., and Wolf, K. (2003). Tumour-cell invasion and migration: diversity and escape mechanisms. Nat. Rev. Cancer *3*, 362–374.

Fukuyama, M., Rokutan, K., Sano, T., Miyake, H., Shimada, M., and Tashiro, S. (2005). Overexpression of a novel superoxide-producing enzyme, NADPH oxidase 1, in adenoma and well differentiated adenocarcinoma of the human colon. Cancer Lett. *221*, 97–104.

Gardel, M.L., Schneider, I.C., Aratyn-Schaus, Y., and Waterman, C.M. (2010). Mechanical integration of actin and adhesion dynamics in cell migration. Annu. Rev. Cell Dev. Biol. *26*, 315–333.

Gedaly, R., Angulo, P., Hundley, J., Daily, M.F., Chen, C., and Evers, B.M. (2012). PKI-587 and Sorafenib Targeting PI3K/AKT/mTOR and Ras/Raf/MAPK Pathways Synergistically Inhibit HCC Cell Proliferation. J. Surg. Res. *176*, 542–548.

Geiszt, M., Kopp, J.B., Várnai, P., and Leto, T.L. (2000). Identification of renox, an NAD(P)H oxidase in kidney. Proc. Natl. Acad. Sci. U. S. A. *97*, 8010–8014.

Giannelli, G., Mazzocca, A., Fransvea, E., Lahn, M., and Antonaci, S. (2011). Inhibiting TGF-β signaling in hepatocellular carcinoma. Biochim. Biophys. Acta *1815*, 214–223.

Giannelli, G., Villa, E., and Lahn, M. (2014). Transforming growth factor-β as a therapeutic target in hepatocellular carcinoma. Cancer Res. *74*, 1890–1894.

Gilgenkrantz, H., and Collin de l'Hortet, A. (2011). New insights into liver regeneration. Clin. Res. Hepatol. Gastroenterol. *35*, 623–629.

Glasauer, A., and Chandel, N.S. (2014). Targeting antioxidants for cancer therapy. Biochem. Pharmacol.

Gonzalez-Rodriguez, A., Clampit, J.E., Escribano, O., Benito, M., Rondinone, C.M., and Valverde, A.M. (2007). Developmental switch from prolonged insulin action to increased insulin sensitivity in protein tyrosine phosphatase 1B-deficient hepatocytes. Endocrinology *148*, 594–608.

Gorin, Y., and Block, K. (2013). Nox4 and diabetic nephropathy: With a friend like this, who needs enemies? Free Radic. Biol. Med. *61C*, 130–142.

Gorin, Y., Ricono, J.M., Kim, N.-H., Bhandari, B., Choudhury, G.G., and Abboud, H.E. (2003). Nox4 mediates angiotensin II-induced activation of Akt/protein kinase B in mesangial cells. Am. J. Physiol. Renal Physiol. *285*, F219–F229.

Goyal, P., Weissmann, N., Rose, F., Grimminger, F., Schäfers, H.J., Seeger, W., and Hänze, J. (2005). Identification of novel Nox4 splice variants with impact on ROS levels in A549 cells. Biochem. Biophys. Res. Commun. *329*, 32–39.

Grise, F., Bidaud, A., and Moreau, V. (2009). Rho GTPases in hepatocellular carcinoma. Biochim. Biophys. Acta *1795*, 137–151.

Guichard, C., Moreau, R., Pessayre, D., Epperson, T.K., and Krause, K.-H. (2008). NOX family NADPH oxidases in liver and in pancreatic islets: a role in the metabolic syndrome and diabetes? Biochem. Soc. Trans. *36*, 920–929.

Hanahan, D., and Weinberg, R.A. (2000). The hallmarks of cancer. Cell *100*, 57–70.

Hanahan, D., and Weinberg, R.A. (2011). Hallmarks of cancer: the next generation. Cell *144*, 646–674.

Hayashi, H., and Sakai, T. (2011). Animal models for the study of liver fibrosis: new insights from knockout mouse models. Am. J. Physiol. Gastrointest. Liver Physiol. *300*, G729–G738.

Hecker, L., Vittal, R., Jones, T., Jagirdar, R., Luckhardt, T.R., Horowitz, J.C., Pennathur, S., Martinez, F.J., and Thannickal, V.J. (2009). NADPH Oxidase-4 Mediates Myofibroblast Activation and Fibrogenic Responses to Lung Injury. Nat. Med. *15*, 1077–1081.

Hecker, L., Cheng, J., and Thannickal, V.J. (2012). Targeting NOX enzymes in pulmonary fibrosis. Cell. Mol. Life Sci. CMLS *69*, 2365–2371.

Hecker, L., Logsdon, N.J., Kurundkar, D., Kurundkar, A., Bernard, K., Hock, T., Meldrum, E., Sanders, Y.Y., and Thannickal, V.J. (2014). Reversal of persistent fibrosis in aging by targeting Nox4-Nrf2 redox imbalance. Sci. Transl. Med. *6*, 231ra47.

Heindryckx, F., Colle, I., and Van Vlierberghe, H. (2009). Experimental mouse models for hepatocellular carcinoma research. Int. J. Exp. Pathol. *90*, 367–386.

Heldin, C.-H., Vanlandewijck, M., and Moustakas, A. (2012). Regulation of EMT by TGFβ in cancer. FEBS Lett. *586*, 1959–1970.

Helmcke, I., Heumüller, S., Tikkanen, R., Schröder, K., and Brandes, R.P. (2009). Identification of structural elements in Nox1 and Nox4 controlling localization and activity. Antioxid. Redox Signal. *11*, 1279–1287.

Hernandes, M.S., and Britto, L.R.G. (2012). NADPH oxidase and neurodegeneration. Curr. Neuropharmacol. *10*, 321–327.

Hernandez-Gea, V., Toffanin, S., Friedman, S.L., and Llovet, J.M. (2013). Role of the Microenvironment in the Pathogenesis and Treatment of Hepatocellular Carcinoma. Gastroenterology *144*, 512–527.

Herrera, B., Alvarez, A.M., Sánchez, A., Fernández, M., Roncero, C., Benito, M., and Fabregat, I. (2001a). Reactive oxygen species (ROS) mediates the mitochondrial-dependent apoptosis induced by transforming growth factor (beta) in fetal hepatocytes. FASEB J. Off. Publ. Fed. Am. Soc. Exp. Biol. *15*, 741–751.

Herrera, B., Fernández, M., Alvarez, A.M., Roncero, C., Benito, M., Gil, J., and Fabregat, I. (2001b). Activation of caspases occurs downstream from radical oxygen species production, Bcl-xL down-regulation, and early cytochrome C release in apoptosis induced by transforming growth factor beta in rat fetal hepatocytes. Hepatol. Baltim. Md *34*, 548–556.

Herrera, B., Murillo, M.M., Alvarez-Barrientos, A., Beltrán, J., Fernández, M., and Fabregat, I. (2004). Source of early reactive oxygen species in the apoptosis induced by transforming growth factor-beta in fetal rat hepatocytes. Free Radic. Biol. Med. *36*, 16–26.

Hilenski, L.L., Clempus, R.E., Quinn, M.T., Lambeth, J.D., and Griendling, K.K. (2004). Distinct subcellular localizations of Nox1 and Nox4 in vascular smooth muscle cells. Arterioscler. Thromb. Vasc. Biol. *24*, 677–683.

Hiraga, R., Kato, M., Miyagawa, S., and Kamata, T. (2013). Nox4-derived ROS signaling contributes to TGF-β-induced epithelial-mesenchymal transition in pancreatic cancer cells. Anticancer Res. *33*, 4431–4438.

Hoidal, J.R., Brar, S.S., Sturrock, A.B., Sanders, K.A., Dinger, B., Fidone, S., and Kennedy, T.P. (2003). The role of endogenous NADPH oxidases in airway and pulmonary vascular smooth muscle function. Antioxid. Redox Signal. *5*, 751–758.

Holmström, K.M., and Finkel, T. (2014). Cellular mechanisms and physiological consequences of redox-dependent signalling. Nat. Rev. Mol. Cell Biol. *15*, 411–421.

Hsieh, C.-H., Shyu, W.-C., Chiang, C.-Y., Kuo, J.-W., Shen, W.-C., and Liu, R.-S. (2011). NADPH oxidase subunit 4-mediated reactive oxygen species contribute to cycling hypoxia-promoted tumor progression in glioblastoma multiforme. PloS One *6*, e23945.

Hu, T., Ramachandrarao, S.P., Siva, S., Valancius, C., Zhu, Y., Mahadev, K., Toh, I., Goldstein, B.J., Woolkalis, M., and Sharma, K. (2005). Reactive oxygen species production via NADPH oxidase mediates TGF-beta-induced cytoskeletal alterations in endothelial cells. Am. J. Physiol. Renal Physiol. *289*, F816–F825.

Huang, D., Du, X., Yuan, R., Chen, L., Liu, T., Wen, C., Huang, M., Li, M., Hao, L., and Shao, J. (2014). Rock2 promotes the invasion and metastasis of hepatocellular carcinoma by modifying MMP2 ubiquitination and degradation. Biochem. Biophys. Res. Commun.

Hubackova, S., Krejcikova, K., Bartek, J., and Hodny, Z. (2012). IL1- and TGFβ-Nox4 signaling, oxidative stress and DNA damage response are shared features of replicative, oncogene-induced, and drug-induced paracrine “bystander senescence.” Aging *4*, 932–951.

Hurd, T.R., DeGennaro, M., and Lehmann, R. (2012). Redox regulation of cell migration and adhesion. Trends Cell Biol. *22*, 107–115.

Ikushima, H., and Miyazono, K. (2010). TGFβ signalling: a complex web in cancer progression. Nat. Rev. Cancer *10*, 415–424.

Ilina, O., and Friedl, P. (2009). Mechanisms of collective cell migration at a glance. J. Cell Sci. *122*, 3203–3208.

Inagaki, Y., Kushida, M., Higashi, K., Itoh, J., Higashiyama, R., Hong, Y.Y., Kawada, N., Namikawa, K., Kiyama, H., Bou-Gharios, G., et al. (2005). Cell type-specific intervention of transforming growth factor beta/Smad signaling suppresses collagen gene expression and hepatic fibrosis in mice. Gastroenterology *129*, 259–268.

Iwaisako, K., Jiang, C., Zhang, M., Cong, M., Moore-Morris, T.J., Park, T.J., Liu, X., Xu, J., Wang, P., Paik, Y.-H., et al. (2014). Origin of myofibroblasts in the fibrotic liver in mice. Proc. Natl. Acad. Sci. U. S. A. *111*, E3297–E3305.

Iwakiri, Y., Shah, V., and Rockey, D.C. (2014). Vascular pathobiology in chronic liver disease and cirrhosis – Current status and future directions. J. Hepatol. *0*.

Jarman, E.R., Khambata, V.S., Cope, C., Jones, P., Roger, J., Ye, L.Y., Duggan, N., Head, D., Pearce, A., Press, N.J., et al. (2014). An inhibitor of NADPH oxidase-4 attenuates established pulmonary fibrosis in a rodent disease model. Am. J. Respir. Cell Mol. Biol. *50*, 158–169.

Jha, J.C., Gray, S.P., Barit, D., Okabe, J., El-Osta, A., Namikoshi, T., Thallas-Bonke, V., Wingler, K., Szyndralewiez, C., Heitz, F., et al. (2014). Genetic targeting or pharmacologic inhibition of NADPH oxidase nox4 provides renoprotection in long-term diabetic nephropathy. J. Am. Soc. Nephrol. JASN *25*, 1237–1254.

Jiang, J.X., Venugopal, S., Serizawa, N., Chen, X., Scott, F., Li, Y., Adamson, R., Devaraj, S., Shah, V., Gershwin, M.E., et al. (2010). NOX2 plays a key role in stellate cell activation and liver fibrogenesis in vivo. Gastroenterology *139*, 1375–1384.e4.

Jiang, J.X., Chen, X., Serizawa, N., Szyndralewiez, C., Page, P., Schroder, K., Brandes, R.P., Devaraj, S., and Torok, N.J. (2012). Liver fibrosis and hepatocyte apoptosis are

attenuated by GKT137831 a novel NOX4/NOX1 inhibitor in vivo. Free Radic. Biol. Med. *53*, 289–296.

Jobling, M.F., Mott, J.D., Finnegan, M.T., Jurukovski, V., Erickson, A.C., Walian, P.J., Taylor, S.E., Ledbetter, S., Lawrence, C.M., Rifkin, D.B., et al. (2006). Isoform-specific activation of latent transforming growth factor beta (LTGF-beta) by reactive oxygen species. Radiat. Res. *166*, 839–848.

Kalluri, R., and Weinberg, R.A. (2009). The basics of epithelial-mesenchymal transition. J. Clin. Invest. *119*, 1420–1428.

Kalyanaraman, B. (2013). Teaching the basics of redox biology to medical and graduate students: Oxidants, antioxidants and disease mechanisms. Redox Biol. *1*, 244–257.

Kanda, Y., Hinata, T., Kang, S.W., and Watanabe, Y. (2011). Reactive oxygen species mediate adipocyte differentiation in mesenchymal stem cells. Life Sci. *89*, 250–258.

Katsuno, Y., Lamouille, S., and Derynck, R. (2013). TGF-β signaling and epithelial-mesenchymal transition in cancer progression. Curr. Opin. Oncol. *25*, 76–84.

Kim, E.Y., Anderson, M., and Dryer, S.E. (2012). Insulin increases surface expression of TRPC6 channels in podocytes: role of NADPH oxidases and reactive oxygen species. Am. J. Physiol. Renal Physiol. *302*, F298–F307.

Kim, G.-Y., Mercer, S.E., Ewton, D.Z., Yan, Z., Jin, K., and Friedman, E. (2002). The stress-activated protein kinases p38 alpha and JNK1 stabilize p21(Cip1) by phosphorylation. J. Biol. Chem. *277*, 29792–29802.

Kim, J.-S., Yeo, S., Shin, D.-G., Bae, Y.-S., Lee, J.-J., Chin, B.-R., Lee, C.-H., and Baek, S.-H. (2010a). Glycogen synthase kinase 3beta and beta-catenin pathway is involved in toll-like receptor 4-mediated NADPH oxidase 1 expression in macrophages. FEBS J. *277*, 2830–2837.

Kim, K.S., Choi, H.W., Yoon, H.E., and Kim, I.Y. (2010b). Reactive oxygen species generated by NADPH oxidase 2 and 4 are required for chondrogenic differentiation. J. Biol. Chem. *285*, 40294–40302.

Kitamura, K., Nakamoto, Y., Akiyama, M., Fujii, C., Kondo, T., Kobayashi, K., Kaneko, S., and Mukaida, N. (2002). Pathogenic roles of tumor necrosis factor receptor p55-mediated signals in dimethylnitrosamine-induced murine liver fibrosis. Lab. Investig. J. Tech. Methods Pathol. *82*, 571–583.

Kleinschnitz, C., Grund, H., Wingler, K., Armitage, M.E., Jones, E., Mittal, M., Barit, D., Schwarz, T., Geis, C., Kraft, P., et al. (2010). Post-stroke inhibition of induced NADPH oxidase type 4 prevents oxidative stress and neurodegeneration. PLoS Biol. *8*.

Kodama, R., Kato, M., Furuta, S., Ueno, S., Zhang, Y., Matsuno, K., Yabe-Nishimura, C., Tanaka, E., and Kamata, T. (2013). ROS-generating oxidases Nox1 and Nox4 contribute to oncogenic Ras-induced premature senescence. Genes Cells Devoted Mol. Cell. Mech. *18*, 32–41.

Kung, J.W.C., Currie, I.S., Forbes, S.J., and Ross, J.A. (2010). Liver Development, Regeneration, and Carcinogenesis. J. Biomed. Biotechnol. *2010*.

Kuroda, J., Ago, T., Matsushima, S., Zhai, P., Schneider, M.D., and Sadoshima, J. (2010). NADPH oxidase 4 (Nox4) is a major source of oxidative stress in the failing heart. Proc. Natl. Acad. Sci. U. S. A. *107*, 15565–15570.

## VIII. REFERENCES


Lambeth, J.D., and Neish, A.S. (2014). Nox Enzymes and New Thinking on Reactive Oxygen: A Double-Edged Sword Revisited. Annu. Rev. Pathol. Mech. Dis. *9*, 119–145.

Lambeth, J.D., Kawahara, T., and Diebold, B. (2007). Regulation of Nox and Duox enzymatic activity and expression. Free Radic. Biol. Med. *43*, 319–331.

Lämmermann, T., and Sixt, M. (2009). Mechanical modes of “amoeboid” cell migration. Curr. Opin. Cell Biol. *21*, 636–644.

Lamouille, S., Xu, J., and Derynck, R. (2014). Molecular mechanisms of epithelial-mesenchymal transition. Nat. Rev. Mol. Cell Biol. *15*, 178–196.

Lee, C.F., Ullevig, S., Kim, H.S., and Asmis, R. (2013a). Regulation of Monocyte Adhesion and Migration by Nox4. PloS One *8*, e66964.

Lee, J.H., Kim, J.H., Kim, J.S., Chang, J.W., Kim, S.B., Park, J.S., and Lee, S.K. (2013b). AMP-activated protein kinase inhibits TGF-β-, angiotensin II-, aldosterone-, high glucose-, and albumin-induced epithelial-mesenchymal transition. Am. J. Physiol. Renal Physiol. *304*, F686–F697.

Lee, J.K., Edderkaoui, M., Truong, P., Ohno, I., Jang, K.-T., Berti, A., Pandol, S.J., and Gukovskaya, A.S. (2007). NADPH oxidase promotes pancreatic cancer cell survival via inhibiting JAK2 dephosphorylation by tyrosine phosphatases. Gastroenterology *133*, 1637–1648.

Lee, S.R., Kwon, K.S., Kim, S.R., and Rhee, S.G. (1998). Reversible inactivation of protein-tyrosine phosphatase 1B in A431 cells stimulated with epidermal growth factor. J. Biol. Chem. *273*, 15366–15372.

Li, H., Liu, Q., Wang, N., and Xu, J. (2011). Correlation of different NADPH oxidase homologues with late endothelial progenitor cell senescence induced by angiotensin II: effect of telmisartan. Intern. Med. Tokyo Jpn. *50*, 1631–1642.

Li, S., Tabar, S.S., Malec, V., Eul, B.G., Klepetko, W., Weissmann, N., Grimminger, F., Seeger, W., Rose, F., and Hänze, J. (2008). NOX4 regulates ROS levels under normoxic and hypoxic conditions, triggers proliferation, and inhibits apoptosis in pulmonary artery adventitial fibroblasts. Antioxid. Redox Signal. *10*, 1687–1698.

Li, X.R., Ji, F., Ouyang, J., Wu, W., Qian, L.Y., and Yang, K.Y. (2006). Overexpression of RhoA is associated with poor prognosis in hepatocellular carcinoma. Eur. J. Surg. Oncol. J. Eur. Soc. Surg. Oncol. Br. Assoc. Surg. Oncol. *32*, 1130–1134.

Liu, H., Pan, Z., Li, A., Fu, S., Lei, Y., Sun, H., Wu, M., and Zhou, W. (2008). Roles of chemokine receptor 4 (CXCR4) and chemokine ligand 12 (CXCL12) in metastasis of hepatocellular carcinoma cells. Cell. Mol. Immunol. *5*, 373–378.

Llovet, J.M. (2014). Liver cancer: Time to evolve trial design after everolimus failure. Nat. Rev. Clin. Oncol.

Llovet, J.M., and Bruix, J. (2008). Molecular Targeted Therapies in Hepatocellular Carcinoma. Hepatol. Baltim. Md *48*, 1312–1327.

Von Löhneysen, K., Noack, D., Wood, M.R., Friedman, J.S., and Knaus, U.G. (2010). Structural insights into Nox4 and Nox2: motifs involved in function and cellular localization. Mol. Cell. Biol. *30*, 961–975.

Lu, J.P., Monardo, L., Bryskin, I., Hou, Z.F., Trachtenberg, J., Wilson, B.C., and Pinthus,

J.H. (2010). Androgens induce oxidative stress and radiation resistance in prostate cancer cells though NADPH oxidase. Prostate Cancer Prostatic Dis. *13*, 39–46.

Lyle, A.N., Deshpande, N.N., Taniyama, Y., Seidel-Rogol, B., Pounkova, L., Du, P., Papaharalambus, C., Lassegue, B., and Griendling, K.K. (2009). Poldip2, a novel regulator of Nox4 and cytoskeletal integrity in vascular smooth muscle cells. Circ. Res. *105*, 249–259.

Maalouf, R.M., Eid, A.A., Gorin, Y.C., Block, K., Escobar, G.P., Bailey, S., and Abboud, H.E. (2012). Nox4-derived reactive oxygen species mediate cardiomyocyte injury in early type 1 diabetes. Am. J. Physiol. Cell Physiol. *302*, C597–C604.

MacDonald, G.A., Bridle, K.R., Ward, P.J., Walker, N.I., Houglum, K., George, D.K., Smith, J.L., Powell, L.W., Crawford, D.H., and Ramm, G.A. (2001). Lipid peroxidation in hepatic steatosis in humans is associated with hepatic fibrosis and occurs predominately in acinar zone 3. J. Gastroenterol. Hepatol. *16*, 599–606.

Mair, M., Zollner, G., Schneller, D., Musteanu, M., Fickert, P., Gumhold, J., Schuster, C., Fuchsbichler, A., Bilban, M., Tauber, S., et al. (2010). Signal Transducer and Activator of Transcription 3 Protects From Liver Injury and Fibrosis in a Mouse Model of Sclerosing Cholangitis. Gastroenterology *138*, 2499–2508.

Malarkey, D.E., Johnson, K., Ryan, L., Boorman, G., and Maronpot, R.R. (2005). New Insights into Functional Aspects of Liver Morphology. Toxicol. Pathol. *33*, 27–34.

Malhi, H., and Gores, G.J. (2008). Cellular and Molecular Mechanisms of Liver Injury. Gastroenterology *134*, 1641–1654.

Mallat, A., and Lotersztajn, S. (2013). Cellular mechanisms of tissue fibrosis. 5. Novel insights into liver fibrosis. Am. J. Physiol. Cell Physiol. *305*, C789–C799.

Mani, S.A., Guo, W., Liao, M.-J., Eaton, E.N., Ayyanan, A., Zhou, A.Y., Brooks, M., Reinhard, F., Zhang, C.C., Shipitsin, M., et al. (2008). The epithelial-mesenchymal transition generates cells with properties of stem cells. Cell *133*, 704–715.

Manickam, N., Patel, M., Griendling, K.K., Gorin, Y., and Barnes, J.L. (2014). RhoA/Rho kinase mediates TGF-β1-induced kidney myofibroblast activation through Poldip2/Nox4-derived reactive oxygen species. Am. J. Physiol. Renal Physiol. *307*, F159–F171.

Mao, S.A., Glorioso, J.M., and Nyberg, S.L. (2014). Liver regeneration. Transl. Res. J. Lab. Clin. Med. *163*, 352–362.

Maraldi, T., Prata, C., Caliceti, C., Vieceli Dalla Sega, F., Zambonin, L., Fiorentini, D., and Hakim, G. (2010). VEGF-induced ROS generation from NAD(P)H oxidases protects human leukemic cells from apoptosis. Int. J. Oncol. *36*, 1581–1589.

Martínez-Palacián, A., del Castillo, G., Suárez-Causado, A., García-Álvaro, M., de Morena-Frutos, D., Fernández, M., Roncero, C., Fabregat, I., Herrera, B., and Sánchez, A. (2013). Mouse hepatic oval cells require Met-dependent PI3K to impair TGF-β-induced oxidative stress and apoptosis. PloS One *8*, e53108.

Martin-Garrido, A., Brown, D.I., Lyle, A.N., Dikalova, A., Seidel-Rogol, B., Lassègue, B., San Martín, A., and Griendling, K.K. (2011). NADPH oxidase 4 mediates TGF-β-induced smooth muscle α-actin via p38MAPK and serum response factor. Free Radic. Biol. Med. *50*, 354–362.

Martinon, F., Chen, X., Lee, A.-H., and Glimcher, L.H. (2010). TLR activation of the transcription factor XBP1 regulates innate immune responses in macrophages. Nat. Immunol.

*11*, 411–418.

Masamune, A., Watanabe, T., Kikuta, K., Satoh, K., and Shimosegawa, T. (2008). NADPH oxidase plays a crucial role in the activation of pancreatic stellate cells. Am. J. Physiol. Gastrointest. Liver Physiol. *294*, G99–G108.

Matsuzaki, K., Date, M., Furukawa, F., Tahashi, Y., Matsushita, M., Sugano, Y., Yamashiki, N., Nakagawa, T., Seki, T., Nishizawa, M., et al. (2000). Regulatory mechanisms for transforming growth factor beta as an autocrine inhibitor in human hepatocellular carcinoma: implications for roles of smads in its growth. Hepatol. Baltim. Md *32*, 218–227.

Menshikov, M., Plekhanova, O., Cai, H., Chalupsky, K., Parfyonova, Y., Bashtrikov, P., Tkachuk, V., and Berk, B.C. (2006). Urokinase plasminogen activator stimulates vascular smooth muscle cell proliferation via redox-dependent pathways. Arterioscler. Thromb. Vasc. Biol. *26*, 801–807.

Michalopoulos, G.K. (2007). Liver regeneration. J. Cell. Physiol. *213*, 286–300.

Michalopoulos, G.K. (2010). Liver Regeneration after Partial Hepatectomy. Am. J. Pathol. *176*, 2–13.

De Minicis, S., and Brenner, D.A. (2007). NOX in liver fibrosis. Arch. Biochem. Biophys. *462*, 266–272.

De Minicis, S., Seki, E., Paik, Y.-H., Österreicher, C.H., Kodama, Y., Kluwe, J., Torozzi, L., Miyai, K., Benedetti, A., Schwabe, R.F., et al. (2010). Role and cellular source of nicotinamide adenine dinucleotide phosphate oxidase in hepatic fibrosis. Hepatology *52*, 1420–1430.

Mitra, S.K., Hanson, D.A., and Schlaepfer, D.D. (2005). Focal adhesion kinase: in command and control of cell motility. Nat. Rev. Mol. Cell Biol. *6*, 56–68.

Ben Mkaddem, S., Pedruzzi, E., Werts, C., Coant, N., Bens, M., Cluzeaud, F., Goujon, J.M., Ogier-Denis, E., and Vandewalle, A. (2010). Heat shock protein gp96 and NAD(P)H oxidase 4 play key roles in Toll-like receptor 4-activated apoptosis during renal ischemia/reperfusion injury. Cell Death Differ. *17*, 1474–1485.

De Mochel, N.S.R., Seronello, S., Wang, S.H., Ito, C., Zheng, J.X., Liang, T.J., Lambeth, J.D., and Choi, J. (2010). Hepatocyte NAD(P)H oxidases as an endogenous source of reactive oxygen species during hepatitis C virus infection. Hepatol. Baltim. Md *52*, 47–59.

Moeini, A., Cornellà, H., and Villanueva, A. (2012). Emerging signaling pathways in hepatocellular carcinoma. Liver Cancer *1*, 83–93.

Mondol, A.S., Tonks, N.K., and Kamata, T. (2014). Nox4 redox regulation of PTP1B contributes to the proliferation and migration of glioblastoma cells by modulating tyrosine phosphorylation of coronin-1C. Free Radic. Biol. Med. *67*, 285–291.

Monga, S. (Paul) S. (2014). Role and Regulation of β-Catenin Signaling During Physiological Liver Growth. Gene Expr. *16*, 51–62.

Montezano, A.C., and Touyz, R.M. (2014). Reactive oxygen species, vascular Noxs, and hypertension: focus on translational and clinical research. Antioxid. Redox Signal. *20*, 164–182.

Montezano, A.C., Burger, D., Ceravolo, G.S., Yusuf, H., Montero, M., and Touyz, R.M. (2011). Novel Nox homologues in the vasculature: focusing on Nox4 and Nox5. Clin. Sci. Lond. Engl. 1979 *120*, 131–141.

Moreno-Càceres, J., Caja, L., Mainez, J., Mayoral, R., Martín-Sanz, P., Moreno-Vicente,

R., Del Pozo, M.Á., Dooley, S., Egea, G., and Fabregat, I. (2014). Caveolin-1 is required for TGF-β-induced transactivation of the EGF receptor pathway in hepatocytes through the activation of the metalloprotease TACE/ADAM17. Cell Death Dis. *5*, e1326.

Morris, S.M., Baek, J.Y., Koszarek, A., Kanngurn, S., Knoblaugh, S.E., and Grady, W.M. (2012). Transforming growth factor-beta signaling promotes hepatocarcinogenesis induced by p53 loss. Hepatol. Baltim. Md *55*, 121–131.

Morrison, C.D., Parvani, J.G., and Schiemann, W.P. (2013). The relevance of the TGF-β Paradox to EMT-MET programs. Cancer Lett. *341*, 30–40.

Moustakas, A., and Heldin, C.-H. (2012). Induction of epithelial-mesenchymal transition by transforming growth factor β. Semin. Cancer Biol. *22*, 446–454.

Murata, M., Matsuzaki, K., Yoshida, K., Sekimoto, G., Tahashi, Y., Mori, S., Uemura, Y., Sakaida, N., Fujisawa, J., Seki, T., et al. (2009). Hepatitis B virus X protein shifts human hepatic transforming growth factor (TGF)-beta signaling from tumor suppression to oncogenesis in early chronic hepatitis B. Hepatol. Baltim. Md *49*, 1203–1217.

Murillo, M.M., del Castillo, G., Sánchez, A., Fernández, M., and Fabregat, I. (2005). Involvement of EGF receptor and c-Src in the survival signals induced by TGF-beta1 in hepatocytes. Oncogene *24*, 4580–4587.

Murillo, M.M., Carmona-Cuenca, I., Del Castillo, G., Ortiz, C., Roncero, C., Sánchez, A., Fernández, M., and Fabregat, I. (2007). Activation of NADPH oxidase by transforming growth factor-beta in hepatocytes mediates up-regulation of epidermal growth factor receptor ligands through a nuclear factor-kappaB-dependent mechanism. Biochem. J. *405*, 251–259.

Murphy, M.P. (2009). How mitochondria produce reactive oxygen species. Biochem. J. *417*, 1–13.

Nalesnik, M.A., and Michalopoulos, G.K. (2012). Growth factor pathways in development and progression of hepatocellular carcinoma. Front. Biosci. Sch. Ed. *4*, 1487–1515.

Nault, J.C., Mallet, M., Pilati, C., Calderaro, J., Bioulac-Sage, P., Laurent, C., Laurent, A., Cherqui, D., Balabaud, C., Zucman-Rossi, J., et al. (2013). High frequency of telomerase reverse-transcriptase promoter somatic mutations in hepatocellular carcinoma and preneoplastic lesions. Nat. Commun. *4*, 2218.

Nikolaou, K., Tsagaratou, A., Eftychi, C., Kollias, G., Mosialos, G., and Talianidis, I. (2012). Inactivation of the deubiquitinase CYLD in hepatocytes causes apoptosis, inflammation, fibrosis, and cancer. Cancer Cell *21*, 738–750.

Nimnual, A.S., Taylor, L.J., and Bar-Sagi, D. (2003). Redox-dependent downregulation of Rho by Rac. Nat. Cell Biol. *5*, 236–241.

Oberhammer, F., Fritsch, G., Pavelka, M., Froschl, G., Tiefenbacher, R., Purchio, T., and Schulte-Hermann, R. (1992). Induction of apoptosis in cultured hepatocytes and in the regressing liver by transforming growth factor-beta 1 occurs without activation of an endonuclease. Toxicol. Lett. *64-65 Spec No*, 701–704.

Ortiz, C., Caja, L., Sancho, P., Bertran, E., and Fabregat, I. (2008). Inhibition of the EGF receptor blocks autocrine growth and increases the cytotoxic effects of doxorubicin in rat hepatoma cells: role of reactive oxygen species production and glutathione depletion. Biochem. Pharmacol. *75*, 1935–1945.

Ortiz, C., Caja, L., Bertran, E., Gonzalez-Rodriguez, Á., Valverde, Á.M., Fabregat, I., and

Sancho, P. (2012). Protein-tyrosine phosphatase 1B (PTP1B) deficiency confers resistance to transforming growth factor-β (TGF-β)-induced suppressor effects in hepatocytes. J. Biol. Chem. *287*, 15263–15274.

Padua, D., and Massagué, J. (2009). Roles of TGFbeta in metastasis. Cell Res. *19*, 89–102.

Paik, Y.H., and Brenner, D.A. (2011). NADPH oxidase mediated oxidative stress in hepatic fibrogenesis. Korean J. Hepatol. *17*, 251–257.

Paik, Y.-H., Iwaisako, K., Seki, E., Inokuchi, S., Schnabl, B., Osterreicher, C.H., Kisseleva, T., and Brenner, D.A. (2011). The nicotinamide adenine dinucleotide phosphate oxidase (NOX) homologues NOX1 and NOX2/gp91(phox) mediate hepatic fibrosis in mice. Hepatol. Baltim. Md *53*, 1730–1741.

Paik, Y.-H., Kim, J., Aoyama, T., De Minicis, S., Bataller, R., and Brenner, D.A. (2013). Role of NADPH Oxidases in Liver Fibrosis. Antioxid. Redox Signal. *20*, 2854–2872.

Paletta-Silva, R., Rocco-Machado, N., and Meyer-Fernandes, J.R. (2013). NADPH Oxidase Biology and the Regulation of Tyrosine Kinase Receptor Signaling and Cancer Drug Cytotoxicity. Int. J. Mol. Sci. *14*, 3683–3704.

Park, H.S., Jung, H.Y., Park, E.Y., Kim, J., Lee, W.J., and Bae, Y.S. (2004a). Cutting edge: direct interaction of TLR4 with NAD(P)H oxidase 4 isozyme is essential for lipopolysaccharide-induced production of reactive oxygen species and activation of NF-kappa B. J. Immunol. Baltim. Md 1950 *173*, 3589–3593.

Park, S.S., Eom, Y.-W., Kim, E.H., Lee, J.H., Min, D.S., Kim, S., Kim, S.-J., and Choi, K.S. (2004b). Involvement of c-Src kinase in the regulation of TGF-beta1-induced apoptosis. Oncogene *23*, 6272–6281.

Parri, M., and Chiarugi, P. (2010). Rac and Rho GTPases in cancer cell motility control. Cell Commun. Signal. CCS *8*, 23.

Parri, M., Buricchi, F., Giannoni, E., Grimaldi, G., Mello, T., Raugei, G., Ramponi, G., and Chiarugi, P. (2007). EphrinA1 activates a Src/focal adhesion kinase-mediated motility response leading to rho-dependent actino/myosin contractility. J. Biol. Chem. *282*, 19619–19628.

Parsons, J.T., Horwitz, A.R., and Schwartz, M.A. (2010). Cell adhesion: integrating cytoskeletal dynamics and cellular tension. Nat. Rev. Mol. Cell Biol. *11*, 633–643.

Parzefall, W., Freiler, C., Lorenz, O., Koudelka, H., Riegler, T., Nejabat, M., Kainzbauer, E., Grasl-Kraupp, B., and Schulte-Hermann, R. (2014). Superoxide deficiency attenuates promotion of hepatocarcinogenesis by cytotoxicity in NADPH oxidase knockout mice. Arch. Toxicol.

Pawlak, K., Zolbach, K., Borawski, J., Mysliwiec, M., Kovalchuk, O., Chyczewski, L., and Pawlak, D. (2008). Chronic viral hepatitis C, oxidative stress and the coagulation/fibrinolysis system in haemodialysis patients. Thromb. Res. *123*, 166–170.

Pellicoro, A., Ramachandran, P., Iredale, J.P., and Fallowfield, J.A. (2014). Liver fibrosis and repair: immune regulation of wound healing in a solid organ. Nat. Rev. Immunol. *14*, 181–194.

Perlemuter, G., Lettéron, P., Carnot, F., Zavala, F., Pessayre, D., Nalpas, B., and Bréchot, C. (2003). Alcohol and hepatitis C virus core protein additively increase lipid peroxidation and synergistically trigger hepatic cytokine expression in a transgenic mouse model. J. Hepatol. *39*, 1020–1027.

Peshavariya, H., Jiang, F., Taylor, C.J., Selemidis, S., Chang, C.W.T., and Dusting, G.J. (2009). Translation-linked mRNA destabilization accompanying serum-induced Nox4 expression in human endothelial cells. Antioxid. Redox Signal. *11*, 2399–2408.

Peshavariya, H.M., Liu, G.-S., Chang, C.W.T., Jiang, F., Chan, E.C., and Dusting, G.J. (2014). Prostacyclin signaling boosts NADPH oxidase 4 in the endothelium promoting cytoprotection and angiogenesis. Antioxid. Redox Signal. *20*, 2710–2725.

Petritsch, C., Beug, H., Balmain, A., and Oft, M. (2000). TGF-beta inhibits p70 S6 kinase via protein phosphatase 2A to induce G(1) arrest. Genes Dev. *14*, 3093–3101.

Pociask, D.A., Sime, P.J., and Brody, A.R. (2004). Asbestos-derived reactive oxygen species activate TGF-beta1. Lab. Investig. J. Tech. Methods Pathol. *84*, 1013–1023.

Prasanphanich, A.F., Arencibia, C.A., and Kemp, M.L. (2014). Redox processes inform multivariate transdifferentiation trajectories associated with TGFβ-induced epithelial-mesenchymal transition. Free Radic. Biol. Med. *76C*, 1–13.

Presser, L.D., McRae, S., and Waris, G. (2013). Activation of TGF-β1 promoter by hepatitis C virus-induced AP-1 and Sp1: role of TGF-β1 in hepatic stellate cell activation and invasion. PloS One *8*, e56367.

Principe, D.R., Doll, J.A., Bauer, J., Jung, B., Munshi, H.G., Bartholin, L., Pasche, B., Lee, C., and Grippo, P.J. (2014). TGF-β: duality of function between tumor prevention and carcinogenesis. J. Natl. Cancer Inst. *106*, djt369.

Proell, V., Mikula, M., Fuchs, E., and Mikulits, W. (2005). The plasticity of p19 ARF null hepatic stellate cells and the dynamics of activation. Biochim. Biophys. Acta *1744*, 76–87.

Proell, V., Carmona-Cuenca, I., Murillo, M.M., Huber, H., Fabregat, I., and Mikulits, W. (2007). TGF-beta dependent regulation of oxygen radicals during transdifferentiation of activated hepatic stellate cells to myofibroblastoid cells. Comp. Hepatol. *6*, 1.

Ramakrishna, G., Rastogi, A., Trehanpati, N., Sen, B., Khosla, R., and Sarin, S.K. (2013). From Cirrhosis to Hepatocellular Carcinoma: New Molecular Insights on Inflammation and Cellular Senescence. Liver Cancer *2*, 367–383.

Rani, B., Cao, Y., Malfettone, A., Tomuleasa, C., Fabregat, I., and Giannelli, G. (2014). Role of the tissue microenvironment as a therapeutic target in hepatocellular carcinoma. World J. Gastroenterol. WJG *20*, 4128–4140.

Ranjan, P., Anathy, V., Burch, P.M., Weirather, K., Lambeth, J.D., and Heintz, N.H. (2006). Redox-dependent expression of cyclin D1 and cell proliferation by Nox1 in mouse lung epithelial cells. Antioxid. Redox Signal. *8*, 1447–1459.

Ribeiro-Pereira, C., Moraes, J.A., Souza, M. de J., Laurindo, F.R., Arruda, M.A., and Barja-Fidalgo, C. (2014). Redox modulation of FAK controls melanoma survival--role of NOX4. PloS One *9*, e99481.

Riehle, K.J., Dan, Y.Y., Campbell, J.S., and Fausto, N. (2011). New concepts in liver regeneration. J. Gastroenterol. Hepatol. *26 Suppl 1*, 203–212.

Rousset, F., Nguyen, M.V.C., Grange, L., Morel, F., and Lardy, B. (2013). Heme oxygenase-1 regulates matrix metalloproteinase MMP-1 secretion and chondrocyte cell death via Nox4 NADPH oxidase activity in chondrocytes. PloS One *8*, e66478.

Rozga, J. (2002). Hepatocyte proliferation in health and in liver failure. Med. Sci. Monit. Int.

Med. J. Exp. Clin. Res. *8*, RA32–RA38.

Sadok, A., and Marshall, C.J. (2014). Rho GTPases: masters of cell migration. Small GTPases *5*, e29710.

Sadok, A., Pierres, A., Dahan, L., Prévôt, C., Lehmann, M., and Kovacic, H. (2009). NADPH oxidase 1 controls the persistence of directed cell migration by a Rho-dependent switch of alpha2/alpha3 integrins. Mol. Cell. Biol. *29*, 3915–3928.

Sahai, E., and Marshall, C.J. (2002). ROCK and Dia have opposing effects on adherens junctions downstream of Rho. Nat. Cell Biol. *4*, 408–415.

Salmeen, A., Park, B.O., and Meyer, T. (2010). The NADPH oxidases NOX4 and DUOX2 regulate cell cycle entry via a p53-dependent pathway. Oncogene *29*, 4473–4484.

Samarakoon, R., Overstreet, J.M., and Higgins, P.J. (2013a). TGF-β signaling in tissue fibrosis: redox controls, target genes and therapeutic opportunities. Cell. Signal. *25*, 264–268.

Samarakoon, R., Dobberfuhl, A.D., Cooley, C., Overstreet, J.M., Patel, S., Goldschmeding, R., Meldrum, K.K., and Higgins, P.J. (2013b). Induction of renal fibrotic genes by TGF-β1 requires EGFR activation, p53 and reactive oxygen species. Cell. Signal. *25*, 2198–2209.

Sampson, N., Koziel, R., Zenzmaier, C., Bubendorf, L., Plas, E., Jansen-Dürr, P., and Berger, P. (2011). ROS signaling by NOX4 drives fibroblast-to-myofibroblast differentiation in the diseased prostatic stroma. Mol. Endocrinol. Baltim. Md *25*, 503–515.

Sánchez, A., and Fabregat, I. (2009). Genetically modified animal models recapitulating molecular events altered in human hepatocarcinogenesis. Clin. Transl. Oncol. Off. Publ. Fed. Span. Oncol. Soc. Natl. Cancer Inst. Mex. *11*, 208–214.

Sánchez, A., Alvarez, A.M., Benito, M., and Fabregat, I. (1996). Apoptosis induced by transforming growth factor-beta in fetal hepatocyte primary cultures: involvement of reactive oxygen intermediates. J. Biol. Chem. *271*, 7416–7422.

Sánchez, A., Alvarez, A.M., Benito, M., and Fabregat, I. (1997). Cycloheximide prevents apoptosis, reactive oxygen species production, and glutathione depletion induced by transforming growth factor beta in fetal rat hepatocytes in primary culture. Hepatol. Baltim. Md *26*, 935–943.

Sánchez, A., Pagan, R., Alvarez, A.M., Roncero, C., Vilaró, S., Benito, M., and Fabregat, I. (1998). Transforming growth factor-beta (TGF-beta) and EGF promote cord-like structures that indicate terminal differentiation of fetal hepatocytes in primary culture. Exp. Cell Res. *242*, 27–37.

Sánchez, A., Alvarez, A.M., López Pedrosa, J.M., Roncero, C., Benito, M., and Fabregat, I. (1999). Apoptotic response to TGF-beta in fetal hepatocytes depends upon their state of differentiation. Exp. Cell Res. *252*, 281–291.

Sancho, P., and Fabregat, I. (2010). NADPH oxidase NOX1 controls autocrine growth of liver tumor cells through up-regulation of the epidermal growth factor receptor pathway. J. Biol. Chem. *285*, 24815–24824.

Sancho, P., and Fabregat, I. (2011). The NADPH oxidase inhibitor VAS2870 impairs cell growth and enhances TGF-β-induced apoptosis of liver tumor cells. Biochem. Pharmacol. *81*, 917–924.

Sancho, P., Bertran, E., Caja, L., Carmona-Cuenca, I., Murillo, M.M., and Fabregat, I.

(2009). The inhibition of the epidermal growth factor (EGF) pathway enhances TGF-beta-induced apoptosis in rat hepatoma cells through inducing oxidative stress coincident with a change in the expression pattern of the NADPH oxidases (NOX) isoforms. Biochim. Biophys. Acta *1793*, 253–263.

Sancho, P., Martín-Sanz, P., and Fabregat, I. (2011). Reciprocal regulation of NADPH oxidases and the cyclooxygenase-2 pathway. Free Radic. Biol. Med. *51*, 1789–1798.

Sancho, P., Mainez, J., Crosas-Molist, E., Roncero, C., Fernandez-Rodriguez, C.M., Pinedo, F., Huber, H., Eferl, R., Mikulits, W., and Fabregat, I. (2012). NADPH Oxidase NOX4 Mediates Stellate Cell Activation and Hepatocyte Cell Death during Liver Fibrosis Development. PLoS ONE *7*.

Sanz-Moreno, V. (2012). Tumour Invasion: A New Twist on Rac-Driven Mesenchymal Migration. Curr. Biol. *22*, R449–R451.

Sanz-Moreno, V., and Marshall, C.J. (2010). The plasticity of cytoskeletal dynamics underlying neoplastic cell migration. Curr. Opin. Cell Biol. *22*, 690–696.

Sawey, E.T., Chanrion, M., Cai, C., Wu, G., Zhang, J., Zender, L., Zhao, A., Busuttil, R.W., Yee, H., Stein, L., et al. (2011). Identification of a therapeutic strategy targeting amplified FGF19 in liver cancer by Oncogenomic screening. Cancer Cell *19*, 347–358.

Schilder, Y.D.C., Heiss, E.H., Schachner, D., Ziegler, J., Reznicek, G., Sorescu, D., and Dirsch, V.M. (2009). NADPH oxidases 1 and 4 mediate cellular senescence induced by resveratrol in human endothelial cells. Free Radic. Biol. Med. *46*, 1598–1606.

Schimanski, C.C., Bahre, R., Gockel, I., Müller, A., Frerichs, K., Hörner, V., Teufel, A., Simiantonaki, N., Biesterfeld, S., Wehler, T., et al. (2006). Dissemination of hepatocellular carcinoma is mediated via chemokine receptor CXCR4. Br. J. Cancer *95*, 210–217.

Scholzen, T., and Gerdes, J. (2000). The Ki-67 protein: from the known and the unknown. J. Cell. Physiol. *182*, 311–322.

Schrader, J., Gordon-Walker, T.T., Aucott, R.L., van Deemter, M., Quaas, A., Walsh, S., Benten, D., Forbes, S.J., Wells, R.G., and Iredale, J.P. (2011). Matrix stiffness modulates proliferation, chemotherapeutic response, and dormancy in hepatocellular carcinoma cells. Hepatol. Baltim. Md *53*, 1192–1205.

Schröder, K. (2014). NADPH oxidases in redox regulation of cell adhesion and migration. Antioxid. Redox Signal. *20*, 2043–2058.

Schröder, K., Helmcke, I., Palfi, K., Krause, K.-H., Busse, R., and Brandes, R.P. (2007). Nox1 mediates basic fibroblast growth factor-induced migration of vascular smooth muscle cells. Arterioscler. Thromb. Vasc. Biol. *27*, 1736–1743.

Schröder, K., Wandzioch, K., Helmcke, I., and Brandes, R.P. (2009). Nox4 acts as a switch between differentiation and proliferation in preadipocytes. Arterioscler. Thromb. Vasc. Biol. *29*, 239–245.

Schröder, K., Zhang, M., Benkhoff, S., Mieth, A., Pliquett, R., Kosowski, J., Kruse, C., Luedike, P., Michaelis, U.R., Weissmann, N., et al. (2012). Nox4 is a protective reactive oxygen species generating vascular NADPH oxidase. Circ. Res. *110*, 1217–1225.

Schuppan, D., and Kim, Y.O. (2013). Evolving therapies for liver fibrosis. J. Clin. Invest. *123*, 1887–1901.

## VIII. REFERENCES


Schwarz, K.B., Kew, M., Klein, A., Abrams, R.A., Sitzmann, J., Jones, L., Sharma, S., Britton, R.S., Di Bisceglie, A.M., and Groopman, J. (2001). Increased hepatic oxidative DNA damage in patients with hepatocellular carcinoma. Dig. Dis. Sci. *46*, 2173–2178.

Sciarretta, S., Zhai, P., Shao, D., Zablocki, D., Nagarajan, N., Terada, L.S., Volpe, M., and Sadoshima, J. (2013). Activation of NADPH oxidase 4 in the endoplasmic reticulum promotes cardiomyocyte autophagy and survival during energy stress through the protein kinase RNA-activated-like endoplasmic reticulum kinase/eukaryotic initiation factor 2α/activating transcription factor 4 pathway. Circ. Res. *113*, 1253–1264.

Scioli, M.G., Cervelli, V., Arcuri, G., Gentile, P., Doldo, E., Bielli, A., Bonanno, E., and Orlandi, A. (2014). High insulin-induced down-regulation of Erk-1/IGF-1R/FGFR-1 signaling is required for oxidative stress-mediated apoptosis of adipose-derived stem cells. J. Cell. Physiol. *229*, 2077–2087.

Sedeek, M., Callera, G., Montezano, A., Gutsol, A., Heitz, F., Szyndralewiez, C., Page, P., Kennedy, C.R.J., Burns, K.D., Touyz, R.M., et al. (2010). Critical role of Nox4-based NADPH oxidase in glucose-induced oxidative stress in the kidney: implications in type 2 diabetic nephropathy. Am. J. Physiol. Renal Physiol. *299*, F1348–F1358.

Sedeek, M., Gutsol, A., Montezano, A.C., Burger, D., Nguyen Dinh Cat, A., Kennedy, C.R.J., Burns, K.D., Cooper, M.E., Jandeleit-Dahm, K., Page, P., et al. (2013). Renoprotective effects of a novel Nox1/4 inhibitor in a mouse model of Type 2 diabetes. Clin. Sci. Lond. Engl. 1979 *124*, 191–202.

Segal, B.H., Romani, L., and Puccetti, P. (2009). Chronic granulomatous disease. Cell. Mol. Life Sci. CMLS *66*, 553–558.

Seki, E., De Minicis, S., Osterreicher, C.H., Kluwe, J., Osawa, Y., Brenner, D.A., and Schwabe, R.F. (2007). TLR4 enhances TGF-beta signaling and hepatic fibrosis. Nat. Med. *13*, 1324–1332.

Seki, S., Kitada, T., and Sakaguchi, H. (2005). Clinicopathological significance of oxidative cellular damage in non-alcoholic fatty liver diseases. Hepatol. Res. Off. J. Jpn. Soc. Hepatol. *33*, 132–134.

Senturk, S., Mumcuoglu, M., Gursoy-Yuzugullu, O., Cingoz, B., Akcali, K.C., and Ozturk, M. (2010). Transforming growth factor-beta induces senescence in hepatocellular carcinoma cells and inhibits tumor growth. Hepatology *52*, 966–974.

Seoane, J. (2006). Escaping from the TGFbeta anti-proliferative control. Carcinogenesis *27*, 2148–2156.

Seoane, J., Le, H.-V., Shen, L., Anderson, S.A., and Massagué, J. (2004). Integration of Smad and forkhead pathways in the control of neuroepithelial and glioblastoma cell proliferation. Cell *117*, 211–223.

Serrander, L., Cartier, L., Bedard, K., Banfi, B., Lardy, B., Plastre, O., Sienkiewicz, A., Forro, L., Schlegel, W., and Krause, K.-H. (2007). NOX4 activity is determined by mRNA levels and reveals a unique pattern of ROS generation. Biochem. J. *406*, 105–114.

Shen, Y., Hirsch, D.S., Sasiela, C.A., and Wu, W.J. (2008). Cdc42 regulates E-cadherin ubiquitination and degradation through an epidermal growth factor receptor to Src-mediated pathway. J. Biol. Chem. *283*, 5127–5137.

Shiose, A., Kuroda, J., Tsuruya, K., Hirai, M., Hirakata, H., Naito, S., Hattori, M., Sakaki, Y.,

and Sumimoto, H. (2001). A novel superoxide-producing NAD(P)H oxidase in kidney. J. Biol. Chem. *276*, 1417–1423.

Shono, T., Yokoyama, N., Uesaka, T., Kuroda, J., Takeya, R., Yamasaki, T., Amano, T., Mizoguchi, M., Suzuki, S.O., Niiro, H., et al. (2008). Enhanced expression of NADPH oxidase Nox4 in human gliomas and its roles in cell proliferation and survival. Int. J. Cancer J. Int. Cancer *123*, 787–792.

Sia, D., and Villanueva, A. (2011). Signaling Pathways in Hepatocellular Carcinoma. Oncology *81*, 18–23.

Sirker, A., Zhang, M., and Shah, A.M. (2011). NADPH oxidases in cardiovascular disease: insights from in vivo models and clinical studies. Basic Res. Cardiol. *106*, 735–747.

Si-Tayeb, K., Lemaigre, F.P., and Duncan, S.A. (2010). Organogenesis and Development of the Liver. Dev. Cell *18*, 175–189.

Liu-Smith, F., Dellinger, R., and Meyskens, F.L. (2014). Updates of reactive oxygen species in melanoma etiology and progression. Arch. Biochem. Biophys.

Song, K., Wang, H., Krebs, T.L., and Danielpour, D. (2006). Novel roles of Akt and mTOR in suppressing TGF-beta/ALK5-mediated Smad3 activation. EMBO J. *25*, 58–69.

Spano, D., Heck, C., De Antonellis, P., Christofori, G., and Zollo, M. (2012). Molecular networks that regulate cancer metastasis. Semin. Cancer Biol. *22*, 234–249.

Spear, B.T., Jin, L., Ramasamy, S., and Dobierzewska, A. (2006). Transcriptional control in the mammalian liver: liver development, perinatal repression, and zonal gene regulation. Cell. Mol. Life Sci. CMLS *63*, 2922–2938.

Stanley, A., Hynes, A., Brakebusch, C., and Quondamatteo, F. (2012). Rho GTPases and Nox dependent ROS production in skin. Is there a connection? Histol. Histopathol. *27*, 1395–1406.

Stanley, A., Thompson, K., Hynes, A., Brakebusch, C., and Quondamatteo, F. (2013). NADPH Oxidase Complex-Derived Reactive Oxygen Species, the Actin Cytoskeleton, and Rho GTPases in Cell Migration. Antioxid. Redox Signal. *20*, 2026–2042.

Sturrock, A., Cahill, B., Norman, K., Hueckstead, T.P., Hill, K., Sanders, K., Karwande, S.V., Stringham, J.C., Bull, D.A., Gleich, M., et al. (2006). Transforming growth factor-beta1 induces Nox4 NAD(P)H oxidase and reactive oxygen species-dependent proliferation in human pulmonary artery smooth muscle cells. Am. J. Physiol. Lung Cell. Mol. Physiol. *290*, L661–L673.

Sturrock, A., Hueckstead, T.P., Norman, K., Sanders, K., Murphy, T.M., Chitano, P., Wilson, K., Hoidal, J.R., and Kennedy, T.P. (2007). Nox4 mediates TGF-beta1-induced retinoblastoma protein phosphorylation, proliferation, and hypertrophy in human airway smooth muscle cells. Am. J. Physiol. Lung Cell. Mol. Physiol. *292*, L1543–L1555.

Suh, Y.A., Arnold, R.S., Lassegue, B., Shi, J., Xu, X., Sorescu, D., Chung, A.B., Griendling, K.K., and Lambeth, J.D. (1999). Cell transformation by the superoxide-generating oxidase Mox1. Nature *401*, 79–82.

Suzuki, Y., Hattori, K., Hamanaka, J., Murase, T., Egashira, Y., Mishiro, K., Ishiguro, M., Tsuruma, K., Hirose, Y., Tanaka, H., et al. (2012). Pharmacological inhibition of TLR4-NOX4 signal protects against neuronal death in transient focal ischemia. Sci. Rep. *2*.

Tabrizian, P., Roayaie, S., and Schwartz, M.E. (2014). Current management of

hepatocellular carcinoma. World J. Gastroenterol. WJG *20*, 10223–10237.

Takac, I., Schröder, K., Zhang, L., Lardy, B., Anilkumar, N., Lambeth, J.D., Shah, A.M., Morel, F., and Brandes, R.P. (2011). The E-loop is involved in hydrogen peroxide formation by the NADPH oxidase Nox4. J. Biol. Chem. *286*, 13304–13313.

Teufelhofer, O., Parzefall, W., Kainzbauer, E., Ferk, F., Freiler, C., Knasmüller, S., Elbling, L., Thurman, R., and Schulte-Hermann, R. (2005). Superoxide generation from Kupffer cells contributes to hepatocarcinogenesis: studies on NADPH oxidase knockout mice. Carcinogenesis *26*, 319–329.

Tian, X.Y., Yung, L.H., Wong, W.T., Liu, J., Leung, F.P., Liu, L., Chen, Y., Kong, S.K., Kwan, K.M., Ng, S.M., et al. (2012). Bone morphogenic protein-4 induces endothelial cell apoptosis through oxidative stress-dependent p38MAPK and JNK pathway. J. Mol. Cell. Cardiol. *52*, 237–244.

Toffanin, S., Hoshida, Y., Lachenmayer, A., Villanueva, A., Cabellos, L., Minguez, B., Savic, R., Ward, S.C., Thung, S., Chiang, D.Y., et al. (2011). MicroRNA-based classification of hepatocellular carcinoma and oncogenic role of miR-517a. Gastroenterology *140*, 1618–1628.e16.

Tormos, A.M., Taléns-Visconti, R., Nebreda, A.R., and Sastre, J. (2013). p38 MAPK: A dual role in hepatocyte proliferation through reactive oxygen species. Free Radic. Res. *47*, 905–916.

Tovar, V., Alsinet, C., Villanueva, A., Hoshida, Y., Chiang, D.Y., Solé, M., Thung, S., Moyano, S., Toffanin, S., Mínguez, B., et al. (2010). IGF activation in a molecular subclass of hepatocellular carcinoma and pre-clinical efficacy of IGF-1R blockage. J. Hepatol. *52*, 550–559.

Tsochatzis, E.A., Bosch, J., and Burroughs, A.K. (2014). Liver cirrhosis. The Lancet *383*, 1749–1761.

Ueno, S., Campbell, J., and Fausto, N. (2006). Reactive oxygen species derived from NADPH oxidase system is not essential for liver regeneration after partial hepatectomy. J. Surg. Res. *136*, 260–265.

Ullevig, S., Zhao, Q., Lee, C.F., Seok Kim, H., Zamora, D., and Asmis, R. (2012). NADPH oxidase 4 mediates monocyte priming and accelerated chemotaxis induced by metabolic stress. Arterioscler. Thromb. Vasc. Biol. *32*, 415–426.

Ushio-Fukai, M. (2009). Compartmentalization of redox signaling through NADPH oxidase-derived ROS. Antioxid. Redox Signal. *11*, 1289–1299.

Utsunomiya, T., Shimada, M., Imura, S., Morine, Y., Ikemoto, T., and Mori, M. (2010). Molecular signatures of noncancerous liver tissue can predict the risk for late recurrence of hepatocellular carcinoma. J. Gastroenterol. *45*, 146–152.

Vacca, M., Degirolamo, C., Massafra, V., Polimeno, L., Mariani-Costantini, R., Palasciano, G., and Moschetta, A. (2013). Nuclear receptors in regenerating liver and hepatocellular carcinoma. Mol. Cell. Endocrinol. *368*, 108–119.

Valdés, F., Alvarez, A.M., Locascio, A., Vega, S., Herrera, B., Fernández, M., Benito, M., Nieto, M.A., and Fabregat, I. (2002). The epithelial mesenchymal transition confers resistance to the apoptotic effects of transforming growth factor Beta in fetal rat hepatocytes. Mol. Cancer Res. MCR *1*, 68–78.

Valdés, F., Murillo, M.M., Valverde, A.M., Herrera, B., Sánchez, A., Benito, M., Fernández,

M., and Fabregat, I. (2004). Transforming growth factor-beta activates both pro-apoptotic and survival signals in fetal rat hepatocytes. Exp. Cell Res. *292*, 209–218.

Vaquero, E.C., Edderkaoui, M., Pandol, S.J., Gukovsky, I., and Gukovskaya, A.S. (2004). Reactive oxygen species produced by NAD(P)H oxidase inhibit apoptosis in pancreatic cancer cells. J. Biol. Chem. *279*, 34643–34654.

Vega, S., Morales, A.V., Ocaña, O.H., Valdés, F., Fabregat, I., and Nieto, M.A. (2004). Snail blocks the cell cycle and confers resistance to cell death. Genes Dev. *18*, 1131–1143.

Verbon, E.H., Post, J.A., and Boonstra, J. (2012). The influence of reactive oxygen species on cell cycle progression in mammalian cells. Gene *511*, 1–6.

Villanueva, A., Newell, P., Chiang, D.Y., Friedman, S.L., and Llovet, J.M. (2007). Genomics and signaling pathways in hepatocellular carcinoma. Semin. Liver Dis. *27*, 55–76.

Villanueva, A., Hernandez-Gea, V., and Llovet, J.M. (2013). Medical therapies for hepatocellular carcinoma: a critical view of the evidence. Nat. Rev. Gastroenterol. Hepatol. *10*, 34–42.

Wagner, B., Ricono, J.M., Gorin, Y., Block, K., Arar, M., Riley, D., Choudhury, G.G., and Abboud, H.E. (2007). Mitogenic signaling via platelet-derived growth factor beta in metanephric mesenchymal cells. J. Am. Soc. Nephrol. JASN *18*, 2903–2911.

Wallace, M.C., and Friedman, S.L. (2014). Hepatic Fibrosis and the Microenvironment: Fertile Soil for Hepatocellular Carcinoma Development. Gene Expr. *16*, 77–84.

Wang, K., Lim, H.Y., Shi, S., Lee, J., Deng, S., Xie, T., Zhu, Z., Wang, Y., Pocalyko, D., Yang, W.J., et al. (2013). Genomic landscape of copy number aberrations enables the identification of oncogenic drivers in hepatocellular carcinoma. Hepatol. Baltim. Md *58*, 706–717.

Wang, L., Clutter, S., Benincosa, J., Fortney, J., and Gibson, L.F. (2005). Activation of transforming growth factor-beta1/p38/Smad3 signaling in stromal cells requires reactive oxygen species-mediated MMP-2 activity during bone marrow damage. Stem Cells Dayt. Ohio *23*, 1122–1134.

Wang, S.-C., Lin, X.-L., Li, J., Zhang, T.-T., Wang, H.-Y., Shi, J.-W., Yang, S., Zhao, W.-T., Xie, R.-Y., Wei, F., et al. (2014). MicroRNA-122 triggers mesenchymal-epithelial transition and suppresses hepatocellular carcinoma cell motility and invasion by targeting RhoA. PloS One *9*, e101330.

Wang, W., Yang, L.-Y., Huang, G.-W., Lu, W.-Q., Yang, Z.-L., Yang, J.-Q., and Liu, H.-L. (2004). Genomic analysis reveals RhoC as a potential marker in hepatocellular carcinoma with poor prognosis. Br. J. Cancer *90*, 2349–2355.

Weinberg, F., and Chandel, N.S. (2009). Reactive oxygen species-dependent signaling regulates cancer. Cell. Mol. Life Sci. CMLS *66*, 3663–3673.

Wells, R.G. (2010). The epithelial-to-mesenchymal transition in liver fibrosis: here today, gone tomorrow? Hepatol. Baltim. Md *51*, 737–740.

Weyemi, U., and Dupuy, C. (2012). The emerging role of ROS-generating NADPH oxidase NOX4 in DNA-damage responses. Mutat. Res. *751*, 77–81.

Weyemi, U., Caillou, B., Talbot, M., Ameziane-El-Hassani, R., Lacroix, L., Lagent-Chevallier, O., Al Ghuzlan, A., Roos, D., Bidart, J.-M., Virion, A., et al. (2010). Intracellular

expression of reactive oxygen species-generating NADPH oxidase NOX4 in normal and cancer thyroid tissues. Endocr. Relat. Cancer *17*, 27–37.

Weyemi, U., Lagente-Chevallier, O., Boufraqech, M., Prenois, F., Courtin, F., Caillou, B., Talbot, M., Dardalhon, M., Al Ghuzlan, A., Bidart, J.-M., et al. (2012). ROS-generating NADPH oxidase NOX4 is a critical mediator in oncogenic H-Ras-induced DNA damage and subsequent senescence. Oncogene *31*, 1117–1129.

Weyemi, U., Redon, C.E., Parekh, P.R., Dupuy, C., and Bonner, W.M. (2013). NADPH Oxidases NOXs and DUOXs as putative targets for cancer therapy. Anticancer Agents Med. Chem. *13*, 502–514.

Wiesner, S., Lange, A., and Fässler, R. (2006). Local call: from integrins to actin assembly. Trends Cell Biol. *16*, 327–329.

Wilkes, M.C., Mitchell, H., Penheiter, S.G., Doré, J.J., Suzuki, K., Edens, M., Sharma, D.K., Pagano, R.E., and Leof, E.B. (2005). Transforming growth factor-beta activation of phosphatidylinositol 3-kinase is independent of Smad2 and Smad3 and regulates fibroblast responses via p21-activated kinase-2. Cancer Res. *65*, 10431–10440.

De Wit, R., Capello, A., Boonstra, J., Verkleij, A.J., and Post, J.A. (2000). Hydrogen peroxide inhibits epidermal growth factor receptor internalization in human fibroblasts. Free Radic. Biol. Med. *28*, 28–38.

Wojciak-Stothard, B., Tsang, L.Y.F., and Haworth, S.G. (2005). Rac and Rho play opposing roles in the regulation of hypoxia/reoxygenation-induced permeability changes in pulmonary artery endothelial cells. Am. J. Physiol. Lung Cell. Mol. Physiol. *288*, L749–L760.

Wu, Y., Qiao, X., Qiao, S., and Yu, L. (2011). Targeting integrins in hepatocellular carcinoma. Expert Opin. Ther. Targets *15*, 421–437.

Wynn, T.A., and Barron, L. (2010). Macrophages: master regulators of inflammation and fibrosis. Semin. Liver Dis. *30*, 245–257.

Xu, Z., Chen, L., Leung, L., Yen, T.S.B., Lee, C., and Chan, J.Y. (2005). Liver-specific inactivation of the Nrf1 gene in adult mouse leads to nonalcoholic steatohepatitis and hepatic neoplasia. Proc. Natl. Acad. Sci. U. S. A. *102*, 4120–4125.

Xue, Z.-F., Wu, X.-M., and Liu, M. (2013). Hepatic regeneration and the epithelial to mesenchymal transition. World J. Gastroenterol. WJG *19*, 1380–1386.

Yadav, D., Hertan, H.I., Schweitzer, P., Norkus, E.P., and Pitchumoni, C.S. (2002). Serum and liver micronutrient antioxidants and serum oxidative stress in patients with chronic hepatitis C. Am. J. Gastroenterol. *97*, 2634–2639.

Yamaura, M., Mitsushita, J., Furuta, S., Kiniwa, Y., Ashida, A., Goto, Y., Shang, W.H., Kubodera, M., Kato, M., Takata, M., et al. (2009). NADPH oxidase 4 contributes to transformation phenotype of melanoma cells by regulating G2-M cell cycle progression. Cancer Res. *69*, 2647–2654.

Yan, F., Wang, Y., Wu, X., Peshavariya, H.M., Dusting, G.J., Zhang, M., and Jiang, F. (2014). Nox4 and redox signaling mediate TGF-β-induced endothelial cell apoptosis and phenotypic switch. Cell Death Dis. *5*, e1010.

Yoon, S.-O., Yun, C.-H., and Chung, A.-S. (2002). Dose effect of oxidative stress on signal transduction in aging. Mech. Ageing Dev. *123*, 1597–1604.

## VIII. REFERENCES


Yu, J.H., Zhu, B.-M., Riedlinger, G., Kang, K., and Hennighausen, L. (2012). The liver-specific tumor suppressor STAT5 controls expression of the reactive oxygen species-generating enzyme NOX4 and the proapoptotic proteins PUMA and BIM in mice. Hepatol. Baltim. Md *56*, 2375–2386.

Yu, L.-X., Yan, H.-X., Liu, Q., Yang, W., Wu, H.-P., Dong, W., Tang, L., Lin, Y., He, Y.-Q., Zou, S.-S., et al. (2010). Endotoxin accumulation prevents carcinogen-induced apoptosis and promotes liver tumorigenesis in rodents. Hepatology *52*, 1322–1333.

Zeisberg, M., and Kalluri, R. (2013). Cellular Mechanisms of Tissue Fibrosis. 1. Common and organ-specific mechanisms associated with tissue fibrosis. Am. J. Physiol. - Cell Physiol. *304*, C216–C225.

Zender, L., Villanueva, A., Tovar, V., Sia, D., Chiang, D.Y., and Llovet, J.M. (2010). Cancer Gene Discovery in Hepatocellular Carcinoma. J. Hepatol. *52*, 921–929.

Zhang, D.Y., and Friedman, S.L. (2012). Fibrosis-Dependent Mechanisms of Hepatocarcinogenesis. Hepatol. Baltim. Md *56*, 769–775.

Zhang, C., Lan, T., Hou, J., Li, J., Fang, R., Yang, Z., Zhang, M., Liu, J., and Liu, B. (2014). NOX4 promotes non-small cell lung cancer cell proliferation and metastasis through positive feedback regulation of PI3K/Akt signaling. Oncotarget *5*, 4392–4405.

Zhang, M., Brewer, A.C., Schröder, K., Santos, C.X.C., Grieve, D.J., Wang, M., Anilkumar, N., Yu, B., Dong, X., Walker, S.J., et al. (2010). NADPH oxidase-4 mediates protection against chronic load-induced stress in mouse hearts by enhancing angiogenesis. Proc. Natl. Acad. Sci. U. S. A. *107*, 18121–18126.

Van Zijl, F., Mair, M., Csiszar, A., Schneller, D., Zulehner, G., Huber, H., Eferl, R., Beug, H., Dolznig, H., and Mikulits, W. (2009). Hepatic tumor-stroma crosstalk guides epithelial to mesenchymal transition at the tumor edge. Oncogene *28*, 4022–4033.

# IX. ANNEXES

OPEN ACCESS Freely available online

PLOS ONE

# NADPH Oxidase NOX4 Mediates Stellate Cell Activation and Hepatocyte Cell Death during Liver Fibrosis Development

**Patricia Sancho[1], Jèssica Mainez[1], Eva Crosas-Molist[1], César Roncero[2], Conrado M. Fernández-Rodriguez[3], Fernando Pinedo[4], Heidemarie Huber[5], Robert Eferl[5,6], Wolfgang Mikulits[5], Isabel Fabregat[1,7]***

**1** Biological Clues of the Invasive and Metastatic Phenotype Group, Bellvitge Biomedical Research Institute (IDIBELL), L'Hospitalet, Barcelona, Spain, **2** Departamento de Bioquímica y Biología Molecular II, Facultad de Farmacia, Universidad Complutense and Instituto de Investigación Sanitaria del Hospital Clínico San Carlos (IdISSC), Madrid, Spain, **3** Service of Gastroenterology, Hospital Universitario Fundación Alcorcón and Universidad Rey Juan Carlos, Alcorcón, Madrid, Spain, **4** Unit of Pathology, Hospital Universitario Fundación Alcorcón, Alcorcón, Madrid, Spain, **5** Department of Medicine I, Division: Institute of Cancer Research, Medical University of Vienna, Vienna, Austria, **6** Ludwig Boltzmann Institute for Cancer Research (LBI-CR), Vienna, Austria, **7** Department of Physiological Sciences II, University of Barcelona, Barcelona, Spain

## Abstract

A role for the NADPH oxidases NOX1 and NOX2 in liver fibrosis has been proposed, but the implication of NOX4 is poorly understood yet. The aim of this work was to study the functional role of NOX4 in different cell populations implicated in liver fibrosis: hepatic stellate cells (HSC), myofibroblats (MFBs) and hepatocytes. Two different mice models that develop spontaneous fibrosis ($Mdr2^{-/-}/p19^{ARF-/-}$, $Stat3^{\Delta hc}/Mdr2^{-/-}$) and a model of experimental induced fibrosis ($CCl_4$) were used. In addition, gene expression in biopsies from chronic hepatitis C virus (HCV) patients or non-fibrotic liver samples was analyzed. Results have indicated that NOX4 expression was increased in the livers of all animal models, concomitantly with fibrosis development and TGF-β pathway activation. *In vitro* TGF-β-treated HSC increased NOX4 expression correlating with transdifferentiation to MFBs. Knockdown experiments revealed that NOX4 downstream TGF-β is necessary for HSC activation as well as for the maintenance of the MFB phenotype. NOX4 was not necessary for TGF-β-induced epithelial-mesenchymal transition (EMT), but was required for TGF-β-induced apoptosis in hepatocytes. Finally, NOX4 expression was elevated in patients with hepatitis C virus (HCV)-derived fibrosis, increasing along the fibrosis degree. In summary, fibrosis progression both *in vitro* and *in vivo* (animal models and patients) is accompanied by increased NOX4 expression, which mediates acquisition and maintenance of the MFB phenotype, as well as TGF-β-induced death of hepatocytes.

**Citation:** Sancho P, Mainez J, Crosas-Molist E, Roncero C, Fernández-Rodriguez CM, et al. (2012) NADPH Oxidase NOX4 Mediates Stellate Cell Activation and Hepatocyte Cell Death during Liver Fibrosis Development. PLoS ONE 7(9): e45285. doi:10.1371/journal.pone.0045285

**Editor:** Marie Jose Goumans, Leiden University Medical Center, The Netherlands

**Received** May 7, 2012; **Accepted** August 15, 2012; **Published** September 26, 2012



**Funding:** This work was supported by grants to IF from the Ministerio de Ciencia e Innovación (MICINN), Spain (BFU2009-07219 and ISCIII-RTICC RD06/0020) and AGAUR-Generalitat de Catalunya (2009SGR-312). The work of WM was supported by the European Union, FP7 Health Research project number HEALTH-F4-2008-202047. JM and EC-M were recipients of pre-doctoral fellowships from the FPI and FPU programs, respectively, MICINN, Spain. The funders had no role in study design, data collection and analysis, decision to publish, or preparation of the manuscript.

**Competing Interests:** The authors have declared that no competing interests exist.

* E-mail: ifabregat@idibell.cat

## Introduction

Liver fibrosis is the final consequence of many chronic liver injuries [1]. Hepatic stellate cells (HSCs) are activated to myofibroblasts (MFBs), which are mainly responsible for collagen deposition during hepatic fibrogenesis. Once injured, hepatocytes undergo apoptosis. The transforming growth factor-beta (TGF-β), whose levels increase during the development of liver fibrosis, could be involved in both processes [2]. Thus, TGF-β inhibits growth and induces apoptosis of hepatocytes and also contributes to the activation of HSCs [3,4].

The generation of reactive oxygen species (ROS) plays relevant roles in hepatic fibrosis and recent works point to NADPH oxidases (NOX) as a key source of ROS in the fibrotic liver [5]. Two NOX isoforms, NOX1 and NOX2, mediate pro-fibrogenic effects in endogenous liver cells [6,7,8]. However, less is known about the possible role in liver fibrosis of another isoform, NOX4, which is highly expressed in hepatocytes and HSCs [8]. We previously reported that NOX4 mediates TGF-β-induced apoptosis in hepatocytes in primary culture [9] and causes ROS production upon the *in vitro* transdifferentiation of activated HSCs to MFBs [3]. In other fibrotic models, NOX4 accounts for ROS-induced fibroblast and mesangial cell activation, playing an essential role in TGF-β1-mediated fibroblast differentiation into a profibrotic myofibroblast phenotype and matrix production [10]. Indeed, TGF-β induces NOX4 expression in lung mesenchymal cells, which mediates MFB activation and fibrogenic responses to lung injury [11]. In this same line of evidence, ROS signaling by NOX4 is required for TGF-β-induced differentiation of fibroblasts into MFB in heart [12], kidney [13] and diseased prostatic stroma [14].

The aim of this work was to analyze whether NOX4 expression is modulated in experimental animal models of liver fibrosis and during the development of human liver fibrogenesis. We demonstrate that NOX4 expression increases in parallel to liver

fibrotic processes and may be required for TGF-β-induced activation of HSC and for the maintenance of the MFB phenotype. In hepatocytes, NOX4 causes cell death but does not mediate epithelial-mesenchymal transition (EMT). These results open new perspectives for the involvement of NOXes in liver fibrosis and for the potential development of new therapeutic targeted tools.

## Materials and Methods

### Ethics statement

Mice were housed in accordance with European laws and with the general regulations specified by the Good Scientific Practices Guidelines of the Medical University of Vienna. From Spain, the approval for all the experiments related to the study of liver fibrosis in experimental animal models was applied to the General Direction of Environment and Biodiversity, Government of Catalonia, and approved with the number #4589, 2011 (document enclosed). Human tissues were collected with the required approvals from the Institutional Review Board (Comité Ético de Investigación Clínica del Hospital Universitario Fundación Alcorcón) and patient's written consent conformed to the ethical guidelines of the 1975 Declaration of Helsinki (both documents are enclosed).

### Reagents and antibodies

TGF-β was from Merck (Darmstadt, Germany). Fetal bovine serum was from Sera Laboratories International (Cinder Hill, UK). Glutathione-ethyl-ester (GEE), Diphenyleneiodonium chloride (DPI) and Butylated hydroxyanisole (BHA) were from Sigma (St Louis, USA). The caspase-3 substrate Ac-DEVD-AMC was from Pharmingen (San Diego, CA, USA). Antibodies: mouse anti-β-actin (clone AC-15, Sigma), rabbit anti-cleaved caspase-3 (Asp-175) from Cell Signaling Technology (Danvers, MA, USA), anti-F4/80 (Abcam, Cambridge, UK), mouse anti-E-cadherin (BD Pharmingen, NJ, USA), rabbit anti-ki67 (Abcam), mouse anti-NOX2 (Santa Cruz Biotechnology, CA, USA), anti-NOX4 raised by Sigma-Genosys against a peptide corresponding to the C-terminal loop region (aminoacids 499–511), mouse anti-α-SMA (Sigma, St Louis, USA), rabbit anti-phospho-Smad2 (Ser465/467) and rabbit anti-phospho-Smad3 (Ser423/425) from Cell Signaling Technology, goat anti-Smad2/3, anti-Smad7 and anti-TGF-β from Santa Cruz Biotechnology and mouse anti-vimentin (Sigma, St Louis, USA).

### Mice

Three animal experimental models of liver fibrosis were used for this study: two genetically modified mice and one drug-induced model. $Mdr2^{-/-}/p19^{ARF-/-}$ double null mice [15] displayed a fibrotic phenotype comparable to $Mdr2^{-/-}$ mice, widely used as a model for experimental liver fibrosis [16,17], characterized by severe hepatic injury and large periductal accumulation of MFBs, but showed the additional advantage of allowing the isolation of immortal cells for *in vitro* experiments [15]. $Stat3^{\Delta hc}/Mdr2^{-/-}$ mice show Stat3 conditional inactivation specifically in hepatocytes and cholangiocytes in a $Mdr2^{-/-}$ background [18], which strongly aggravates liver injury and fibrosis. Animals were sacrificed to evaluate liver histology at 2 and 7 weeks of age. C.B-17/IcrHsd-$Prkcd^{scid}$ (SCID) mice have been used as control. For $CCl_4$ experiments, $CCl_4$ (Sigma, St Louis, USA) was diluted 1:4 in ultrapure Olive Oil (Sigma, St Louis, USA) and injected intraperitoneally at a concentration of 1.5 mg per gram of body weight into 3-month old C57BL/6J mice. The treatment was performed two times a week for 6 weeks to induce hepatic fibrosis. Mice were sacrificed 3 days after the last injection and liver samples were collected and processed for immunohistochemical analysis.

### Cell models and cell culture conditions

No commercial cell lines have been used in this study. Mice stellate cells, myofibroblasts and hepatocytes were obtained in our or colleagues' laboratories and used in previous published works [14,18,19]: 1) By employing $p19^{ARF}$ deficiency, we established a non-transformed murine HSC model to investigate their plasticity and the dynamics of HSC activation [19]. The immortal cell line, referred to as M1-4HSC, showed stellate cell characteristics including the expression of desmin, glial fibrillary acidic protein, alpha-smooth muscle actin and pro-collagen I [19]. Treatment of these non-tumorigenic M1-4HSC with pro-fibrogenic TGF-β1 provoked a morphological transition to a myofibroblastoid cell type which was accompanied by enhanced cellular turnover and impaired migration [19]. These cells have been used in this study to analyze the role of NOX4 in the *in vitro* activation of HSC to MFB; 2) *In vivo*-activated MFBs derived from physiologically inflamed livers of $Mdr2/p19^{ARF}$ double-null mice were obtained as previously described [15] and used in this study in *in vitro* experiments to analyze the role of NOX4 in maintaining the myofibroblast phenotype; 3) Finally, hepatocytes from wild-type mice were isolated and immortalized with a puromycin-resistance retroviral vector pBabe encoding Simian virus 40 large T antigen (LTAg), as described [20] and were generously provided by Dr. AM Valverde (Madrid, Spain). These cells were used in this study to analyze the potential role of NOX4 in the TGF-β-induced effects related to fibrosis development, i.e., epithelial-mesenchymal transitions and apoptosis. For cell culture, cells were grown in DMEM (Lonza, Basel, Switzerland) supplemented with 10% FBS and maintained in a humidified atmosphere of 37°C, 5% CO2.

### Human samples

Biopsies from 28 chronic hepatitis C virus (HCV) patients showing different degrees of fibrosis or control liver samples extracted in surgeries from colorectal cancer patients with hepatic metastasis were collected in the Hospital Universitario de Alcorcón (Madrid, Spain). The control group was formed by 10 patients in whom liver biopsy was performed by altered function test. Liver biopsy examination revealed normal histology or minimal change.

### Immunohistochemistry and immunocytochemistry studies

For immunohistochemistry, sections of 4 μm-thick paraffin-embedded livers were stained with hematoxylin and eosine (H&E) or Trichrome (Sigma) for collagen staining using standard procedures. The immunostaining was performed by incubating primary antibodies (diluted from 1:50 to 1:100) overnight at 4°C and by visualization with the Vectastain ABC kit (Vector Laboratories, Burlingame, CA). Immunocytochemistry studies were performed as described previously [21]. Representative images were taken with a Spot 4.3 digital camera and edited in Adobe Photoshop. Cells were visualized in an Olympus BX-60 with the appropriate filters.

### Analysis of cell number

Cell number was analyzed after crystal violet staining [4].

### Total ROS production

Intracellular ROS content was measured by staining with the fluorescent probe $H_2$DCF-DA as described previously [22].

### Analysis of caspase-3 activity

Caspase-3 activity was analyzed fluorimetrically upon incubation of 20 µg of cell lysates with 6.6 µg/mL Ac-DEVD-AMC for 2 hours at 37°C [22]. Results are calculated as units of caspase-3 activity per microgram of protein per hour.

### Analysis of gene expression

RNeasy Mini Kit (Qiagen, Valencia, CA, USA) was used for total RNA isolation. Reverse transcription (RT) was carried out using the High Capacity Reverse Transcriptase kit (Applied Biosystems, Foster City, CA, USA), and 500 ng of total RNA from each sample for complementary DNA synthesis. PCR products in semiquantitative reactions were obtained after 30–35 cycles of amplification at annealing temperatures of 57–62°C, and analyzed by 1.5% agarose gel electrophoresis. Expression of *18S* was analyzed as a loading control, as indicated. The –RT channel contained RNA that had not been treated with the RT mixture.

For Real-Time quantitative PCR, expression levels were determined in duplicate in an ABIPrism7700 System, using the Sybr® Green PCR Master Mix (Applied Biosystems).

All the primers used for both semiquantitative PCR or Real-Time quantitative PCR reactions are listed in Suppl. Table 1 and 2, respectively.

### Western blot analysis

Total protein extracts and Western Blot procedure were carried out as previously described [22,23]. Antibodies were used at 1:1000, except β-actin (1:3000). Protein concentration was measured with the BCA$^{TM}$ Protein Assay kit (Pierce, Rockford, USA).

### Knock-down assays

Cells at 70% confluence were transiently transfected with 50 nM siRNA during 8 hours using TransIT-siQuest following manufacturer's instructions (Mirus, Madison, USA). Oligos were obtained from Sigma-Genosys (Suffolk, UK). The oligo sequences were as follows: unsilencing: GUAAGACACGACUUAUCGC; mouse NOX4: CAAGAAGAUUGUUGGAUAA. The unsilencing siRNA used was selected from previous works [22]. Specific oligos with maximal knock-down efficiency were selected among three different sequences for each gene.

### Statistics

All data represented at least three experiments and expressed as the mean ± SEM. Differences between groups were compared using either Student's t test or one-way ANOVA associated with the Dunnett's test. Statistical significance was assumed when $p<0.05$.

## Results

### Activation of the TGF-β/NOX4 pathway in fibrosis development

Mdr2$^{-/-}$ mice represent a widely used model for experimental liver fibrosis [16,17] and are characterized by chronic liver injury and large periductal accumulation of MFBs. Similarly, Mdr2$^{-/-}$/p19$^{ARF-/-}$ double null mice [15] displayed a fibrotic phenotype comparable to Mdr2$^{-/-}$ mice which allows, on one hand, investigation of *in vivo* fibrosis development and, on the other hand, isolation of MFBs for *in vitro* experiments that become immortalized upon loss of p19$^{ARF}$, a gene involved in the negative control of cell cycle [15]. As observed in Mdr2$^{-/-}$ mice, Mdr2$^{-/-}$/p19$^{ARF-/-}$ mice developed spontaneous fibrosis characterized by periductal accumulation of collagen and MFBs, as well as an increased number of Kupffer cells (F4/80 positive) (Suppl. Fig. 1). Importantly, these periductal changes were accompanied by damage of the hepatic parenchyma and compensatory hepatocyte proliferation, since we could not only detect increased apoptosis by cleaved caspase-3, but also increased numbers of Ki67 positive cells, (Fig. 1A). Fibrotic cells, easily recognized by their elongated form, condensed nuclei and positive expression for alpha-Smooth Muscle Actin (α-SMA) (Suppl. Fig. 1), stained for Ki67, but not for apoptosis. Of note, dying hepatocytes were mostly detected in the surrounding tissue of these fibrotic areas. Stat3$^{Alb\text{c}}$/Mdr2$^{-/-}$ mice represent a mouse model with conditional inactivation of Stat3 in hepatocytes and cholangiocytes of Mdr2$^{-/-}$ mice [18]. Loss of the hepatoprotective transcription factor Stat3 strongly aggravated liver injury and fibrosis of the Mdr2$^{-/-}$ fibrotic phenotype (Suppl. Fig. 2) leading to premature lethality. The compensatory hepatocyte proliferation due to parenchymal liver damage was severely reduced in this model (Suppl. Fig. 2, Fig. 1B).

Previous reports have indicated that several profibrotic genes are up-regulated at early stages of fibrosis development in Mdr2$^{-/-}$ mice, highlighting the major pro-fibrotic cytokine, TGF-β [24]. In agreement with these previous results, we found that both TGF-β and its downstream signal molecule, phospho-Smad2, were increased during fibrosis development in both animal models as analyzed by immunohistochemistry (Fig. 2 and Suppl. Fig. 3). Phospho-Smad2 staining intensity was higher at 2 weeks and decreased over time, inversely correlating with Smad7 level, a TGF-β pathway inhibitor. Importantly, NOX4 level was also found elevated in these fibrosis models in both hepatocytes and fibroblastoid cells. In the case of hepatocytes, NOX4 expression was more intense in those cells surrounding the MFBs area (Fig. 3A), which was coincident with the regions showing positive cells for cleaved caspase-3 (Suppl. Fig. 4). Interestingly, these observations were corroborated in a model of chemically-induced fibrosis by $CCl_4$ injection (Suppl. Fig. 5). CCl4 model has been widely used as an experimental model of chronic damage to the liver that produces fibrogenesis and may mimic the situation of human chronic liver diseases. These data together suggest that changes in the expression of NOX4 occur in different experimental animal models of hepatic fibrosis.

Since lack of p19$^{ARF}$ allows the culture of spontaneously immortalized cells, we isolated and cultured both HSC in an inactive state from p19$^{ARF-/-}$ non fibrotic livers and activated MFB from Mdr2$^{-/-}$/p19$^{ARF-/-}$ fibrotic livers, as described in the Materials and Methods section. These MFB, which have suffered the activation process *in vivo* during spontaneous fibrosis development in Mdr2$^{-/-}$/p19$^{ARF-/-}$mice, showed increased expression of NOX1, NOX2 and NOX4 at the mRNA level when compared to p19$^{ARF-/-}$ inactive HSC (Fig. 3B–D, left graphs). Thus, these results suggest that these NOX isoforms may be induced during the HSC activation process. In addition, and corroborating the results at the tissue level, immortalized hepatocytes showed very high NOX4 expression when compared to HSC or MFB, which was further up-regulated when they were treated with TGF-β (Fig. 3B, right graph). NOX1 expression was also predominantly expressed in hepatocytes, but was down-regulated by TGF-β in *in vitro* experiments (Fig. 3C, right graph). NOX2 was predominantly expressed in MFBs and was not affected by TGF-β in hepatocytes (Fig. 3D).

### Role of NOX4 in HSC activation and MFBs phenotype maintenance

Since NOX4 seemed to increase during the transdifferentiation process of HSC to MFBs and its role in this process is completely

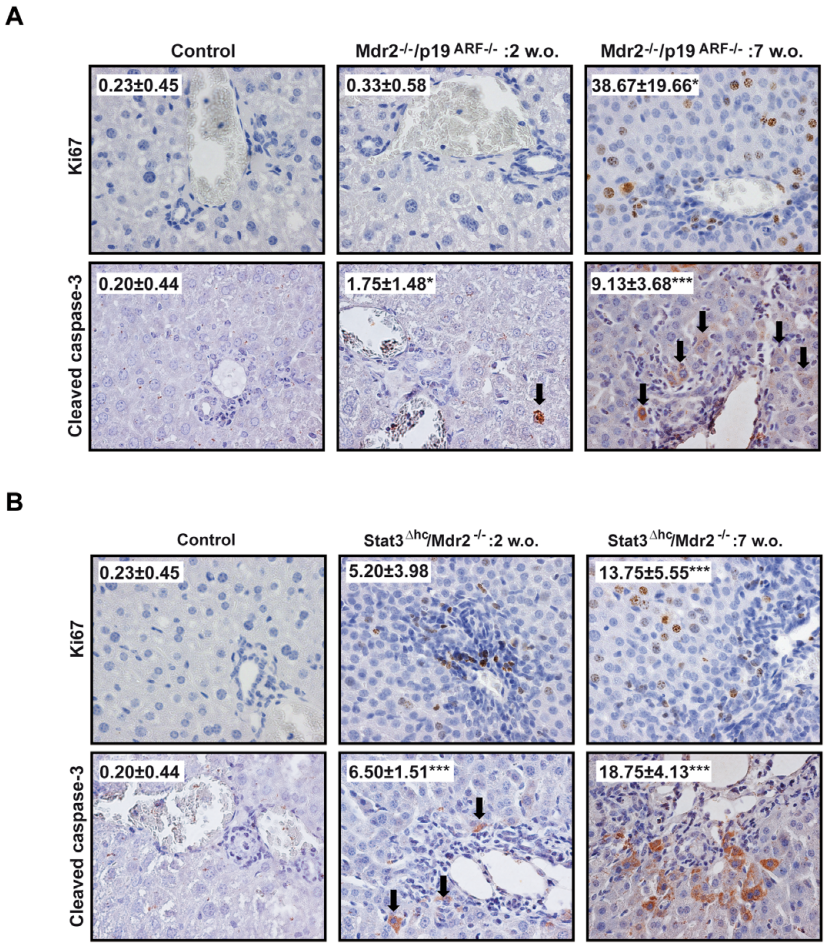


**Figure 1. Fibrosis development in Mdr2$^{-/-}$/p19$^{ARF-/-}$ and Stat3$^{\Delta hc}$/Mdr2$^{-/-}$ mice is accompanied by hepatocellular proliferation and apoptosis.** Representative 60x histological sections of livers from control or 2 or 7 weeks-old Mdr2$^{-/-}$/p19$^{ARF-/-}$ *(A)* and Stat3$^{\Delta hc}$/Mdr2$^{-/-}$ mice *(B)*: Ki67 (upper row) and cleaved caspase-3 (lower row). Inset: quantification of positive cells for each marker. Data represent the mean ± SEM of the number of positive cells in at least ten different fields. Student's t test calculated versus control sections (*p<0.05; **p<0.01;***p<0.001).
doi:10.1371/journal.pone.0045285.g001

unknown, we decided to focus our study on the potential role of NOX4 in the *in vitro* activation of HSC with TGF-β. As expected, TGF-β treatment induced HSC activation, featured by increase in α-SMA levels and E-cadherin down-regulation, which was accompanied by NOX1, NOX2 and NOX4 up-regulation (Fig. 4A). In the absence of TGF-β, this activation was not observed (Suppl. Fig. 6). Regulation of α-SMA at the protein level correlated with parallel changes at the mRNA level, along with up-regulation of vimentin and the extracellular matrix genes collagen I and fibronectin (Fig. 4B). The same panel shows that all these changes in gene expression induced by TGF-β were inhibited when NOX4 was knocked-down in cultured HSC cells. Importantly, phenotypical changes induced by TGF-β during the transdifferentiation process, such as morphological alterations and increased expression and reorganization of α-SMA and vimentin, were impaired when NOX4 was targeted knock-down (Fig. 4C). No apparent changes in the viability of these cells were observed in NOX4 deficient cells (results not shown).

Since TGF-β and NOX4 appeared to play a crucial role in the activation of HSC, we next wondered if they could play a role in the maintenance of the activated MFB phenotype. For this purpose, firstly we treated isolated Mdr2$^{-/-}$/p19$^{ARF-/-}$ MFBs during 72 hours with LY364947, an inhibitor of the TGF-β receptor I (TβRI), in *in vitro* experiments. As shown in Figure 5A, inhibition of the TβRI reversed the MFB phenotype, measured as expression of pro-fibrotic genes, which correlated with a decrease in NOX4 mRNA levels. Importantly, this fact implicates plasticity of the MFB phenotype suggesting that it is possible to reverse the MFB activated state towards a more inactive HSC-like phenotype. It is worthy to note that blocking the TGF-β pathway down-

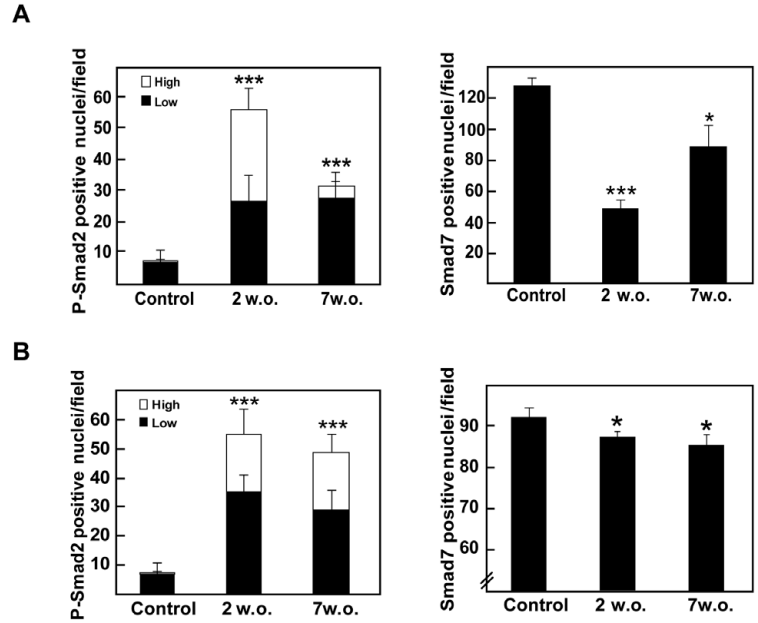


**Figure 2. TGF-β pathway is activated at early stages of fibrosis in Mdr2$^{-/-}$/p19$^{ARF-/-}$ and Stat3$^{\Delta hc}$/Mdr2$^{-/-}$ mice.** 60x histological sections of livers from control or 2 or 7 weeks-old Mdr2$^{-/-}$/p19$^{ARF-/-}$ *(A)* and Stat3$^{\Delta hc}$/Mdr2$^{-/-}$ mice *(B)* were stained with phospho-Smad2 or Smad7 and the number of positive cells was quantified. Left graph: positive nuclei for phospho-Smad2 with low or high signal intensity. Right graph: positive nuclei for Smad7. Data represent the mean ± SEM of cells in at least ten different fields. Student's t test calculated versus control sections (*p<0.05; **p<0.01;***p<0.001).
doi:10.1371/journal.pone.0045285.g002

regulated TGF-β expression, indicating the existence of an autocrine positive feed-back loop implicated in the maintenance of the MFB properties. In addition, as shown in Fig. 5B, NOX4 knock-down produced a similar change as the one found with the TβRI inhibitor. Indeed, the expression of pro-fibrotic genes, as well as α-SMA and vimentin expression and organization, were significantly diminished when NOX4 was knocked-down, cells acquiring an HSC-like morphology (Fig. 5C). Furthermore, desmin expression, as a marker of activated stellate cells, decreased when NOX4 was knocked-down, correlating with the reversion of MFB phenotype. However, NOX4 silencing was unable to inhibit the expression of either TGF-β or its receptor (Fig. 5B, 5D), and it did not alter Smad2/3 phosphorylation status (Fig. 5D).

These results together suggest that NOX4 acts downstream TGF-β and controls the expression of different pro-fibrotic genes; however, autocrine expression of the cytokine in MFB, and activation of its downstream immediate signals, i.e., Smads, seems to be independent of NOX4.

It is interesting to point out that NOX4 expression at the mRNA level in both HSC and MFB was much higher than the expression of the other isoforms NOX1 and NOX2 (50-fold higher than NOX2 and 25-fold higher than NOX1 in hepatocytes; 80-fold higher than NOX2 and 60-fold higher than NOX1 in HSC: Suppl. Fig. 7), which may explain why neither NOX1 nor NOX2 replaces NOX4 function.

## Role of NOX4 in hepatocytes

Finally, we decided to study the putative role of NOX4 in TGF-β-induced effects in hepatocytes. As shown in Fig. 6A, NOX4 expression was significantly up-regulated reaching the maximum mRNA levels at 12 h and the maximum protein level at 24–48 hours upon TGF-β treatment. As we and others have previously reported in several experimental models, induction of apoptosis by TGF-β was impaired when NOX4 was knocked-down (Fig. 6B). These *in vitro* data support the immunohistochemistry studies, where elevated NOX4 expression seemed to correlate with the areas of higher apoptosis of hepatocytes (Suppl. Fig 4). Interestingly, supplementation of cell culture medium with either antioxidants or a general inhibitor of NADPH oxidases (DPI) blocked TGF-β-induced ROS production and caspase-3 activation in hepatocytes (Suppl. Fig. 8A, B). In a similar way, a permeable form of GSH and DPI also attenuated changes in gene expression addressed by TGF-β in HSC (Suppl. Fig. 8C), highlighting the relevant role played by ROS in these processes.

We have previously reported that some liver cells are able to impair the pro-apoptotic effects of TGF-β and undergo EMT, characterized by cytoskeleton rearrangement and changes in gene expression leading to a mesenchymal phenotype with up-regulation of Snail, vimentin and α-SMA and loss of E-cadherin expression [21,25]. In view of the results regarding apoptosis, we next wondered whether NOX4 could be mediating TGF-β-induced EMT *in vitro*. NOX4 knock-down did not influence TGF-β-induced cytoskeletal changes, neither affected the expression of several EMT-related genes (Fig. 6C, D). In summary, NOX4 is

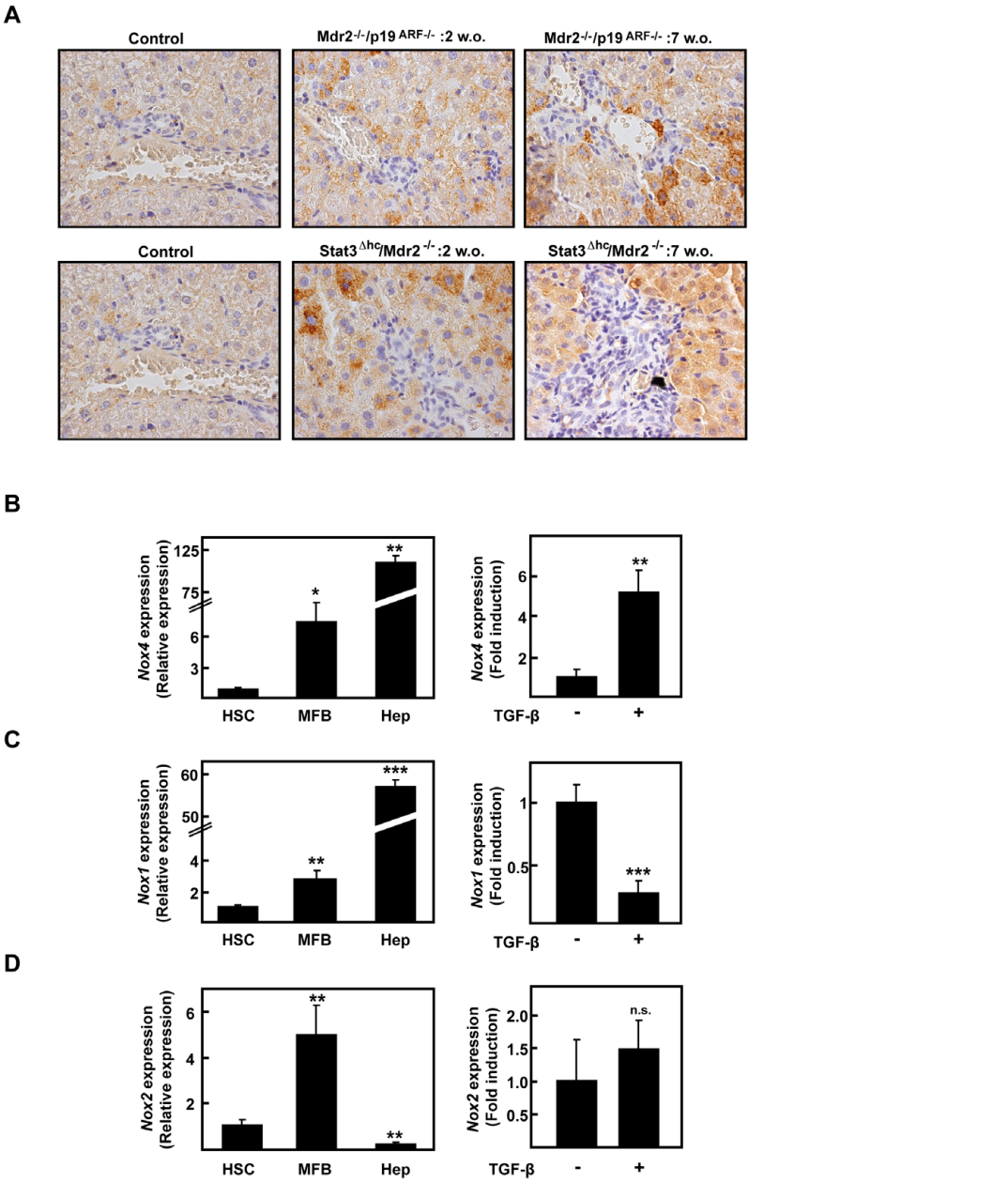


**Figure 3. NOX4 expression is increased concomitant with fibrosis development in Mdr2$^{-/-}$/p19$^{ARF-/-}$ and Stat3$^{\Delta hc}$/Mdr2$^{-/-}$ mice.** (*A*) Representative 60x photographs from NOX4 immunohistochemistry performed in control or 2 or 7 weeks-old livers. *(B, C, D)* Real time PCR of *NOX4, NOX1* or *NOX2. Left*: comparison of cultures of inactive stellate cells (HSC) isolated from p19$^{ARF-/-}$ mice, *in vivo* activated myofibroblats (MFB) isolated from fibrotic Mdr2$^{-/-}$/p19$^{ARF-/-}$ livers and wild type immortalized hepatocytes (Hep) (see Materials and Methods section). *Right:* immortalized hepatocytes treated or not with 2 ng/ml TGF-β. Data represent the mean ± SEM of three independent experiments, and were calculated relative to HSC (left) or untreated hepatocytes (right) respectively, which were given an arbitrary value of 1. Student's t test calculated versus HSC cells in the left column (*p<0.05; **p<0.01) or untreated hepatocytes in the right column (**p<0.01).
doi:10.1371/journal.pone.0045285.g003

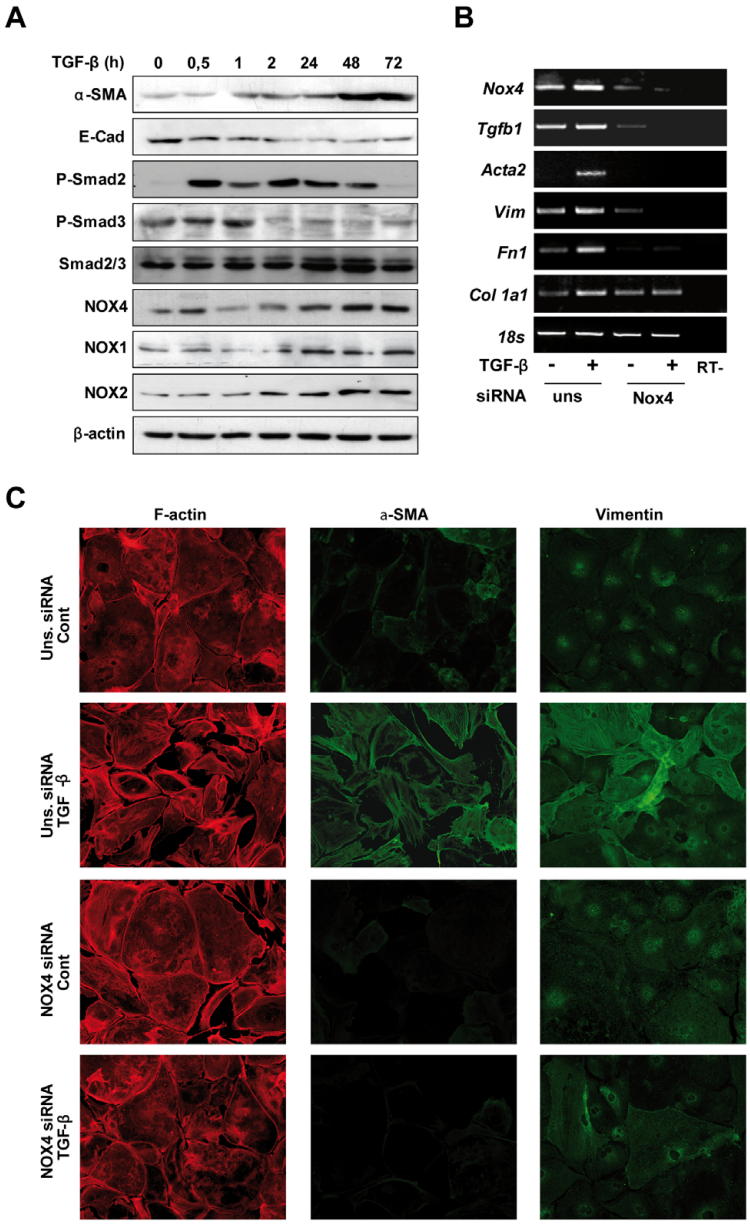


**Figure 4. NOX4 knock-down inhibits TGF-β-dependent HSC activation.** (*A*) $p19^{ARF-/-}$ HSC cells at early passages were treated for the indicated times with 2 ng/ml TGF-β and a Western blot of total extracts was performed. β-actin was used as loading control. Additional information to this experiment is presented in Suppl. Fig. 6, where the expression of the different proteins in HSC cultured for 24, 48 and 72 h in the absence of treatments is shown, as well as densitometric analysis of the Western blots. In (*B*) and (*C*), $p19^{ARF-/-}$ HSC cells were transfected with either an unsilencing siRNA (uns siRNA) or a specific siRNA for NOX4 (NOX4 siRNA) and then treated or not with 2 ng/ml TGF-β during 48 hours, when it was performed: (*B*) RT-PCR of *NOX4*, α-SMA (*Acta2*), vimentin (*vim*), fibronectin (*Fn1*) and collagen I (*Col1a1*); (*C*) immunofluorescence images of F-actin, α-SMA and vimentin. A representative image for each RT-PCR *(B)* or immunofluorescence staining *(C)* is shown. *18S* was used as loading control in *B*. Since HSC are very sensitive to serum deprivation, all experiments were carried out in the presence of 10% FBS.
doi:10.1371/journal.pone.0045285.g004

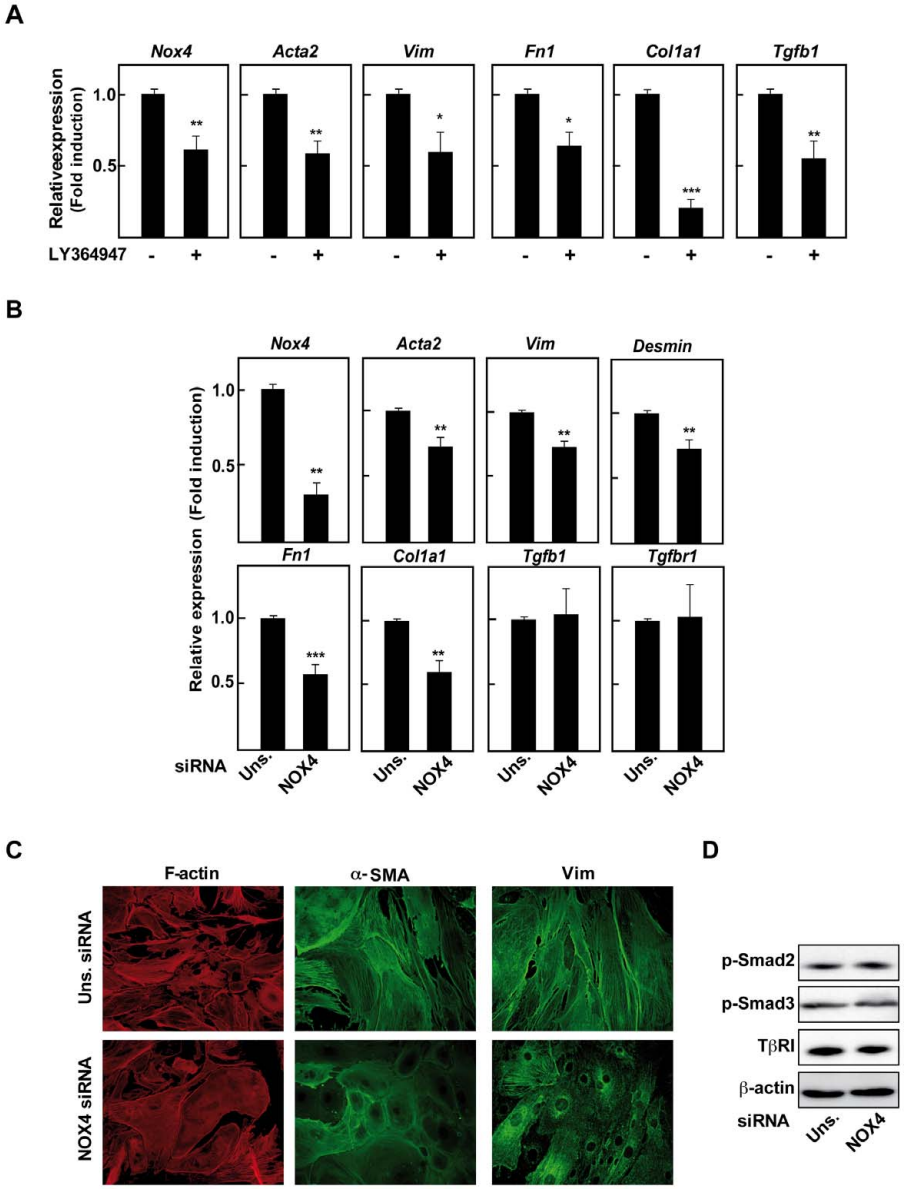


**Figure 5. NOX4 downstream autocrine TGF-β is necessary to maintain the activated phenotype of cultured Mdr2$^{-/-}$/p19$^{ARF-/-}$ MFB.** MFB isolated from fibrotic Mdr2$^{-/-}$/p19$^{ARF-/-}$ livers were used. *(A)* Real time PCR of Mdr2$^{-/-}$/p19$^{ARF-/-}$ MFB treated for 72 hours with 10 μM LY36494 (TRβI inhibitor): *NOX4*, α-SMA (*Acta2*), vimentin (*vim*), fibronectin (*Fn1*), collagen I (*Col1a1*) and TGF-$\beta_1$ (*Tgfb1*). In *B–D*, Mdr2$^{-/-}$/p19$^{ARF-/-}$ MFB were transfected with either an unsilencing siRNA (uns siRNA) or a specific siRNA for NOX4 (NOX4 siRNA) for 72 hours, when it was performed: *(B)* Real time PCR of the indicated genes. *(C)* Immunofluorescence staining of F-actin, α-SMA and vimentin. *(D)* Western blot of total lysates. β-actin was used as loading control. Data represent the mean ± SEM of three to six independent experiments, and were calculated relative to untreated MFB *(A)* or unsilencing-transfected cells *(B)* (*$p<0.05$; **$p<0.01$).
doi:10.1371/journal.pone.0045285.g005

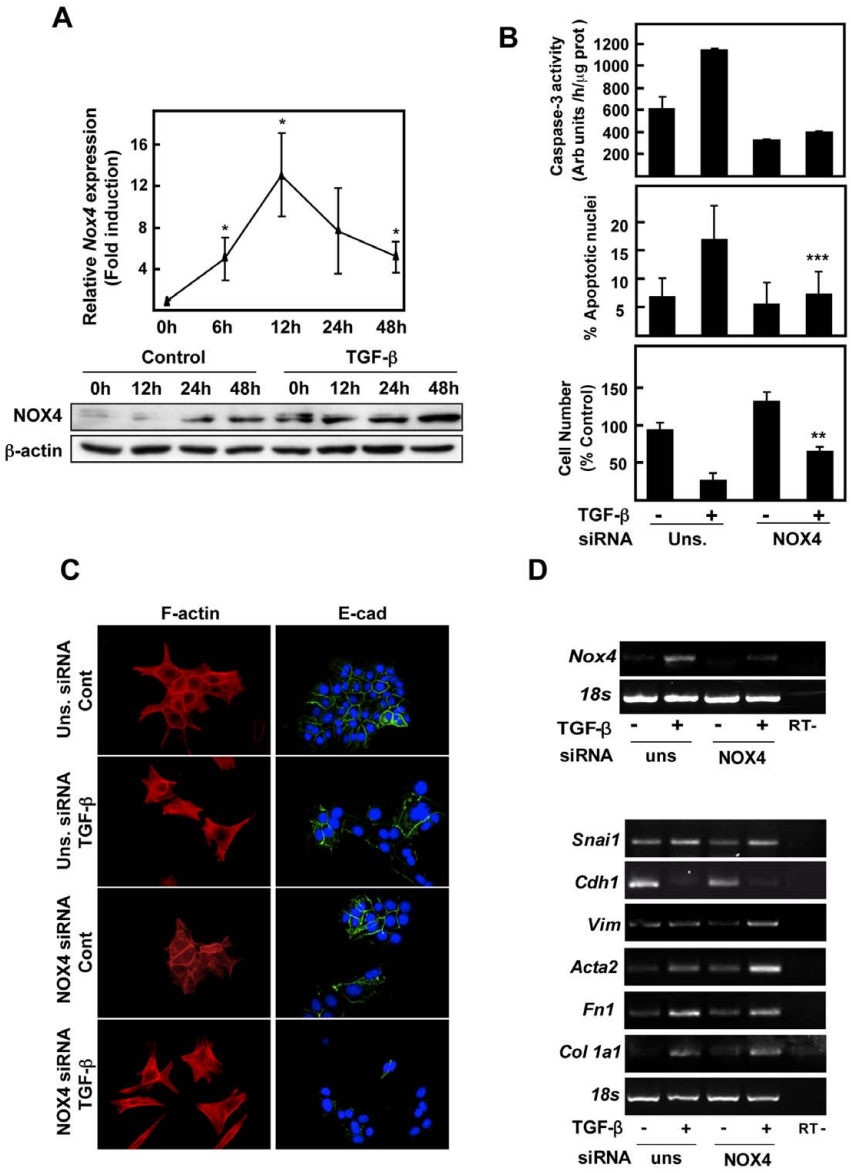


**Figure 6. NOX4 is required for apoptosisbut not necessary for the EMT process, induced by TGF-β in hepatocytes.** *(A)* TGF-β induces NOX4 expression in hepatocytes. NOX4 transript and protein levels were determined by Real time-PCR (upper panel) and western blot (lower panel), respectively, at the indicated times of treatment with 2 ng/ml TGF-β. In *B–D*, immortalized hepatocytes were transfected with either an unsilencing siRNA (uns siRNA) or a specific siRNA for NOX4 (NOX4 siRNA), serum-depleted for 4 hours and, finally, treated or not with 2 ng/ml TGF-β. *(B)* Cell death analysis: activation of caspase-3 activity at 16 hours, where the peak of maximal activation was found *(upper graph)*; percentage of cells with apoptotic nuclei at 48 h upon nuclear staining with DAPI *(middle graph)*; loss in cell viability at 48 h *(lower graph)*. Data represent the mean ± SEM of three independent experiments. Student's t test calculated comparing TGF-β-treated cells between the two conditions with the different siRNAs (**$p<0.01$; ***$p<0.001$). *(C)* Fluorescence microscopy staining for F-actin and E-cadherin at 48 hours. *(D)* Representative RT-PCR of the indicated genes after 3 h of treatment to observe the effects on *Nox4* expression (upper panel) and 48 h of treatment to analyze the effects on EMT-related genes (bottom panel). *18S* was used as loading control.
doi:10.1371/journal.pone.0045285.g006

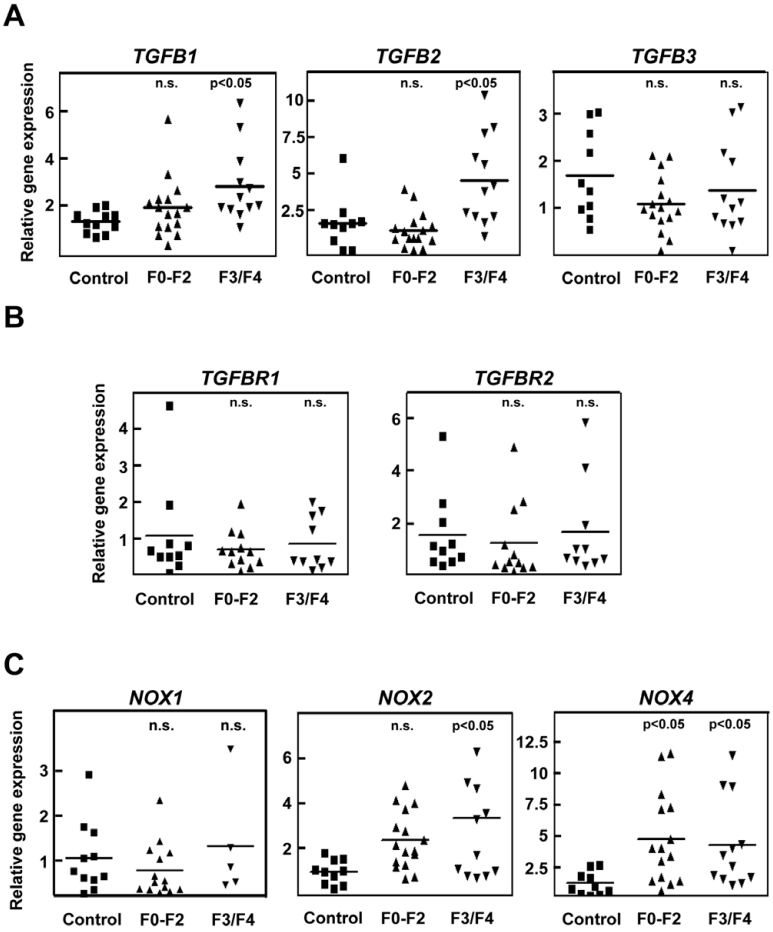


**Figure 7. TGF-β1 and 2, NOX2 and NOX4 are up-regulated in human samples from patients with HCV-derived fibrosis.** Samples from patients showing control livers (control; n = 10), low or mildly fibrotic livers (F0–F2; n = 16) or severely fibrotic and cirrhotic livers (F3/F4; n = 12). Real time determination of TGF-$\beta_1$(*TGFB1*), TGF-$\beta_2$ (*TGFB2*), TGF-$\beta_3$ (*TGFB3*) (*A*), TGFβRI and TGFβRII (*TGFBR1*, *TGFBR2*) (*B*), and *NOX1*, *NOX2* and *NOX4* (*C*). Statistic was calculated using one-way ANOVA associated with Dunnett's test.
doi:10.1371/journal.pone.0045285.g007

implicated in apoptosis but not in the EMT process that TGF-β induces in hepatocytes.

### Up-regulation of TGF-β and NOX4 in human samples from HCV infected patients

Since our *in vivo* and *in vitro* results in animal models pointed to a crucial role for NOX4 in fibrosis development, we next studied the situation in human samples. For this reason, we chose patients suffering from different degrees of liver fibrosis associated to HCV infection, who were classified as having mildly fibrotic livers (F0–F2) or severely fibrotic and cirrhotic livers (F3/F4) (Table 1). Comparing with samples from control livers, we performed real time PCR determinations of the three isoforms of TGF-β and the corresponding receptors, and also NOX1, NOX2 and NOX4. As shown in Fig. 7, TGF-β1 shows a clear tendency to increase from F0/F2 stages, showing significant enhanced levels in F3/F4 patients. TGF-β2 was also significantly increased in the F3/F4 stage (Fig. 7A). No relevant changes in the expression of their receptors were observed. Interestingly, NOX1 expression did not show any significant change (Fig. 7C, left graph), but NOX2 and NOX4 were significantly up-regulated in fibrotic livers, being the relative increase in NOX4 higher than that observed for NOX2 (Fig. 7C).

## Discussion

Chronic liver disease often progresses to fibrosis and finally to cirrhosis, which is a preneoplastic condition [1]. Thus far, there are no direct therapies aimed at liver fibrosis reversal, therefore innovative antifibrogenic approaches are needed [26]. Different models of hepatic fibrosis have been used to study the molecular

**Table 1.** Demographic, virological and histopathological characteristics of patients with chronic hepatitis C.

| | | |
|---|---|---|
| Age (yr) (Median and range) | | 46 (31–67) |
| Gender (M/F) | | 17/11 |
| Baseline Viral load ($\times 10^3$ IU/ml) (Mean $\pm$ SD) | | 1.36±2.05 |
| Genotype distribution (%) | Ia | 7.14 |
| | Ib | 75.00 |
| | II | 3.57 |
| | III | 14.28 |
| Activity distribution (n, %) (METAVIR) | 0 | 0 (0) |
| | 1 | 11 (39.28) |
| | 2 | 14 (50.00) |
| | 3 | 3 (10.71) |
| | 4 | 0 (0) |
| Fibrosis distribution (n, %) (METAVIR) | 0 | 1 (3.57) |
| | 1 | 11 (39.28) |
| | 2 | 4 (14.28) |
| | 3 | 7 (25.00) |
| | 4 | 5 (17.85) |

Tissue of liver biopsies from 28 patients with chronic hepatitis C in different stages of liver fibrosis was examined for the gene expression analysis shown in Fig. 7.

doi:10.1371/journal.pone.0045285.t001

pathogenesis of this disease. From these studies, several key generalizations have been done [1]: i) TGF-β is the most potent liver pro-fibrogenic cytokine; ii) oxidative stress induces liver fibrosis; iii) blocking normal liver regeneration by massive hepatocyte apoptosis turns out to be pro-fibrogenic. One of the most studied mechanisms of fibrogenesis actually influenced by ROS is myofibroblast activation. Previous reports and results presented in this manuscript have revealed that stellate cell transdifferentiation into myofibroblast is inhibited by antioxidants [27,28]. NOX4 downstream TGF-β has been described as the main mediator for myofibroblast activation in different organs such as heart [12], lung [11], kidney [13] and diseased prostatic stroma [14]. However, very few were known about the role of NOX4 in liver fibrosis. Results presented here indicate that induction of NOX4 occurs in three different animal models of liver fibrosis and in chronic HCV infection in humans, associated with activation of the TGF-β pathway, appearance of fibrotic areas and hepatocyte proliferation and apoptosis. NOX4 may play a key role in liver fibrosis development, downstream TGF-β, at two different levels: i) *in vitro* experiments reveal that NOX4 is required for both HSC activation and maintenance of the activated phenotype in MFBs and ii) hepatocytes respond to TGF-β by inducing NOX4 that is required for its pro-apoptotic response, which might be relevant to blunt regeneration and create a pro-fibrogenic microenvironment.

However, the role of NOX proteins in liver fibrogenesis is not only circumscribed to NOX4. Thus, studies performed in $Nox1^{-/-}$, $Nox2^{-/-}$ or $p47phox^{-/-}$ mice have pointed out the importance of NOX1 and NOX2 in fibrosis development [5,29,30]. Our results indicate that expression of NOX4 at the mRNA levels is much higher than those found for NOX1 and NOX2 in HSCs and hepatocytes, and functions are not redundant, since knock-down of NOX4 in these cells cause effects that cannot be prevented by the other NOXes. It is possible that each isoform plays differential roles in liver fibrosis. Indeed, it has been suggested that NOX1 promotes myofibroblast proliferation by PTEN inactivation to positively regulate an Akt/FOXO4/p27 signaling pathway [29]. NOX2, highly expressed in macrophages and bone marrow-derived cells [8] may be acting in the process of phagocytosis of dead hepatocytes [30]. NOX1 activity might also contribute to the inflammatory process promoting COX-2 expression and prostaglandin synthesis in hepatocytes [31]. Interestingly, whereas the revised version of this manuscript was being prepared, evidences for the role of dual NOX4/NOX1 pharmacological inhibitors in decreasing both the apparition of fibrogenic markers and hepatocyte apoptosis *in vivo*, upon bile duct ligation, were reported [32], highlighting the relevant role of NOX1 and NOX4 in liver fibrosis and opening new perspectives for its treatment.

Hepatic fibrosis has been considered as an irreversible process but recent experimental and clinical data indicate that removal of the pro-fibrotic agent or condition may reverse liver fibrosis [33]. Results presented in this manuscript suggest that either TβRI inhibition or NOX4 silencing reverses the MFB phenotype, decreasing the expression of extracellular matrix genes, such as collagen I or fibronectin, down-regulating α-SMA and vimentin expression and changing cell morphology, which loses myofibroblastic appearance. Since it has been recently proposed that NOX4 modulates α-SMA and procollagen I (alpha1) expression in pulmonary fibrosis by controlling activation of Smad2/3 [34], we checked the effect of silencing NOX4 on TGF-β levels and Smad2/3 phosphorylation. Our results have indicated that NOX4 clearly acts downstream TGF-β-independently from Smads activation. It also has been described that NOX4 is critical for maintenance of smooth muscle gene expression in vascular smooth muscle cells [35], where ROS production impairs the TGF-β-induced phosphorylation of Ser103 on serum response factor (SRF) and reduces its transcriptional activity. Thus, NOX4 may play an important role associated with the α-SMA phenotype, being not only important in fibrotic processes, but also in cardiovascular physiology.

We have previously described that liver cells respond to TGF-β *in vitro* undergoing EMT [25,36]. The role of EMT is perhaps the most intriguing and controversial of recent hypothesis on the origin mechanisms of liver fibrosis [37]. Strong evidences indicate that hepatocytes from transgenic animals that overexpress Snail (a master gene involved in EMT through its capacity to repress E-cadherin gene, among others) fully undergo EMT [38] and may propagate liver fibrosis progression [39]. However, under normal genetic background, data from different experimental approaches in animals and humans show controversy [40]. Our results show that EMT occurs in hepatocytes *in vitro*, but NOX4 is not required for this process. However, NOX4 mediates TGF-β-induced cell death that is prevented in the presence of antioxidants. In agreement with these results, it has been recently proposed a role for NOX4 in epithelial cell death during development of bleomycin-induced lung fibrosis [41]. Using a model of NOX4-deficient mice, authors demonstrated that these animals were resistant to fibrosis due to the abrogation of TGF-β-induced apoptosis in epithelial cells. Prevention of apoptosis impaired fibrosis development, although inflammation was comparable to wild-type. A similar situation may occur in liver fibrosis, where engulfment of apoptotic bodies by HSC contributes to induce their activation [7]. Indeed, hepatocyte apoptosis not only would facilitate fibrosis through blocking liver regeneration, but it could play an active role. In this line of evidence, inhibiting apoptosis decreased the liver profibrogenic response [7,42]. Additionally to the crucial role of NOX4 in TGF-β-induced cell death, recent

results indicate that it may be also required for apoptosis induced by other stimuli in liver cells, such as FasL and TNF-α/actinomycin D [32].

Finally, the finding that NOX4 is induced during the progression of a HCV disease reinforces the hypothesis of a role for NOX4 in human liver fibrosis. The magnitude of NOX4 up-regulation is higher than that observed for its co-partner NOX2 and, interestingly, we could not find any significant change in the expression of NOX1. NOX4 induction is observed at early stages of the disease when increases of TGF-β1 and 2 are not significant yet. This could be mediated by release of inflammatory signals that, indeed, up-regulate NOX4 in hepatocytes [31]. Furthermore, different reports support that HCV induces a persistent elevation and increased nuclear localization of NOX4 in *in vitro* assays in hepatocytes, a process that was TGF-β-dependent [43,44]. Collectively, all these data provide evidences to propose that HCV-induced NOX4 may contribute to ROS production and may be related to HCV-induced liver disease. Results presented in this manuscript support that NOX4 could play an essential role inducing activation of stellate cells and apoptosis of hepatocytes under these conditions of human disease, contributing to the development of liver fibrosis.

Development of first-in-class series of NOX4 inhibitors for the potential treatment of fibrotic diseases, cardiovascular and metabolic syndromes is in progress [45]. Liver fibrosis might be considered for future clinical trials with these drugs. Likewise, ROS and NOX4 induced by TGF-β have proved to be therapeutic targets of polyenylphosphatidylcholine in the suppression of human stellate cell activation [46]. Since NOX4 is mainly expressed in hepatocytes and HSC [8], according to the results presented in this manuscript, NOX4 inhibitors would specifically prevent HSC activation and hepatocytes cell death, without altering the role of other NOXes, such as NOX2, which might play defense function in Kupffer cells. In advanced stages of the disease, NOX4 inhibitors might be able to reverse the fibrotic phenotype acting on MFBs. Furthermore, and not less important, we demonstrate that silencing NOX4 prevents fibrogenesis but has no effect on TGF-β-mediated Smads phosphorylation. Indeed, the use of pharmacological drugs targeting NOX4 expression/activation would inhibit fibrogenesis without blocking other beneficial effects of TGF-β, such as growth inhibition in the epithelial cells, which prevents initiation of a pre-neoplastic stage.

In summary, here we show that NOX4 expression is elevated in the livers of experimental in vivo models of liver fibrosis and in patients with chronic HCV-derived infection, increasing along the fibrosis degree. NOX4, downstream TGF-β pathway, would play a role in the acquisition and maintenance of the MFB phenotype, as well as in mediating death of hepatocytes, which provokes inflammation and facilitates extracellular matrix deposit.

## Supporting Information

**Figure S1 Fibrosis development in Mdr2$^{-/-}$/p19$^{ARF-/-}$ mice.** Representative histological sections of livers from control or 2 or 7 weeks-old Mdr2$^{-/-}$/p19$^{ARF-/-}$ mice. H&E, trichrome C staining and immunohistochemistru of F4/80, α-SMA, E-cadherin (E-cad) or vimentin (Vim) are shown.
(TIF)

**Figure S2 Fibrosis development in Stat3$^{\Delta hc}$/Mdr2$^{-/-}$ mice.** Representative histological sections of livers from control or 2 or 7 weeks-old Stat3$^{\Delta hc}$/Mdr2$^{-/-}$ mice. H&E, trichrome C staining and immunohistochemistru of F4/80, α-SMA, E-cadherin (E-cad) or vimentin (Vim) are shown.
(TIF)

**Figure S3 TGF-β pathway is activated in Mdr2$^{-/-}$/p19$^{ARF-/-}$ and Stat3$^{\Delta hc}$/Mdr2$^{-/-}$ mice.** Immunohistochemistry analysis of TGF-β, phospho-Smad2 or Smad7 in Mdr2$^{-/-}$/p19$^{ARF-/-}$ (**A**) and Stat3$^{\Delta hc}$/Mdr2$^{-/-}$ mice (**B**).
(TIF)

**Figure S4 NOX4 expression in hepatocytes correlates with activation of caspase-3 in fibrotic tissues from Mdr2$^{-/-}$/p19$^{ARF-/-}$ mice.** Immunohistochemistry analysis of NOX4 and the active form (cleaved) of caspase-3 in: hepatocytes around the vascular (up) or fibrotic (bottom) areas (**A**); two serial sections showing coincidence in the expression of both proteins in the same cells (**B**).
(TIF)

**Figure S5 NOX4 expression is increased concomitant with fibrosis development in $CCl_4$ injection.** Liver samples were collected and processed for immunohistochemical analysis. Representative results for NOX4, cleaved caspase-3 and Ki67 are shown.
(TIF)

**Figure S6 Additional information to Figure 4.** Expression of the different proteins analyzed in the Western blot of Figure 4A in HSC cells cultures for 24, 48 and 72 h in the absence of treatments (**A**). Quantitation of the intensity of the bands through densitometric analysis, relative to loading (β-actin) is shown above each band. A similar quantification approach for Western blot in Figure 4A is shown in **B**.
(TIF)

**Figure S7 Role of NOX4 knock-down with specific siRNA on the expression of NOX4, NOX2 and NOX1 in HSC (A) and MFB (B).** p19$^{ARF-/-}$ HSC cells (**A**) and Mdr2$^{-/-}$/p19$^{ARF-/-}$ MFB (**B**) were transfected with either an unsilencing siRNA (uns. siRNA) or a specific siRNA for NOX4 (NOX4 siRNA) as described in Figs. 4 and 5, respectively. In the case of HSC (**A**), cells were either not treated or treated with TGF-β (2 ng/ml), as indicated in the figure. Data shown correspond to the real-time PCR analysis of the mRNA levels of NOX4, NOX2 and NOX1, which were calculated relative to 18S expression. In order to compare the expression level among the different isoforms, we gave an arbitrary value of 1 to NOX4 expression under basal conditions in both HSC (**A**) and MFB (**B**), and all the data are referred to this value. Mean ± S.E.M. is shown and the specific value of the mean detailed above each bar.
(TIF)

**Figure S8 Role of antioxidants (GEE and BHA) or a NADPH oxidase inhibitor (DPI) on the effects of TGF-β on ROS production and apoptosis in hepatocytes (A and B, respectively) and activation of HSC (C).** Cells were pre-incubated during 30 min with 1 μM DPI, 2 mM GEE or 200 μM BHA, as indicated in each figure, before adding 2 ng/ml of TGF-β. The same concentrations of the agents were maintained during all the TGF-β treatment. **A.** After 3 h of treatment in hepatocytes, intracellular content of ROS was analyzed through fluorimetric assay as detailed in the Materials and Methods section. Data represent the mean ± S.E.M. of 3 independent experiments in triplicate and are referred to the value in untreated cells (100%). **B.** After 16 h of treatment in hepatocytes, proteins were collected for caspase-3 analysis. Data represent the mean ± S.E.M. of 3 independent experiments in duplicate and are expressed as arbitrary units per hour and per microgram of protein. **C.** After 48 h of treatment in HSC, RNA was collected for analysis of expression by RT-PCR of the genes

detailed in the figure. A representative experiment out of 3 is shown.
(TIF)

**Table S1 Mouse primer sequences used for semiquantitative PCR.**
(DOC)

**Table S2 Mouse and human primer sequences used for quantitative real-time PCR.**
(DOC)

## Acknowledgments

We acknowledge the encouraging advices of Dr. Victor Thannickal (University of Alabama at Birmingham, USA) and the excellent technical support of Esther Bertran, Greta Ripoll and Judit Lopez. We also thank Dr. Valeria Poli for providing the floxed Stat3 mice. We dedicate this manuscript to the memory of Dr. Nelson Fausto, Professor of Pathology and Senior Advisor to the Dean of the School of Medicine and former Chairman of the Department of Pathology at the University of Washington Medical School, died last April. We enthusiastically acknowledge his continuous help for the development of our research line, his inspiration, his advices and his friendship.

## Author Contributions

Conceived and designed the experiments: PS WM IF. Performed the experiments: PS JM EC-M CR HH. Analyzed the data: PS CR CMF-R WM IF. Contributed reagents/materials/analysis tools: CMF-R FP RE. Wrote the paper: PS IF.

## References

1. Brenner DA (2009) Molecular pathogenesis of liver fibrosis. Trans Am Clin Climatol Assoc 120: 361–368.
2. Matsuzaki K (2009) Modulation of TGF-beta signaling during progression of chronic liver diseases. Front Biosci 14: 2923–2934.
3. Proell V, Carmona-Cuenca I, Murillo MM, Huber H, Fabregat I, et al. (2007) TGF-beta dependent regulation of oxygen radicals during transdifferentiation of activated hepatic stellate cells to myofibroblastoid cells. Comp Hepatol 6: 1.
4. Sanchez A, Alvarez AM, Benito M, Fabregat I (1996) Apoptosis induced by transforming growth factor-beta in fetal hepatocyte primary cultures: involvement of reactive oxygen intermediates. J Biol Chem 271: 7416–7422.
5. De Minicis S, Seki E, Paik YH, Osterreicher CH, Kodama Y, et al. (2010) Role and cellular source of nicotinamide adenine dinucleotide phosphate oxidase in hepatic fibrosis. Hepatology 52: 1420–1430.
6. Aram G, Potter JJ, Liu X, Wang L, Torbenson MS, et al. (2009) Deficiency of nicotinamide adenine dinucleotide phosphate, reduced form oxidase enhances hepatocellular injury but attenuates fibrosis after chronic carbon tetrachloride administration. Hepatology 49: 911–919.
7. Jiang JX, Venugopal S, Serizawa N, Chen X, Scott F, et al. (2010) Reduced nicotinamide adenine dinucleotide phosphate oxidase 2 plays a key role in stellate cell activation and liver fibrogenesis in vivo. Gastroenterology 139: 1375–1384.
8. Paik YH, Iwaisako K, Seki E, Inokuchi S, Schnabl B, et al. (2011) The nicotinamide adenine dinucleotide phosphate oxidase (NOX) homologues NOX1 and NOX2/gp91(phox) mediate hepatic fibrosis in mice. Hepatology 53: 1730–1741.
9. Carmona-Cuenca I, Roncero C, Sancho P, Caja L, Fausto N, et al. (2008) Upregulation of the NADPH oxidase NOX4 by TGF-beta in hepatocytes is required for its pro-apoptotic activity. J Hepatol 49: 965–976.
10. Barnes JL, Gorin Y (2011) Myofibroblast differentiation during fibrosis: role of NAD(P)H oxidases. Kidney Int 79: 944–956.
11. Hecker L, Vittal R, Jones T, Jagirdar R, Luckhardt TR, et al. (2009) NADPH oxidase-4 mediates myofibroblast activation and fibrogenic responses to lung injury. Nat Med 15: 1077–1081.
12. Cucoranu I, Clempus R, Dikalova A, Phelan PJ, Ariyan S, et al. (2005) NAD(P)H oxidase 4 mediates transforming growth factor-beta1-induced differentiation of cardiac fibroblasts into myofibroblasts. Circ Res 97: 900–907.
13. Bondi CD, Manickam N, Lee DY, Block K, Gorin Y, et al. (2010) NAD(P)H oxidase mediates TGF-beta1-induced activation of kidney myofibroblasts. J Am Soc Nephrol 21: 93–102.
14. Sampson N, Koziel R, Zenzmaier C, Bubendorf L, Plas E, et al. (2011) ROS signaling by NOX4 drives fibroblast-to-myofibroblast differentiation in the diseased prostatic stroma. Mol Endocrinol 25: 503–515.
15. van Zijl F, Mair M, Csiszar A, Schneller D, Zulehner G, et al. (2009) Hepatic tumor-stroma crosstalk guides epithelial to mesenchymal transition at the tumor edge. Oncogene 28: 4022–4033.
16. Baghdasaryan A, Claudel T, Kosters A, Gumhold J, Silbert D, et al. Curcumin improves sclerosing cholangitis in Mdr2−/− mice by inhibition of cholangiocyte inflammatory response and portal myofibroblast proliferation. Gut 59: 521–530.
17. Barikbin R, Neureiter D, Wirth J, Erhardt A, Schwinge D, et al. Induction of heme oxygenase 1 prevents progression of liver fibrosis in Mdr2 knockout mice. Hepatology 55:553–562.
18. Mair M, Zollner G, Schneller D, Musteanu M, Fickert P, et al. (2010) Signal transducer and activator of transcription 3 protects from liver injury and fibrosis in a mouse model of sclerosing cholangitis. Gastroenterology 138: 2499–2508.
19. Proell V, Mikula M, Fuchs E, Mikulits W (2005) The plasticity of p19 ARF null hepatic stellate cells and the dynamics of activation. Biochim Biophys Acta 1744: 76–87.
20. Gonzalez-Rodriguez A, Clampit JE, Escribano O, Benito M, Rondinone CM, et al. (2007) Developmental switch from prolonged insulin action to increased insulin sensitivity in protein tyrosine phosphatase 1B-deficient hepatocytes. Endocrinology 148: 594–608.
21. Caja L, Ortiz C, Bertran E, Murillo MM, Miro-Obradors MJ, et al. (2007) Differential intracellular signalling induced by TGF-beta in rat adult hepatocytes and hepatoma cells: implications in liver carcinogenesis. Cell Signal 19: 683–694.
22. Sancho P, Bertran E, Caja L, Carmona-Cuenca I, Murillo MM, et al. (2009) The inhibition of the epidermal growth factor (EGF) pathway enhances TGF-beta-induced apoptosis in rat hepatoma cells through inducing oxidative stress coincident with a change in the expression pattern of the NADPH oxidases (NOX) isoforms. Biochim Biophys Acta 1793: 253–263.
23. Murillo MM, Carmona-Cuenca I, Del Castillo G, Ortiz C, Roncero C, et al. (2007) Activation of NADPH oxidase by transforming growth factor-beta in hepatocytes mediates up-regulation of epidermal growth factor receptor ligands through a nuclear factor-kappaB-dependent mechanism. Biochem J 405: 251–259.
24. Fickert P, Fuchsbichler A, Wagner M, Zollner G, Kaser A, et al. (2004) Regurgitation of bile acids from leaky bile ducts causes sclerosing cholangitis in Mdr2 (Abcb4) knockout mice. Gastroenterology 127: 261–274.
25. Valdes F, Alvarez AM, Locascio A, Vega S, Herrera B, et al. (2002) The epithelial mesenchymal transition confers resistance to the apoptotic effects of transforming growth factor Beta in fetal rat hepatocytes. Mol Cancer Res 1: 68–78.
26. de Andrade JA, Thannickal VJ (2009) Innovative approaches to the therapy of fibrosis. Curr Opin Rheumatol 21: 649–655.
27. Abhilash PA, Harikrishnan R, Indira M (2012) Ascorbic acid supplementation down-regulates the alcohol induced oxidative stress, hepatic stellate cell activation, cytotoxicity and mRNA levels of selected fibrotic genes in guinea pigs. Free Radic Res 46: 204–213.
28. Foo NP, Lin SH, Lee YH, Wu MJ, Wang YJ (2011) alpha-Lipoic acid inhibits liver fibrosis through the attenuation of ROS-triggered signaling in hepatic stellate cells activated by PDGF and TGF-beta. Toxicology 282: 39–46.
29. Cui W, Matsuno K, Iwata K, Ibi M, Matsumoto M, et al. (2011) NOX1/nicotinamide adenine dinucleotide phosphate, reduced form (NADPH) oxidase promotes proliferation of stellate cells and aggravates liver fibrosis induced by bile duct ligation. Hepatology 54: 949–958.
30. Jiang JX, Venugopal S, Serizawa N, Chen X, Scott F, et al. (2010) Reduced nicotinamide adenine dinucleotide phosphate oxidase 2 plays a key role in stellate cell activation and liver fibrogenesis in vivo. Gastroenterology 139: 1375–1384.
31. Sancho P, Martin-Sanz P, Fabregat I (2011) Reciprocal regulation of NADPH oxidases and the cyclooxygenase-2 pathway. Free Radic Biol Med 51: 1789–1798.
32. Jiang JX, Chen X, Serizawa N, Szyndralewicz C, Page P, et al. (2012) Liver fibrosis and hepatocyte apoptosis are attenuated by GKT137831, a novel NOX4/NOX1 inhibitor in vivo. Free Radic Biol Med 53:289–296.
33. Povero D, Busletta C, Novo E, di Bonzo LV, Cannito S, et al. (2010) Liver fibrosis: a dynamic and potentially reversible process. Histol Histopathol 25: 1075–1091.
34. Amara N, Goven D, Prost F, Muloway R, Crestani B, et al. NOX4/NADPH oxidase expression is increased in pulmonary fibroblasts from patients with idiopathic pulmonary fibrosis and mediates TGFbeta1-induced fibroblast differentiation into myofibroblasts. Thorax 65: 733–738.
35. Martin-Garrido A, Brown DI, Lyle AN, Dikalova A, Seidel-Rogol B, et al. NADPH oxidase 4 mediates TGF-beta-induced smooth muscle alpha-actin via p38MAPK and serum response factor. Free Radic Biol Med 50: 354–362.
36. Caja L, Bertran E, Campbell J, Fausto N, Fabregat I (2011) The transforming growth factor-beta (TGF-beta) mediates acquisition of a mesenchymal stem cell-like phenotype in human liver cells. J Cell Physiol 226: 1214–1223.
37. Wells RG (2011) The epithelial-to-mesenchymal transition in liver fibrosis: here today, gone tomorrow? Hepatology 51: 737–740.
38. Franco DL, Mainez J, Vega S, Sancho P, Murillo MM, et al. (2010) Snail1 suppresses TGF-beta-induced apoptosis and is sufficient to trigger EMT in hepatocytes. J Cell Sci 123: 3467–3477.

39. Rowe RG, Lin Y, Shimizu-Hirota R, Hanada S, Neilson EG, et al. (2011) Hepatocyte-derived Snail1 propagates liver fibrosis progression. Mol Cell Biol 31: 2392–2403.
40. Dooley S, Hamzavi J, Ciuclan L, Godoy P, Ilkavets I, et al. (2008) Hepatocyte-specific Smad7 expression attenuates TGF-beta-mediated fibrogenesis and protects against liver damage. Gastroenterology 135: 642–659.
41. Carnesecchi S, Deffert C, Donati Y, Basset O, Hinz B, et al. (2011) A key role for NOX4 in epithelial cell death during development of lung fibrosis. Antioxid Redox Signal 15: 607–619.
42. Mitchell C, Robin MA, Mayeuf A, Mahrouf-Yorgov M, Mansouri A, et al. (2009) Protection against hepatocyte mitochondrial dysfunction delays fibrosis progression in mice. Am J Pathol 175: 1929–1937.
43. Boudreau HE, Emerson SU, Korzeniowska A, Jendrysik MA, Leto TL (2009) Hepatitis C virus (HCV) proteins induce NADPH oxidase 4 expression in a transforming growth factor beta-dependent manner: a new contributor to HCV-induced oxidative stress. J Virol 83: 12934–12946.
44. de Mochel NS, Seronello S, Wang SH, Ito C, Zheng JX, et al. (2010) Hepatocyte NAD(P)H oxidases as an endogenous source of reactive oxygen species during hepatitis C virus infection. Hepatology 52: 47–59.
45. Laleu B, Gaggini F, Orchard M, Fioraso-Cartier L, Cagnon L, et al. (2010) First in class, potent, and orally bioavailable NADPH oxidase isoform 4 (Nox4) inhibitors for the treatment of idiopathic pulmonary fibrosis. J Med Chem 53: 7715–7730.
46. Ikeda R, Ishii K, Hoshikawa Y, Azumi J, Arakaki Y, et al. (2011) Reactive oxygen species and NADPH oxidase 4 induced by transforming growth factor beta1 are the therapeutic targets of polyenylphosphatidylcholine in the suppression of human hepatic stellate cell activation. Inflamm Res 60: 597–604.

HEPATOLOGY
Official Journal of the American Association for the Study of Liver Diseases

# Overactivation of the TGF-$\beta$ Pathway Confers a Mesenchymal-Like Phenotype and CXCR4-Dependent Migratory Properties to Liver Tumor Cells

Esther Bertran,[1] Eva Crosas-Molist,[1] Patricia Sancho,[1] Laia Caja,[1] Judit Lopez-Luque,[1] Estanislao Navarro,[1] Gustavo Egea,[2] Raquel Lastra,[3] Teresa Serrano,[4] Emilio Ramos,[3] and Isabel Fabregat[1,5]

**Transforming growth factor-beta (TGF-$\beta$) is an important regulatory suppressor factor in hepatocytes. However, liver tumor cells develop mechanisms to overcome its suppressor effects and respond to this cytokine by inducing other processes, such as the epithelial-mesenchymal transition (EMT), which contributes to tumor progression and dissemination. Recent studies have placed chemokines and their receptors at the center not only of physiological cell migration but also of pathological processes, such as metastasis in cancer. In particular, CXCR4 and its ligand, stromal cell-derived factor 1$\alpha$ (SDF-1$\alpha$) / chemokine (C-X-C motif) ligand 12 (CXCL12) have been revealed as regulatory molecules involved in the spreading and progression of a variety of tumors. Here we show that autocrine stimulation of TGF-$\beta$ in human liver tumor cells correlates with a mesenchymal-like phenotype, resistance to TGF-$\beta$-induced suppressor effects, and high expression of CXCR4, which is required for TGF-$\beta$-induced cell migration. Silencing of the TGF-$\beta$ receptor1 (TGFBR1), or its specific inhibition, recovered the epithelial phenotype and attenuated CXCR4 expression, inhibiting cell migratory capacity. In an experimental mouse model of hepatocarcinogenesis (diethylnitrosamine-induced), tumors showed increased activation of the TGF-$\beta$ pathway and enhanced CXCR4 levels. In human hepatocellular carcinoma tumors, high levels of CXCR4 always correlated with activation of the TGF-$\beta$ pathway, a less differentiated phenotype, and a cirrhotic background. CXCR4 concentrated at the tumor border and perivascular areas, suggesting its potential involvement in tumor cell dissemination. *Conclusion*: A crosstalk exists among the TGF-$\beta$ and CXCR4 pathways in liver tumors, reflecting a novel molecular mechanism that explains the protumorigenic effects of TGF-$\beta$ and opens new perspectives for tumor therapy. (HEPATOLOGY 2013;58:2032-2044)**

Transforming growth factor-beta (TGF-$\beta$) is an important regulatory suppressor factor; however, paradoxically, it also modulates other processes that contribute to tumorigenesis, such as fibrosis, immune regulation, microenvironment modification, and cell invasion.[1] Indeed, in addition to its suppressor effects, TGF-$\beta$ induces antiapoptotic signals in fetal hepatocytes and hepatoma cells,[2,3] through activation of the epidermal growth factor receptor (EGFR) pathway.[4] Cells that survive to TGF-$\beta$-induced apoptotic signals undergo epithelial-mesenchymal transition (EMT).[3,5,6] Upon progression of liver cancer, EMT is considered a key process that may drive intrahepatic metastasis.[7] TGF-$\beta$ levels are increased in hepatocellular carcinoma (HCC) tissue, plasma, and urine and decreased in patients who

*Abbreviations: CDH1, E-cadherin; CK-18, cytokeratin; CXCL12/SDF-1$\alpha$, stromal cell-derived factor 1$\alpha$; DEN, diethylnitrosamine; EGFR, the epidermal growth factor receptor; EMT, epithelial-mesenchymal transition; HCC, hepatocellular carcinoma; TGF-$\beta$, transforming growth factor-beta; TGFBR1, transforming growth factor-beta receptor-1*

*From the [1]Bellvitge Biomedical Research Institute (IDIBELL), L'Hospitalet de Llobregat, Barcelona, Spain; [2]Department of Cell Biology, Immunology and Neuroscience, University of Barcelona, Spain; [3]Department of Surgery, Liver Transplant Unit, University Hospital of Bellvitge, Barcelona, Spain; [4]Pathological Anatomy Service, University Hospital of Bellvitge, Barcelona, Spain; [5]Department of Physiological Sciences-II, University of Barcelona, Spain.*

*Received February 4, 2013; accepted June 15, 2013.*

*Supported by grants to I.F. from the Ministry of Economy and Competitiveness (MINECO), Spain (BFU2009-07219, BFU2012-35538, and ISCIII-RTICC RD06/0020) and AGAUR-Generalitat de Catalunya (2009SGR-312). E.C-M. was the recipient of a predoctoral fellowship from the FPU program, Ministry of Education, Culture and Sport, Spain.*

underwent effective therapy for HCC.[8] Liver tumors expressing late TGF-$\beta$-responsive genes (antiapoptotic and EMT-related genes) display a higher invasive phenotype and increased tumor recurrence when compared to those that show an early TGF-$\beta$ signature (suppressor genes).[9] Interestingly, blocking TGF-$\beta$ up-regulates E-cadherin and reduces migration and invasion of HCC cells.[10]

Recent studies place chemokines and their receptors at the center not only of physiological cell migration, but also of pathological processes, such as metastasis in cancer.[11] In particular, CXCR4 and its ligand, stromal cell-derived factor 1$\alpha$ (SDF-1$\alpha$) / chemokine (C-X-C motif) ligand 12 (CXCL12), have been revealed as important molecules involved in the spreading and progression of a variety of tumors.[12] Different data suggest that molecular strategies to inhibit the CXCR4/CXCL12 pathway could be of therapeutic use for the treatment of HCC.[13] CXCR4 is up-regulated in human HCC,[14] correlating with progression of the disease.[15] Its ligand CXCL12 stimulates human hepatoma cell growth, migration, and invasion.[14] We have recently described that TGF-$\beta$ up-regulates CXCR4 in rat hepatoma cells[16] and sensitizes cells to respond to CXCL12, which mediates cell scattering and survival. These results suggest a crosstalk between the increased protumorigenic response to TGF-$\beta$ and the establishment of a functional CXCR4/CXCL12 axis. Nothing is known about whether a similar situation occurs in human liver tumorigenesis.

The aim of this work was to analyze whether autocrine stimulation of TGF-$\beta$ in human liver tumors may induce up-regulation, and/or intracellular reorganization, of CXCR4, which, concomitant with the EMT process induced by this factor, would contribute to the enhancement of cell migration and invasion.

## Materials and Methods

***Ethics Statement.*** Approval for experiments related to the study of liver carcinogenesis in experimental animal models was obtained from the General Direction of Environment and Biodiversity, Government of Catalonia, #4589, 2011. All animals received humane care and study protocols comply with the institution's guidelines. Human tissues were collected with the required approvals from the Institutional Review Board (Comité Ético de Investigación Clínica del Hospital Universitario de Bellvitge) and patient's written consent conformed to the ethical guidelines of the 1975 Declaration of Helsinki.

***Cell Culture.*** Cell lines used in this study were from commercial sources. Hep3B, HepG2, and PLC/PRF/5 were obtained from the European Collection of Cell Cultures (ECACC). SNU449 were obtained from the American Tissue Culture Collection (ATCC). Huh7 and HLF cells were from the Japanese Collection of Research Bioresources (JCRB Cell Bank) and were kindly provided by Dr. Perales (University of Barcelona, Spain) and Dr. Giannelli (University of Bari, Italy), respectively. Cell lines were never used in the laboratory for longer than 4 months after receipt or resuscitation.

HepG2 and Hep3B were maintained in modified Eagle's medium (MEM) medium, PLC/PRF/5 and Huh7 in Dulbecco's modified Eagle's medium (DMEM) medium, SNU449 and HLF in RPMI medium. Neonatal mice hepatocytes were immortalized as described[17] and cultured in DMEM. All media (Lonza, Basel, Switzerland) were supplemented with 10% fetal bovine serum (FBS; Sera Laboratories International, Cinder Hill, UK) and cells maintained in a humidified atmosphere of 37°C, 5% $CO_2$. Analysis of cell viability was performed by Crystal violet staining.[3]

***Immunofluorescence Staining.*** Fluorescence microscopy studies were performed as described[3] (further details in the Supporting Materials and Methods). Cells were visualized with a Nikon eclipse 80i microscope with the appropriate filters. Representative images were taken with a Nikon DS-Ri1 digital camera. ImageJ software (National Institutes of Health [NIH], Bethesda, MD) was used to analyze fluorescence from TIFF images captured using the same exposure conditions.

***Immunohistochemistry.*** Human HCC tissues were obtained from the Pathological Anatomy Service, University Hospital of Bellvitge, Barcelona. Paraffin-embedded tissues were cut into 4-$\mu$m-thick sections, incubated with the specific primary antibody overnight at 4°C, and binding developed with the Vectastain ABC kit (Vector

*Address reprint requests to: Isabel Fabregat, Bellvitge Biomedical Research Institute (IDIBELL), Gran Via de L'Hospitalet, 199, 08908 L'Hospitalet de Llobregat, Barcelona, Spain. E-mail: ifabregat@idibell.cat; fax: 34 932 607426.*



*View this article online at wileyonlinelibrary.com.*

*DOI 10.1002/hep.26597*

*Potential conflict of interest: Nothing to report.*

*Additional Supporting Information may be found in the online version of this article.*

Laboratories, Burlingame, CA). Further information is supplied in the Supporting Materials and Methods.

***Western Blot Analysis.*** Total protein extracts and western blotting procedures were carried out as described.[3] Source of antibodies are detailed in the Supporting Materials and Methods.

***Analysis of Gene Expression.*** RNeasy Mini Kit (Qiagen, Valencia, CA) was used for total RNA isolation. Reverse transcription (RT) was carried out using the High Capacity Reverse Transcriptase kit (Applied Biosystems, Foster City, CA), and 500 ng of total RNA from each sample for complementary DNA synthesis. For details about semiquantitative and real-time polymerase chain reaction (PCR) reactions, see the Supporting Materials and Methods.

***RNA Interference Assays.*** Cells at 70% confluence were transiently transfected with 50 nM small interfering RNA (siRNA) for 8 hours using TransIT-siQuest following the manufacturer's instructions (Mirus, Madison, WI). For stable transfection of short hairpin RNA (shRNA), cells at 50%-60% confluence were transfected with MATra-A reagent (IBA, Germany) according to the manufacturer's recommendation (15 minutes on the magnet plate, 2 $\mu$g/mL of shRNA plasmid). Four different plasmids of TGFBRI shRNA were transfected separately or combined, as well as a control shRNA. Protocols used were as described.[18] For siRNA sequences and further experimental details, see the Supporting Materials and Methods.

***Migration Assays.*** Cell motility was examined by two different methods: (1) a wound-healing assay[16] and (2) real-time migration assay through the xCELLigence system (Roche Applied Science). For the wound-healing assay, cells were grown at basal conditions to 95% confluence and monolayers were scratched with a pipette tip (0 hours). Cell migration was recorded by phase contrast microscopy (Olympus IX-70) at 48 hours after wound scratch. For real-time monitoring of cell migration, the xCELLigence system was used; $4 \times 10^4$ cells/well were seeded onto the top chamber of a CIM plate, which features microelectronic sensors integrated on the underside of the microporous membrane of a Boyden-like chamber. CIM plates were placed onto the Real-Time Cell Analyzer (RTCA) station (xCELLigence System, Roche, Mannheim, Germany). Cell migration was continuously monitored by measuring changes in the electrical impedance at the electrode/cell interface, as a population of cells migrated from the top to the bottom chamber. Continuous values are represented as cell index (CI), a dimensionless parameter that reflects a relative change in measured electrical impedance, and quantified as a slope ($h^{-1}$) of the first 5 hours.

***Diethylnitrosamine (DEN)-Induced Hepatocarcinogenesis in Mice.*** Male mice at day 15 of age received intraperitoneal injections of DEN (5 mg/kg) diluted in saline buffer, control animals were injected with saline buffer intraperitoneally. At 6, 9, and 12 months of age, mice were sacrificed and their livers removed. For histological studies, liver lobes were fixed in 4% paraformaldehyde overnight and paraffin-embedded for immunohistochemistry staining. Total RNA was isolated from frozen tissues to analyze gene expression by real-time quantitative PCR. Three to four animals/condition and two different tissue pieces/animal were processed for RNA extraction.

***Statistics.*** All data represent at least three experiments and are expressed as the mean ± SEM. Differences between groups were compared using either Student $t$ test or one-way analysis of variance (ANOVA) associated with Dunnett's test. Statistical significance was assumed when $P < 0.05$. The analysis was performed using GraphPad Prism software (Graph-Pad for Science, San Diego, CA). For data from human samples, statistical significance between means was determined by the nonparametric Mann-Whitney $U$ test. Correlation between TGF-$\beta$ and CXCR4 mRNA levels was determined by the Pearson correlation coefficient.

## Results

***Mesenchymal-Like Phenotype in HCC Cells Correlates With SMADs Activation and Resistance to TGF-β-Induced Suppressor Effects.*** In order to evaluate the relevance of the autocrine stimulation of TGF-$\beta$ pathway in the acquisition of mesenchymal-like features, we analyzed the phenotype of six different human liver tumor cell lines whose characteristics are detailed in Supporting Table 1. A correlation between the decrease in E-cadherin and cytokeratin-18 (CK-18) expression, characteristics of an epithelial phenotype, and the appearance of cells expressing vimentin (a mesenchymal intermediate filament) was observed (Fig. 1A). The acquisition of a mesenchymal-like phenotype occurred concomitantly with an increase in the expression of *TGFB1* (Fig. 1B) and with nuclear localization of both SMAD2 and SMAD3 (Supporting Fig. 1). Analysis of TGF-$\beta$ in the culture medium revealed increased amounts of this cytokine in mesenchymal-like versus epithelial cell lines. Furthermore, conditioned medium from mesenchymal-like HCC cells induced higher Smad2 phosphorylation in immortalized mice hepatocytes (Supporting Fig. 1). With the exception of the HepG2 cells that show mutations in *NRAS* and are

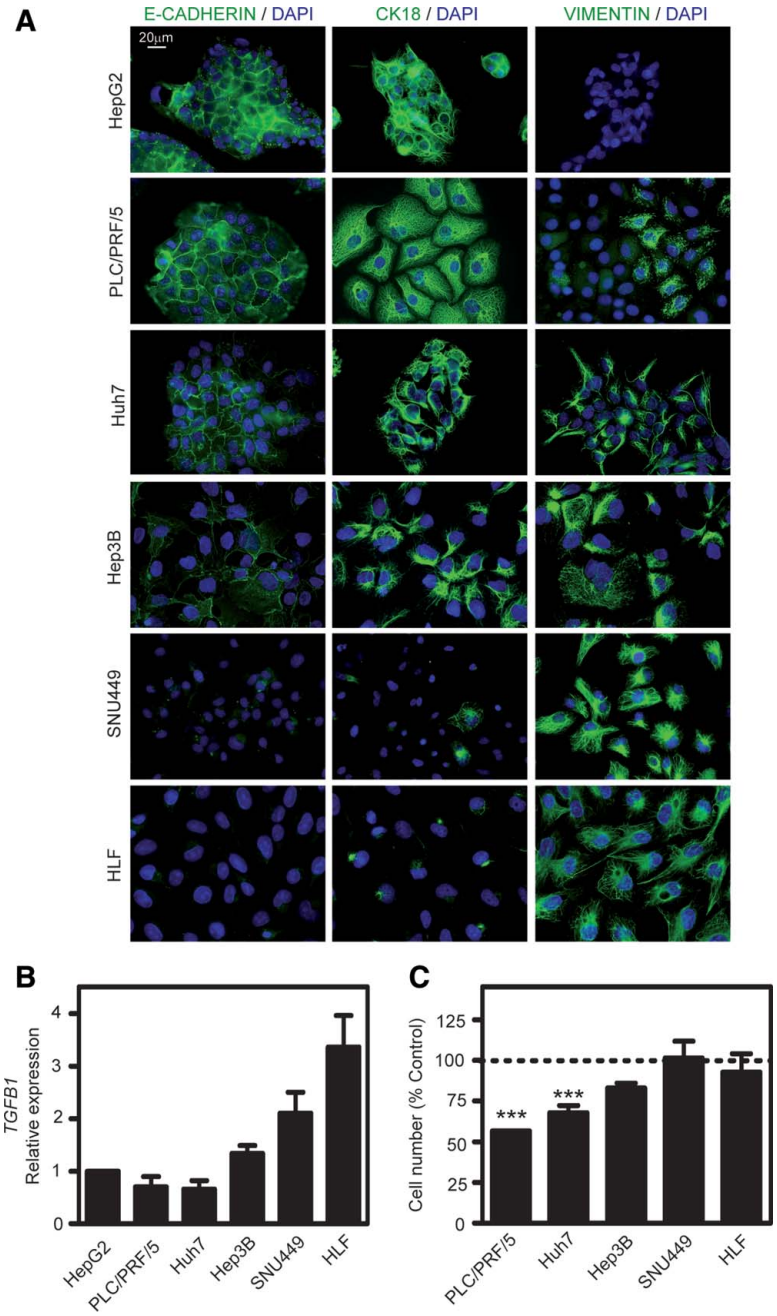


Fig. 1. Autocrine stimulation of the TGF-$\beta$ pathway in HCC cells correlate with a mesenchymal-like phenotype and resistance to TGF-$\beta$-induced suppressor effects. HepG2, PLC/PRF/5, Huh7, Hep3B, SNU449, HLF were cultured under standard conditions in 10% FBS. (A) Immunofluorescence of E-cadherin (green), CK-18 (green), vimentin (green), and DAPI (blue). (B) *TGFB* expression levels determined by real-time PCR. Mean $\pm$ SEM (n = 5). (C) Effect of 48 hours of treatment with 2 ng/mL TGF-$\beta$ on cell viability, analyzed by Crystal violet staining: data were calculated relative to zero time and represent the mean $\pm$ SEM of at least six independent experiments. Student *t* test was calculated versus zero time for each cell type: $***P < 0.001$.

resistant to TGF-$\beta$-induced suppressor effects,[19] the epithelial phenotype correlated with response to TGF-$\beta$ as a cytostatic factor, whereas cells with a mesenchymal-like phenotype did not arrest proliferation in the presence of TGF-$\beta$ (Fig. 1C). This behavior confirms a previous classification of these cell lines according to the TGF-$\beta$ signature[9] (early for PLC/PRF/5 and Huh7; late for SNU449, HLF). Results in Hep3B indicate that these cells represent a transition from an epithelial to a mesenchymal-like phenotype, since they showed decreased expression of E-cadherin and simultaneous expression of epithelial (CK-18) and mesenchymal (vimentin) intermediate filaments (Fig. 1A). Interestingly, this mixed phenotype correlated with a high activation of the TGF-$\beta$ pathway (Supporting Fig. 1) and lower suppressor response to this cytokine (Fig. 1C). In summary, mesenchymal-like phenotype in HCC cell lines correlates with autocrine stimulation of the TGF-$\beta$ pathway and resistance to TGF-$\beta$-induced suppressor effects.

***Mesenchymal-Like Phenotype in HCC Cells Correlates With CXCR4 Up-regulation and Asymmetric Distribution, Which Is Required for Cell Migration.*** The analysis of the cytoskeleton organization reflected that cells with more mesenchymal phenotype presented F-actin located in stress fibers, whereas the more epithelial ones showed more pericellular distribution (Fig. 2A, left panels). Cells with mesenchymal characteristics showed CXCR4 in an asymmetric distribution in a great percentage of them (Fig. 2A, right panels). HepG2 cells showed homogeneous distribution of CXCR4 with no apparent polarization, whereas in the epithelial Huh7 and PLC/PRF/5 localization of CXCR4 was variable, with some cells showing polarized areas, but a great percentage containing homogeneous intracellular localization (Fig. 2A, right panels, quantification of the protrusions in Fig. 2B). Furthermore, analysis of *CXCR4* expression at the messenger RNA (mRNA) levels revealed that cells with mesenchymal-like characteristics presented a higher expression of *CXCR4*, when compared with the more epithelial ones (such as HepG2) (Fig. 2C). Levels of *TGFB1* mRNA showed correlation not only with the mesenchymal-like phenotype, but also with *CXCR4* levels (Fig. 2D). In agreement with their mesenchymal characteristics and F-actin distribution, the migratory capacity of Hep3B and SNU449 was much higher than that observed in HepG2, analyzed through the xCELLigence technology or in a wound-healing assay (Fig. 2E,F). Interestingly, in mesenchymal-like cells, such as Hep3B (Fig. 2G) or SNU449 (results not shown), the cells in the migration front showed a strong polarization of CXCR4. The presence of AMD3100, a well-known inhibitor of the CXCR4 receptor, inhibited migration of both Hep3B and SNU449 (Fig. 2F). Furthermore, only cells that showed *CXCR4* elevated expression and asymmetrical distribution, such as SNU449, responded to CXCL12 inducing migration, whereas HepG2 cells did not (Supporting Fig. 2). All these results together indicate that autocrine stimulation of the TGF-$\beta$ pathway in HCC cell lines correlates with activation of the CXCR4/CXCL12 axis, which mediates cell migration.

***Targeting TGF-β Receptor I Attenuates the Mesenchymal Phenotype, Decreases CXCR4 Expression, and Impairs Cell Migration in HCC Cells.*** To analyze whether the autocrine stimulation of the TGF-$\beta$ pathway induces CXCR4 expression and/or its asymmetric distribution, we stably silenced *TGFBR1* expression with specific shRNA in Hep3B (Fig. 3A) and PLC-PRF5 cells (Supporting Fig. 3). Increase in E-cadherin, which presented a pericellular distribution, and decrease in vimentin expression were observed in *TGFBR1*-silenced Hep3B cells (Fig. 3B,C, left). Cytoskeleton organization changed in the absence of *TGFBR1* expression, showing a more pericellular distribution and fewer stress fibers (Fig. 3C,D). *CXCR4* expression was inhibited in these cells (Fig. 3B,C, right, and D), which correlated with a significantly lower capacity to migrate (Fig. 3E). Silencing of *TGFBR1* also correlated with reorganization of cytoskeleton and attenuation of *CXCR4* expression and asymmetric distribution in PLC/PRF/5 cells (Supporting Fig. 3). A pharmacological inhibitor of the kinase activity of TGFBR1, LY36497, which attenuated SMAD2 phosphorylation in HCC cells both in the absence or presence of TGF-$\beta$ (Supporting Fig. 4), decreased *CXCR4* levels (Fig. 4A), increased E-cadherin (*CDH1*) mRNA levels (although changes were more moderate and less significant than the *TGFBR1* silencing: Supporting Fig. 4), reorganized the cytoskeleton and decreased the percentage of cells with an asymmetric distribution of CXCR4 (Fig. 4B). Interestingly, treatment with LY36497 inhibited the capacity of cells to close the wound in migration experiments (Fig. 4C). In summary, TGF-$\beta$ signaling is responsible for up-regulation and asymmetric distribution of CXCR4 in HCC cells.

***Mice Tumors From DEN-Induced Liver Carcinogenesis Show High Expression of Both TGF-β1 and CXCR4.*** In order to know whether the TGF-$\beta$/CXCR4 crosstalk shows significance during *in vivo* hepatocarcinogenesis, we started with the analysis of tumors in a model of DEN-induced experimental liver tumorigenesis in mice. At different times after a single

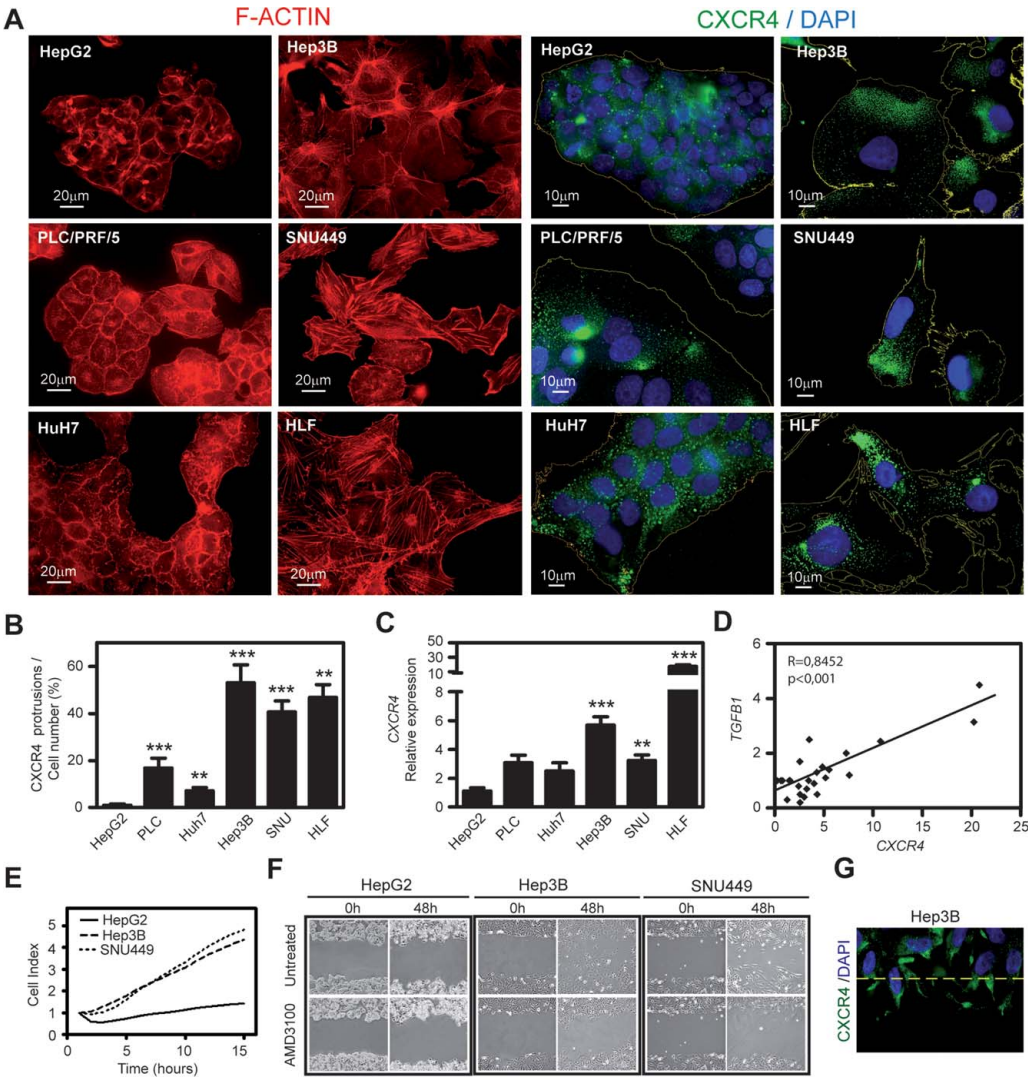


Fig. 2. Overactivation of the TGF-$\beta$ pathway correlates with high expression and asymmetric distribution of CXCR4, which is required for cell migration. (A) Immunofluorescence of F-ACTIN (red), CXCR4 (green), and DAPI (blue). (B) Percentage of CXCR4 protrusions/cell number. (C) *CXCR4* mRNA levels by real-time PCR relative to HepG2 levels. (B,C) Mean ± SEM (n = 3). Student *t* test versus HepG2 cells: $^{**}P < 0.01$, $^{***}P < 0.001$. (D) Correlation among *TGFB* and *CXCR4* mRNA levels in the individual analyses performed in the different cell lines. (E) Real-time migration assay (xCELLigence system, Roche). (F) Cells were untreated or treated with 1 $\mu$g/mL AMD3100. Wound-healing assay (48 hours after wound scratch). (G) Immunofluorescence of CXCR4 (green) and DAPI (blue) of Hep3B, 10 minutes after wound scratch. (E-G) Representative experiments (n = 3).

dose of DEN in 15-day-old animals, liver was collected and analyzed. The appearance of tumors was observed microscopically in all male mice at 9 months of age, but clear macroscopic observation of relevant tumor masses was not observed until 12 months (Supporting Fig. 5). Real-time PCR analysis revealed a progressive increase in the expression of *TGFB1, TGFBR1,* and *CXCR4* in livers from mice of 9 to 12 months of age (Fig. 5A). Increased expression of *TGFB1* correlated with a higher percentage of cells

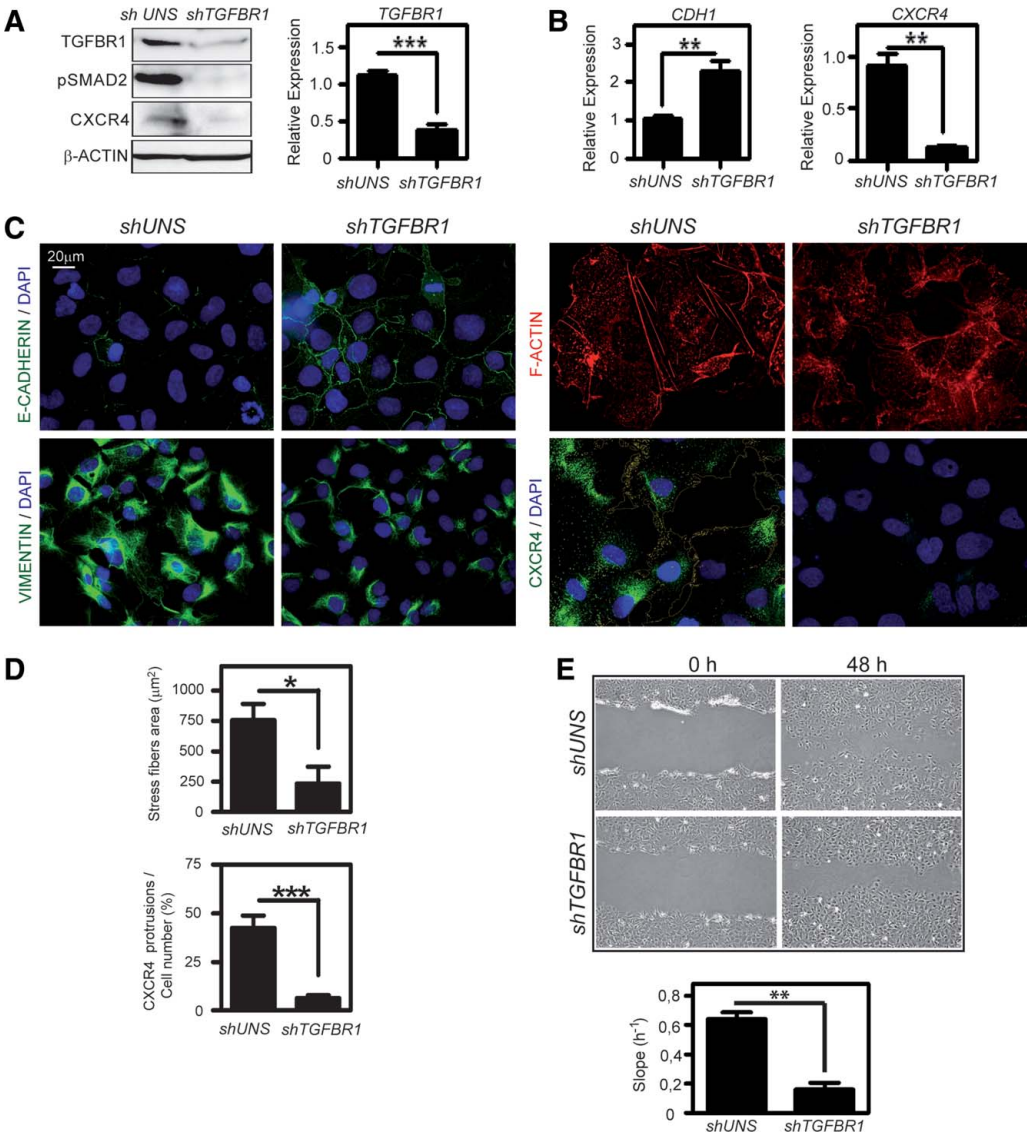


Fig. 3. Stable silencing of TGFBR1 recovers the epithelial phenotype and attenuates CXCR4 expression, inhibiting cell migratory capacity. Hep3B cells were stably transfected with an unspecific shRNA (Hep3B-shUns) or a pool of four different shRNAs against TGFBRI, as detailed in the Supporting Materials and Methods, (Hep3B-shTGFBR1) and were comparatively studied: (A) western blot (left) and real-time PCR of *TGFBRI* (right). (B) E-cadherin (*CDH1*) and *CXCR4* expression levels by real-time PCR. (C) Immunofluorescence of: left: E-cadherin (green), vimentin (green), and DAPI (blue); right: F-ACTIN (red), CXCR4 (green), and DAPI (blue). (D) Quantitative analysis of the F-ACTIN stress fibers area (top) and the number of CXCR4 protrusions relative to the number of cells (bottom). (E) Analysis of cell migration. Top: wound-healing experiment (48 hours after wound scratch). Bottom: real-time migration assay (xCELLigence system). (A, left, C, E, top) Representative experiments (n = 3). (A, right, B, D, E, bottom) Mean ± SEM (n = 3). Student *t* test $*P < 0.05$, $**P < 0.01$, $***P < 0.001$.

showing nuclear localization of phospho-SMAD2 and phospho-SMAD3 in immunohistochemical studies (Fig. 5B). Cells in the border of the tumor presented the maximal level of CXCR4 expression (Fig. 5C). Importantly, it was possible to observe some CXCR4-positive cells invading the stroma. The expression of

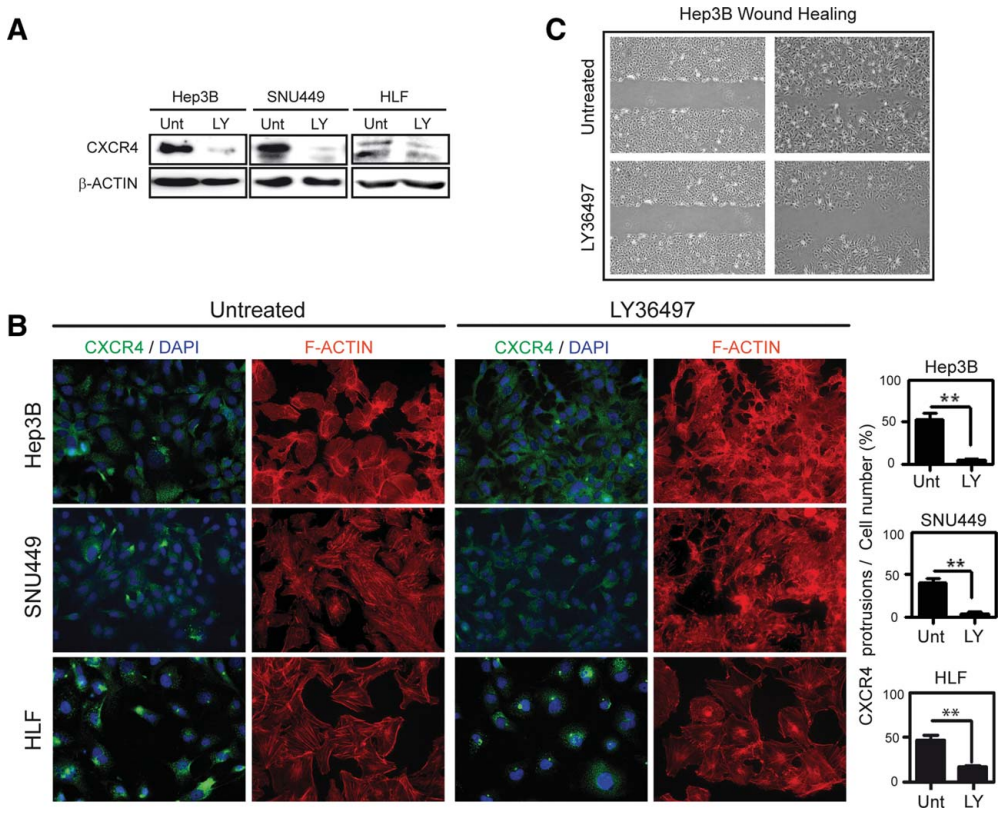


Fig. 4. Pharmacological inhibition of TGFBR1 kinase activity prevents CXCR4 expression and polarization in the mesenchymal HCC cell lines. Hep3B, SNU449, and HLF cells were incubated in the presence or absence of 3 $\mu$M LY36497 for 48 hours. (A) Western blot analysis of CXCR4. A representative experiment of three is shown. (B) Immunofluorescence of F-ACTIN (red), CXCR4 (green), and DAPI (blue). Percentage of CXCR4 protrusions/cell number is represented on the right of each picture as the mean $\pm$ SEM of three independent experiments. Student *t* test versus untreated cells: $^{**}P < 0.01$. (C) Wound-healing experiment in Hep3B cells with or without 3 $\mu$M LY36497 at 48 hours after wound scratch.

CXCL12/SDF-1$\alpha$ was concentrated in perivascular or ductal cells, which could induce the stimulus for cells to migrate toward these areas. Furthermore, we found that immortalized mice hepatocytes in culture were able to respond to TGF-$\beta$ by inducing *CXCR4* expression, a process that was SMAD2/3-dependent (Fig. 5D). In summary, tumor cells in the DEN-induced mice model of liver tumorigenesis show increased activation of the TGF-$\beta$ pathway, which correlates with enhanced CXCR4 levels that concentrates particularly in the cells of the tumor border line.

***Expression of CXCR4 in Human HCC Tissues Correlates With an Active TGF-β Pathway and Is Concentrated in Areas of Cell Spreading.*** Finally, we wanted to know whether TGF-$\beta$1 signaling and CXCR4 expression correlated in human HCC tissues. We analyzed tissues from 17 patients with HCC from different etiologies (Table 1). Heterogeneity among HCC tumors, with variable expression of *TGFB1* and its receptor *TGFBR1*, was observed. Nevertheless, when calculated as the mean among the patients, the expression was significantly increased in tumor tissues versus their surrounding nontumoral tissues. Analysis of *CXCR4* was also variable, but again the tendency was to an increased expression in the tumor tissues (Fig. 6A). However, the most interesting way to dissect the results was individually (Fig. 6B), considering each patient independently. In all the patients showing increased expression of *CXCR4, TGFB1* expression was also enhanced, with the exception of patient 8, who presented *CXCR4* expression mainly in areas of infiltration (results not shown). This patient suffered from an autoimmune disease. This direct correlation was not necessarily true the other way around, since some

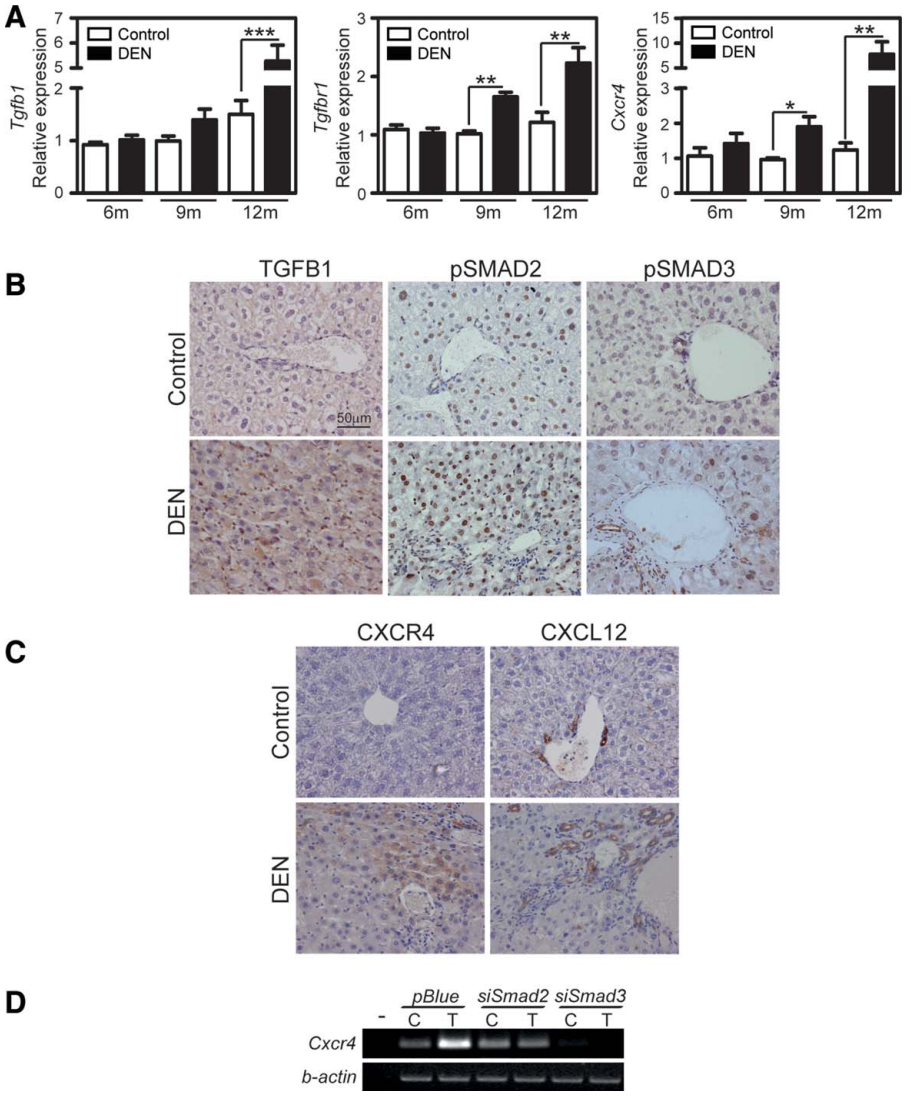


Fig. 5. Tumorigenesis in mice following DEN treatment is associated with increased TGF-$\beta$ and CXCR4 signaling. (A) *Tgfb, Tgfbrl,* and *Cxcr4* transcript levels analyzed by real-time PCR in control liver (PBS treatment) versus tumoral tissues in animals at 6, 9, and 12 months of age. Data represent mean ± SEM (n = 4 in control animals; 3 in DEN-treated animals; analysis in two different pieces of tissue/animal). Student *t* test $*P < 0.05$, $**P < 0.01$, $***P < 0.001$. (B,C) Immunohistochemistry analysis of serial sections of liver from mice after DEN or PBS treatment (12 months). (D) Effect of transient knockdown of SMAD2 or SMAD3 on *Cxcr4* mRNA levels analyzed by RT-PCR in immortalized neonatal hepatocytes treated during 24 hours with or without 2 ng/mL TGF-$\beta$. A representative experiment (n = 3).

patients with increased expression of *TGFB1* did not show higher expression of *CXCR4* (patients 9, 10, 13, 17). Of note, the increased expression of *TGFB1* at the mRNA level correlated with higher levels of TGFB1 protein in the tissues from these patients, not only in the tumoral cells but also in the surrounding stroma and perivascular areas (Fig. 6B,C). Nuclear location of phospho-SMAD2 confirmed the activation of the TGF-$\beta$ signaling. In a similar way to that observed in the mice model, CXCR4-positive cells were mainly located in the border of the tumor or in the perivascular area (Fig. 6B,C) and CXCL12

**Table 1. Patient and Tumor Characteristics**

| Case | Age/Sex | Etiology | Background | Size (cm) | Tumoral Focus/ Satellite Nodules | Histological Grade | Microscopic Vascular Invasion | Macroscopic Vascular Invasion | pT / Stage |
|---|---|---|---|---|---|---|---|---|---|
| 1 | 46/M | Alc | LC | 3 | 1/0 | 3 | No | No | 1 / I |
| 2 | 50/M | Alc, HCV | LC | 2,5 | 2/0 | 2-3 | No | No | 2 / II |
| 3 | 75/M | Alc | LC | 3 | 1/0 | 3 | No | No | 1 / I |
| 4 | 49/F | U | NL | 27 | 1/0 | 3 | No | No | 1 / I |
| 5 | 78/F | U | NL | 7,5 | 1/1 | 3 | Yes | No | 2 / II |
| 6 | 50/M | Alc | LC | 2 | 9/0 | 2 | Yes | No | 2 / II |
| 7 | 69/M | HCV | LC | 3 | - | 3 | No | Yes | 1 / I |
| 8 | 65/F | Aut | LC | 6 | 5/0 | 2 | Yes | No | 3 / IIIa |
| 9 | 61/M | HCV | LC | 2,5 | - | 2 | No | No | 2 / II |
| 10 | 62/M | HCV | LC | 4,5 | 1/0 | 3 | No | No | 1 / I |
| 11 | 74/M | U | NL | 6 | 1/0 | 2 | No | No | 1 / I |
| 12 | 52/M | HCV | LC | 3,8 | 1/0 | 2 | No | No | 1 / I |
| 13 | 82/M | U | NL | 7 | 1/0 | 1-2 | No | No | 1 / I |
| 14 | 46/M | HCV | LC | 8,5 | 1/multi | 3 | Yes | No | 2a / II |
| 15 | 71/M | U | NL | 20 | 1/multi | 2 | Yes | No | 2 / II |
| 16 | 64/M | HCV | LC | 3,3 | 1/0 | 3 | No | No | 1 / I |
| 17 | 71/M | HCV | LC | 4,5 | 1/1 | 2-3 | No | No | 1 / I |

Gender: F (female); M (male). Histological grade according to the criteria of Edmondson and Steiner: 1, well differentiated; 2, moderately differentiated; 3, poorly differentiated; 4, undifferentiated. Etiology: HBV (hepatitis B virus); HCV (hepatitis C virus); NBNC (HBV(-), HCV(-)); alcohol (heavy alcohol use); U (unknown etiology); Aut (autoimmune); background: NL (normal liver); LC (liver cirrhosis).

expression was found in the stroma, infiltration areas, and in ductal and perivascular cells. It is worth noting that it was possible to observe CXCR4-positive cells trying to invade the vasculature and infiltrating the peritumoral capsule (Fig. 6D). Interestingly, CXCR4-positive tumor cells surrounding vascular areas showed disorganization of E-cadherin, which reflects a less differentiated, more mesenchymal, and migratory phenotype (Fig. 6C). In fact, the highest expression of both TGF-$\beta$ and CXCR4 significantly correlated with the lowest stages of differentiation in the HCC patients analyzed (Supporting Fig. 6A). Furthermore, patients with a cirrhotic background showed the highest levels of CXCR4 and, interestingly, the tumor surrounding (cirrhotic) tissue from these patients contained significantly higher levels of both TGF-$\beta$ and CXCR4 when compared with the surrounding tissue from noncirrhosis patients (Supporting Fig. 6B). Immunohistochemical analysis of CXCR4 in tissues from patients with different grades of fibrosis (no tumors yet) revealed progressive increase in the expression of this protein, which correlated with higher activation of the TGF-$\beta$ pathway, analyzed as SMAD2 phosphorylation (Supporting Fig. 6C).

In summary, a great percentage of HCC tumors express high levels of CXCR4 that is always coincident with activation of the TGF-$\beta$ pathway and correlates with a dedifferentiation stage and a cirrhotic background. CXCR4 concentrates particularly in the cells of the tumor border and in the perivascular areas, a fact that may suggest its potential involvement in tumor cell migration.

## Discussion

In addition to the clear evidence for TGF-$\beta$ signaling as a liver tumor suppressor, different studies have identified overexpression of TGF-$\beta$1 in HCC, which correlates with tumor progression and a bad prognosis.[9,10] The ability of TGF-$\beta$ to contribute to tumor progression depends on the capacity of the cells to overcome its growth inhibitory and proapoptotic effects. Different mechanisms could account for this resistance, among others: (1) alteration of oncogenic pathways, such as Ras/Erks or p53[19,20]; (2) alterations in the TGF-$\beta$ suppressor arm, such as dysregulation of embryonic liver fodrin (ELF, a crucial SMAD3/4 adaptor)[21] or up-regulation of SMAD7[22,23]; or (3) interaction with hepatitis B virus X (HBx) protein.[24] Tumor cells that overcome TGF-$\beta$ suppressor effects become susceptible to respond to these cytokine-inducing other effects, such as EMT processes that contribute to either fibrosis and/or tumor dissemination.[25] Furthermore, TGF-$\beta$ may exert multiple effects on the microenvironment, as well as on vasculogenesis.[26] For all these reasons, the TGF-$\beta$ signaling pathway is starting to be considered as a pharmaceutical target in HCC.[8] However, whereas interference with TGF-$\beta$ signaling in various short-term animal models has provided promising results, liver disease progression in humans is a process of decades with different phases where targeting of TGF-$\beta$ might have both beneficial and/or adverse effects.[27] Indeed, dissecting the downstream signals that govern the protumorigenic effects of the

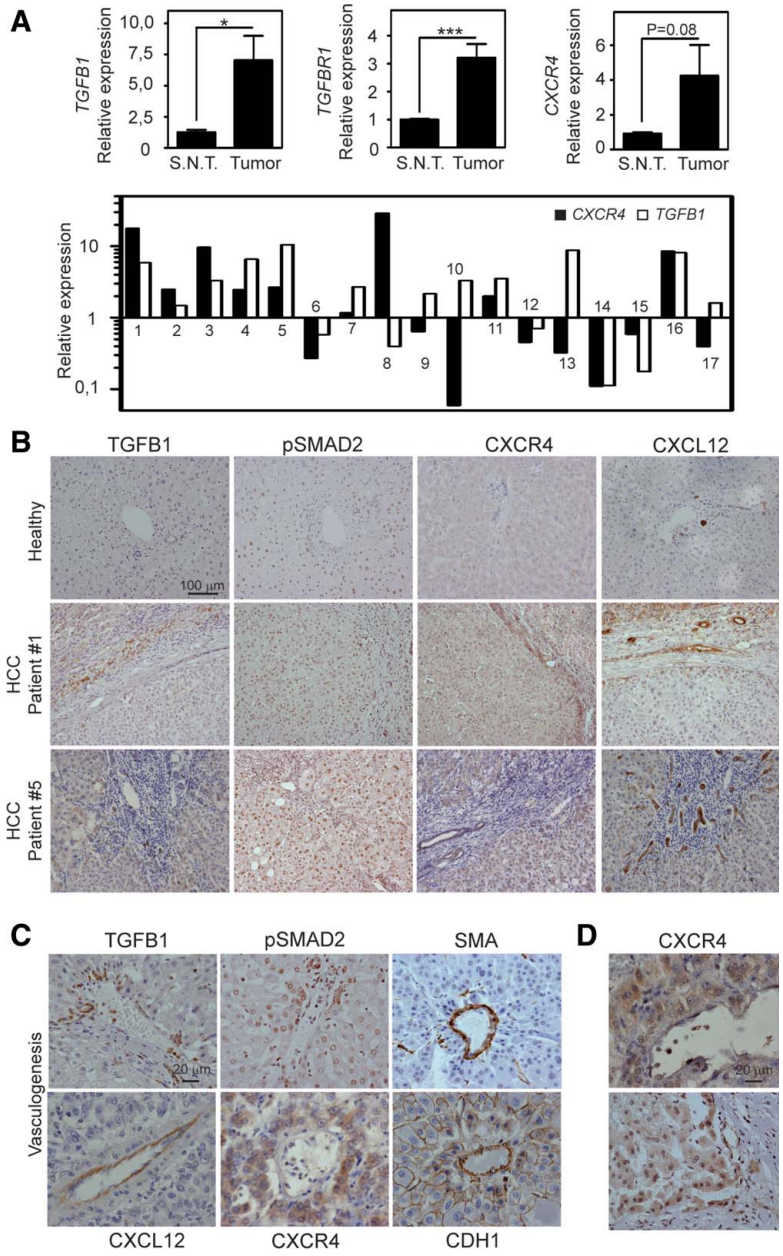


Fig. 6. High expression of CXCR4 correlates with activation of the TGF-$\beta$ pathway and a less differentiated phenotype in HCC tumor tissues. (A) *TGFB, TGFBRI,* and *CXCR4* transcript levels analyzed by real-time PCR, comparing tumor versus surrounding tissue in 17 HCC patients (up). Relative expression of *TGFB and CXCR4* of each individual tumor versus its respective surrounding tissue, represented in a logarithmic scale for a better understanding of changes observed (down). (B) Immunohistochemistry analysis of serial sections in two representative HCC patients (1 and 5), compared with healthy tissue. (C) Immunohistochemistry analysis of tumor arteries. (D) Magnification of different CXCR4 localizations within the tumor.

TGF-$\beta$ pathway in liver tumor cells may help in the design of more specific targeted therapies for downstream TGF-$\beta$ receptors and/or to select patients in whom a potential positive response to TGF-$\beta$ inhibitors is predicted.

In this work, we show that some human HCC cells display a mesenchymal-like phenotype and migratory capacity under basal conditions, which is coincident with overactivation of the TGF-$\beta$ pathway. An inverse correlation between the mesenchymal-like phenotype and the response to TGF-$\beta$ as a tumor suppressor is observed. In liver cancer cells EMT, through Snail1 up-regulation, overcomes TGF-$\beta$-induced tumor-suppressor effects, switching its response to tumor progression, making cells resistant to cell death and prone to acquire invasive properties.[28] Furthermore, correlating with the autocrine stimulation of TGF-$\beta$, HCC cells express high levels of CXCR4, which is asymmetrically distributed and concentrated at the presumptive cell migratory front and mediates cell migration. Interestingly, both mesenchymal-like features and expression/polarization of CXCR4 are attenuated in cells where TGFBR1 expression is decreased with a specific shRNA, which correlates with the impairment of their migratory capacity. Although previous reports had reported the overexpression of TGF-$\beta$ in HCC[9,10] and the correlation of CXCR4 expression with invasive potential of HCC cells,[13,15,29,30] this is the first study demonstrating that the tumor-promoting function of TGF-$\beta$ signaling involves CXCR4/CXCL12, which results in enhanced migration in human liver tumor cells. Furthermore, activation of CXCR4 would affect several major signaling pathways related not only to cell migration, but also to proliferation and survival,[16] which may have relevant consequences in tumor progression.[31]

The results presented here also indicate that in the animal model of DEN-induced liver carcinogenesis, expression of TGF-$\beta$1 and CXCR4 is progressively increased, reaching maximum levels at late stages where tumors are macroscopically observed. We have also proven that in cultures of immortalized hepatocytes, TGF-$\beta$ induces CXCR4 expression, a process that requires activation of both SMAD2 and SMAD3. In fact, an integrative genomic analysis of CXCR4 transcriptional regulation had previously suggested that TGF-$\beta$, Nodal, and Activin signals may induce CXCR4 upregulation based on SMAD2/3 and FOX family members.[32] The study in humans also indicates that a relevant percentage of liver tissues from HCC patients show a higher expression of CXCR4, which is always coincident with overactivation of the TGF-$\beta$ pathway and correlates with a less differentiated phenotype and cirrhotic background. Cells that present a higher amount and polarized localization of CXCR4 are located in the borders of the tumor, in the migratory fronts, or in the perivascular zone, coincident with high expression of TGF-$\beta$ in these areas. Interestingly, expression of CXCL12 is higher in the peritumoral cells, which suggest a paracrine regulation of the CXCR4 pathway. Indeed, overactivation of the TGF-$\beta$ pathway sensitizes tumor cells to respond to CXCL12 produced by tumoral surrounding tissue. All these results together support the existence of crosstalk among TGF-$\beta$ and CXCR4 pathways in HCC human tumors, which may contribute to tumor progression and dissemination.

The inhibition of the TGF-$\beta$ pathway is emerging as a new therapeutic tool in cancer.[33] Since it regulates several steps in tumor progression, blocking this mediator should have multiple beneficial effects.[8] However, based on the results presented here, from both *in vitro* and *in vivo* experiments, the heterogeneity of the tumors might condition the response to these inhibitors. Indeed, overactivation of the TGF-$\beta$ pathway differs among the different cell lines tested, as well as among the different tissues from patients. Interestingly, a strong correlation between TGF-$\beta$ overactivation and mesenchymal-like and migratory phenotypes is observed, locating CXCR4 as a target of TGF-$\beta$ both in cell lines and in HCC patients. From these results, CXCR4 localization in the migratory fronts of tumor tissues, coincident with high expression of TGF-$\beta$ and/or high nuclear localization of p-SMAD2, may be used as biomarkers to predict the beneficial response to therapeutic agents that act on the TGF-$\beta$ pathway. Increasing evidence demonstrates that activation of the CXCR4/CXCL12 pathway is a potential mechanism of tumor resistance to both conventional therapies and biological agents by way of complementary actions.[34] The use of TGF-$\beta$ inhibitors, or inhibitors of the CXCR4/CXCL12 pathway, might increase the response to other therapeutic drugs when used in combination.

In conclusion, overactivation of the TGF-$\beta$ pathway in HCC cells confers on them a mesenchymal-like phenotype and migratory properties through activation of the CXCR4/CXCL12 axis, a mechanism that would contribute to tumor progression in HCC patients. CXCR4 localization in the migratory fronts of tumor tissues, coincident with overactivation of the TGF-$\beta$ signaling, may be considered in the future as a prognostic factor to predict patient response to drugs that target the TGF-$\beta$ pathway.

*Acknowledgment:* The authors thank Greta Ripoll for technical support and participation in the analysis of the DEN model of hepatocarcinogenesis by Dr. Joana Visa (and the IDIBELL animal core facility) and graduate student Miguel Reina. We thank Drs. Perales and Giannelli for providing cells.

## References

1. Massague J. TGFbeta in cancer. Cell 2008;134:215-230.
2. Valdes F, Murillo MM, Valverde AM, Herrera B, Sanchez A, Benito M, et al. Transforming growth factor-beta activates both pro-apoptotic and survival signals in fetal rat hepatocytes. Exp Cell Res 2004;292:209-218.
3. Caja L, Ortiz C, Bertran E, Murillo MM, Miro-Obradors MJ, Palacios E, et al. Differential intracellular signalling induced by TGF-beta in rat adult hepatocytes and hepatoma cells: implications in liver carcinogenesis. Cell Signal 2007;19:683-694.
4. Murillo MM, del Castillo G, Sanchez A, Fernandez M, Fabregat I. Involvement of EGF receptor and c-Src in the survival signals induced by TGF-beta1 in hepatocytes. Oncogene 2005;24:4580-4587.
5. Gotzmann J, Huber H, Thallinger C, Wolschek M, Jansen B, Schulte-Hermann R, et al. Hepatocytes convert to a fibroblastoid phenotype through the cooperation of TGF-beta1 and Ha-Ras: steps towards invasiveness. J Cell Sci 2002;115:1189-1202.
6. Valdes F, Alvarez AM, Locascio A, Vega S, Herrera B, Fernandez M, et al. The epithelial mesenchymal transition confers resistance to the apoptotic effects of transforming growth factor beta in fetal rat hepatocytes. Mol Cancer Res 2002;1:68-78.
7. Reichl P, Haider C, Grubinger M, Mikulits W. TGF-beta in epithelial to mesenchymal transition and metastasis of hepatocellular carcinoma. Curr Pharm Des 2012;18:4135-4147.
8. Giannelli G, Mazzocca A, Fransvea E, Lahn M, Antonaci S. Inhibiting TGF-beta signaling in hepatocellular carcinoma. Biochim Biophys Acta 2011;1815:214-223.
9. Coulouarn C, Factor VM, Thorgeirsson SS. Transforming growth factor-beta gene expression signature in mouse hepatocytes predicts clinical outcome in human cancer. Hepatology 2008;47:2059-2067.
10. Fransvea E, Angelotti U, Antonaci S, Giannelli G. Blocking transforming growth factor-beta up-regulates E-cadherin and reduces migration and invasion of hepatocellular carcinoma cells. Hepatology 2008;47: 1557-1566.
11. Sheu BC, Chang WC, Cheng CY, Lin HH, Chang DY, Huang SC. Cytokine regulation networks in the cancer microenvironment. Front Biosci 2008;13:6255-6268.
12. Zlotnik A. New insights on the role of CXCR4 in cancer metastasis. J Pathol 2008;215:211-213.
13. Li W, Gomez E, Zhang Z. Immunohistochemical expression of stromal cell-derived factor-1 (SDF-1) and CXCR4 ligand receptor system in hepatocellular carcinoma. J Exp Clin Cancer Res 2007;26:527-533.
14. Sutton A, Friand V, Brule-Donneger S, Chaigneau T, Ziol M, Sainte-Catherine O, et al. Stromal cell-derived factor-1/chemokine (C-X-C motif) ligand 12 stimulates human hepatoma cell growth, migration, and invasion. Mol Cancer Res 2007;5:21-33.
15. Schimanski CC, Bahre R, Gockel I, Muller A, Frerichs K, Horner V, et al. Dissemination of hepatocellular carcinoma is mediated via chemokine receptor CXCR4. Br J Cancer 2006;95:210-217.
16. Bertran E, Caja L, Navarro E, Sancho P, Mainez J, Murillo MM, et al. Role of CXCR4/SDF-1alpha in the migratory phenotype of hepatoma cells that have undergone epithelial-mesenchymal transition in response to the transforming growth factor-beta. Cell Signal 2009;21:1595-1606.
17. Gonzalez-Rodriguez A, Clampit JE, Escribano O, Benito M, Rondinone CM, Valverde AM. Developmental switch from prolonged insulin action to increased insulin sensitivity in protein tyrosine phosphatase 1B-deficient hepatocytes. Endocrinology 2007;148:594-608.
18. Caja L, Sancho P, Bertran E, Ortiz C, Campbell JS, Fausto N, et al. The tyrphostin AG1478 inhibits proliferation and induces death of liver tumor cells through EGF receptor-dependent and independent mechanisms. Biochem Pharmacol 2011;82:1583-1592.
19. Caja L, Sancho P, Bertran E, Iglesias-Serret D, Gil J, Fabregat I. Overactivation of the MEK/ERK pathway in liver tumor cells confers resistance to TGF-{beta}-induced cell death through impairing up-regulation of the NADPH oxidase NOX4. Cancer Res 2009;69:7595-7602.
20. Morris SM, Baek JY, Koszarek A, Kanngurn S, Knoblaugh SE, Grady WM. Transforming growth factor-beta signaling promotes hepatocarcinogenesis induced by p53 loss. Hepatology 2012;55:121-131.
21. Baek HJ, Lim SC, Kitisin K, Jogunoori W, Tang Y, Marshall MB, et al. Hepatocellular cancer arises from loss of transforming growth factor beta signaling adaptor protein embryonic liver fodrin through abnormal angiogenesis. Hepatology 2008;48:1128-1137.
22. Matsuzaki K, Date M, Furukawa F, Tahashi Y, Matsushita M, Sugano Y, et al. Regulatory mechanisms for transforming growth factor beta as an autocrine inhibitor in human hepatocellular carcinoma: implications for roles of SMADs in its growth. Hepatology 2000;32:218-227.
23. Dooley S, Weng H, Mertens PR. Hypotheses on the role of transforming growth factor-beta in the onset and progression of hepatocellular carcinoma. Dig Dis 2009;27:93-101.
24. Murata M, Matsuzaki K, Yoshida K, Sekimoto G, Tahashi Y, Mori S, et al. Hepatitis B virus X protein shifts human hepatic transforming growth factor (TGF)-beta signaling from tumor suppression to oncogenesis in early chronic hepatitis B. Hepatology 2009;49:1203-1217.
25. Moustakas A, Heldin CH. Induction of epithelial-mesenchymal transition by transforming growth factor beta. Semin Cancer Biol 2012;22: 446-454.
26. Fransvea E, Mazzocca A, Antonaci S, Giannelli G. Targeting transforming growth factor (TGF)-betaRI inhibits activation of beta1 integrin and blocks vascular invasion in hepatocellular carcinoma. Hepatology 2009;49:839-850.
27. Dooley S, ten Dijke P. TGF-beta in progression of liver disease. Cell Tissue Res 2012;347:245-256.
28. Franco DL, Mainez J, Vega S, Sancho P, Murillo MM, de Frutos CA, et al. Snail1 suppresses TGF-beta-induced apoptosis and is sufficient to trigger EMT in hepatocytes. J Cell Sci 2010;123:3467-3477.
29. Liu H, Pan Z, Li A, Fu S, Lei Y, Sun H, et al. Roles of chemokine receptor 4 (CXCR4) and chemokine ligand 12 (CXCL12) in metastasis of hepatocellular carcinoma cells. Cell Mol Immunol 2008;5:373-378.
30. Li N, Guo W, Shi J, Xue J, Hu H, Xie D, et al. Expression of the chemokine receptor CXCR4 in human hepatocellular carcinoma and its role in portal vein tumor thrombus. J Exp Clin Cancer Res 2010; 29:156.
31. Zhang XH, Wang Q, Gerald W, Hudis CA, Norton L, Smid M, et al. Latent bone metastasis in breast cancer tied to Src-dependent survival signals. Cancer Cell 2009;16:67-78.
32. Katoh M, Katoh M. Integrative genomic analyses of CXCR4: transcriptional regulation of CXCR4 based on TGFbeta, Nodal, Activin signaling and POU5F1, FOXA2, FOXC2, FOXH1, SOX17, and GFI1 transcription factors. Int J Oncol 2010;36:415-420.
33. Seoane J. The TGFBeta pathway as a therapeutic target in cancer. Clin Transl Oncol 2008;10:14-19.
34. Duda DG, Kozin SV, Kirkpatrick ND, Xu L, Fukumura D, Jain RK. CXCL12 (SDF1alpha)-CXCR4/CXCR7 pathway inhibition: an emerging sensitizer for anticancer therapies? Clin Cancer Res 2011;17:2074-2080.

Free Radical Biology and Medicine 69 (2014) 338–347

Contents lists available at ScienceDirect

Free Radical Biology and Medicine

journal homepage: www.elsevier.com/locate/freeradbiomed

Original Contribution

# The NADPH oxidase NOX4 inhibits hepatocyte proliferation and liver cancer progression

Eva Crosas-Molist [a], Esther Bertran [a], Patricia Sancho [a,1], Judit López-Luque [a], Joan Fernando [a], Aránzazu Sánchez [b], Margarita Fernández [b], Estanis Navarro [a], Isabel Fabregat [a,c,*]

[a] Bellvitge Biomedical Research Institute, L'Hospitalet de Llobregat, 08908 Barcelona, Spain
[b] Departamento de Bioquímica y Biología Molecular II, Facultad de Farmacia, Universidad Complutense, Instituto de Investigación Sanitaria del Hospital Clínico San Carlos, 28080 Madrid, Spain
[c] Departament de Ciències Fisiològiques II, Universitat de Barcelona, Campus de Bellvitge, Barcelona, Spain

ARTICLE INFO

*Article history:*
Received 24 October 2013
Received in revised form
23 January 2014
Accepted 28 January 2014
Available online 6 February 2014

*Keywords:*
NOX4
NADPH oxidase
Reactive oxygen species
Hepatocyte proliferation
Hepatocellular carcinoma
Liver cancer
Liver regeneration
Hepatocarcinogenesis
Free radicals

ABSTRACT

The NADPH oxidase NOX4 has emerged as an important source of reactive oxygen species in signal transduction, playing roles in physiological and pathological processes. NOX4 mediates transforming growth factor-β-induced intracellular signals that provoke liver fibrosis, and preclinical assays have suggested NOX4 inhibitors as useful tools to ameliorate this process. However, the potential consequences of sustained treatment of liver cells with NOX4 inhibitors are yet unknown. The aim of this work was to analyze whether NOX4 plays a role in regulating liver cell growth either under physiological conditions or during tumorigenesis. In vitro assays proved that stable knockdown of NOX4 expression in human liver tumor cells increased cell proliferation, which correlated with a higher percentage of cells in S/G2/M phases of the cell cycle, downregulation of p21(CIP1/WAF1), increase in cyclin D1 protein levels, and nuclear localization of β-catenin. Silencing of NOX4 in untransformed human and mouse hepatocytes also increased their in vitro proliferative capacity. In vivo analysis in mice revealed that NOX4 expression was downregulated under physiological proliferative situations of the liver, such as regeneration after partial hepatectomy, as well as during pathological proliferative conditions, such as diethylnitrosamine-induced hepatocarcinogenesis. Xenograft experiments in athymic mice indicated that NOX4 silencing conferred an advantage to human hepatocarcinoma cells, resulting in earlier onset of tumor formation and increase in tumor size. Interestingly, immunochemical analyses of NOX4 expression in human liver tumor cell lines and tissues revealed decreased NOX4 protein levels in liver tumorigenesis. Overall, results described here strongly suggest that NOX4 would play a growth-inhibitory role in liver cells.



Reactive oxygen species (ROS) are intracellular physiological signals, but also disease triggers. Their relative excess or shortage is potentially deleterious [1]. The NADPH oxidase (NOX) family has emerged in the past years as important sources of ROS in signal transduction [2]. NOX-derived ROS may modulate gene expression, cytoskeleton remodeling, migration, and differentiation, as well as cell proliferation and death [1,2]. The first NOX described was the respiratory burst NADPH oxidase complex, whose catalytic subunit is now known as NOX2. The other family members have been cloned and studied in the past 15 years. The NOX family consists of seven members, NOX1–5 and two dual oxidases (DUOX1 and 2), which share analogies in structure and catalytic function, because all of them mediate the reduction of oxygen using NADPH as an electron donor. However, important differences in regulation and cellular functions are observed among them. The functional analysis of the isoenzyme NOX4 revealed unique characteristics compared to other NADPH oxidases [3]. NOX4 associates with their regulators (p22phox or Poldip2) in intracellular membranes, where the superoxide anion is rapidly converted to $H_2O_2$ [3,4]. It is believed that $H_2O_2$ is responsible for the majority of NOX4 downstream effects. None of the known cytosolic oxidase proteins nor

*Abbreviations:* DEN, diethylnitrosamine; HCC, hepatocellular carcinoma; NOX, NADPH oxidase; ROS, reactive oxygen species; TGF-β, transforming growth factor β

* Corresponding author at: Bellvitge Biomedical Research Institute, L'Hospitalet de Llobregat, 08908 Barcelona, Spain. Fax: +34 932 607426.
*E-mail address:* ifabregat@idibell.cat (I. Fabregat).
[1] Present address: Spanish National Cancer Research Center, Madrid, Spain.

http://dx.doi.org/10.1016/j.freeradbiomed.2014.01.040
0891-5849 

the GTPase Rac is required for its activity, which seems to be regulated mainly at the transcriptional level [3,5,6]. Strong pieces of evidence support the role of NOX4 in various pathologies. In particular, NOX4 has been proposed to be a relevant mediator of fibrotic processes in lung [7] or liver [8]. For these reasons there is an increasing interest in the development and test of new NOX inhibitors that could be clinically useful to ameliorate fibrosis [9–11]. However, what could be the consequences of sustained treatment with NOX4 inhibitors? This is an unanswered question yet.

In the liver, NOXs play relevant roles mediating transforming growth factor-β (TGF-β) actions. In stellate cells, NOX4 signals for their activation to myofibroblasts, but in hepatocytes, it mediates cell death [8]. A similar situation occurs in the lung [12]. ROS generated by NOX4 are required for the mitochondrial-mediated apoptosis induced by TGF-β in hepatocytes [13], through modulation of the expression of the proapoptotic genes BIM and BMF [14]. TGF-β is a well-known tumor suppressor factor in epithelial cells through its capacity to inhibit growth as well as to induce apoptosis. Indeed, inhibition of NOX4 in epithelial cells might lead to a situation in which protumorigenic processes would be favored because of the lack of a suppressor gene. However, this is a hypothesis that remains to be proved.

The aim of this work was to analyze whether NOX4 plays a role in regulating liver cell growth either under physiological conditions or during liver tumorigenesis. Overall, results described here strongly suggest that NOX4 would play a growth-inhibitory role in liver cells.

## Material and methods

### *Reagents*

Human recombinant TGF-β1 was from Calbiochem (La Jolla, CA, USA). Fetal bovine serum (FBS) was from Sera Laboratories International (Cinder Hill, UK). Anti-NOX4 rabbit polyclonal antiserum was raised by Sigma–Genosys (Suffolk, UK) against a peptide corresponding to the C-terminal loop region (amino acids 499–511). Specificity was tested by ELISA with the purified peptide [14]. This NOX4 antibody is currently available from Merck Millipore (Billerica, MA, USA; Cat. No. ABC459).

### *Cell culture*

Hep3B and PLC/PRF/5 cell lines were obtained from the European Collection of Cell Cultures. HLF cells were from the Japanese Collection of Research Bioresources (JCRB Cell Bank) and were kindly provided by Dr. Giannelli (University of Bari, Bari, Italy). The human liver cell line CCL-13 (Chang liver, CHL) was from the American Type Culture Collection. Neonatal mouse hepatocytes were immortalized as described previously [15]. Hep3B cells were maintained in minimal essential medium, HLF in RPMI medium, and PLC/PRF/5, CHL, and neonatal mouse hepatocytes in Dulbecco's modified Eagle's medium, supplemented with 10% fetal bovine serum, in a humidified atmosphere at 37 °C, 5% $CO_2$.

### *Knockdown assays*

For stable transfection of short hairpin (sh) RNA, cells at 50–60% confluence were transfected with MAtra-A reagent (IBA GmbH, Goettingen, Germany) at a dilution of 1:600 in complete medium, according to the manufacturer's recommendation (15 min on the magnet plate), using 2 μg/ml shRNA plasmid. Four different plasmids of NOX4 shRNA were transfected, as well as a control nonspecific shRNA. After 24 h, the medium was changed to complete medium, and selection of transfected cells was done with puromycin (for 50 days before experiments). ShRNA plasmids were selected from Mission SH, Sigma (Madrid, Spain) and the sequences were the following: No. 1, CCGGGAGCCTCAGCATCTGTTCTTACTCGAGTAAGAACAGATGCTGAGGCTCTTTTTG; No. 2, CCGGCCCTCAACTTCTCAGTGAATTCTCGAGAATTCACTGAGAAGTTGAGGGTTTTTG; No. 3, CCGGCAGAGTTTACCCAGCACAAATCTCGAGATTTGTGCTGGGTAAACTCTGTTTTTG; and No. 4, CCGGGCTGTATATTGATGGTCCTTTCTCGAGAAAGGACCATCAATATACAGCTTTTTG. The protocols used were previously described [16,17].

For transient small interfering (si) RNA transfection, cells at 70% confluence were transfected using TransIT-siQuest (Mirus, Madison, WI, USA) at 1:300 dilution in complete medium, as described previously [18]. Oligos were obtained from Sigma–Genosys. Oligo sequences were the following: unsilencing, 5′-GUAAGACACGACUUAUCGC-3′; human NOX4, 5′-GCCUCUACAUAUGCAAUAA-3′, and mouse Nox4, 5′-CAAGAAGAUUGUUGGAUAA-3′. The unsilencing siRNA used was selected from previous works [19].

### *Partial hepatectomy in mice*

Animals used in this study were male C57/BL6 mice, ages 10 to 14 weeks. Partial hepatectomies were performed by removal of two-thirds of the adult mouse liver, according to the method described by Higgins and Anderson [20]. Mice were euthanized at 2, 8, 24, 48, and 72 h and 7days after the surgery and tissue samples were frozen immediately in liquid nitrogen for RNA extraction or fixed in 4% paraformaldehyde for immunohistochemistry analysis.

### *Diethylnitrosamine (DEN)-induced hepatocarcinogenesis in mice*

Male mice at day 15 of age received intraperitoneal injections of DEN (5 mg/kg) diluted in saline buffer, control animals were injected with saline buffer intraperitoneally. After 6, 9, or 12 months, the mice were sacrificed and their livers removed. For histological studies, liver lobes were fixed in 4% paraformaldehyde overnight and paraffin-embedded for immunohistochemistry staining. Total RNA was isolated from these tissues to analyze gene expression by real-time quantitative PCR.

### *Xenograft model of subcutaneous tumor growth in vivo*

Athymic nude mice were purchased from Harlan Laboratories. A total of 16 male mice, 7 weeks of age, were used. Hep3B cells transfected with either a control shRNA or a NOX4 silencing shRNA (shNOX4(No. 3)) were grown in the presence of 10% FBS. Then, the cells were trypsinized and counted, being diluted at a final concentration of $5 \times 10^7$ cells/ml in HBSS. A total of 16 nude mice were randomly divided into two groups (shControl and shNOX4 (No. 3), 8 mice per group) and the cell suspension (0.1 ml/mouse) was subcutaneously injected into the left flank of the mouse. Tumor growth was measured every 2 days.

### *Crystal violet staining*

Cells were washed twice with phosphate-buffered saline and the remaining viable adherent cells were stained with crystal violet (0.2% in 2% ethanol) and analyzed spectrophotometrically, as described previously [21].

### *Analysis of caspase-3 activity*

Fluorimetric analysis of caspase-3 activity was determined as described previously [22], with 20 μg protein extract. Fluorescence was measured in a Fluostar Optima microplate fluorescence reader. A unit of caspase-3 activity is the amount of active enzyme

necessary to produce an increase in 1 fluorescence unit and results are presented as units of caspase-3 activity/h/μg protein.

*DNA synthesis assay*

After incubation of cells for 48 h, DNA synthesis was evaluated by [*methyl*-$^3$H]thymidine (GE Healthcare, Barcelona, Spain) incorporation into trichloroacetic acid (TCA)-precipitable material during the last 40 h, as described previously [23].

*Analysis of DNA content by flow cytometry*

Cell ploidy was estimated by flow cytometry DNA analysis [24]. Cell cycle analysis was carried out using the software ModFit LTTM (Verity Software House, USA).

*Measurement of redox state*

The oxidation-sensitive fluorescent probe 2′,7′-dichlorodihydrofluorescein diacetate ($H_2$DCFDA; from Invitrogen, UK) was used to analyze the intracellular oxidant levels [19]. Extracellular $H_2O_2$ was measured in intact cells using horseradish peroxidase-linked Amplex Ultra Red (Invitrogen). Briefly, Amplex Ultra Red (50 μM) and horseradish peroxidase (0.1 U/ml) were added to the cellular samples for 2 h. Fluorescence readings were made in duplicate in a 96-well plate at ex/em 530/590 nm using 100 μl samples of medium. Fluorescence was measured in a Fluostar Optima microplate fluorescence reader and expressed as percentage of control after correction for protein content with $H_2$DCFDA and for cell number (crystal violet assay) with Amplex Ultra Red.

*Analysis of gene expression*

RNeasy Mini Kit (Qiagen, Valencia, CA, USA) was used for total RNA isolation. Reverse transcription was carried out using the High Capacity reverse transcriptase kit (Applied Biosystems, Foster City, CA, USA) and 1 μg of total RNA from each sample for complementary DNA synthesis. For real-time quantitative PCR, expression levels were determined in duplicate in an ABI Prism7700 system, using the Sybr Green PCR master mix (Applied Biosystems) for mouse primers and in a LightCycler 480 real-time PCR system, using the LightCycler 480 SYBR Green I Master (Roche Applied Science) for human primers. Reactions were performed with the specific primers listed in Table 1.

*Western blot analysis*

Total protein extracts and Western blotting procedures were carried out as described previously [19,25]. The antibodies used were mouse anti-β-actin (clone AC-15) from Sigma–Aldrich (St. Louis, MO, USA), rabbit anti-NOX4 raised by Sigma–Genosys [14], and rabbit anti-cyclin D1 (M-20) from Santa Cruz Biotechnology (Santa Cruz, CA, USA). Antibodies were used at 1:1000 dilutions, except β-actin (1:3000). Protein concentration was measured with a BCA protein assay kit (Pierce).

*Immunofluorescence staining*

Fluorescence microscopy studies were performed as described previously [25]. For rabbit anti-NOX4 (Sigma–Genosys) staining, cells were fixed with 4% paraformaldehyde in phosphate-buffered saline. For rabbit anti-Ki67 (Abcam, Cambridge, UK) and mouse anti-β-catenin (BD Transduction Laboratories, Erembodegem, Belgium) staining, cells were fixed with 4% paraformaldehyde in phosphate-buffered saline and permeabilized with 0.2% Triton X-100. The secondary antibodies Alexa Fluor 488-conjugated anti-rabbit and anti-mouse immunoglobulin were from Molecular Probes (Eugene, OR, USA). Blue signal represents the nuclear DNA staining with DAPI from Sigma–Aldrich. Cells were visualized in a Nikon Eclipse 80i microscope with the appropriate filters. Representative images were taken with a Nikon DS-Ri1 digital camera. NOX4 staining was visualized on a Leica TCS SP5 spectral confocal microscope with a HCX PL APO λ blue 63 × 1.4 oil objective lens and excited with the 488-nm laser line of an argon laser. Acquisition software was Leica Application Suite Advanced Fluorescence (LAS AF). The projections of Z stacks are shown. Fluorescence intensity was quantified using Fiji open source software.

**Table 1**
Specific primers used in this study.

| Primer | Sequence |
|---|---|
| Human CDKN1A forward | 5′-TGTCACTGTCTTGTACCCTTG-3′ |
| Human CDKN1A reverse | 5′-GGCGTTTGGAGTGGTAGAA-3′ |
| Human NOX4 forward | 5′-GCAGGAGAACCAGGAGATTG-3′ |
| Human NOX4 reverse | 5′-CACTGAGAAGTTGAGGGCATT-3′ |
| Human L32 forward | 5′-AACGTCAAGGAGCTGGAAG-3′ |
| Human L32 reverse | 5′-GGGTTGGTGACTCTGATGG-3′ |
| Mouse Nox4 forward | 5′-TCCAAGCTCATTTCCCACAG-3′ |
| Mouse Nox4 reverse | 5′-CGGAGTTCCATTACATCAGAGG-3′ |
| Mouse p22phox forward | 5′-ACACAGTGGTATTTCGGCG-3′ |
| Mouse p22phox reverse | 5′-CAGGTACTTCTGTCCACATCG-3′ |
| Mouse 18S forward | 5′-CGAGACTCTGGCATGCTAA-3′ |
| Mouse 18S reverse | 5′-CGCCACTTGTCCCTCTAAG-3′ |

*Immunohistochemistry*

Paraffin-embedded samples, both from xenografts and from partial hepatectomy experiments, were cut into 4-μm-thick sections and stained with hematoxylin and eosin (H&E) or the following primary antibodies (diluted from 1:50 to 1:100): rabbit anti-Ki67 (Abcam), rabbit anti-cleaved caspase-3 (Asp-175) (Cell Signaling Technology, Danvers, MA, USA), and rabbit anti-NOX4 (Sigma–Genosys). The primary antibodies were incubated overnight at 4 °C and binding developed with the Vectastain ABC kit (Vector Laboratories, Burlingame, CA, USA). Tissues were visualized in a Nikon Eclipse 80i microscope with the appropriate filters. Representative images were taken with a Nikon DS-Ri1 digital camera.

*Tissue array*

A human liver tissue array (Cat. No. Z7020056; BioChain Institute, San Francisco, CA, USA) containing duplicates of 70 cases covering (1) HCC and a few samples of other types of liver cancer, (2) 3 cases of other nonmalignant liver tissues, and (3) 2 normal liver tissues was used. Rabbit anti-NOX4 (Sigma–Genosys) was used as a primary antibody. The same procedure as for immunohistochemistry was used. Staining was quantified by densitometry using the software Quantity One (Bio-Rad Laboratories, Hercules, CA, USA) and the ratio between each case and the mean of normal tissues was represented.

*Statistical analyses*

All data represent at least three experiments and are express as the mean ± SEM. Differences between groups were compared using Student's *t* test. Statistical significance was assumed when $p < 0.05$.

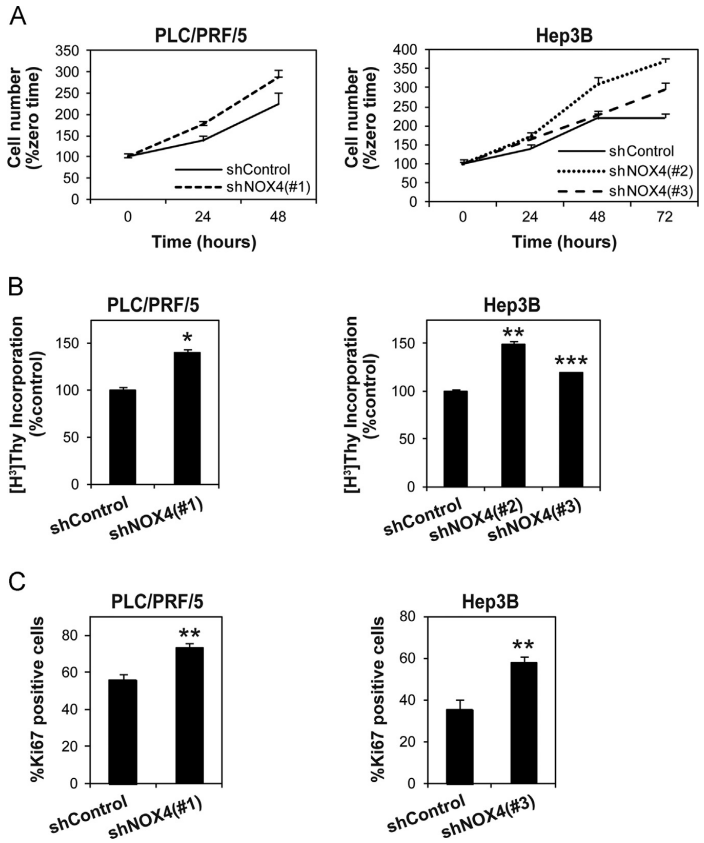


**Fig. 1.** Stable silencing of NOX4 confers a proliferative advantage to human HCC cells. Comparison of the proliferative capacity of NOX4-silenced cells (shNOX4) versus cells transfected with a nonspecific shRNA (shControl). The cell line and the shNOX4 used are indicated. (A) Number of viable cells analyzed by crystal violet at the times indicated. Results are expressed as a percentage of increase relative to time 0. (B) DNA synthesis, analyzed as [$^3$H]thymidine incorporation (48 h) and expressed as a percentage of the control (nonspecific-shRNA-transfected) cells. (C) Detection of proliferative cells through immunocytochemistry with an anti-Ki67 antibody; quantification of the positive nuclei expressed as a percentage of total nuclei number. Data are means ± SEM of three independent experiments. Student's *t* test versus control (nonspecific-shRNA-transfected) cells was used in (B) and (C): $^*p < 0.05$, $^{**}p < 0.01$, $^{***}p < 0.001$.

## Results

### *In vitro analysis of the effect of silencing NOX4 on the proliferation of liver tumor and untransformed cells*

To know the role of NOX4 on liver tumor cell growth, we targeted NOX4 for knockdown with specific shRNA in the HCC cell lines PLC/PRF/5 and Hep3B and selected stable clones (Supplementary Fig. 1). Western blot revealed specific reduction of a 60-kDa band, the expected size for NOX4, as well as of two additional bands of slightly smaller size (Supplementary Fig. 1A). NOX4-targeting knockdown correlated with a decrease in intracellular oxidant levels, through $H_2$DCFDA fluorescence analysis, as well as in extracellular hydrogen peroxide levels, through Amplex red assay (Supplementary Fig. 1B). To analyze the loss of NOX4 function we evaluated the cell response to TGF-β in terms of apoptosis, a process that requires NOX4 [13]. As expected, TGF-β-induced activation of caspase-3 was significantly diminished when NOX4 was knocked down (Supplementary Fig. 1C).

We first decided to analyze the effect of canceling NOX4 on in vitro growth of HCC cells. For this, we performed experiments to compare the proliferative capacity of NOX4-silenced cells versus their respective controls. Two different cell lines were analyzed (PLC/PRF/5 and Hep3B), with similar results. Cell number, as well as DNA synthesis analyzed as [$^3$H]thymidine incorporation into TCA-precipitable material or Ki67-positive cells, was significantly increased in NOX4-knockdown cells (Fig. 1). Enhancement of cell proliferation correlated with significant lower percentage of cells in G1 phase of the cell cycle and significant increase in the percentage of cells in S phase (Fig. 2A). Previous reports had proposed a role for NOX4 in TGF-β-induced senescence through upregulation of p21(CIP1/WAF1) and p15INK4b [26]. For this, we decided to analyze the expression of these cyclin-dependent kinase inhibitors. We found that attenuation of NOX4 expression provoked a decrease in the transcript levels of *CDKN1A* (p21) (Fig. 2B). No significant changes in *p15INK4b* were observed (results not shown). Correlating with this, analysis of cyclin D1 protein by Western blot revealed higher levels in NOX4-silenced versus control cells (Fig. 2C). Interestingly, HCC cells in which NOX4 expression was knocked down showed higher nuclear localization of β-catenin (Fig. 2D). To know whether the role of NOX4 in controlling proliferation was a specific characteristic of tumor cells or whether it also occurs in untransformed cells, we performed experiments of transient targeting knockdown of NOX4

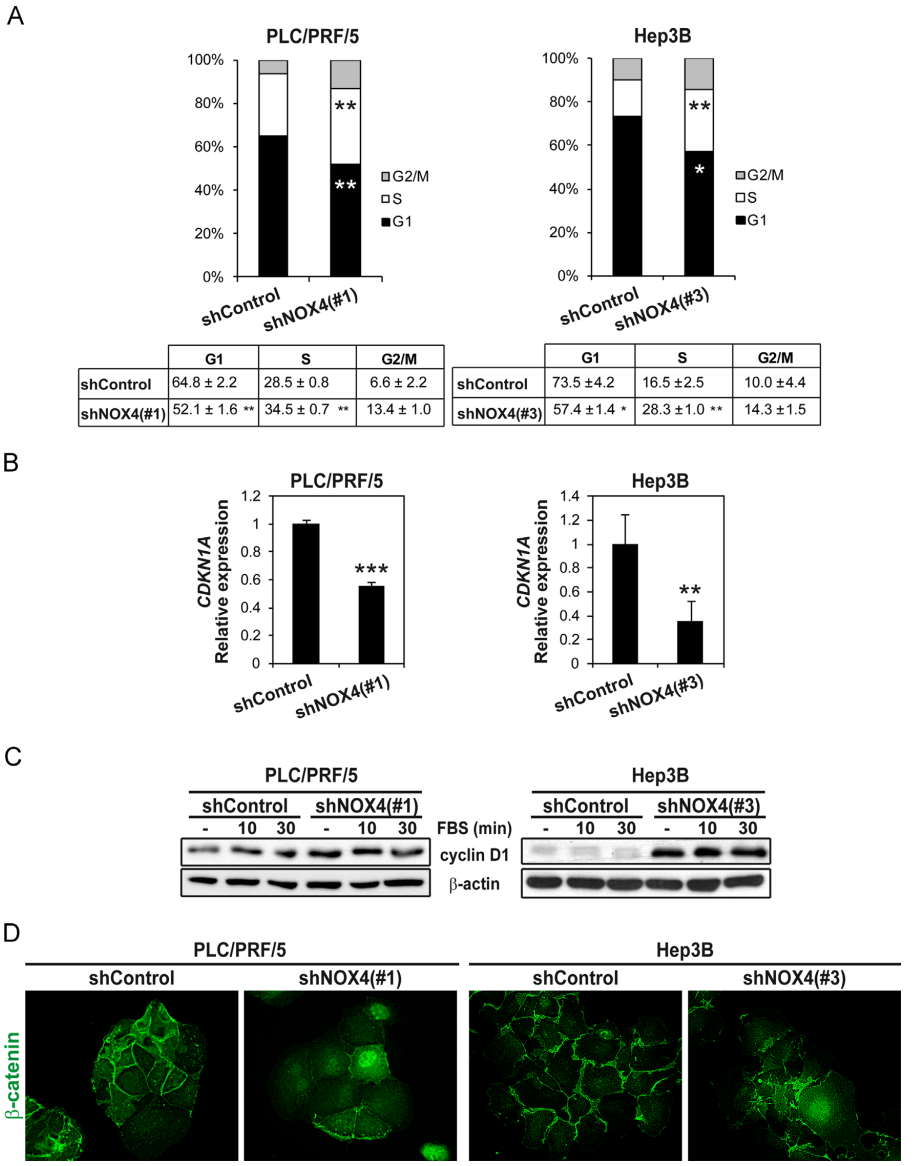


| | G1 | S | G2/M |
|---|---|---|---|
| shControl | 64.8 ± 2.2 | 28.5 ± 0.8 | 6.6 ± 2.2 |
| shNOX4(#1) | 52.1 ± 1.6 ** | 34.5 ± 0.7 ** | 13.4 ± 1.0 |

| | G1 | S | G2/M |
|---|---|---|---|
| shControl | 73.5 ±4.2 | 16.5 ±2.5 | 10.0 ±4.4 |
| shNOX4(#3) | 57.4 ±1.4 * | 28.3 ±1.0 ** | 14.3 ±1.5 |

**Fig. 2.** Stable silencing of NOX4 increases the proportion of HCC cells in proliferating phases of the cell cycle. The cell line and the shNOX4 used are indicated. (A) Analysis of the percentage of cells in the various phases of the cell cycle in control and NOX4-silenced (shNOX4) cells. (B) Analysis of *CDKN1A* expression by real-time PCR. (C) Analysis of cyclin D1 by Western blot at 10 and 30 min after 10% FBS stimulation. (D) Immunofluorescence analysis of β-catenin (green). Data in (A) and (B) are means ± SEM of at least three independent experiments. Student's *t* test versus control (nonspecific-shRNA-transfected) cells was used: $^{*}p < 0.05$, $^{**}p < 0.01$, $^{***}p < 0.001$. (C) and (D) show a representative experiment.

in the untransformed human hepatocyte cell line CHL and in an immortalized mouse hepatocyte cell line. As shown in Fig. 3, silencing of NOX4 (Fig. 3A), which correlated with a significant decrease in the intracellular oxidant levels (Fig. 3B), significantly increased the growth of both cell lines (Fig. 3C). All these results indicated that NOX4 negatively controls the proliferation of liver tumor and untransformed cells.

*NOX4 expression is downregulated during liver regeneration after partial hepatectomy in mice*

Because results described above indicated an inverse correlation between NOX4 expression and liver cell growth in in vitro experiments, we hypothesized that NOX4 expression may inversely correlate with hepatocyte proliferation under physiological

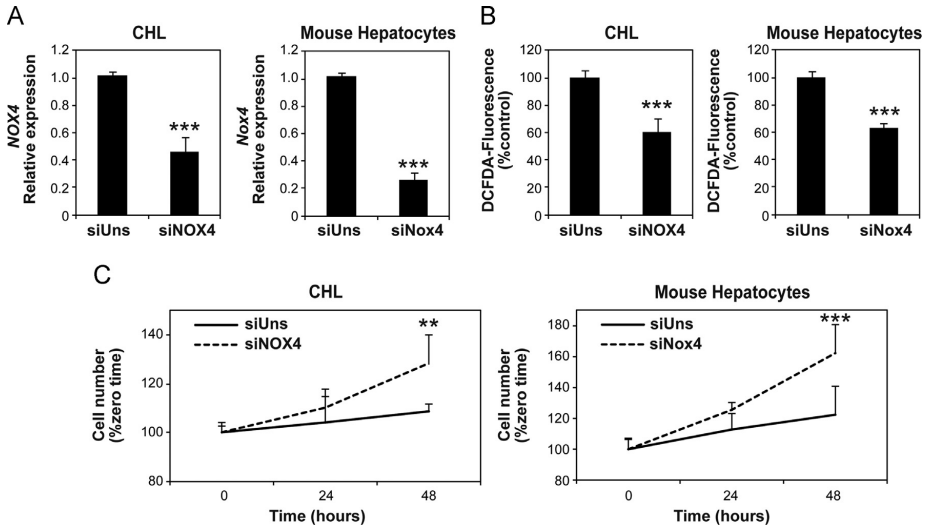


**Fig. 3.** NOX4-targeted knockdown increases proliferation in both human and mouse hepatocytes. CHL cells and mouse hepatocytes were transfected with an unsilencing siRNA (siUns) or a specific NOX4 siRNA (siNOX4). (A) Analysis of NOX4 mRNA expression by real-time PCR. (B) Analysis of intracellular oxidant levels. (C) Number of viable cells analyzed by crystal violet at the indicated times. Results are expressed as a percentage of increase relative to time 0. Student's *t* test versus control (nonspecific-siRNA-transfected) cells was used: $^{**}p < 0.01$, $^{***}p < 0.001$.

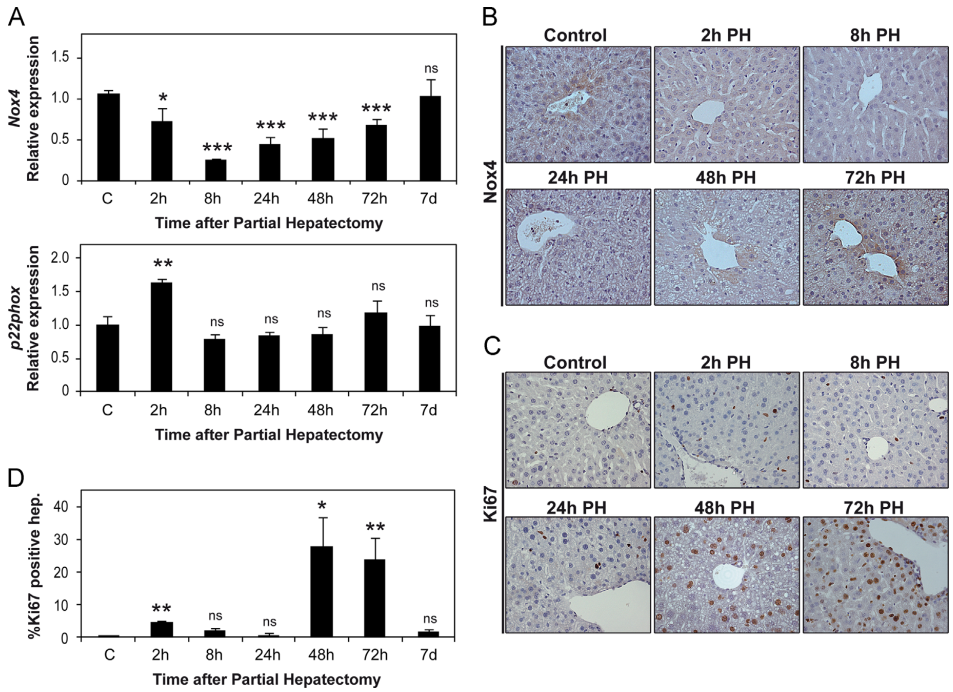


**Fig. 4.** Downregulation of NOX4 during liver regeneration after partial hepatectomy in mice. (A) Analysis of NOX4 and p22phox mRNA expression by real-time PCR at the indicated times after partial hepatectomy. Immunohistochemistry of (B) NOX4 and (C) Ki67 at the indicated times after partial-hepatectomy. (D) Quantification of the percentage of Ki67-labeled nuclei. Data in (A) and (D) are means ± SEM of at least three mice per group. Student's *t* test versus control was used: $^{*}p < 0.05$, $^{**}p < 0.01$, $^{***}p < 0.001$.

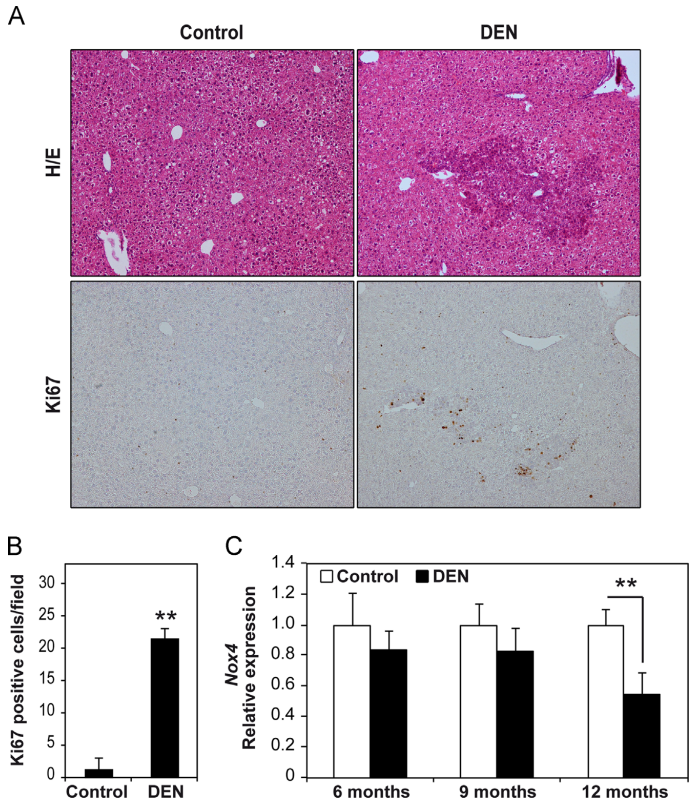


**Fig. 5.** Tumorigenesis in mice after DEN treatment is associated with decreased NOX4 expression. (A) Immunohistochemistry of 12-month-old mouse livers. Top: H&E stain. Bottom: immunohistochemistry of Ki67. (B) Quantification of the number of Ki67-labeled nuclei per field. (C) *NOX4* transcript levels analyzed by real-time PCR in control liver (PBS treatment) versus tumoral tissues in animals at 6, 9, and 12 months of age. Data represent means ± SEM (number of animals: 4 control animals; 3 DEN-treated animals; analysis in two different pieces of tissue/animal). Student's *t* test was used: $^{**}p < 0.01$.

and/or pathological situations where proliferation of liver cells takes place. To confirm this hypothesis, we studied changes in the expression of NOX4 after two-thirds partial hepatectomy in mice, a situation that pushes hepatocytes to leave the G0 phase of the cell cycle to proliferate and regenerate the liver. As shown in Fig. 4A, partial hepatectomy provoked a downregulation of NOX4 expression between 2 and 72 h, which completely recovered after 7 days, without changes in *p22phox* expression, correlating with lower NOX4 protein levels in hepatocytes analyzed by immunohistochemistry (Fig. 4B). This effect preceded the peak of maximal DNA synthesis in hepatocytes (Fig. 4C and D). Thus, in vivo liver cell proliferation correlates with a decrease in NOX4 expression.

*Inverse correlation between NOX4 expression and liver tumor progression in experimental animal models*

The treatment of mice with DEN at day 15 of age provokes a situation of liver injury that develops in the appearance of liver tumors between 9 and 12 months of age in mice. We had previously reported the use of this model for analyzing molecular mechanisms of liver tumorigenesis [27]. At 12 months of age all the male mice presented multifocal liver tumors, well recognized as neoplastic areas where proliferating cells were localized (Fig. 5A and B). We decided to analyze NOX4 mRNA levels in the livers of DEN-treated mice at 6, 9, and 12 months of age. Interestingly, a significant decrease in NOX4 expression was observed in 12-month-old animals, coincident with the appearance of liver tumors. These results indicated that in vivo liver tumor cell proliferation also correlates with a decrease in NOX4 expression in an experimental model in mice.

Considering all the results described above we hypothesized that silencing of NOX4 expression may increase the tumorigenic capacity of HCC cells. To confirm this hypothesis, we studied the tumor formation and progression capacities of control and NOX4-knockdown Hep3B cells in xenograft experiments into athymic nude mice (Fig. 6A and B). Results indicated that attenuation of NOX4 significantly increased the cell tumorigenic capacity, as tumors appeared earlier and reached a much higher volume than those induced by shControl Hep3B cells. Maintenance of the decrease in NOX4 expression in tumors from NOX4-knockdown HCC cells was corroborated by immunohistochemical analysis of the tumor tissues (Supplementary Fig. 2). Interestingly, increased rate in tumor progression correlated with significant enhancement in tumor cell proliferation (Fig. 6C). Number of apoptotic cells was low in both cohorts of tumors (Fig. 6D) and when caspase-3 activity was analyzed in tissues, although a tendency to decrease was observed in the tumors originating from NOX4-knockdown cells, the effect was not statistically significant (Fig. 6E).

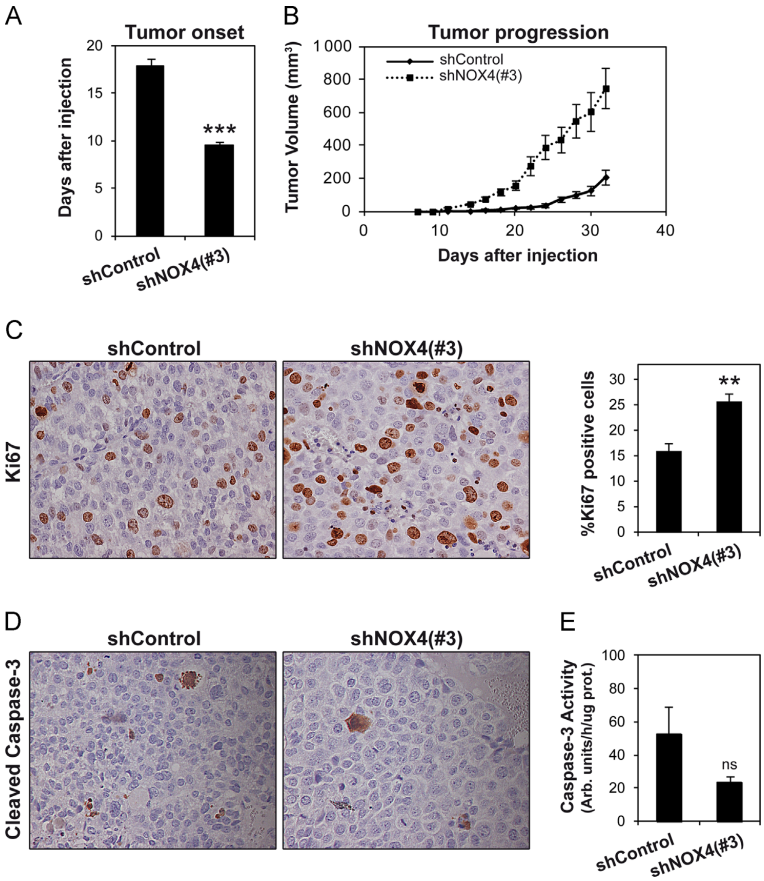


**Fig. 6.** Stable silencing of NOX4 in human HCC cells increases their tumorigenic capacity when injected subcutaneously into athymic nude mice. Hep3B cells stably transfected with a plasmid containing either an shRNA against NOX4 (shNOX4(No. 3)) or an unsilencing sequence (shControl) were injected subcutaneously into athymic nude mice. (A) Number of days after injection when tumors appeared. (B) Tumor volumes over time. (C) Left: immunohistochemistry of Ki67. Right: quantification of the percentage of labeled nuclei. (D) Immunohistochemistry of cleaved caspase-3. (E) Analysis of caspase-3 activity. Data are means ± SEM of at least six mice per group. Student's *t* test versus control (nonspecific-shRNA-transfected cells) was used: $^{**}p < 0.01$, $^{***}p < 0.001$.

*Human liver tumors show decreased levels of NOX4 protein*

Owing to the observed effect of targeting NOX4 knockdown on liver tumor progression in animal models, we decided to evaluate NOX4 protein levels in human HCC cell lines as well as in tissues from human liver tumors (Fig. 7). Immunofluorescence analysis in normal hepatocytes (CHL) and different HCC cell lines (PLC/PRF/5, Hep3B, and HLF) revealed that NOX4 is downregulated in transformed cell lines compared to normal cells (Fig. 7A). A tissue array that contained 65 samples (in duplicate) of liver tumors, of which 62 were HCC, as well as 2 samples (in duplicate) of healthy tissue (as control) and 3 samples (in duplicate) of nonmalignant lesions, was used for immunohistochemical analysis of NOX4. It was evidenced that most of the HCC tissues showed lower NOX4 expression compared to the control samples or even compared to the nonmalignant lesions (Fig. 7B). Interestingly, although few samples were included to get significant results, spots from cholangiocarcinoma and hepatoblastoma also showed lower NOX4 levels. Quantitative analysis corroborated decreased levels of NOX4 in most of the tumor samples (Fig. 7B, right). In 47% of the cases the ratio of NOX4 expression in tumor versus healthy tissues was lower than 0.8, and in 13% of the cases it was lower than 0.5.

## Discussion

The recent discovery of new members of the NADPH oxidase family opened up perspectives about the roles of these ROS-producing enzymes in human physiology and pathology. However, we are only at the beginning of understanding the players and their interactions. The recent implication of these enzymes in pathological processes, such as cardiovascular diseases or fibrosis, prompted the discovery of drugs that target their function and ameliorate the diseases. However, it is necessary to dissect all the functions of these enzymes to predict what would be the consequences of their targeting. NOX4 has been proved to mediate fibrosis in the liver [8] and NOX inhibitors are being tested in preclinical assays as a new therapy in liver fibrosis [9,10]. However, results presented in this article indicate that NOX4 may also play a tumor suppressor function in the liver. A variety of evidence supports this hypothesis: (1) targeting NOX4 confers selective

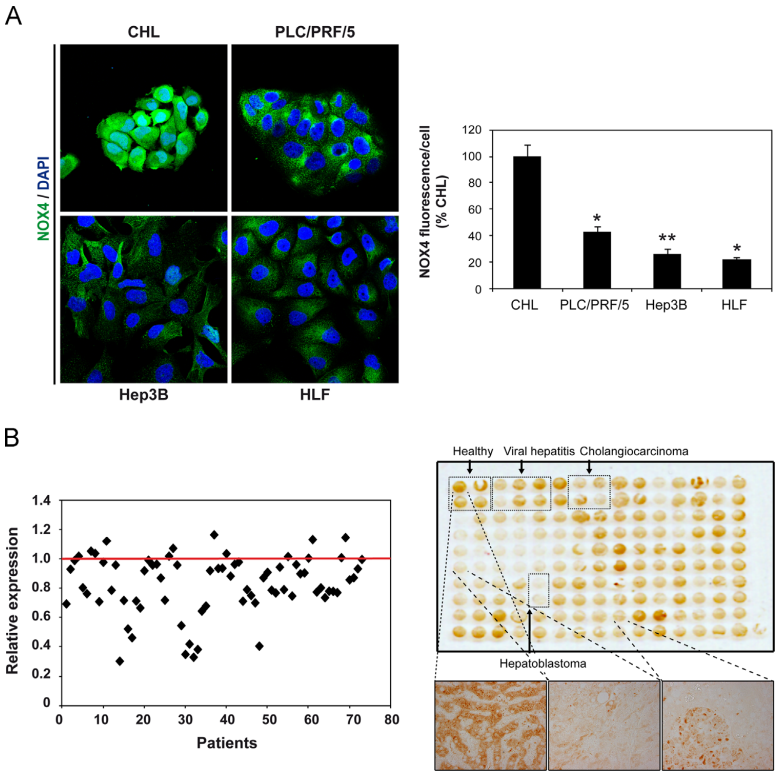


**Fig. 7.** NOX4 is downregulated in both human HCC cell lines and tissues. (A) Left: NOX4 (green) and DAPI (blue) staining in human hepatocytes (CHL) and human HCC cell lines (PLC/PRF/5, Hep3B, and HLF). Right: quantification of NOX4 fluorescence per cell represented as percentage versus CHL. Data are means ± SEM and Student's *t* test versus normal hepatocytes (CHL) was used: $^{*}p < 0.05$, $^{**}p < 0.01$. (B) Right top: macro overview of the NOX4 immunohistochemistry staining of the human liver tumor tissue array. Spots corresponding to healthy donors, viral hepatitis patients, cholangiocarcinoma, or hepatoblastoma are indicated. All the other spots correspond to hepatocellular carcinoma. Right bottom: representative microscopy images of one of the healthy liver spots and two of the HCC patients' spots. Left: densitometric quantification of each HCC tissue spot versus healthy tissue. Red line represents healthy tissue values.

advantage to liver cells to proliferate in vitro; (2) during liver regeneration after two-thirds partial hepatectomy in mice, a process that requires hepatocytes to leave quiescence and enter the cell cycle, *NOX4* expression is transiently downregulated; 3) liver tumorigenesis in an experimental model in mice correlates with downregulation of *NOX4;* (4) targeting NOX4 in HCC cells confers an advantage for tumor progression in a xenograft model of in vivo tumorigenesis; and (5) lower levels of NOX4 are found in human HCC cell lines and in a great percentage of human liver tumor tissues.

Correct progression through the cell cycle and its precise regulation is essential to an organism for proliferation and survival. The production of ROS in early growth factor-induced signaling pathways has led to the proposal that ROS regulate the G0 to G1 transition of the cell cycle through the regulation of cyclin D1 expression [28]. Furthermore, recent results indicate that NOX4 in human normal fibroblasts is required to suppress the p53-dependent checkpoint of proliferation [29]. However, various pieces of evidence locate ROS and, in particular, oxidative stress induced by NOX4 in a completely opposite role, i.e., inducing cell cycle arrest and cell death through either senescence or apoptosis. A possible explanation for these pleiotropic and sometimes contradictory actions of ROS may be related to the intracellular compartment where ROS are produced. NOX4 is associated with intracellular compartments, including the endoplasmic reticulum (ER), mitochondria, and nucleus. Nuclear NOX4 has been proposed to mediate ROS-induced DNA damage that leads to a loss of replicative potential and subsequent senescence [30,31]. In this same line of evidence, NOX4 mediates TGF-β-induced senescence in HCC cells through upregulation of p21(CIP1/WAF1) and p15INK4b [26].

Intracellular NOX4-derived ROS may also mediate signal transduction in normal cells by regulating redox-sensitive cysteine residues in specific effector proteins including tyrosine phosphatases [32]. Indeed, ER localization of NOX4 is critical for the regulation of protein tyrosine phosphatase (PTP1B), also an ER resident, through redox-mediated signaling. NOX4-mediated oxidation and inactivation of PTP1B in the ER serves as a regulatory switch for epidermal growth factor (EGF) receptor trafficking and specifically acts to terminate EGF (and maybe other growth factors) signaling [33].

Here we show that physiological proliferative situations in the liver, such as liver regeneration after partial hepatectomy in mice, or neoplastic liver pathologies, such as that found in the mouse model of DEN-induced hepatocarcinogenesis, concur with significant decreases in NOX4 expression. These results, together with the higher tumorigenic capacity of NOX4-silenced HCC cells in xenograft experiments in mice, point to the in vivo relevance of the in vitro results, in that the attenuation of NOX4 expression is coincident with a higher proportion of cells in the S phase of the

cell cycle, downregulation of *CDKN1A* (p21), and upregulation of cyclin D1. Interestingly, NOX4-knockdown cells show nuclear translocation of β-catenin and it has been reported that HCCs with β-catenin activation display significantly higher proliferation rate and larger tumor size compared with β-catenin-negative tumors [34]. All these results together indicate that NOX4 in liver tumor cells acts as a growth inhibitor, compatible with its potential role in counteracting growth factor signals and/or inducing senescence. In support of this, it is worth noting that NOX4 levels appear to be decreased in a cohort of tissues from human liver tumors, most of them HCC.

In conclusion, our results suggest a role for NOX4 as a redox enzyme involved in controlling proliferation of liver cells. Overall, NOX4 would play an essential tumor suppressor role in the liver. Considering that fibrotic processes frequently develop in cirrhosis, which is a preneoplastic situation, it is necessary to be cautious in the use of NOX4 inhibitors in these pathologies.

## Acknowledgments

This work was supported by grants to I.F. from the Ministry of Economy and Competitiveness, Spain (BFU2009-07219, BFU2012-35538, ISCIII-RTICC RD06/0020, and RD12-0036-0029) and AGAUR-Generalitat de Catalunya (2009SGR-312). E.C.-M. was the recipient of a predoctoral fellowship from the FPU program, Ministry of Education, Culture, and Sport, Spain. J.L.-L. and J.F. were recipients of predoctoral fellowships from the Bellvitge Biomedical Research Institute (IDIBELL) program. We thank Dr. Esther Castaño (Serveis Cientificotècnics, Institut d'Investigació Biomèdica de Bellvitge, Universitat de Barcelona) for her technical assistance with the flow cytometry, Dr. Carmen Casal for her technical assistance with the confocal microscope, and the team of the Animal Core Facility of IDIBELL for their help in tumorigenesis experiments in mice.

## Appendix A. Supplementary material

Supplementary data associated with this article can be found in the online version at http://dx.doi.org/10.1016/j.freeradbiomed.2014.01.040.

## References

[1] Altenhofer, S.; Kleikers, P. W.; Radermacher, K. A.; Scheurer, P.; Hermans, J. J. R.; Schiffers, P.; et al. The NOX toolbox: validating the role of NADPH oxidases in physiology and disease. *Cell. Mol. Life Sci.* **69:**2327–2343; 2012.

[2] Brown, D. I.; Griendling, K. K. Nox proteins in signal transduction. *Free Radic. Biol. Med.* **47:**1239–1253; 2009.

[3] Martyn, K. D.; Frederick, L. M.; von Loehneysen, K.; Dinauer, M. C.; Knaus, U. G. Functional analysis of Nox4 reveals unique characteristics compared to other NADPH oxidases. *Cell. Signalling* **18:**69–82; 2006.

[4] Lyle, A. N.; Deshpande, N. N.; Taniyama, Y.; Seidel-Rogol, B.; Pounkova, L.; Du, P.; et al. Poldip2, a novel regulator of Nox4 and cytoskeletal integrity in vascular smooth muscle cells. *Circ. Res.* **105:**249–259; 2009.

[5] Lambeth, J. D.; Kawahara, T.; Diebold, B. Regulation of Nox and Duox enzymatic activity and expression. *Free Radic. Biol. Med.* **43:**319–331; 2007.

[6] Serrander, L.; Cartier, L.; Bedard, K.; Banfi, B.; Lardy, B.; Plastre, O.; et al. NOX4 activity is determined by mRNA levels and reveals a unique pattern of ROS generation. *Biochem. J.* **406:**105–114; 2007.

[7] Hecker, L.; Vittal, R.; Jones, T.; Jagirdar, R.; Luckhardt, T. R.; Horowitz, J. C.; et al. NADPH oxidase-4 mediates myofibroblast activation and fibrogenic responses to lung injury. *Nat. Med.* **15:**1077–1081; 2009.

[8] Sancho, P.; Mainez, J.; Crosas-Molist, E.; Roncero, C.; Fernandez-Rodriguez, C. M.; Pinedo, F.; et al. NADPH oxidase NOX4 mediates stellate cell activation and hepatocyte cell death during liver fibrosis development. *PLoS One* **7:**e45285; 2012.

[9] Aoyama, T.; Paik, Y. H.; Watanabe, S.; Laleu, B.; Gaggini, F.; Fioraso-Cartier, L.; et al. Nicotinamide adenine dinucleotide phosphate oxidase in experimental liver fibrosis: GKT137831 as a novel potential therapeutic agent. *Hepatology* **56:**2316–2327; 2012.

[10] Jiang, J. X.; Chen, X.; Serizawa, N.; Szyndralewiez, C.; Page, P.; Schroder, K.; et al. Liver fibrosis and hepatocyte apoptosis are attenuated by GKT137831, a novel NOX4/NOX1 inhibitor in vivo. *Free Radic. Biol. Med.* **53:**289–296; 2012.

[11] Laleu, B.; Gaggini, F.; Orchard, M.; Fioraso-Cartier, L.; Cagnon, L.; Houngninou-Molango, S.; et al. First in class, potent, and orally bioavailable NADPH oxidase isoform 4 (Nox4) inhibitors for the treatment of idiopathic pulmonary fibrosis. *J. Med. Chem.* **53:**7715–7730; 2010.

[12] Carnesecchi, S.; Deffert, C.; Donati, Y.; Basset, O.; Hinz, B.; Preynat-Seauve, O.; et al. A key role for NOX4 in epithelial cell death during development of lung fibrosis. *Antioxid. Redox Signaling* **15:**607–619; 2011.

[13] Carmona-Cuenca, I.; Roncero, C.; Sancho, P.; Caja, L.; Fausto, N.; Fernandez, M.; et al. Upregulation of the NADPH oxidase NOX4 by TGF-beta in hepatocytes is required for its pro-apoptotic activity. *J. Hepatol.* **49:**965–976; 2008.

[14] Caja, L.; Sancho, P.; Bertran, E.; Iglesias-Serret, D.; Gil, J.; Fabregat, I. Overactivation of the MEK/ERK pathway in liver tumor cells confers resistance to TGF-{beta}-induced cell death through impairing up-regulation of the NADPH oxidase NOX4. *Cancer Res.* **69:**7595–7602; 2009.

[15] Gonzalez-Rodriguez, A.; Clampit, J. E.; Escribano, O.; Benito, M.; Rondinone, C. M.; Valverde, A. M. Developmental switch from prolonged insulin action to increased insulin sensitivity in protein tyrosine phosphatase 1B-deficient hepatocytes. *Endocrinology* **148:**594–608; 2007.

[16] Caja, L.; Sancho, P.; Bertran, E.; Fabregat, I. Dissecting the effect of targeting the epidermal growth factor receptor on TGF-beta-induced-apoptosis in human hepatocellular carcinoma cells. *J. Hepatol.* **55:**351–358; 2011.

[17] Caja, L.; Sancho, P.; Bertran, E.; Ortiz, C.; Campbell, J. S.; Fausto, N.; et al. The tyrphostin AG1478 inhibits proliferation and induces death of liver tumor cells through EGF receptor-dependent and independent mechanisms. *Biochem. Pharmacol.* **82:**1583–1592; 2011.

[18] Sancho, P.; Martin-Sanz, P.; Fabregat, I. Reciprocal regulation of NADPH oxidases and the cyclooxygenase-2 pathway. *Free Radic. Biol. Med.* **51:**1789–1798; 2011.

[19] Sancho, P.; Bertran, E.; Caja, L.; Carmona-Cuenca, I.; Murillo, M. M.; Fabregat, I. The inhibition of the epidermal growth factor (EGF) pathway enhances TGF-beta-induced apoptosis in rat hepatoma cells through inducing oxidative stress coincident with a change in the expression pattern of the NADPH oxidases (NOX) isoforms. *Biochim. Biophys. Acta* **1793:**253–263; 2009.

[20] Higgins, G.; Anderson, G. M. Experimental pathology of the liver: restoration of the liver of the white rat following partial surgical removal. *Arch. Pathol.* **12:**186–202; 1931.

[21] Sanchez, A.; Alvarez, A. M.; Benito, M.; Fabregat, I. Apoptosis induced by transforming growth factor-beta in fetal hepatocyte primary cultures: involvement of reactive oxygen intermediates. *J. Biol. Chem.* **271:**7416–7422; 1996.

[22] Murillo, M. M.; del Castillo, G.; Sanchez, A.; Fernandez, M.; Fabregat, I. Involvement of EGF receptor and c-Src in the survival signals induced by TGF-beta1 in hepatocytes. *Oncogene* **24:**4580–4587; 2005.

[23] de Juan, C.; Benito, M.; Alvarez, A.; Fabregat, I. Differential proliferative response of cultured fetal and regenerating hepatocytes to growth factors and hormones. *Exp. Cell Res.* **202:**495–500; 1992.

[24] Valdes, F.; Alvarez, A. M.; Locascio, A.; Vega, S.; Herrera, B.; Fernandez, M.; et al. The epithelial mesenchymal transition confers resistance to the apoptotic effects of transforming growth factor beta in fetal rat hepatocytes. *Mol. Cancer Res.* **1:**68–78; 2002.

[25] Caja, L.; Ortiz, C.; Bertran, E.; Murillo, M. M.; Miro-Obradors, M. J.; Palacios, E.; et al. Differential intracellular signalling induced by TGF-beta in rat adult hepatocytes and hepatoma cells: implications in liver carcinogenesis. *Cell. Signalling* **19:**683–694; 2007.

[26] Senturk, S.; Mumcuoglu, M.; Gursoy-Yuzugullu, O.; Cingoz, B.; Akcali, K. C.; Ozturk, M. Transforming growth factor-beta induces senescence in hepatocellular carcinoma cells and inhibits tumor growth. *Hepatology* **52:**966–974; 2010.

[27] Bertran, E.; Crosas-Molist, E.; Sancho, P.; Caja, L.; Lopez-Luque, J.; Navarro, E.; et al. Overactivation of the TGF-β pathway confers a mesenchymal-like phenotype and CXCR4-dependent migratory properties to liver tumor cells. *Hepatology* **58:**2032–2044; 2013.

[28] Burch, P. M.; Heintz, N. H. Redox regulation of cell-cycle re-entry: cyclin D1 as a primary target for the mitogenic effects of reactive oxygen and nitrogen species. *Antioxid. Redox Signaling* **7:**741–751; 2005.

[29] Salmeen, A.; Park, B. O.; Meyer, T. The NADPH oxidases NOX4 and DUOX2 regulate cell cycle entry via a p53-dependent pathway. *Oncogene* **29:**4473–4484; 2010.

[30] Weyemi, U.; Dupuy, C. The emerging role of ROS-generating NADPH oxidase NOX4 in DNA-damage responses. *Mutat. Res.* **751:**77–81; 2012.

[31] Weyemi, U.; Lagente-Chevallier, O.; Boufraqech, M.; Prenois, F.; Courtin, F.; Caillou, B.; et al. ROS-generating NADPH oxidase NOX4 is a critical mediator in oncogenic H-Ras-induced DNA damage and subsequent senescence. *Oncogene* **31:**1117–1129; 2012.

[32] Finkel, T. Signal transduction by reactive oxygen species. *J. Cell Biol.* **194:**7–15; 2011.

[33] Chen, K.; Kirber, M. T.; Xiao, H.; Yang, Y.; Keaney Jr J. F. Regulation of ROS signal transduction by NADPH oxidase 4 localization. *J. Cell Biol.* **181:**1129–1139; 2008.

[34] Calvisi, D. F.; Conner, E. A.; Ladu, S.; Lemmer, E. R.; Factor, V. M.; Thorgeirsson, S. S. Activation of the canonical Wnt/beta-catenin pathway confers growth advantages in c-Myc/E2F1 transgenic mouse model of liver cancer. *J. Hepatol.* **42:**842–849; 2005.